INFORMATION TO USERS

This manuscript has been reproduced from the microfilm master. UMI films the text directly from the original or copy submitted. Thus, some thesis and dissertation copies are in typewriter face, while others may be from any type of computer printer.

The quality of this reproduction is dependent upon the quality of the copy submitted. Broken or indistinct print, colored or poor quality illustrations and photographs, print bleedthrough, substandard margins, and improper alignment can adversely affect reproduction.

In the unlikely event that the author did not send UMI a complete manuscript and there are missing pages, these will be noted. Also, if unauthorized copyright material had to be removed, a note will indicate the deletion.

Oversize materials (e.g., maps, drawings, charts) are reproduced by sectioning the original, beginning at the upper left-hand corner and continuing from left to right in equal sections with small overlaps.

ProQuest Information and Learning
300 North Zeeb Road, Ann Arbor, MI 48106-1346 USA
800-521-0600

UNIVERSITÉ DE SHERBROOKE

TECHNETIUM–99M COMPLEXES WITH 2-PYROLLYLTHIONES: A NEW CLASS OF RADIOPHARMACEUTICALS FOR MEDICAL IMAGING

Svetlana Victorovna Selivanova

Département de Médecine nucléaire et de radiobiologie

Thèse présentée à la Faculté de médecine
en vue de l'obtention du grade de
philosophiae doctor (Ph.D.) en radiobiologie

Sherbrooke, Québec, Canada
2001

to my parents

CONTENTS

LIST OF ILLUSTRATIONS

Figures

Schemes

Tables

LIST OF SYMBOLS AND ABBREVIATIONS

$5HT_2$	serotonin receptor subtype 2
ATP	adenosine triphosphate
BBB	blood-brain barrier
COSY	correlation spectroscopy
DADS	bisamidedithiol
DADT	diaminedithiol
DHT	5α-dihydrotestosterone
dmpe	1,2-bis(dimethylphosphino)ethane
DMSA	dimercaptosuccinic acid
DTPA	diethylenetriaminepantaacetic acid
EC	ethylenedicysteine
ECD	ethyl cysteinate dimer
EDTMP	ethylenediaminetetramethylene phosphonic acid
EMT6	tumour type
ERPF	effective renal plasma flow
FSA	formamidine sulphinic acid
GAM	N-mercaptoacetylglycine
GFR	glomerular filtration rate
HAG_3	hydroxyacetylglycylglycylglycine
HEDP	hydroxyethylidene diphosphonate
HIDA	hepatobiliary iminodiacetic acid

HMDP	hydroxymethylene diphosphonate
HMPAO	hexamethylpropyleneamineoxime; 3,6,6,9-tetramethyl-4,8-diazaundecane-2,10-dione dioxime
HPLC	high pressure liquid chromatography
MAG_3	mercaptoacetylglycylglycylglycine
MDP	methylene diphosphonate
MIBI	(2-methoxy-2-methylpropyl)isonitrile
NBA	nitrobenzil alcohol
NMR	nuclear magnetic resonance
NOE	Nuclear Overhauser Effect
NOESY	Nuclear Overhauser Effect spectroscopy
OIH	*ortho*-iodohippurate
PAH	*p*-aminohippurate
PAHIDA	para-[(biscarboxymethylaminomethyl)carbamino]-hippuric acid
Q12	^{99m}Tc(III)-furifosmin; trans-(1,2-bis(dihydro-2,2,5,5-tetra-methyl-3 (2H) furanone-4-methylene-imino)ethane) bis(tris-(3-methoxy-1-propyl)phosphine)technetium(III)-99m
rCBF	regional cerebral blood flow
SPECT	single photon emission computed tomography
TLC	thin layer chromatography
UV	ultra-violet
$EtOH_{aq.}$	aqueous ethanol

pH	value of the medium acidity, logarithm of the protons concentration in the solution
pK_a	ionisation constant (logarithm)
λ	wavelength, nm
ε	molar extinction coefficient
$\lg \varepsilon$	decimal logarithm of the molar extinction coefficient
χ_A	atomic magnetic susceptibility

ABSTRACT

Technetium-99m (^{99m}Tc) is the most useful radioisotope in medical imaging due to its favourable nuclear characteristics, wide availability and low cost. Since ^{99m}Tc is a metal, it must be chelated using appropriate ligands to impart affinity for target tissues.

A series of new 2-pyrrolylthiones were synthesised as potential ligands for transition metals, particularly ^{99m}Tc, and were fully characterised. Both lipophilic and water-soluble compounds were obtained. Chemical reactions of the 2-pyrrolylthiones were studied. It was found that physical and chemical properties of these ligands are highly dependent on the substituents in the outer periphery of the molecule.

Transition metals such as *Ni*, *Cu*, *Co*, *Cd*, and *Zn* react smoothly with synthesised 2-pyrrolylthiones. A general complexation procedure was developed for technetium and rhenium. ^{99}Tc and non-radioactive *Re* complexes were used to establish the chemical structure of the new ^{99m}Tc compounds and to study their properties.

Labelling of the 2-pyrrolylthiones with ^{99m}Tc was performed. The biodistribution and pharmacokinetics of the selected complexes were studied. The biodistribution pattern of the new ^{99m}Tc-complexes greatly depends on their lipophilicity. Chemical changes in the ligand periphery, from highly lipophilic through amphiphilic to water-soluble, allow for fine turning of the biological properties of the corresponding technetium complexes.

Novel 2-pyrrolylthiones would provide a new class of radiopharmaceuticals

for medical imaging, where the periphery of the radiopharmaceutical can be modified according to desirable properties, while the central technetium core remains the same.

RESUME

Technetium-99m (^{99m}Tc) est le radio-isotope le plus utile dans l'imagerie médicale en raison de ses caractéristiques nucléaires favorables, disponibilité et coût. Posséder les propriétés métalliques, ^{99m}Tc doit être chélatée en utilisant les ligands appropriés pour donner l'affinité pour des tissus de cible.

Une série de nouveau 2-pyrrolylthiones a été synthétisée en tant que ligands potentiels pour les métaux de transition, en particulier ^{99m}Tc, et a été entièrement caractérisée. Des composés liphophiles et hydrophiles ont été obtenus. Des réactions chimiques du 2-pyrrolylthiones ont été étudiées. On l'a constaté que les propriétés physiques et chimiques de ces ligands dépendent fortement des substituants dans la périphérie externe de la molécule.

Les métaux de transition tels que les *Ni*, *Cu*, *Co*, *Cd*, et *Zn* réagissent sans à-coup avec 2-pyrrolylthiones synthétisé. Un procédé général de complexation a été développé pour le technetium et le rhénium. Complexes de ^{99}Tc et de rhénium non radioactifs ont été employés pour établir la structure chimique des nouveaux composés de ^{99m}Tc et pour étudier leurs propriétés.

Marquage du 2-pyrrolylthiones avec ^{99m}Tc a été exécuté. Le biodistribution et la pharmacocinétique des complexes choisis sont ont été étudiés. La configuration de biodistribution du nouveau ^{99m}Tc-complexes dépend considérablement de leur lipophilicity. Les changements chimiques dans la périphérie de ligand tiennent compte de la rotation fine des propriétés biologiques des complexes correspondants de technetium.

La serie de 2-pyrrolylthiones fournirait une nouvelle classe des produits radiopharmaceutiques pour l'imagerie médicale, où la périphérie du produit radiopharmaceutique peut être modifiée selon les propriétés souhaitables, alors que le noyau central de technetium demeure le même.

INTRODUCTION

The role of nuclear medicine in health care has expanded rapidly over the past few decades. The design and development of new radiopharmaceuticals plays here a great role. The search for more specific, more stable, more convenient radiopharmaceuticals continues and attracts the attention of a wide range of scientists and medical specialists.

^{99m}Tc-radiopharmaceuticals are the most useful imaging agents in clinic. This is due to extremely favourable nuclear characteristics of ^{99m}Tc-radioisotope, its wide availability and low cost.

The element technetium is not found in nature. Thus, it is absent in molecules of a living organism. There is a basic difference between the chemistry of ^{99m}Tc-compounds and other radionuclides[1] used in medical imaging, such as ^{11}C, ^{13}N, and ^{15}O that are radioactive analogues of naturally occurring atoms, or radiohalogens, which can covalently bind to organic molecules. Due to its metallic properties, ^{99m}Tc must be chelated using appropriate ligands – chelating agents – to impart affinity for target tissues. A chelating agent is an organic molecule, which binds strongly to metal ions using one or more covalent, or coordination links. The resulting complex can be designed as "metal essential" or "metal tagged".

"Technetium essential", or the first generation agents are small molecules where *Tc* is an essential part of the structure. The biodistribution and targeting ability

[1] A *radionuclide* is a nucleus with a set of characteristic properties, such as the specific nucleon composition, the mode of radioactive decay and type of emissions, the transition energy, and the average lifetime of a nucleus of the radionuclide before it undergoes radioactive decay.

of these radiopharmaceuticals depend on their size, charge, and lipophilicity and are determined by blood flow or perfusion. Most ^{99m}Tc-based imaging agents that are approved for clinical use are considered first generation radiopharmaceuticals.

"Technetium tagged" – second generation agents – have a more sophisticated structure and chemistry. These are biologically active molecules, typically a small peptide, which act as an agonist or antagonist for a specific receptor site, or a monoclonal antibody, which are labelled with ^{99m}Tc directly or through a chelating group. The targeting ability of such radiopharmaceuticals depends on the biologically active moiety of the complex, which carries ^{99m}Tc to the target organ. Tissue uptake and retention depend on a specific biochemical process or binding to a specific receptor.

^{99m}Tc can be attached to a carrier molecule using a bifunctional chelating agent (the conjugate or bifunctional chelate approach). Sometimes the mass of the tagged chelating system comprising *Tc* is large enough to double the size and mass of the original bioactive molecule. These changes can have serious consequences for the properties of resulting complexes in terms of biodistribution and targeting ability of the radiopharmaceutical. The site of attachment to the small bioactive molecule, the size, charge and lipophilicity of the conjugate and the length of the covalent linker all need to be optimised for maximum receptor binding. It is a challenge to attach a technetium moiety to a bioactive molecule and preserve the biochemical properties of the original small molecule. The bifunctional chelate approach has found wide application in labelling of antibodies and their fragments (Arano, 1999; Dilworth and Parrott, 1998).

Another route in the design of *Tc*-radiopharmaceuticals is the integrated approach, where the metal ion is incorporated in the structure of the carrier molecule. This involves the design of a biologically active molecule, where ^{99m}Tc is an essential part of the molecular structure, such that the *Tc*-complex mimics the parent molecule. To date none of such synthesised mimics display satisfactory biological properties and lack stability under *in vitro* binding condition. The conjugate and integrated synthetic approaches are both currently at their early stages of development.

The aim of this work was to find an improved ^{99m}Tc radiopharmaceutical, through the synthesis and evaluation a series of new chelating agents. In particular we sought to find a chelator, which would allow for easy substitution around its core to give exceptional dynamics and versatility to the resulting complex. 2-Pyrrolylthiones were selected to study their potential as chelating agents for technetium and rhenium. All synthesised 2-pyrrolylthiones were able to react with a range of metal ions forming stable complexes.

We found that two of the newly synthesised water-soluble radiopharmaceuticals were taken up by the kidneys. The pharmacokinetics of these compounds is comparable and, in certain aspects, superior to that of the existing kidney imaging agent ^{99m}Tc-DMSA. Biodistribution studies in the rat suggest that these novel complexes may be a useful alternative to ^{99m}Tc-DMSA as a kidney scanning agent.

This work is an invention of a new technetium core with an easily varied periphery, which allows for the synthesis of novel derivatives with potential properties for medical imaging (Kudrevich *et al.*).

Since the new 2-pyrrolylthiones were found to be good chelating agents, they might well find applications in different biological, medical, and other fields where chelators play an important role.

CHAPTER 1: Biomedical chemistry of technetium-99m

1.1. ***Chemical element technetium***

1.1.1. Brief history of the discovery

The element *technetium* (*Tc*) has the atomic number 43, an atomic weight of 98, and the electron configuration $[Kr]5s^2 4d^5$. Mendelejeff predicted it on the basis of the periodic table as eka-manganese (Mendelejeff, 1872). Perrier and Segré discovered the element 43 in 1937 (Perrier and Segré, 1937). It was obtained by irradiating molybdenum with deuterons in the Berkeley cyclotron. The element 43 was the first element to be produced artificially from where comes its name – technetos, which means "artificial" in Greek. Perrier and Segré discovered technetium-95 and technetium-97m with half-lives of 60 and 90 days respectively. The long-lived isotope technetium-99 (^{99}Tc), on which most of the chemistry of the element is based, was studied at trace level in 1939 (Seaborg and Segré, 1939) and was synthesised in weighable quantities in 1946 (Motta *et al.*, 1947).

Since the discovery of technetium, searches for the element in terrestrial material have been made. Finally in 1962, ^{99}Tc was isolated and identified in African pitchblende (a uranium rich ore) in extremely minute quantities as a spontaneous fission product of uranium-238 (Kenna and Kuroda, 1962). It is currently believed that the existence of stable technetium isotopes seems very unlikely.

1.1.2. Tc-Isotopes

Currently, more than thirty isotopes of technetium have been reported (^{85}Tc-^{115}Tc). All *Tc* isotopes are radioactive. Three of them are long-lived isotopes: ^{97}Tc ($t_{1/2} = 2.6 \times 10^6$ years), ^{98}Tc ($t_{1/2} = 4.2 \times 10^6$ years), and ^{99}Tc ($t_{1/2} = 2.1 \times 10^5$ years). The most useful isotope of technetium is technetium-99m (^{99m}Tc, "m" stands for *metastable*[2] state, the prefix "*meta*" derives from the Greek word "almost") (Saha, 1998). It is used mainly in nuclear medicine because of its short half-life of 6.01 hours and the convenient energy of the gamma ray emission of 141 *keV*.

1.1.3. Physical, chemical and nuclear characteristics

Metal technetium is a bright, silvery grey metal. It crystallises in hexagonal close-packed arrangement with metallic radii of 1.358Å for a twelve coordination (Mooney, 1947) and is weakly paramagnetic ($\chi_A = 270\times10^{-6}$ c.g.s. units at 298°K) (Nelson *et al.*, 1954).

Technetium exhibits valencies from seven to zero. The common oxidation states of technetium are +7, +5, and +4. Under oxidising conditions technetium (VII) is stable as the pertechnetate ion, TcO_4^-. Chemically, technetium powder is readily oxidised, which is not the case for massive metal. Technetium does not dissolve in hydrochloric acid of any concentration, but will dissolve in dilute or concentrated

[2] Metastable (or isomeric) state is an arrangment of nucleons within a nucleus, which is unstable but has relatively long lifetime before transforming to another state.

nitric and concentrated sulphuric acids. It easily reacts with fluorine, less with chlorine and combines with sulphur at elevated temperatures (Peacock, 1966). The chemistry of technetium is believed to be similar to that of rhenium. This point of view is very controversial however, because technetium and rhenium compounds often behave substantially differently, exhibiting different lipophilicities, redox-potentials and stability.

Almost all of the chemistry of technetium is based on the ^{99}Tc isotope, which is a weak β-emitter ($\beta_{max} = 0.3\ MeV$). The handling of ^{99}Tc on a small scale (< 0.05 g) does not present a serious health hazard, provided elementary precautions are taken. The radiation is effectively stopped by ordinary laboratory glassware, and there is no associated γ-radiation. Even for larger quantities (< 0.25 g) the health hazard is small, provided the operator maintains a distance of at least 30 cm from the working area to avoid the small amount of soft X-rays produced by the action of the β-emission on glass. Therefore, the essential requirements for safe handling of ^{99}Tc are a well-ventilated box, monitoring of working area and avoidance of manipulations, where compound could escape to atmosphere (Peacock, 1966). Nevertheless, the handling of technetium must be performed in a special laboratory approved for the radioisotope use.

As was noticed previously, the most useful radioisotope of technetium is ^{99m}Tc. The methods of synthesis, separation and analysis are different for ^{99m}Tc, compare to ^{99}Tc because of the trace amounts of ^{99m}Tc used. The quantity of a ligand taken for complexation is usually exceeds the quantity needed to chelate all ^{99m}Tc ions available for reaction. An excess of the ligand should be separated at time of

purification. Separation and purification is often done using HPLC with UV and radioactivity detectors. Different spectroscopic and chromatographic methods and electrophoresis are used to identify and analyse ^{99m}Tc compounds. ^{99m}Tc emits γ-rays of 140 *keV* with 89% abundance, which can be detected using scintillation cameras also know as gamma cameras. Images of its distribution pattern can be obtained by recording the emitting radiation. The energy of ^{99m}Tc is close to optimum for medical imaging with gamma cameras (contemporary detectors can absorb γ-rays of 30-300 *keV*, and 140 *keV* of ^{99m}Tc is just in the middle of the range). The radioisotope's half-life of 6 hours is long enough to complete synthesis and purification, inject radiopharmaceutical into a patient and perform imaging. On the other hand, it is short enough to minimise the radiation dose to the patient. Work with ^{99m}Tc must be done in an approved laboratory, in a well-ventilated hood behind a lead barrier shield, and gloves should be worn for handling radioactivity.

1.1.4. $^{99}Mo/^{99m}Tc$ generator

Until 1960, ^{99m}Tc was available only in small amounts and its price was quite high. After the discovery of the $^{99}Mo/^{99m}Tc$ generator it became routinely available and economical. The possibility to have a $^{99}Mo/^{99m}Tc$ generator at virtually any hospital makes ^{99m}Tc the most popular isotope in diagnostic nuclear medicine. The generator is based on transient equilibrium between parent and daughter radionuclides, ^{99}Mo and ^{99m}Tc respectively. $^{99}MoO_4^{2-}$ is absorbed on an alumina column inside a lead shield. There is a vial, which provides a saline solution to elute

pertechnetate $^{99m}TcO_4^-$, and another one to collect the eluted solution. The column is connected to the vials with stainless steal tubing, shielded by lead. This construction is then shielded by another lead jacket to prevent escape of radiation. The generator can be eluted daily and is replaced once a week.

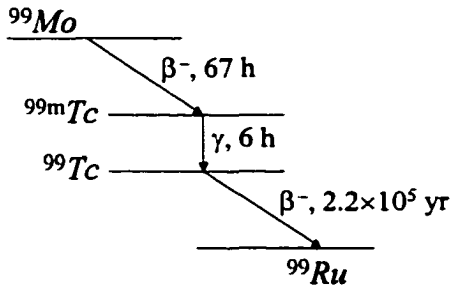

Figure 1. Decay scheme for molybdenum-99.

1.2. ***Technetium based radiopharmaceuticals of the first generation***

1.2.1. First ^{99m}Tc radiopharmaceutical

Accumulation of pertechnetate in the thyroid of animals was demonstrated in 1953 (Baumann *et al.*, 1953). The first report on the use of technetium for medical imaging appeared in 1963 and involved the use of $^{99m}TcO_4^-$ for the visualisation of the liver by scintillation scanning, following administration and hepatic localisation of the parent molybdenum-99 radionuclide (Sorensen and Archambault, 1963; Sorensen and Archambault, 1964). Later ^{99m}Tc pertechnetate was evaluated for brain scanning (McAfee *et al.*, 1964). In 1964 ^{99m}Tc pertechnetate was used for the diagnosis of thyroid disease (Harper, 1964; Andros *et al.*, 1965), based on the principle that the pertechnetate anion behaves similarly to iodide, which is known to be taken up by the thyroid. The biodistribution and targeting ability of this

radiopharmaceutical depends solely on the size and charge of the complex. This was the first of a series of so-called "technetium essential", or the first generation agents.

1.2.2. Brain imaging radiopharmaceuticals

The ideal radiopharmaceutical for brain imaging should be capable of traversing an intact blood-brain barrier[3] (BBB), accumulate in the brain and stay there long enough to perform the imaging. Therefore, useful complexes must be moderately lipophilic and have an overall neutral charge.

Research at the University of Missouri in the 1980s and further development at Amersham International led to the commercially successful agent Ceretec™ based on the hexamethylpropyleneamineoxime proligand (HMPAO hexametazime; 3,6,6,9-tetramethyl-4,8-diazaundecane-2,10-dione dioxime) (Holmes *et al.*, 1985; Leonard *et al.*, 1986; Neirinckx *et al.*, 1987). The proligand loses three protons to form a neutral, square pyramidal technetium(V) mono-oxo complex. (***Figure 2***) (Jurisson *et al.*,

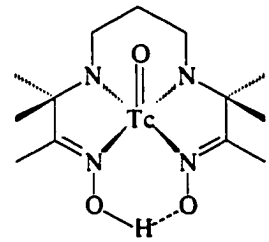

^{99m}Tc-PnAO

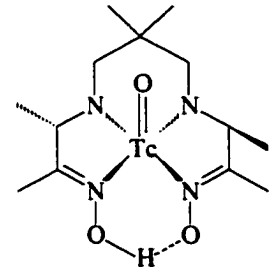

^{99m}Tc-HMPAO

Figure 2. Schematic structures of the technetium complexes with propyleneamineoxime derivatives.

[3] The *blood-brain barrier* (BBB) is a functional mixture of anatomic, physiologic, and metabolic phenomena, which excludes alien substances from entering the brain from the blood, while vitally important substances are easily cross it.

1986; Nikitin and Kulakov, 1997) This complex is approved as a cerebral perfusion imaging agent for evaluation of stroke damage. A previously synthesised (Troutner *et al.*, 1984) technetium complex with propyleneamineoxime (3,3,9,9-tetramethyl-4,8-diazaundecane-2,10-dione dioxime) – ^{99m}*Tc*-PnAO – was shown to be taken up by the rat brain (Volkert *et al.* 1984) but unfortunately it also diffuses rapidly back out of the brain with a half-life too short to allow for imaging (Holm *et al.*, 1985). The final HMPAO derivative was selected from more than one hundred structural variants for its optimal biodistribution characteristics.

The technetium complexes of a wide range of bisamidedithiol (DADS) proligands have been investigated as potential agents for brain imaging. The technetium ethyl cysteinate dimer (^{99m}*Tc*-ECD) complex is commercially available from Dupont as Neurolite™. This compound is one of the recent additions to available radiopharmaceuticals for measuring cerebral blood flow. ^{99m}*Tc*-*L*,*L*-ECD is a neutral, lipophilic *Tc*(V) complex with mono-oxo core and *L*,*L*-ethylcysteine dimer bound to the metal *via* two amine nitrogen and two thiolate sulphur atoms. (***Figure 3***) The complex has two isomers. One of them, *L*,*L*-enantiomer of ECD, is trapped once across the BBB due to the enzymatic hydrolysis of one ester group by an esterase enzyme to give the free acid group, generating a more hydrophilic charged complex. In contrast, the *D*,*D*-enantiomer is inert to the enzymatic hydrolysis and diffuses back across the BBB. Such an enzymatic conversion reaction also occurs in the blood during biodistribution, and although is

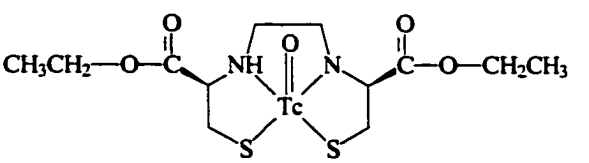

Figure 3. ^{99m}*Tc*-*L*,*L*-ECD

impairs brain uptake, it facilitates clearance from the blood and non-target tissue via the kidneys.

These agents actually provide images of regional cerebral blood flow (rCBF). The regional distribution of the two tracers differs. ^{99m}Tc-HMPAO accumulates more in the thalamus, frontal lobe, temporal lobe and cerebellum than ^{99m}Tc-ECD, which accumulates primarily in the occipital and parietal lobes. There is a considerable difference in the accumulations of the two tracers in the medial temporal lobe (93.9% and 83.1% respectively compared with the mean global cerebral cortical accumulation). The results suggest that ^{99m}Tc-HMPAO and ^{99m}Tc-ECD require specific and separate criteria for diagnosing temporal lobe pathologies.

Interestingly, it was found that brain uptake in rats is not determined by lipophilicity only. Uptake is strongly influenced by substituents on the ligand periphery (Oya *et al.*, 1998). This fact should be taken in consideration when designing novel labelled agents.

1.2.3. Heart imaging radiopharmaceuticals

The design of heart imaging radiopharmaceuticals initially was based on the idea that lipophilic complexes with a mono-positive charge should accumulate in heart tissue *via* the Na^+/K^+ ATPase mechanism as K^+ ion mimics. This concept prompted the synthesis of the cationic ^{99m}Tc complex, $[^{99m}Tc(dmpe)_2Cl_2]^+$, where *dmpe* is 1,2-bis(dimethylphosphino)ethane as a potential myocardial perfusion agent.

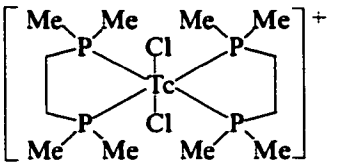

Figure 4. Technetium complex with 1,2-bis(dimethylphosphino)ethane

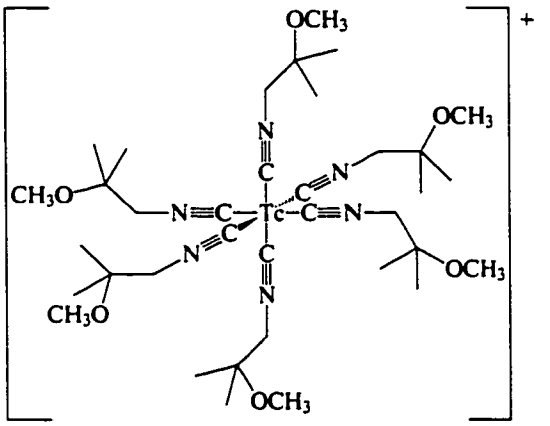

Figure 5.
^{99m}Tc[(2-methoxy-2-methylpropyl)isonitrile]$_6^+$

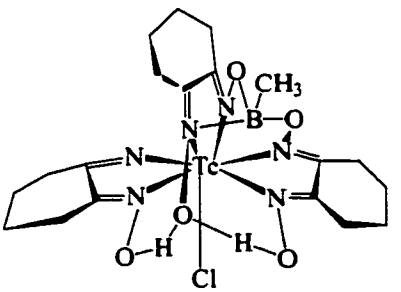

Figure 6. Mixed *Tc* complex with cyclohexane-1,2-dione dioxime and methyl boronic acid

(***Figure 4***) It was later found that this complex undergoes *in vivo* reduction to the neutral *Tc*(II) complex [$^{99m}Tc(dmpe)_2Cl_2$]. Loss of the positive charge results in fast washout from the heart and accumulation in the liver.

Further development of cationic complexes as myocardial perfusion agents led to the approved agent [^{99m}Tc(MIBI)$_6$]$^+$ (known also as ^{99m}Tc-sestamibi) (Cardiolite™, Dupont), where MIBI is (2-methoxy-2-methylpropyl)isonitrile (***Figure 5***) (Piwnica-Worms *et al.*, 1988). The uptake in the human heart reaches about 1.5% of the injected dose, slowly decreasing to 1% after 4 *h*. A good organ to background ratio is achieved due

to low uptake in the blood, lungs, liver, spleen. Animal studies suggest that the methoxy-group of ^{99m}Tc-sestamibi is metabolised in the liver leading to more rapid clearance (Kronauge *et al.*, 1990).

The first approved neutral myocardial perfusion agent is ^{99m}Tc-teboroxime (Cardiotec™, Bristol-Myers Squibb). The complex is prepared by template synthesis where $^{99m}TcO_4^-$ reacts with a mixture of cyclohexane-1,2-dione dioxime and methyl boronic acid with $SnCl_2$ as a reducing agent. Five minutes after injection 2.2% of the administered dose of the *Tc*(III) complex is found in the heart. The mechanism of accumulation is still unknown at this time. The complex exhibits rapid myocardial clearance in normal myocardium.

One of the recent cationic imaging agents is ^{99m}Tc-P53 (where P53 is ethylene-bis-[bis-(2-ethoxyethyl)-phosphine), also known as Tetrofosmine™ or Myoview™ (***Figure*** *7*). In contrast to $[^{99m}Tc(dmpe)_2Cl_2]^+$, Myoview™ contains the dioxo *Tc*(V) core, which does not undergo *in vivo* reduction. The complex contains eight alkoxy groups on the bidentate phosphine ligands that help to reduce the background activity in the blood and liver. Heart uptake of the complex is 1.2% of the injected dose, with slow clearance to 1% at 2 hours post-injection.

A report on the comparison of kit performances of Cardiolite™, Tetrofosmine™, and Technescan™ Q12 has been published (Cagnolini *et al.*, 1998).

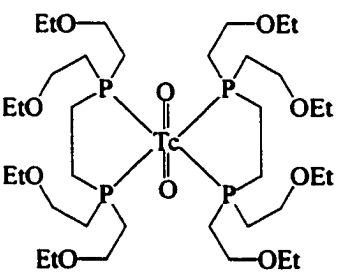

Figure *7.* Tetrofosmine

The uptake and retention mechanism of the mono-cationic ^{99m}Tc complexes in the

myocardium remains unknown. However, it has been shown that accumulation does not involve the Na^+/K^+-ATPase pump. A more likely mechanism of uptake suggests that cations such as $[^{99m}Tc(MIBI)_6]^+$ and ^{99m}Tc-diphosphine complexes accumulate *via* a diffusion mechanism and electrostatic binding due to a high mitochondrial membrane potential (Sands *et al.*, 1985; Piwnica-Worms *et al.*, 1988).

1.2.4. Imaging agents for the hepatobiliary system

The first iminodiacetic acid derivative employed in nuclear medicine was 2,6-dimethylphenylcarbamoylmethyl iminodiacetic acid (lidofenin) (Loberg *et al.*, 1976). Currently, a few analogues of technetium complexes with hepatobiliary iminodiacetic acid (HIDA) are used for imaging of hepatobiliary system (liver, bladder, and intestines). They include ^{99m}Tc-lidofenin (TechneScan™ HIDA, Mallinckrodt), ^{99m}Tc-disofenin (Hepatolite™, Dupont), and ^{99m}Tc-mebrofenin (Choletec™, Bristol-Myers Squibb) (***Figure 8***). All three agents show quite similar behaviour. It was found that the metal to ligand ratio in *Tc*-HIDA is 1:2, that the complex does not contain tin, and that the overall complex charge is –1 (Loberg and Fields, 1978).

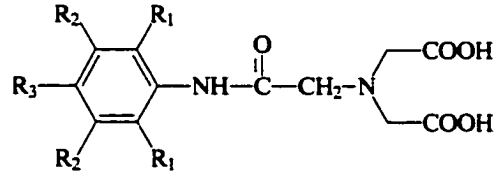

Figure 8. HIDA ligands

Lidofenin: R_1=*CH_3*, R_2=R_3=*H*
Disofenin: R_1=isopropyl, R_2=R_3=*H*
Mebrofenin: R_1=R_3=*CH_3*, R_2=*H* and *Br*

1.2.5. Bone imaging radiopharmaceuticals

^{99m}Tc complexes containing a wide range of diphosphonates, analogues of pyrophosphates, present technetium radiopharmaceuticals for bone imaging. Methylene diphosphonate (MDP), hydroxymethylene diphosphonate (HMDP), hydroxyethylidene diphosphonate (HEDP), and ethylenediaminetetramethylene phosphonic acid (EDTMP) are only a few examples of this class of compounds (***Figure 9***).

Technetium methylene diphosphonate (^{99m}Tc-MDP) is most frequently used in clinic. It is an organic analogue of pyrophosphate and contains an organic P-C-P bond. The agent affixes to the bone surface as a result of a chemisorption process. It was found that after administration ^{99m}Tc-MDP dissociates into its technetium and methylene diphosphonate moieties, which are then adsorbed onto the organic (newly-formed osteoid) and inorganic (forming mineral) phases, respectively (Schwartz *et al.*, 1993). About 40-50% of the compound will be affixed to bone within 3 to 4 hours after injection. Excretion is primarily renal and 70% of the administered dose is eliminated within 6 hours after injection.

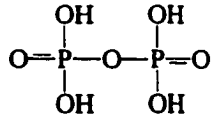

Pyrophosphate

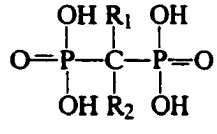

Diphosphonate

Figure 9. Diphosphonates family

MDP: R_1=*H*, R_2=*H*
HEDP: R_1=*OH*, R_2=CH_3
HMDP: R_1=*H*, R_2=*OH*

A ^{99m}Tc- complex with a new ligand from the phosphonate family was reported recently (Demurphy *et al.*, 1996). Technetium forms a

stable and strong complex with 4-amino-1-hydroxybutylidene-1,1-diphosphonate, probably due to the amino group present in the ligand structure. Biological data have not yet been published on this compound.

1.2.6. Radioactive drugs for kidney imaging

Renography using radiotracers allows for the determination of both total and differential renal function and the detection of obstructions in urine flow. Kidney imaging agents can be divided in two groups: radiopharmaceuticals for functional imaging or tubular imaging agents, and radiopharmaceuticals for morphological imaging or glomerular (cortical) imaging agents.

Among the oldest and most widely employed techniques for renal function evaluation are the renal clearance methods directed toward determination of glomerular filtration rate (GFR). The clearance of compounds that undergo extensive tubular excretion in addition to filtration allow the evaluation of functional tubular mass and the estimation of effective renal plasma flow (ERPF).

The standard for ERPF determination is *p*-aminohippurate (PAH): approximately 90% of this compound are extracted from the renal arterial plasma in a single pass through the renal parenchyma. An ^{131}I labelled structural analogue, *ortho*-iodohippurate ([^{131}I]OIH; Hippuran) (***Figure 10***), has been the clinical standard for the past

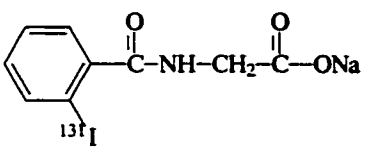

Figure 10. ^{131}I-iodohippurate

40 years (Tubis *et al.*, 1960). Although OIH yields a good approximation of renal plasma flow, the 364 *keV* photon energy of ^{131}I results in poor spatial resolution and the beta emission increases the radiation dose to the patient. Labelling OIH with ^{123}I results in a better imaging agent, but the unavailability and high cost of ^{123}I limits the use of this compound (Thakur *et al.*, 1975).

[^{99m}Tc]-DTPA (where DTPA is diethylenetriaminepentaacetic acid (***Figure 11***)) (Eckelman and Richards, 1970) has received regulatory approval for use as a kidney imaging agent. The structure of this complex has not yet been determined unequivocally, and it is unclear as to whether the complex contains technetium in the IV or V oxidation state. This radiopharmaceutical has very limited clinical applications.

Early attempts to create a ^{99m}Tc-based renal imaging agent focused on the diamine dithiolate (DADT) ligands. ^{99m}Tc-N,N'-bis(mercaptoacetyl)-2,3-diaminopropanoate has a favourable renal clearance profile, but this compound consists of stereoisomers with different rates and specificity for renal clearance (Fritzberg *et al.*, 1982). Therefore, HPLC separation of the desired stereoisomer is required, which makes routine preparation less convenient.

The *para*-aminohippuric acid (PAH) was found almost completely extracted

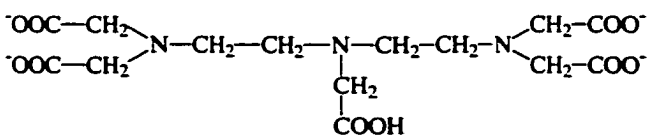

Figure 11. Diethylenetriaminepentaacetic acid

from blood flow by the kidneys. Incorporation of an iminodiacetic acid (IDA) moiety into PAH yielded *p*-[(biscarboxymethylaminomethyl)carbamino]-hippuric acid (PAHIDA) with a clearance of less than 50% of OIH (Chervu *et al.*, 1984).

Later, the triamide mercaptide (N_3S) class of ^{99m}Tc chelating agents was developed (Fritzberg *et al.*, 1986). To date, the ^{99m}Tc-mercaptoacetylglycylglycylglycine (^{99m}Tc-MAG_3) is considered to be one of the most successful agents for functional renal imaging. The structure of ^{99m}Tc-MAG_3 is shown in ***Figure 12***. It has a core of $Tc{=}ON_3S$ with a carboxylic group on the third nitrogen. ^{99m}Tc has a coordination number of 5 and the complex has an overall negative charge of -1. The structure of this radiopharmaceutical was established through direct synthesis and characterisation of the analogous ^{99}Tc complex (Grummon *et al.*, 1995; Nikitin and Kulakov, 1997).

A few minutes post injection, approximately 1-2% of the injected dose of ^{99m}Tc-MAG_3 is found in the kidneys. At the same time, this drug is cleared from the kidney tissue very rapidly. It is the passage into and through the kidneys that provides a measure of renal function (ERPF). Although considered to be the renal imaging agent of choice, ^{99m}Tc-MAG_3 is not free of certain problems associated with its use. For instance, the plasma-protein binding of ^{99m}Tc-MAG_3 is very high (Taylor *et al.*, 1987; Bubeck *et al.*, 1990); the clearance of ^{99m}Tc-MAG_3 is only 50-60% of that of OIH and therefore is not suitable for direct

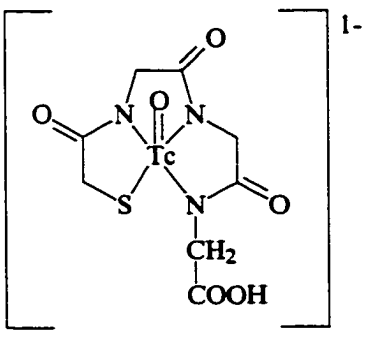

Figure 12. Structure of the ^{99m}Tc-MAG_3 complex

measurement of ERPF. In addition, the preparation of ^{99m}Tc-MAG_3 requires the kit to be heated at 100°C for 10 min, thus adding an inconvenient step in the preparation.

It was found that the polar metabolite of the brain radiopharmaceutical, diethyl Tc-99m-ethylenedicysteine (^{99m}Tc-*L,L*-EC), was rapidly and efficiently excreted by the kidneys in mice (Verbruggen *et al.*, 1990). This observation prompted the evaluation of ^{99m}Tc-*L,L*-EC as a potential renal imaging agent. Studies in mice and baboons showed that the pharmacokinetic properties of ^{99m}Tc-*L,L*-EC are superior to those of ^{99m}Tc-MAG_3. ^{99m}Tc-*L,L*-EC yields a better approximation of ERPF. A number of clinical studies have been conducted to date on patients with a variety of renal disorders comparing ^{99m}Tc-*L,L*-EC and ^{99m}Tc-MAG_3 (Kabasakal *et al.*, 1995; Gupta *et al.* 1995; Kibar *et al.*, 1997). There was no significant difference in the image quality or in the parameters derived from the renogram between the two tracers. The structure of ^{99m}Tc-*L,L*-EC was established through direct synthesis and crystallographic studies (Pirmettis *et al.*, 1994).

MAG_3 is synthesised and supplied in commercial kits as an *S*-benzyl protected derivative. This is necessary due to the low chemical stability of the thiol group toward oxidation. The kit must be kept in the dark after reconstitution to prevent oxidation of the thiol (Mallinckrodt Medical Inc., 1992). To circumvent this problem, an attempt was made to substitute an hydroxyl group in MAG_3 for the thiol (Vanbilloen *et al.*, 1997). The resulting ^{99m}Tc-labeled hydroxyacetyltriglycine (HAG_3) had a slightly higher urinary excretion and faster renal transit than ^{99m}Tc-MAG_3. The faster renal clearance of ^{99m}Tc-HAG_3 can be attributed to its lower plasma protein binding. Although the renal excretion characteristics of ^{99m}Tc-HAG_3

are slightly better than those of ^{99m}Tc-MAG_3 and the labelling is done at room temperature, the chemical stability of ^{99m}Tc-HAG_3 to transchelation is less than that of ^{99m}Tc-MAG_3.

Certain ^{99m}Tc labelled molecules have a high extraction rate from the blood stream by the kidneys combined with a high retention rate in the kidneys. Usually they have a high affinity to the cortex area. These radiopharmaceuticals can be used for morphological imaging.

^{99m}TcO(glucoheptonate)$_2$ (Glucoscan™, Dupont; TechneScan Gluceptate™, Mallinckrodt) is one of the radiopharmaceuticals of this kind. This is an early kidney imaging agent, the precise structure of which has never been determined. Nevertheless, the chemical structure shown on ***Figure 13*** was proposed based on different analytical methods (de Kieviet, 1981). Up to 15 % of injected dose is retained in kidneys, with greater retention in the cortex than in the medulla, giving information on kidney morphology. This complex is no longer widely used as an imaging agent since ultrasound and magnetic resonance imaging have proven more useful for morphologic studies and do not require the use of radiopharmaceuticals. Nevertheless, it is regularly used as a precursor for the synthesis of other *Tc*(V)

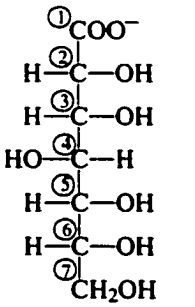

Glucoheptonate

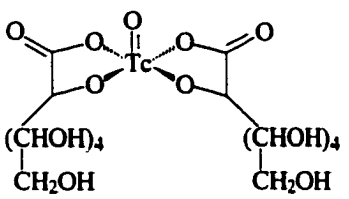

Figure 13. Proposed structure for *TcO*(glucoheptonate)$_2^-$

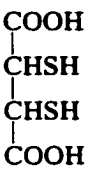

Figure 14. DMSA structure

compounds *via* ligand exchange.

Technetium-99m-dimercaptosuccinic acid (^{99m}Tc-DMSA; Technetium-99m Succimer Injection™) is marketed for morphological studies of the kidneys. However, it is possible also to assess an individual kidney function. Such examinations constitute a useful approach in the diagnosis, location and evaluation of various renal pathologies: inflammation, infection, lithiases, traumatisms, tumours, etc. The *Tc*(III) or *Tc*(V) complex (of unknown structure) is prepared from the reaction of $^{99m}TcO_4^-$ with DMSA in the presence of the reducing agent $SnCl_2$. ^{99m}Tc-DMSA has a specific affinity for the renal cortex. The renal activity increases until 6 to 8 hours after injection in healthy subjects, at which point a steady level of uptake is reached representing some 30% of the activity administered. ^{99m}Tc-DMSA is almost completely bound to proteins at the plasma level. The commercially available kit should be stored in the dark due to its sensitivity to light (MDS Nordion S.A., 1998).

A bidentate chelator N-mercaptoacetylglycine (GAM) was suggested as a ^{99m}Tc-ligand (Gianolli *et al.*, 1996). GAM contains both thiolato sulphur and amido nitrogen similar to MAG_3 and DADS, but it is a bidentate ligand similar to DMSA. The resulting 2:1 complex (^{99m}Tc-2GAM) can adopt either a *cis-* or *trans-* configuration relative to the oxo-technetium core. Biodistribution studies in animals and normal volunteers indicate that ^{99m}Tc-2GAM has biological properties, which are more similar to ^{99m}Tc-DMSA, rather than to ^{99m}Tc-MAG_3 or ^{99m}Tc-DADS. ^{99m}Tc-

2GAM activity in the kidney reaches a plateau more rapidly than ^{99m}Tc-DMSA and thus may be a possible replacement for ^{99m}Tc-DMSA.

A series of biguanide ligands were stadied recently as potential chelators for ^{99m}Tc (Neves *et al.*, 1999). The authors suggest that ^{99m}Tc-complex with unsubstituted biguanide might be a favourable alternative to ^{99m}Tc-DMSA, because of its better clearance and lower absorbed radiation dose.

All the mentioned above imaging agents are organometallic anions. They are transported by organic anion receptors in the renal tubular system. A build-up of organic anions in plasma, which happens in patients suffering from uraemia, can competitively inhibit renal tubular transport of anionic tracers, thereby leading to artificially low estimates of renographic parameters in such patients.

Another tubular transport mechanism, the cationic transporter system, cannot be disrupted by anion accumulation. Tetraazapolyamine chelators, such as cyclam and tetramethylcyclam, were evaluated for their ability to form stable complexes with dioxotechnetium (Herzog *et al.*, 1992). The overall charge of each ^{99m}Tc complex was +1. The magnitude of the plasma protein binding for these organic cations was comparable to that for ^{99m}Tc-EC and significantly less than that for OIH and ^{99m}Tc-MAG_3. The renal clearance of tetraazapolyamines was similar to that of ^{99m}Tc-*L,L*-EC. The mode of excretion of these tracers by the tubule cationic transporter system was clearly identified.

A series of cationic ^{99m}Tc complexes with *N*-substituted pyridoxal derivatives were synthesised and evaluated as renal function agents (Karube *et al.*, 1994). The pyridoxal-derived ^{99m}Tc complexes are rapidly excreted in urine and provide clear

renal scintigrams in a rat model. However, total clearances are lower than that of ^{131}I-OIH or ^{99m}Tc-MAG_3.

1.3. ***Design of the technetium tagged radiopharmaceuticals***

Many researchers are currently devoting their efforts to the synthesis of conjugate complexes where small bioactive molecules are labelled with ^{99m}Tc using bifunctional chelating agent. Receptors, monoclonal antibodies, small peptides are under close attention in these studies (Jurisson and Lydon, 1999; Liu and Edwards, 1999).

1.3.1. Monoclonal antibodies or their fragments

Monoclonal antibodies or their fragments are potentially ideal vehicles to target radioisotopes to specific sites, providing the radiolabel can be introduced without interfering with binding to the receptor site. The relatively large size of whole antibodies generally confers undesirably slow biodistribution kinetics for imaging purposes, and attention is now directed to antibody fragments, which retain the specific binding characteristics (Eckelman, 1995; Arano, 1999). The use of fragments also reduces the possibility of immunogenecity and adverse allergic reactions.

1.3.2. Central nervous system receptors

There are a number of important diseases and psychiatric conditions that are associated with changes in the densities of neurotransmitter receptor sites in the brain. Specially designed radiopharmaceuticals can deliver radioisotopes to the receptor sites to perform the imaging. Cocaine and analogues are the most promising candidates as carrier molecules for ^{99m}Tc as they are antagonists to dopamine transporter receptor.

Recently a tetradentate analogue of tropane, Technepine™, was developed (***Figure 15***) (Madras *et al.*, 1996). Technepine™ demonstrates high affinity *in vitro* binding to the dopamine receptor, and was the first technetium-based agent to be used to image selectively the striatum of non-human primates (Meltzer *et al*, 1997).

Linking of the cocaine derivative *via* the seven-membered ring to a *Tc*(V) oxo-core involving an N_2S_2 ligand forms a conjugate ^{99m}Tc-TRODAT (***Figure 15***). ^{99m}Tc-

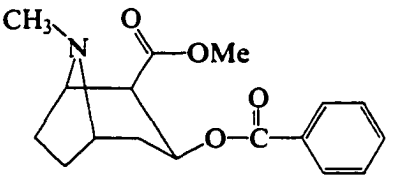

Cocaine

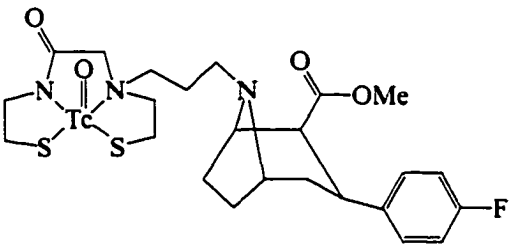

Technepine

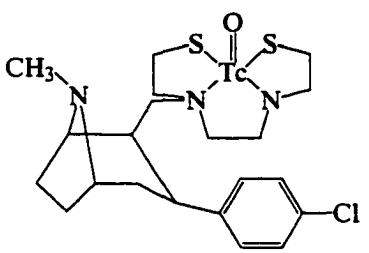

^{99m}Tc-TRODAT

Figure 15. Cocaine and its ^{99m}Tc conjugates

TRODAT exhibits selective uptake in rat striatum (Kung *et al.*, 1997) and provides good contrast for basal ganglia in single photon emission computed tomography (SPECT) images taken of human (Kung *et al.*, 1996). The ^{99m}Tc-TRODAT presents the first human-tested technetium-based SPECT agent that could be used clinically to image the dopamine transporter. Recently, there has been a report on a kit formulation for the synthesis of ^{99m}Tc-TRODAT (Choi *et al.*, 1999). This radiopharmaceutical is the first of second generation agents that can be synthesised using a kit.

This exciting advance confirms the viability of the conjugate approach to ^{99m}Tc imaging of central nervous system receptors.

Several other neuro-receptor selective molecules (primarily for dopamine transporter and seratonin $5HT_2$) have been studied in the last few years (Jurisson and Lydon, 1999).

1.3.3. Steroid receptors

Imaging of prostate and breast cancers can be done with appropriately labelled hormones: most prostate cancers are androgen and progesterone receptor positive, whereas breast cancers are estrogen and progesterone receptor positive. The structures of three relevant hormones are shown in ***Figure 16***.

^{99m}Tc labelling of progesterone has been studied utilising conjugation to N_2S_2 ligands *via* a phenyl spacer (Katzenellenbogen, 1995). A few complexes, where progesterone has been substituted at the 21-, 17α-, 16α,17α-, and 11β - positions

(*Figure 17*), have been reported (DiZio *et al.*, 1991). Only 11β - analogues display remarkably high binding affinity to progesterone receptor: the *syn* pair has an affinity of 161% relative to progesterone. Although the conjugates showed high binding, *in vivo* studies also revealed high level of non-specific binding. Nevertheless, the approach is promising although further fine-tuning of biodistribution characteristics is required.

The major problem of steroid-based technetium chelates is their strong non-specific binding properties under *in vivo* conditions, while *in vitro* cell binding studies give satisfactory results.

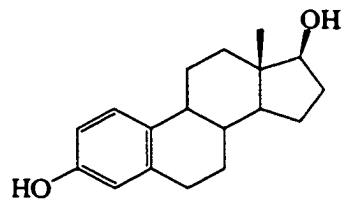

Estradiol

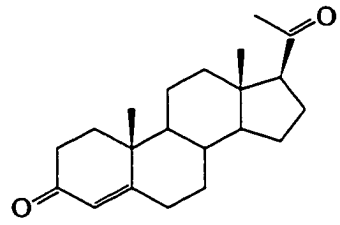

Progesterone

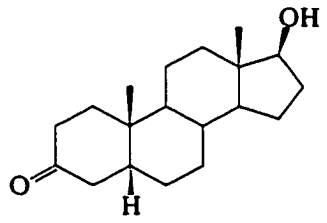

Dihydrotestosterone

Figure 16. Hormones that bind to androgen and progesterone receptors.

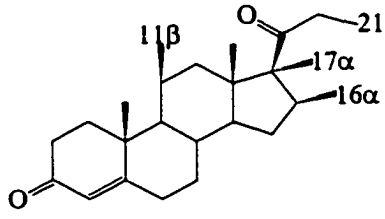

Figure 17. Substituted progesterone

1.4. ***The integrated approach to mimic bioactive molecules***

The ideal *Tc*-radiopharmaceutical would be such that the outer surface of the complex itself contains the groups necessary to deliver the radioisotope to the target organ. This could be achieved by replacing a part of the ligand with a metal chelate system. In this way, there is a minimal change in ligand size, shape and structure, and biological properties of the original molecule can be preserved as well. The steric bulk and the resulting mass of technetium-based complexes are much lower when the technetium unit is incorporated into the bioactive molecule than when the conjugate is attached to the compound. This approach is far more challenging in terms of the chemistry involved, and developments are currently in the early stages.

The integrated approach strategy was primarily used to synthesise hormone mimics for receptor binding (Hom and Katzenellenbogen, 1997, review). A model structure for such a complex is shown in ***Figure 18***, where the overall similarity to progesterone is apparent.

The synthesis of bis-bidentate oxorhenium (V) complex has also been achieved (***Figure 19***). It was designed from the 5a-dihydrotestosterone (DHT) framework as a potential ligand for the androgen receptor (Hom *et al.*, 1996). While modelling suggested that this complex was a good steric mimic of DHT, it exhibited a markedly lower lipophilicity than DHT itself, and showed very low binding for the androgen receptor. The oxo-technetium (V) complex was also formed, but was not characterised owing to its low stability.

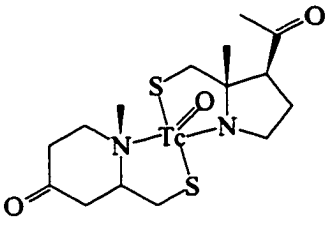

Figure 18. Progesterone bis-bidentate mimic model

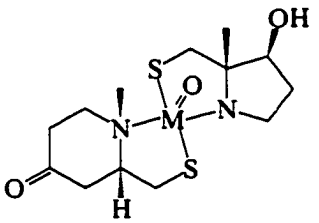

Figure 19. Organometallic mimic of the dihydrotestosterone. M = *Tc*, *Re*.

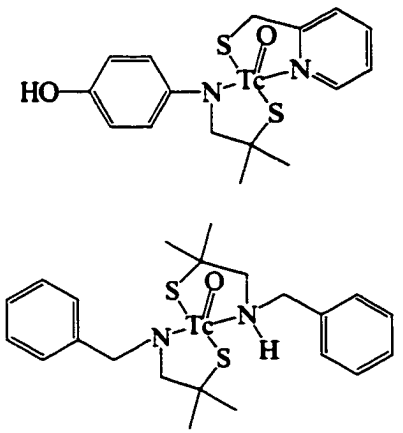

Figure 20. Estradiol technetium mimics

Some initial steps toward producing an analogue of estradiol have been made through the synthesis of bis-bidentate complexes (***Figure 20***). Synthesised compounds have a phenol group, which is essential for estrogen receptor binding, even though their structures are quite different from estradiol. The receptor-binding affinity of such complexes was found to be low (Chi *et al.*, 1994).

There have also been attempts to synthesise rhenium complexes that mimic estradiol structure. The B and C rings of estradiol were replaced with a tetradentate oxo-rhenium(V)-heteroatom core. Although this complex appeared to be a good structural mimic of the hormone, it was surprisingly unstable in aqueous solution, and decomposed to form a tridentate (3+1) complex (***Figure 21***). This was explained by a poor donor ability of the aromatic thioether linkage

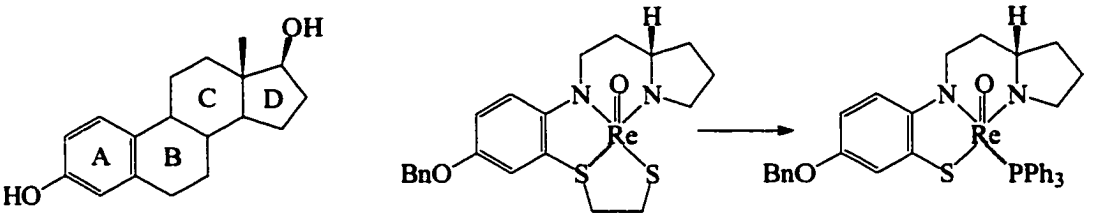

Estradiol

Integrated oxorhenium complex from estradiol template

Figure 21. Estradiol and its integrated oxorhenium complex.

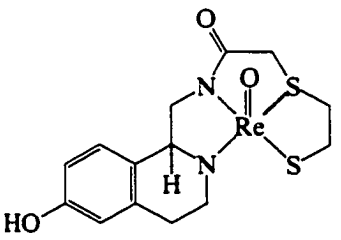

Figure 22. Integrated tetradentate oxometal complex from estradiol template

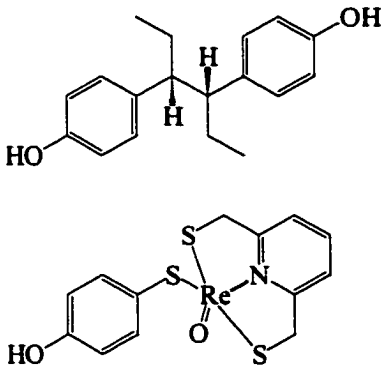

Figure 23. Hexestrol and integrated (3+1) tridentate oxorhenium complex

(Sugano and Katzenellenbogen, 1996).

An alternate design strategy suggested replacing the C and D rings of the steroid (***Figure 22***). This complex was more stable than the bis-bidentate rhenium (V) mimic of DHT. But the complex exhibited low lipophilicity, and relative binding affinity of the complex toward the estrogen receptor was found to be low. The affinity of such compounds may be attributed to the presence of phenolic functions. However, the replacement of the C and D rings with the rhenium chelate reduces binding affinity (Hom and Katzenellenbogen, 1997).

The preparation of a 3+1 system that mimics the structure of non-steroidal estrogen hexestrol (***Figure 23***) has recently been reported

(Hom *et al.*, 1997). *In vivo* biological data on this compound have not been published yet.

As one can note *N,S*-chelating agents are of great importance in ^{99m}Tc-radiopharmaceuticals synthesis. More sophisticated second generation agents or simple small molecules of the first generation agents both use the ability of N,S-ligands to participate in bonding to technetium.

AIM

Available ^{99m}Tc-radiopharmaceuticals are presently limited to single small molecules with fixed structure. There are not many possibilities for modifying the periphery of such ligand molecules in order to fine-tune the solubility of the compound and its pharmacokinetics. Therefore, there is an interest to develop new technetium ligands, which vary the size and lipophilicity of stable ^{99m}Tc-complexes containing the same type of technetium core.

The aim of the present work is to obtain various substituted 2-pyrrolylthiones in order to examine their potential to form complexes with transition metals and to study the properties of such complexes. Furthermore, the suitability of these novel ligands as chelators for radiometals, such as for isotopes of technetium and rhenium, was explored with the goal of creating a new class of radiopharmaceutical compounds for medical imaging.

CHAPTER 2: Results and Discussions

The primary aim of this project was to synthesise porphyrin mimics with an integrated technetium core of potential interest for medical imaging. The outer part of the porphyrin molecule (***Figure 24***) is chemically accessible allowing for the attachment of different substituents to vary the biological biodistribution pattern.

It is well known that metal derivatives of phthalocyanines (tetrabenzotetraazaporphines) (***Figure 25***) can be prepared either by condensation, the so called template synthesis, from a monomer, such as phthalic acid, phthalic anhydride, diiminoisoindoline, or phthalonitrile in the presence of metal ion, or by exchange of the central hydrogen or metal ion from pre-formed phthalocyanine. The last route encounters two major problems. First of all, the initial reactants should be soluble in the same solvent. The second problem is that the selected metal ion should have the proper dimension to allow for insertion into the phthalocyanine core. Unfortunately, technetium ions such as pertechnetate or reduced compounds (i.e. technetium dioxide) do not fit into the porphyrin or phthalocyanine core. Therefore,

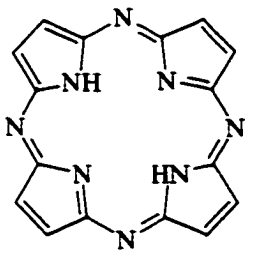

Figure 25. Porphyrin

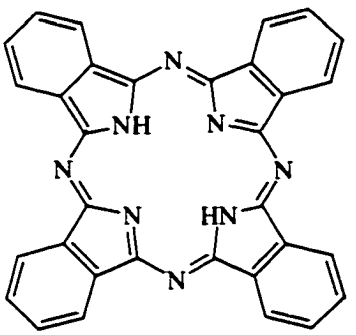

Figure 24. Phthalocyanine

direct insertion of the technetium moieties into the cavity of the phthalocyanine macrocycle failed. (Rousseau, 1985) Accordingly, the template synthesis should be more convenient and promising. The same authors reported such synthesis with a final complex where the technetium core was found in an out-of-plane position. This fact makes it doubtful that the obtained complex is stable enough for biological applications. Nevertheless, preliminary biological tests were conducted showing *in vivo* stability but there were no further results published on the properties of this compound.

It might be possible to imitate the structure of a molecule using smaller sub-units as building blocks. A few classes of molecules would be suitable to build a porphyrin mimic.

Pyrroles and their derivatives have been used for the synthesis of porphyrins. Early work showed different methods to construct porphyrin molecules from dipyrromethanes, dipyrromethenes, or pyrrole itself (Paine, 1978). The methods and routes of these reactions are conventionally determined by the structure of desired final products. Dipyrromethanes and dipyrromethenes are used mostly for the synthesis of symmetric compounds, whereas several pyrrole molecules with different substituents give unsymmetrical porphyrins. The synthetic strategies for such reactions are well established and are still being improved (Gilchrist, 1999; Mamardashvili and Golubchikov, 2000).

To introduce a large metal ion inside the porphyrin mimic, one needs to use building blocks other than dipyrromethanes, such as molecules with increased electron-donor properties. We suggest that a metal ion would form one covalent bond

with a ligand, while another bond would be formed via coordination of metal ion by an electron-donor atom, which would provide a free pair of electrons. This would help to produce more stable complexes. Dipyrromethenes could be considered as possible ligands, but their instability and multi-steps synthesis are inconvenient.

When developing site-specific therapeutic or diagnostic radiopharmaceuticals, many important factors must be considered. It is essential that a metallic radionuclide upon interaction with a chelating agent should form an *in vivo* stable complex with high specific activities and with defined metal to ligand stoichiometry. These requirements narrow the choice to only a few ligand backbones. The detailed understanding of the coordination chemistry of new ligand systems with non-radioactive rhenium or ground[4] isotope ^{99}Tc is important. This knowledge helps to subsequently extent these reactions at the trace level in order to label the chelating agents with ^{99m}Tc. In addition, the ability of the ligand to form radiopharmaceutical complexes under conditions suitable for routine formulation is also an essential consideration.

Thiol groups are known to bind to technetium with high affinity. *N,S*-Bidentate ligands are particularly attractive as potential technetium and rhenium chelators. They have nitrogen as part of a heterocycle and sulphur donor atom as part of the thione or thiol group. There exists continuing interest to study such bidentate chelating agents. A wide range of different *N,S* bidentate and N_xS_{4-x} tetradentate chelating agents have been synthesised over the past years and tested for their capacity to complex technetium (Volkert and Jurisson, 1996).

[4] The most stable arrangement of nucleons within nucleus is called the ground state.

Reports on compounds containing a 2-pyrrolylthione moiety have appeared in the literature (Murase *et al.*, 1991; Kost *et al.*, 1974, Sato and Sunagawa, 1967). However, their potential chelating ability was never addressed.

It has been reported that 2,2'-dipyrrolylthione forms a complex with mercuric chloride (Clezy and Smythe, 1969), although no structures or characteristics of such complexes were provided.

Recently it has been reported that unsubstituted 2,2'-dipyrrolylthione was used as starting material for the synthesis of 5,15-diphenylporphyrin *via* the Raney-Nickel induced hydrodesulphurisation, thereby obtaining 2,2'-dipyrrolylmethane – a key intermediate in porphyrin synthesis (Brückner *et al.*, 1998). The anticipated hydrodesulphurisation, however, did not occur. Instead of the expected product, a *Ni*(II)-2-pyrrolylthione complex was isolated from the reaction. This finding prompted a close look at 2-pyrrolylthiones as *N,S*-donor chelating agents for transition metals. Description of the *Ni*(II), *Co*(II), and *Hg*(II) complexes with unsubstituted 2,2'-dipyrrolylthione can be found in literature (Brückner *et al.*, 2000).

Thus, the use of 2-pyrrolylthiones (***Figure 26***) was suggested as potential ligands for transition metals, including technetium and rhenium. First of all, they contain *N,S* donor atoms, the combination of which can be found in bis-bidentate or tetradentate ligands. The photochemical and spectroscopic properties of the thione group can be advantageous for biological applications. Finally, there are many possibilities to modify the periphery of pyrrolylthiones, which may be useful to study the

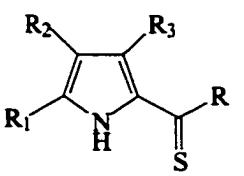

Figure 26. General formula for 2-pyrrolylthiones

biological behaviour of the ligand and its metal complexes as a function of different substituents.

2-Pyrrolylthiones represent a rather unknown class of compounds. There are few groups that have studied pyrrolylthiones and reported on their physical and chemical properties. Previous studies (Clezy and Smythe, 1969; Bruchner *et al.*, 2000) were performed using 2,2'-dipyrrolylthiones, which can be considered as a particular example of 2-pyrrolylthiones, where two usually symmetric pyrroles are bound together *via* a thione group.

Few methods of 2,2'-dipyrrolythione synthesis are described in the literature. The most convenient synthetic pathway to prepare 2,2'-dipyrrolylthiones proceeds through the reaction of initially substituted or unsubstituted pyrrole molecules with thiophosgene (Clezy and Smythe, 1969). The 2-position of the pyrroles must be free to allow for the interaction with thiophosgene. The optimal conditions for the reaction depend primarily on the nature of the substituents in the pyrrole molecule.

Although it seems plausible to use pyrrolic Grignard derivatives for "coupling"-type syntheses of 2-pyrrolylthiones, the experiments with such activated pyrrolic compounds lead to no avail. The possible formation of a tripyrrolic substance was reported in such reactions (Clezy and Smythe, 1969) due to the high electron-acceptor activity of the thione group, which affects the basicity of the pyrrolic nitrogen. It is worth noting that analogous compounds are never formed in the reaction of comparable pyrroles with phosgene (Clezy and Nichol, 1965; Ballantine *et al.*, 1966). To avoid the formation of tripyrrolic compounds, it is suggested to carry out the reaction directly from pyrrole.

Some 2-pyrrolylthiones and dipyrrolylthiones can be obtained from their ketone analogues by converting the carbonyl group into the thiocarbonyl moiety. This reaction would be possible using sulphuration agents such as tetraphosphorus decasulphide (Scheeren *et al.*, 1973) or milder Lawesson's reagent (***Figure 27***) (Shabana *et al.*, 1981).

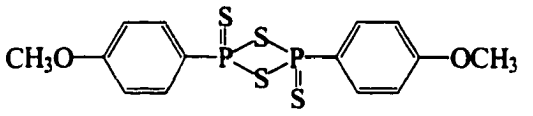

Figure 27. 2,4-bis(4-methoxyphenyl)-1,3-dithia-2,4-diphosphetane-2,4-disulphide

3.1. ***Synthesis of 2-pyrrolylthiones***

The parent unsubstituted or substituted 2-pyrrolylketones **1a-c** served as the precursors for the synthesis of lipophilic 2-pyrrolylthiones. 2-Pyrrolylketone **1a** is commercially available and was used as received. Compounds **1b,c** were obtained using the method suggested in the literature (Pesson *et al.*, 1966) from the appropriate pyrrole activated as its Grignard derivative (***Scheme 1***).

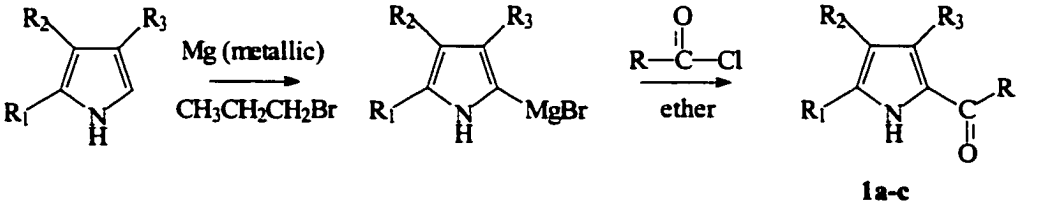

1a-c

a: $R_1=R_2=R_3=H$, R= $-C_6H_5$

b: $R_1=R_2=R_3=H$, R= $-C_6H_4(OCH_3)$

c: $R_1=R_2=R_3=H$, R= $-C_6H_3(OCH_3)_2$

Scheme 1. Synthesis of the 2-pyrrolylketones

Subsequently, compounds **1** were converted into the corespondent thiones **2** (***Scheme 2***). Conversion of the carbonyl group into the thione group was achieved by treatment with Lawesson's reagent. 1,2-Dimethoxyethane is the solvent of choice for this process. The reaction must be conducted under a nitrogen atmosphere and shielded from light. The reaction is complete in 1-12 hours. The final compound was extracted from the reaction mixture with chloroform and washed with water. The yields are good (45-50%).

Alternatively, the conversion of carbonyl groups into the thiocarbonyl moieties was accomplished with P_4S_{10} (***Scheme 2***) using a slightly modified method described in the literature (Lumbroso and Liégeois, 1984; Brückner, 1993). Benzene was used as a solvent. In this case, the reaction was complete in 40 minutes. Unreacted P_4S_{10} was separated from the reaction mixture by filtration. We prefer to use P_4S_{10} as a sulphuration agent for 2-pyrrolylketones because of its better availability, high reactivity, easy work-up of reaction mixtures, and very good yields of desired 2-pyrrolylthiones (up to 65 %).

Final products were purified using column chromatography to give compound

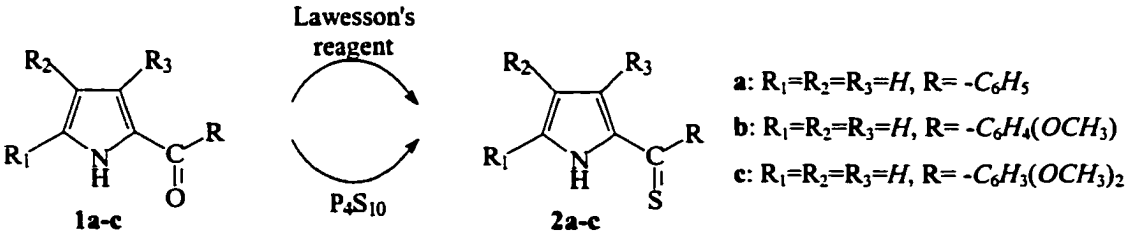

Scheme 2. Conversion of 2-pyrrolylketones into 2-pyrrolylthiones

2b as a bright red crystalline solid and **2c** as red oil, which subsequently crystallised. Compound **2a** has been described in the literature (Lumbroso and Liégeois, 1984) as oil, but repeated purification by column chromatography gave a dark red crystalline solid with low melting point (33-36°C).

Thione **2d** was prepared as suggested in the literature (Clezy *et al.*, 1974) with good yield (55%). This route can be used to obtain other dipyrrolylthiones of symmetric structure (***Scheme 3***).

Synthesised 2-pyrrolylthiones **2** are quite stable in solid state but oxidise fairly easily in solution, particularly when exposed to light.

Because solubility in water could change the physical, chemical and biological properties of the ligands and corresponding complexes, the water-soluble

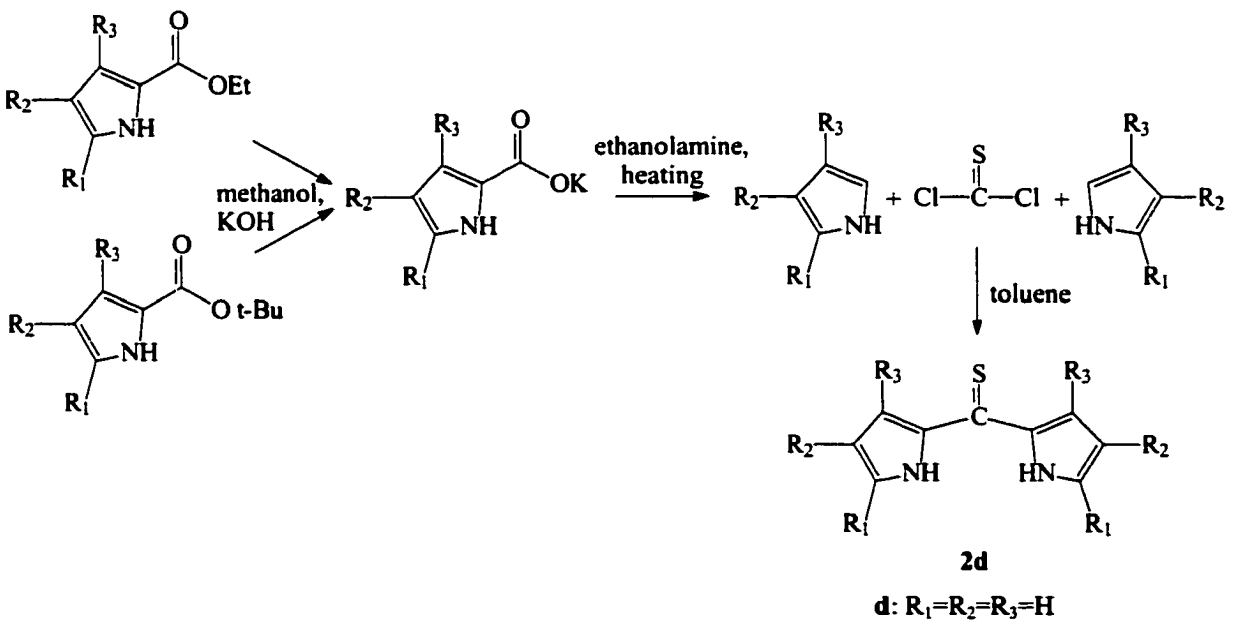

Scheme 3. Synthesis of the symmetric dipyrrolylthiones

analogues of the lipophilic compounds were also prepared. A simple method to change the lipophilicity of the compounds is through the addition of one or more hydrophilic substituents to the pyrrolic ring, for example *via* sulphonation. Several sulphonating agents exist and are used in chemical synthesis (Fieser and Fieser, 1967).

The sulphonation of 2-pyrrolylthiones using pyridine-sulphur trioxide was not successful after reaction time of 24 hours. This signifies that pyridine-sulphur trioxide is too mild a reagent for these compounds. In contrast, the sulphonation of all compounds **2a-d** goes smoothly with 1,4-dioxane-sulphur trioxide as a sulphonating agent (***Scheme 4***). Electrophilic substitution takes place in 4-position of aromatic pyrrolic ring resulting in a sulphonated compound.

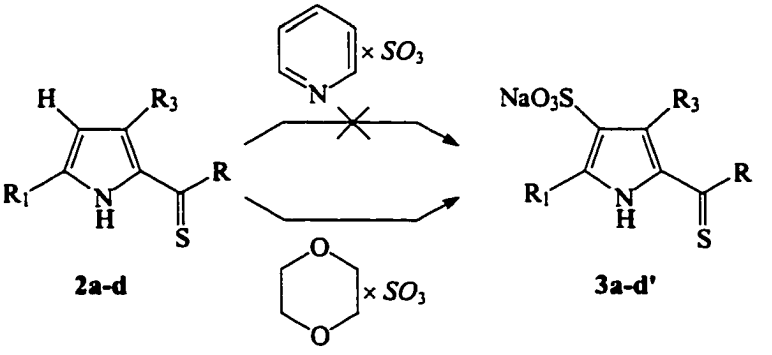

a: R_1=R_3=*H*, R= -C_6H_5
b: R_1=R_3=*H*, R= -$C_6H_4(OCH_3)$
c: R_1=R_3=*H*, R= -$C_6H_3(OCH_3)_2$
d: R_1=R_3=*H*, R= -$C_4H_2(SO_3Na)NH$
d': R_1=R_3=*H*, R= -C_4H_3NH

Scheme 4. Sulphonation of 2-pyrrolylthiones

1,4-Dioxane-sulphur trioxide was synthesised using a literature method (Bordwell and Rondestvedt, 1950). Some difficulties were encountered during product separation. In our hands, filtration of the product at first was not successful. Although we observed large quantity of the precipitate before filtration, most of the precipitate was re-dissolved during the washing step. Reducing the volume of the reaction mixture under vacuum resulted in more stable white precipitate, which was easily collected by filtration. A yield of 89% of the theoretically possible quantity was achieved by repeating this procedure (evaporating-filtration) several times. 1,4-Dioxane-sulphur trioxide is very unstable under atmospheric conditions and is easily hydrolysed in water. Nevertheless, it can be stored in tightly closed vials sealed with Parafilm in the freezer for at least two years. This compound was further used for sulphonation of 2-pyrrolylthiones.

A large excess of sulphonating agent (sometimes up to four equivalents) is required when 1,4-dioxane-sulphur trioxide is pre-dissolved in 1,4-dioxane for further use. We found that sulphonation is more efficient when a two-fold excess of 1,4-dioxane-sulphur trioxide is added gradually as a solid to a substrate dissolved in 1,4-dioxane. The reaction takes place at room temperature in an inert atmosphere and is usually complete in 10 min. Nitrogen atmosphere is crucial to prevent the hydrolysis of 1,4-dioxane-sulphur trioxide and to inhibit the oxidation of 2-pyrrolylthiones. Progress of the reaction is obvious from the colour change, which occurs when the sulphonating agent is added. The reaction mixture becomes yellowish-red and looks thicker, like oil, which can be due to increasing of density and/or liquid surface tension. Completion of the reaction was monitored using TLC. The parent thiones

move on silica-gel plates in chloroform, while water-soluble compounds remain at the origin. Sulphonated ligands migrate in methanol almost with the front of the solvent. The reaction was terminated, when there was no initial pyrrolylthione detected in the reaction mixture. There was still a little amount left of the initial dipyrrolylthione **2d**, but an addition of new portions of the sulphonating agent, increasing the reaction time or heating up to 60°C did not improve the yield.

After the reaction was complete the solvent was evaporated and the product was re-dissolved in water. Aqueous solutions of sulpho-2-pyrrolylthiones are very acidic with pH less than 1. Acidity of these mixtures was adjusted using 0.1 N aqueous *NaOH* to the pH values shown in **Table 1**. It is essential to conduct neutralisation carefully, avoiding rapid pH shift into basic conditions past the titration point. Otherwise, at pH ≥ 8 pyrrolylthione solution changes its colour rapidly from red to brown, which probably reflects product transformation in basic medium. This color change is reversible: once a weak acid solution is added to the mixture to move equilibrium to acidic conditions, the mixture becomes red again. No further observations were made to find out if this color shift is permanent or the reversion will become impossible with time. Thus, it is important to keep acidity of a sulphonated 2-pyrrolylthione solution below pH 5.

Table 1. The final pH of the 2-pyrrolylthiones' solution after neutralisation

	2a	2b	2c	2d
pH	4.6	4.6	4.3	3.6

Next, sulphonation by-products and other impurities were precipitated from aqueous solutions by adding acetone. Acetone was added gradually until a white

precipitate appears. A light brown precipitate was observed only in the case of dipyrrolylthione **2d**. The volume of the added acetone was roughly equal to 4 volumes of the initial solution. The red supernatant obtained after centrifugation was stripped of solvent to give the water-soluble 2-pyrrolylthiones.

Each of 2-pyrrolylthiones **2a-c** yielded a single main product of sulphonation. Purification of these compounds was straightforward. Reversed-phase column chromatography with water as eluent gave pure sulphonated 2-pyrrolylthiones **3a-c** in good yields (40-56 %). There are some side products formed during the synthesis of **3b,c**, which are perhaps disulphonated analogues or 5-substituted isomers, but their yields are too low to perform routine analyses. Separation of the main component from the by-products is easily accomplished on reversed-phase (C_{18} or Phenyl) silica gel due to considerably different chromatographic mobilities of these compounds.

Two reaction products were recovered when 2,2'-dipyrrolylthione **2d** was used as a substrate. They were identified as di- and monosulphonated 2,2'-dipyrrolylthiones **3d** and **3d'**, respectively. The major product is disulphonated compound **3d**, which was obtained in 43% yield. The quantity of separated monosulphonated 2,2'-dipyrrolylthione **3d'** was much lower (12% yield) but sufficient to allow for chemical analyses and syntheses of *Tc* complexes. The retention time of these products differ significantly, allowing for separation by reversed-phase chromatography. Dried samples of the synthesised water-soluble sulpho-2-pyrrolylthiones were used to study their physical and chemical properties.

All synthesised sulphonated compounds **3a-d'** are brightly coloured in various shades of red. They are highly soluble in water and decompose at high temperature

without melting. Synthesised sulpho-2-pyrrolylthiones are strong acids. Because sodium hydroxide has been used to neutralise them during purification, the final products were obtained as sodium salts. Elemental analyses, NMR spectroscopy and crystallographic data suggest that all synthesised compounds were recovered as hydrates with one to three molecules of water retained in the ligand structure.

3.2. *Analysis of the spectroscopic data*

The tautomeric nature of the dipyrrolylthiones has been discussed previously (Clezy and Smythe, 1969). 2-Pyrrolylthiones preserve the same tautomeric structure (***Scheme 5***). The IR spectra of the synthesised lipophilic compounds recorded in chloroform show characteristic weak *SH* absorption near 2550 cm^{-1}, corresponding to the structure of the thiol isomer **2'** (Silversten *et al.*, 1991; Dyer, 1970). However, these pyrrolylthiones have a maximum of medium intensity, which is assigned to the *C=S* stretching frequency (1250-1020 cm^{-1}) (Silversten *et al.*, 1991). The thione group is less polar than the ketone group and has a considerably weaker bond. As a consequence, the band is not intense and appears at lower frequencies, where it is

Scheme 5. Tautomeric structures of 2-pyrrolylthiones

much more susceptible to coupling effects. Therefore, identification presents a challenge. A medium-intensity absorption of *C=S* group occurs at the same region as *C–O* and *C–N* stretching, which suggests that considerable intramolecular interaction may occur between these vibrations. The IR spectra of the water-soluble 2-pyrrolylthiones **3** were recorded in *KBr* pellets. No absorption was found around 2550 cm^{-1}. However, a high intensity maximum is present around 1210-1212 cm^{-1}, which is assigned to the thione structure. Therefore, it is likely that the ligands in solid state exist mainly in the thione form with minor contributions of the other tautomer. The dynamic tautomeric thione-thiol transition exists in solution.

Lipophilic 2-pyrrolylthiones **2** have characteristic UV-visible spectra with intensive absorption around 376-406 nm, attributable to intraligand π—π^* transitions, that can be used for their quantitative detection. UV-visible spectrum of the novel sulpho-2-pyrrolylthiones **3** is similar in shape to that of compounds **2**. The very strong absorption of **3** at 375-397 nm is somewhat red-shifted as compared to the lipophilic analogues. The extinction coefficients are high ($\lg \varepsilon > 4$) and close to the extinction coefficients of lipophilic compounds. In general, the extinction

Table 2. Extinction coefficients ε for the synthesised 2-pyrrolylthiones (λ_{max}, nm ($\lg \varepsilon$))

	a	**b**	**c**	**d**	**d'**
Compounds **2**	392 (4.26)	376 (4.38)	390 (4.29)	406 (4.70)	
Compounds **3**	382 (4.34)	375 (4.40)	382 (4.64)	389 (4.44)	397 (4.03)

coefficients of the water-soluble 2-pyrrolylthiones are slightly higher than those of the lipophilic compounds with the exception of the dipyrrolylthiones **3d,d'** (***Table 2***). These data are in agreement with a comparable study of 2-pyrrolylketones, wherein the peak position was observed to be a function of substituents in the pyrrolic ring (Ballantine, 1966).

Nuclear Magnetic Resonance (NMR) spectra of the 2-pyrrolylthiones show pyrrolic and aromatic *CH* protons at 6.5-8 ppm, which is in good agreement with published data for pyrrolic and aromatic compounds in general (Silversten *et al.*, 1991). The pyrrolic *NH* proton was observed around 9.8 ppm for lipophilic compounds as a single broad peak. This data is in good accordance with experimental results for other 2-pyrrolylthione containing compounds. (Lumbroso and Liégeois, 1984; Murase *et al.*, 1991) A broad peak of the same shape was found at 11.7 ppm for hydrophilic ligands, which was also assigned to the *NH* proton. The shift of almost 2 ppm can be explained by intramolecular hydrogen bonding between the *NH* proton and sulpho-substituent. This proton would have a resonance peak corresponding to the strong acidic nature of the sulpho-group, which is even more shifted towards high frequency than for pyrrolic *NH* proton. It is known that sulphonic acids show a peak around 10-12 ppm (Silversten *et al.*, 1991). Correlated spectroscopy[5] (COSY) and Nuclear Overhauser Effect spectroscopy[6] (2D and selected 1D NOESY) were performed to prove the position of the sulpho-group in the

[5] COSY is useful to determine existence of neighbouring protons in pyrrolic ring. A COSY spectrum yields through bond correlations *via* spin-spin coupling.

[6] NOESY helps to determine protons, which are close in space but not closely connected by chemical bonds. A NOESY spectrum yields through space correlations *via* dipole-dipole coupling known as Nuclear Overhauser Effect (NOE).

pyrrolic ring of the sulphonated 2-pyrrolylthiones. Systematic study of the spectra confirms that two protons in the substituted pyrrolic ring cannot be adjacent, which can be taken as affirmative of the sulpho-group to be positioned at forth carbon in pyrrolic ring.

The results of other analytical methods must be considered to identify the chemical structure of synthesised 2-pyrrolylthiones, since little is known about NMR spectra for this class of compounds.

3.3. Crystallographic study

Single crystal X-ray diffraction studies were performed for selected ligands. Crystal data and selected experimental details are listed in ***Table 3***. The complete results including selected bond lengths and angles are collected in ***Supporting data (Part 2)***.

3,4-Dimethoxyphenyl-2-pyrrolylketone **1c** is a new compound, which was not described previously. An X-ray diffraction study was performed for **1c** to establish its structure. A pale grey-green block crystal with dimensions of 0.76×0.36×0.21 mm was grown by slow evaporation of the solvent (chloroform). The resolved structure is the expected pure ketone (***Figure 28***). The bond lengths around the carbonyl C1-C2 and C1-C7 are 1.453(4) Å and 1.479(4) Å, respectively. The length of O1-C1 bond is somewhat shorter (1.231(3) Å), which is due to its double order. The pyrrolic part of the molecule is found to be in plane with the carbonyl group with a deviation not exceeding 7°. The C7-C10 axis of the phenolic

ring is lying in the same plane, while the phenolic ring itself is found to be at an angle of ca. 36.7° to the plane. The torsion angle O10-C10-C11-O11 is 0.3°. The two methoxy-groups are at a *trans*-position with respect to each other. The methoxy-group, which is *cis* to the carbonyl, is almost in the phenyl ring plane with a deviation of only 2.4°, while another one rises from the plane at 10.1°. The pyrrolic *NH* hydrogen binds to the carbonyl oxygen of another molecule forming relatively weak hydrogen bonds of 2.37 Å.

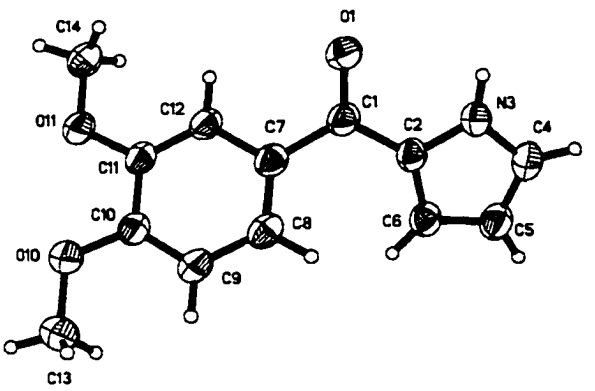

Figure 28. ORTEP drawing and numbering scheme for 3,4-dimethoxyphenyl-2-pyrrolylketone **1c**

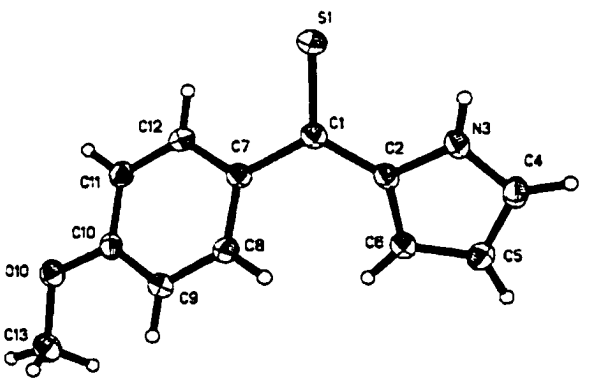

Figure 29. ORTEP drawing and numbering scheme for *p*-methoxyphenyl-2-pyrrolylthione **2b**

The single crystal X-ray diffraction study of compound **2b** results in a thione structure, with the *C=S* bond readily visualised (***Figure 29***). Monoclinic crystals of **2b** with $P2_1/c$ space group are formed *via* the pyrrolic hydrogen-sulphur bonds. Overall the crystal structure is similar to the one above of the ketone. The thiocarbonyl S1=C1 bond is longer than the analogous carbonyl O1=C1 bond of **1c**

Table 3. Crystal data for selected ligands.

Compound	**1c**	**2b**	**3b**
Form	Block	Block	Block
Colour	Pale grey-green	Dark red	Intense violet-pink
Dimensions (mm)	0.76×0.36×0.21	0.58×0.52×0.18	0.57×0.53×0.27
Empirical formula	$C_{13}H_{13}NO_3$	$C_{12}H_{11}NOS$	$C_{12}H_{16}NNaO_7S_2$
Molecular weight	231.244	217.278	373.368
Crystal system	Orthorhombic	Monoclinic	Orthorhombic
Space group	$Pca2_1$	$P2_1/c$	*Pnma*
a (Å)	18.972(8)	11.8386(1)	6.763(3)
b (Å)	9.065(3)	11.9453(1)	7.540(6)
c (Å)	6.867(2)	7.5061(1)	31.641(15)
β (°)		98.676(1)	
V (Å^3)	1181.0(7)	1049.33(2)	1613.5(15)
Z	4	4	4
$D_{calc.}$ (Mg/m^3)	1.3006	1.3753	1.5370
μ (mm^{-1})	0.766	2.490	3.587
Extinction coefficient	0.0205(19)	0.0275(19)	0.0146(12)
R^a ($R_w{}^b$)	0.0616 (0.1485)	0.0402 (0.1118)	0.0286 (0.0817)

[a] $R = \Sigma||F_o| - |F_c|| / \Sigma|F_o|$; [b] $R_w = [\Sigma[w(F_o^2 - F_c^2)^2] / \Sigma[w(F_o^2)^2]]^{1/2}$

as expected due to the larger sulphur atom radii as compared to oxygen. The double-bond S1=C1 has a length of 1.6686(15) Å, which is more than the single bonds C1–C2 and C1–C7 that are 1.426(2) Å and 1.4782(19) Å, respectively. This is in good agreement with crystal data reported for 2,2'-dipyrrolylthione containing complexes (Brückner *et al.*, 2000).

A block crystal of intense violet-pink colour with dimensions of 0.57×0.53×0.27 mm was used to collect the data for compound **3b** (***Supporting data, Part 2***). Its resolved structure is illustrated in ***Figure 30***. The sulphonated analogue **3b** of the general formula $C_{12}H_{16}NNaO_7S_2$ was found to be a sodium salt of the ligand, which is logical considering the method of synthesis and purification, and this is in good accordance with elemental analyses. The ligand itself has a negative charge of -1. Sodium atoms are accommodated between water molecules forming an infinite chain in which each Na^+ ion is surrounded by 6 water oxygens, and each water molecule is bridging two Na^+ ions. In the lattice, the motive shown (see picture in Supporting Data, page S44) is repeated indefinitely in both directions. This chain is an associated cation disordered between negative ligand molecules. The angles around the thione carbon are almost perfect: 119.79(17)°, 120.42(17)°, and 119.78(15)°. The pyrrolic ring is lying in the same plane as the thiocarbonyl group while the phenolic ring is

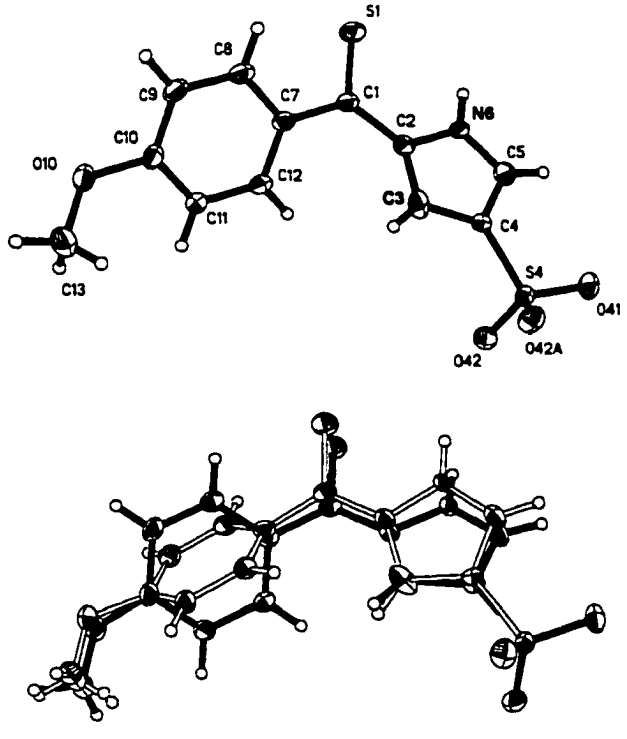

Figure 30. ORTEP drawing and numbering scheme for *p*-methoxyphenyl-4-sulpho-2-pyrrolylthione **3b**. The associated cation omitted for clarity.

rotated around the C1-C7 axis with a deviation of about 35-40° from the plane.

This rotation takes part in the crystal formation. It is of interest to note that the main planes of the two disordered molecules remain roughly parallel, whereas the phenolic rings adopt an orientation of ~70° apart (***Figure 30***). The methoxy-group is not linear and is bent at 122.08(19)°, which is normal for sp^2 hybridisation. The sulpho-group has tetrahedron configuration with angles of ca. 112°. The pyrrolic nitrogen is protonated and participates in hydrogen bonding of the system.

This case is a good demonstration of the fact, that X-ray diffraction data alone cannot identify unequivocally position of the sulpho-group in the pyrrolic ring. Aromatic nature of the structure together with similarity of carbon and nitrogen atoms for the technique might suggest forth position as well as fifth. Consideration of NMR studies results is very important to establish true structure of the sulphonated 2-pyrrolylthiones.

3.4. ***Reactions with small transition metals ions***

Compounds **2** and **3** are potential ligands for transition metals, including such large ions as *Tc* and *Re*. The presence of *N,S* donor atoms in their molecular structure should facilitate formation of ligand-to-metal bonds. A series of screening experiments were performed to evaluate the potential of the sulphonated 2-pyrrolylthiones as chelators in neutral medium. To accomplish this, a range of transition metal complexes with all synthesised water-soluble compounds **3** was

prepared.

Cadmium (*Cd*), cobalt (*Co*), copper (*Cu*), nickel (*Ni*), and zinc (*Zn*) were selected and their complexes with ligands **3a-d** were successfully synthesised (***Scheme 6***). Reactions were performed in neutral medium to mimic synthetic conditions for ^{99m}Tc. Formation of complexes was complete in a few minutes after simply adding the ligand solution to the previously dissolved metal salt.

Metal acetates and metal chlorides were used for reactions. The reaction with the acetates occurs rapidly, which is not the case for the chloride salts. The yields are also significantly higher for complexes made from the acetate salts. This can be explained by the difference in dissociation constants (pK_a) between hydrogen chloride and acetic acid (-2.2 and 4.7 respectively).

Either water or methanol was used as a solvent for complexation reactions. In some instances, we obtained the complexes as precipitates (for example, *Ni* and *Cu* complexes with **3a** in aqueous solution). In other cases, we had to monitor the course of the reaction using spectrophotometry.

All 2-pyrrolylthiones display a characteristic absorption in the UV-visible spectrum around 380 nm. These peaks became broader and progressively shifted toward higher wavelengths upon addition of metal salts to the ligand solutions. The shape and the peak maximum depend on several factors, including valency and oxidation state of the central metal ion, as well as geometric structure of the complex. The results agree with experimental data obtained earlier for 2,2'-dipyrrolylthione complexes (Brückner *et al.*, 2000).

The resulting complexes were purified by either, normal or reversed-phase chromatography, or by using both methods if the sample was not pure enough after the first run. The purified compounds were characterised using spectroscopic methods and elemental analyses.

NMR spectra of the water-soluble complexes are in good agreement with those of the ligands themselves. Aromatic and pyrrolic *CH* protons can be seen where expected while acidic proton disappears from 11.7 ppm, which serves as an additional confirmation of the complex formation. Curiously, two peaks still appear at 11.86 and 11.99 ppm for *Cd* complex with ligand **3a**. The ligand itself shows the only peak in this region at 11.81 ppm. Similar situation exists for *Cu* complex with the same ligand **3a**: this complex has a peak at 11.92 ppm. We suggest that these signals arise not from unprotonated *NH* pyrrolic group but rather from acidic $-SO_3H$ protons. We believe that Na^+ ions were substituted for H^+ in the aqueous solution of the reaction mixture and the resulting compound is not a sodium salt anymore but a sulphonic acid or a mixture of both.

NMR data collected for *Co* and *Cu* complexes do not give good spectra. This

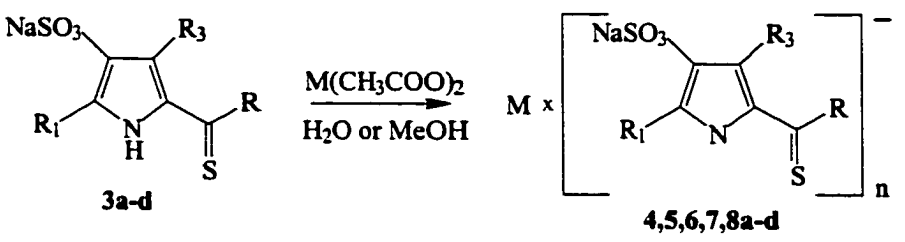

Scheme 6. Reaction of 2-pyrrolylthiones with transition metals. M = *Cd* (**4a-d**), *Co* (**5a-d**), *Cu* (**6a-d**), *Ni* (**7a-d**), *Zn* (**8a-d**); n=1,2.

could be an indicative of their +2 oxidation states, which are paramagnetic. Brückner describes formation of *Co*(III) complex with unsubstituted dipyrrolylthione **2d** in basic conditions starting from *Co*(II) acetate (Brückner *et al.*, 2000) explaining this transformation as oxidation of *Co*(II) by aerial oxygen during reaction. Nevertheless, we strongly support the idea that *Co*(II) complexes were formed with ligands **3a-d**. The reaction conditions in these experiments are very different from those described in reference above. First, the complexation was performed in neutral medium. Secondly, reaction time is only few minutes in case of the ligands **3a-d**, comparing to 12 hours cited in the paper mentioned.

Consistent elemental data for every complex was impossible to obtain. This can be due to high salt formation and/or formation of complexes as mixtures that cannot be separated. The elemental analyses that were successful show formation of 1:1 or 1:2 complexes. Mass-spectra of these compounds exhibit peaks with the corresponding *m/z* ratio. Interestingly, mass spectrum of some complexes (i.e. **5b**, **6b**) exhibit 1:2 peaks even if their elemental analysis shows formation of 1:1 compounds. This cannot be explained until additional analyses are performed, for example, X-ray crystallography.

All the sulpho-pyrrolylthione complexes are formed in aqueous solutions. Our data suggest that water, along with methanol (if used), is always present in the coordination spheres of sulphonated complexes, filling up the space that would otherwise be taken (or not taken) by a second pyrrolylthione. This might explain why we have obtained sulphonated nickel complexes **7a-d** with a ratio of metal:ligand 1:1, as opposed to 1:2 in case of lipophilic nickel 2,2'-dipyrrolylthionates (Brückner *et al.*,

2000).

We believe that sulpho-group does not participate in complex formation. This suggestion came from observation that sulpho-group does not undergo changes in its structure: if starting ligand was used as a sodium salt (**3a-d**), the resulting complex will be most likely a sodium salt also (complexes **4-8a,b,d**; **7c**), if starting ligand was in a sulphonic acid form (**3c**), the resulting complex will be also a sulphonic acid (complexes **4-6,8c**). Thus, one can consider sulphonated 2-pyrrolylthiones **3a-d** as monoanionic ligands in regards to transition metals at described conditions.

Although exact structures of the synthesised metal complexes cannot be established unequivocally from the provided limited picture, we found that most of the formed complexes have a ratio metal:ligand 1:1 with a few exeptions, where 1:2 ratio can be suggested (***Table 4***). Defining the general reactivity for each metal ion and establishing complete structures of the resulting metal complexes is a separate subject and was beyond the scope of this study.

Table 4. Suggested metal-to-ligand ratio in synthesised transition metal complexes

	Cd	**Co**	**Cu**	**Ni**	**Zn**
3a	1:2	1:1	1:1	1:1	1:1
3b	1:1	1:1	1:1	1:1	1:1
3c	1:1	1:2	1:1	1:1	1:1
3d	1:2	1:2	1:1	1:1	1:2

3.5. ***Reactions with technetium and rhenium***

The metastable ^{99m}Tc-compounds could only be synthesised in solutions in minute concentrations (~10^{-9} M). It makes establishing the structure of these compounds by direct methods difficult. We have to assume that such complexes have the same chemical structure as their more stable ^{99g}Tc (or stable *Re*) analogues despite the fact that a ligand is added to the reduced $^{99m}TcO_4^-$ in great excess. One way to establish the identity of new ^{99m}Tc-complexes is to compare their chromatographic properties with those of ^{99}Tc-analogues.

In order to gather structural information on the technetium complexes, we obtained various ^{99}Tc and *Re* analogues with lipophilic and hydrophilic ligands on a macroscopic scale.

The general procedure that was developed for the reaction of 2-pyrrolylthiones **2,3** with TcO_4^- and ReO_4^- in aqueous ethanol or water solution involved the use of a reducing agent in the form of a saturated solution of stannous chloride $SnCl_2$ in 0.1N aqueous *HCl*. The formation of oxo- and hydroxy-metal polymers as side products may occur, particularly in the case of *Re*, due to relative difficulty to reduce *Tc*(VII) and *Re*(VII) to lower oxidation states and easy acidic hydrolysis of the respective moieties.

We explored another reduction method, wherein formamidine sulphinic acid (FSA) was used as a reducing agent (Fritzberg *et al.*, 1977). This procedure was examined for the reduction of the perrhenate ion in a neutral solution. However, treatment of the perrhenate at 60°C for 24 h with FSA did not result in the reduction of ReO_4^-, which was probably due to the low reduction capability of FSA.

Accordingly, $SnCl_2$ was retained in this study to reduce technetium and rhenium ions.

Reduced pertechnetate and perrhenate react smoothly with ligands **2** forming 1:2 stable, soluble complexes **9,10** with very few side products (***Scheme 7***, I). The yields are good and vary from 40% to 90% of the theoretically expected quantities. The complexation reaction is complete in half an hour for *Tc* complexes but can take up to 24 hours for *Re* compounds. In most cases the reaction mixture was heated to 60°C, but reactions will also proceed at room temperature. The reaction was carried out in a nitrogen atmosphere to inhibit hydrolysis and aerial oxidation to unwanted species, which is particularly important for rhenium complexes. The colour of the reaction mixture changes from orange-red to dark brown soon after addition of the

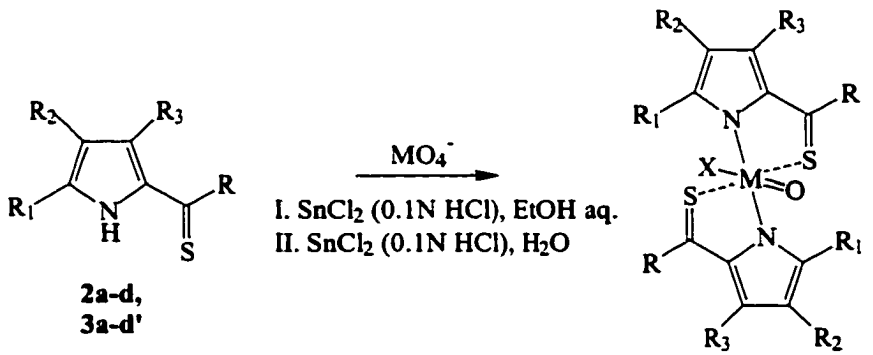

Scheme 7. Synthesis of technetium and rhenium complexes

a: $R_1 = R_3 = H$, $R = -C_6H_5$

b: $R_1 = R_3 = H$, $R = -C_6H_4(OCH_3)$

c: $R_1 = R_3 = H$, $R = -C_6H_3(OCH_3)_2$

d: $R_1 = R_3 = H$, $R = -C_4H_2(SO_3Na)NH$

d': $R_1 = R_3 = H$, $R = -C_4H_3NH$

2: $R_2 = H$

3: $R_2 = SO_3Na$

9: $R_2 = H$, $M = {}^{99}Tc$, $X = -OC_2H_5$

10: $R_2 = H$, $M = Re$, $X = -OC_2H_5$

11: $R_2 = SO_3Na$, $M = {}^{99}Tc$, $X = -OH$

12: $R_2 = SO_3Na$, $M = Re$, $X = -OH$

reagents. The degree of complexation was monitored using TLC on silica gel. The orange-yellow spots of unreacted lipophilic ligands move in chloroform near to the solvent front. Brown-coloured lipophilic complexes move in methanol while the polymers and reduced metal oxides always remain at the origin of the chromatogram.

Synthesised lipophilic ^{99}Tc (**9a-d**) and *Re* (**10a-d**) compounds were isolated and characterised in terms of their identity and purity. All complexes were purified by suitable methods such as normal phase chromatography, re-precipitation from organic solvents, etc. Sometimes a combination of these methods was used to achieve an adequate degree of purification. The complexes are brown crystalline solids. Rhenium complexes decompose at high temperature without melting. All complexes are soluble at different degree in organic solvents such as chloroform, ethyl acetate, acetone, and ethanol.

^{99}Tc complexes with 2-sulphopyrrolylthiones **3** were prepared by mixing three components of the reaction. Stannous chloride was the reducing agent of choice. Reactions were carried out in water (***Scheme 7***, II). Reduced pertechnetate reacted fairly smoothly with all ligands to form stable complexes **11**. The complexation was complete in 15 minutes at 60°C. The course of the reaction was followed using TLC on normal and reversed-phase silica gel. Purification by either normal or reversed-phase chromatography gave ^{99}Tc complexes in good yields (75-95%). A few side products were detected in quantities not sufficient for their characterisation. Compounds **11a-c** were purified using normal phase chromatography with methanol as an eluent. The one step purification is easy and effective. Compounds **11d,d'** are considerably less soluble in organic solvents but they are highly soluble in water.

These two crude products were purified using reversed-phase chromatography with water and methanol as eluents.

Optimal reaction conditions for the complexation (such as solvent, temperature and time of reaction) were found for each system "chelating agent - metal ion".

We attempted to obtain *Re* complexes with ligands **3** using either FSA or $SnCl_2$ to reduce the perrhenate. FSA was found to be inactive, while $SnCl_2$ reduces the perrhenate quite effectively. No immediate changes were observed after mixing the initial reactants at room temperature in inert atmosphere. A brown precipitate starts to appear after heating at 60°C for 15 minutes. The precipitate was separated by centrifugation and washed with water giving products **12** with low yields varying from 12 to 25%. The product does not dissolve well in methanol and other organic solvents, which makes chromatographic purification and spectroscopic analyses in solution problematic. All attempts to purify the material on a reversed-phase column failed. TLC analysis of both precipitate and supernatant suggests that the compound, which forms the precipitate, is still present in the soluble fraction. Further purification of the product isolated from the supernatant was unsuccessful. It is unclear why the yields of the reactions are so low (as compared to the synthesis of the ^{99}Tc complexes) and why *Re* complexes are almost insoluble in water. This could be due to the formation of non-stoichiometric compounds or polymers with possible participation of tin ions. Another possibility is that the sulpho-group at 4-pyrrolic position is lost during complexation, which would lead to final products similar to lipophilic compounds **10**. It remains unclear why such de-sulphonation might occur

in this case; steric interference could be one of the causes. Nevertheless, it is obvious that the behaviour of rhenium is completely different from that of technetium in reactions with sulphonated compounds **3**.

We suggest that the metal binding of these new *Tc* and *Re* complexes occurs at the pyrrolic nitrogen and the sulphur, leaving a pendant uncoordinated pyrrolic (ligands **2d;3d,d'**) or phenolic (ligands **2a-c;3a-c**) ring. We have shown that the periphery of the ring can be modified to change the solubility of the subsequent *Tc* and *Re* complexes, while the central metal core remains the same.

All synthesised complexes were characterised by mass- and UV-visible spectroscopy, ^{1}H NMR, and ^{13}C NMR. Elemental analyses were performed when possible (i.e. for non-radioactive rhenium compounds).

The mass spectrum (SIMS, thioglycerol as matrix) of some water-soluble *Tc* complexes (for example **11c,d,d'**) did not contain the molecular ion peak but rather signals of the ligand. Similar problems with mass-spectroscopy for *Tc* complexes have been reported earlier (Schöster and Zeisler, 1997).

The UV-visible spectra of the ^{99}Tc and *Re* complexes show a broad peak approximately at 430 nm, which is indicative of complex formation. Two minor bands are present for some complexes (e.g. **9b, 10d, 12c**), which can be found at 509 nm and 628-696 nm and correspond to mono- and diprotonated oxo-group respectively. Overall, the UV-visible spectra of synthesised compounds differ from those of pure ligands. The characteristic peaks of the complexes are shifted towards longer wavelengths and are considerably broader. The absence of maxima at 244 and 289 nm, which are characteristic for TcO_4^-, confirms that the reduction was complete

and that other *Tc* products were formed.

Elemental analysis and NMR data suggest that synthesised complexes are isolated as solvates that have one or two molecules of methanol (or ethanol, depending on the solvent used) in the crystal structure. These results are consistent with the data discussed above for synthesised small transition metals complexes, which also mostly exist as solvates. The ^{1}H NMR spectra for compounds **9,10,11a-c** show no peak at 9-11 ppm, which corresponds to the pyrrolic *NH* hydrogen. Only one *NH* hydrogen peak should be observed for the metal complexes with 2,2'-dipyrrolylthione **9,10,11d-d'** around 11.8 ppm. This confirms the complex formation between metal ion and ligand molecule and its stability in solution.

Infrared (IR) spectra for *Re* complexes show strong bands at 900-1000 cm^{-1}, which is the range observed generally for oxo-groups (Barraclough *et al.*, 1959; Bélanger and Beauchamp, 1997). Interpretation of the spectra and peaks assignement are quite difficult in these regions because of high population of various bands, including strong absorbtion resulting from bending vibrations of aromatic rings of the ligands. Hydrophilic complexes have somewhat different IR spectra in this region comparing to lipophilic analogues. In case of sulphonated ligands, the reaction conditions could lead to dioxo compounds of the type $[ReO_2(\text{monoanionic ligand})_2]^-$, which can be distinguished by a strong *O=Re=O* band at 789-825 cm^{-1} in their IR spectra (Bélanger and Beauchamp, 1996). At general, stretching modes of dioxo compounds shift to lower frequency (768-895 cm^{-1}) if comparing to monooxo groups (Nugent and Mayer). A strong band should be observed at 956-962 cm^{-1} for *Tc=O* core (Tisato *et al.*, 1994).

A single crystal X-ray diffraction study was performed for the bis-(*p*-methoxyphenyl-2-pyrrolylthionato)rhenium **10b**. The results show the formation of a trinuclear three-layered structure wherein rhenium atoms are connected by oxygen bridges forming a $[O{=}Re\text{-}O\text{-}Re\text{-}O\text{-}Re{=}O]^{+7}$ axis and six bidentate ligands are coordinated around Re atoms in equatorial planes (***Figure 31***). Such complex structure is uncommon for rhenium. Only two similar examples can be found in the literature (Banbery *et al.*, 1990; Carrondo *et al.*, 1980), which also report the formation of a trinuclear rhenium complex with $O{=}Re\text{-}O\text{-}Re\text{-}O\text{-}Re{=}O$ axial backbone. The bilayered rhenium complexes with heterocyclic nitrogen-containing ligands are described in the literature more often (Bélanger and Beauchamp, 1997; Fortin and Beauchamp, 1998; Bélanger and Beauchamp, 1999; Hansen *et al.*, 2000).

Fractional atomic coordinates from the crystallographic study of $[Re_3O_4(C_{12}H_{10}NOS)_6]^{+1}[ReO_4]^{-1}\cdot 2CH_3CH_2OH$ have been deposited with the Cambridge Crystallographic Data Center. Selected bond lengths and angles are presented in ***Table 5*** (complete list can also be found in ***Supporting data, Part 2***). The structure of the complex is illustrated in ***Figure 31***.

The complex has an overall positive charge of +1 and is associated with an anion. We have established that the anion is ReO_4^-. It seems unlikely that the perrhenate ion could have survived in the presence of $SnCl_2$, but it is an ion, which does not lend itself to reduction easily even when an excess of the reducing agent is present. To our knowledge, a few similar cases, where ReO_4^- acts as a counter-ion to a main molecular cation, were described in the literature (Carrondo *et al.*, 1980; Cotton *et al.*, 1996). The overall charge of the complex (+1) can be explained if one

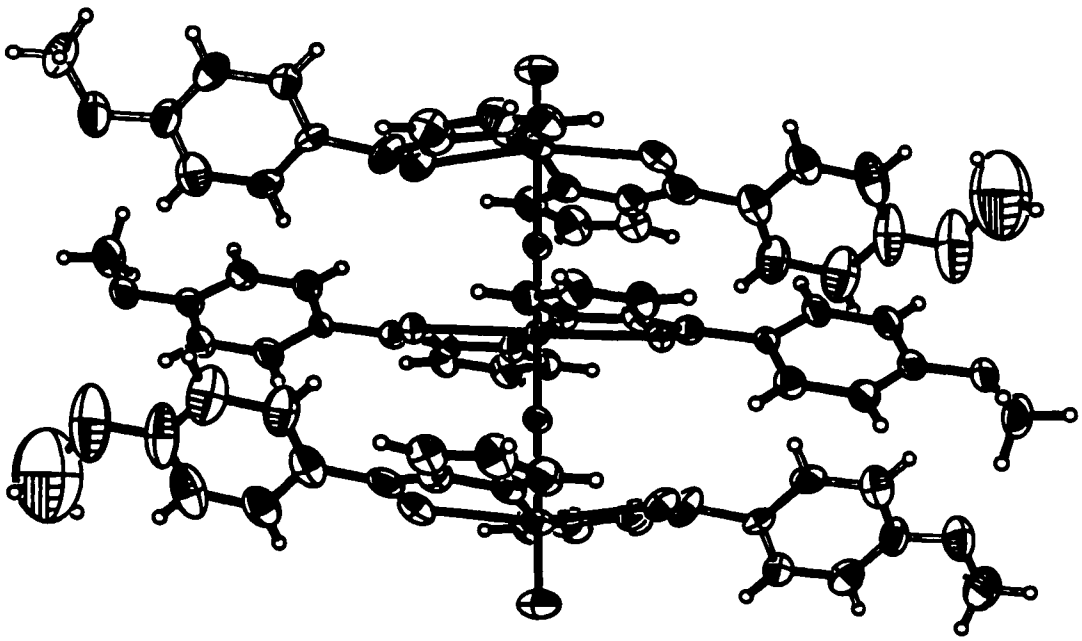

Side view

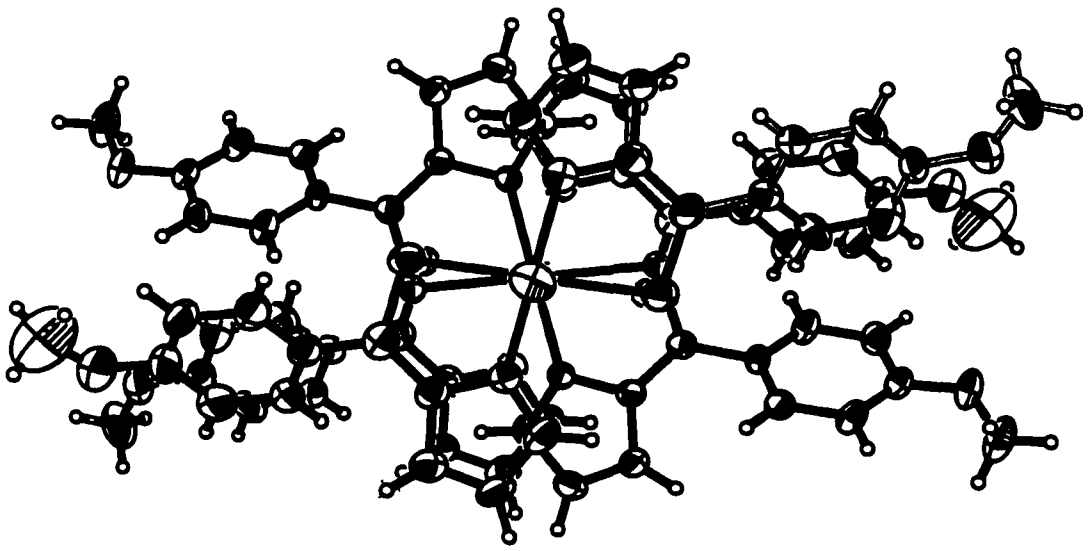

Top view

Figure 31. ORTEP drawing and numbering scheme for *Re* complex **10b**. Ellipsoids correspond to 30% probability

imagines the $[O{=}Re\text{-}O\text{-}Re\text{-}O\text{-}Re{=}O]^{+7}$ backbone as a structure containing three *Re*(V) centres, each of which coordinates two 2-pyrrolylthione ligands forming one covalent and one coordination bond with each centre. The coordination around each *Re* atom is octahedral, which is characteristic of d^2sp^3 hybridisation. Each molecule of the complex is also associated with two molecules of ethanol. These data confirm previously suggested solvatation from the results of NMR spectroscopy and elemental analyses.

The complex contains a near linear $[O{=}Re\text{-}O\text{-}Re\text{-}O\text{-}Re{=}O]^{+7}$ core; the central *-O-Re-O-* part of the molecule is perfectly linear (180°) and the deviation from the linearity is within 2.4° for the terminal parts of the structure. Also, the various lengths of the Re-O bonds suggest their different orders. Thus, the two terminal bonds are the shortest with a mean length of 1.6655(9) Å, whereas the bonds on the other side of the terminal

Table 5. Crystal data for rhenium complex $[Re_3O_4(C_{12}H_{10}NOS)_6]^{+1}[ReO_4]^{-1}\cdot 2CH_3CH_2OH$.

Compound	**9b**
Form	Plate
Colour	Red
Dimensions (mm)	0.27×0.12×0.04
Formula weight	2262.556
Crystal system	Monoclinic
Space group	*C*2/*c*
a (Å)	34.6651(2)
b (Å)	11.5694(1)
c (Å)	24.6839(2)
β (°)	128.0350(4)
V (Å^3)	7797.3(1)
Z	4
$D_{calc.}$ (Mg/m^3)	1.9274
μ (mm^{-1})	13.923
R^a ($R_w{}^b$)	0.0619 (0.1710)

[a] $R = \Sigma||F_o| - |F_c|| / \Sigma|F_o|$;

[b] $R_w = [\Sigma[w(F_o^2 - F_c^2)^2] / \Sigma[w(F_o^2)^2]]^{1/2}$

rhenium atoms are the longest with a mean of 2.082(6) Å. The lengths of the bonds on either side of the central rhenium atom are 1.779(6) Å. Therefore, the oxygen bridges of this structure are asymmetric. These data are similar to those reported for other trinuclear *Re* complexes. (Banbery *et al.*, 1990; Carrondo *et al.*, 1980)

The ligands of the terminal *Re* atoms are almost parallel and overlay one over another with an inter-planar distance of ca. 7.7 Å. Both ligands at each terminal are somewhat pushed from the *Re=O* bond to the centre of the molecule, thereby forming a kind of umbrella. The deviation is no more than 9.5° from the plane and can be attributed to the electronic configuration of the *Re=O* double bond. This explains the fact that the terminal rhenium atoms exhibit distortion from regular octahedral geometry. The ligands of the central *Re* atom are ideally planar, lying almost perpendicular to the *O=Re-O-Re-O-Re=O* axis at an angle of 90.8°. These central ligands are in a *trans*-configuration to the terminal ones. They do not overlay terminal ligands exactly but are displaced counter-clockwise by 6°. Such placement can be defined as favourable in order to accommodate sterically crowded ligands and to stabilise the system.

An interesting observation can be made from the ORTEP drawings (***Supporting data, Part 2, page S66-S67***). These two pictures represent the same molecule, in which the phenolic ring on the top right-hand side is disordered over two orientations (C147-C152 *vs.* C137-C142). This is an unusual disorder, which was found also in crystals of the ligand molecule **3b** (***Figure 30***).

A complicated structure of this compound partially explains its mass-spectrum. For example, the mass-spectrum of bulk compound **10b** contains peaks

corresponding to the fragments $[ReO(ligand)_2]^+$ and $[ReO_2(ligand)_2]^-$ and can be explained as a gain or loss of the bridge oxygen atom. The presence of the peaks with masses corresponding to the complexes of type metal-ligand$_2$ and metal$_2$-ligand$_4$ simultaneously (**9c**) also become not controversial. They can be considered as parts of the large layered structure with a higher molecular mass. The combustion analysis data are close enough to those calculated for the mononuclear 1:2 compound.

Summarising all obtained analytical and spectroscopic data, we could suggest that lipophilic *Re* complexes can be described most likely by the following schematic formulae: $Re^{V}O(OC_2H_5)$(monoanionic ligand)$_2$. The crystals of the trimer could then be a product resulting from slow hydrolysis to $Re^{V}O(OH)$(monoanionic ligand)$_2$ and

Table 6. Selected bond lengths and angles for **10b**.

bond	Distance (Å)	angle	degrees
Re1-O1	1667(8)	O1-Re1-N113	97.9(4)
Re1-N113	2.064(8)	O1-Re1-N133	99.5(3)
Re1-N133	2.066(3)	N113-Re1-N133	162.6(2)
Re1-O2	2.082(6)	O1-Re1-O2	178.2(4)
Re1-S111	2.384(3)	N113-Re1-O2	80.7(3)
Re1-S131	2.406(2)	N133-Re1-O2	81.96(19)
O2-Re2	1.779(6)	O1-Re1-S111	98.3(4)
S111-C111	1.704(10)	N113-Re1-S111	81.6(2)
C111-C112	1.371(11)	N133-Re1-S111	95.79(10)
C111-C117	1.481(9)	O2-Re1-S111	82.66(17)
C112-N113	1.404(11)	O1-Re1-S131	96.4(4)
C112-C116	1.431(12)	N113-Re1-S131	96.0(2)
N113-C114	1.327(11)	N133-Re1-S131	82.12(8)
C114-C115	1.412(13)	O2-Re1-S131	82.56(17)
C115-C116	1.339(12)	S111-Re1-S131	165.22(9)
C117-C118	1.3900	Re2-O2-Re1	177.6(3)
C117-C122	1.3900	C111-S111-Re1	99.5(3)
C118-C119	118.60(13)	C114-N113-Re1	132.4(7)
C119-C120	121.35(11)	C112-N113-Re1	119.6(6)
C120-O123	120.04(11)	C131-S131-Re1	99.47(6)
C120-C121	105.82(13)	O2-Re2-O2^{i}	179.996(2)
C121-C122	121.46(13)	O1-Re1-O2-Re2	28(16)
O123-C123	132.70(14)		

following condensation by formation of an oxo bridge.

We suggest that these results can be extrapolated to the complete family of newly synthesised *Re* complexes **10a-d**, since other characteristics of the compounds in this series look pretty much similar. Because the chemistry of ^{99}Tc is close in many aspects to that of *Re* and considering existence of high mass molecular ions in mass spectra of *Tc* complexes (e.g. **9a**), similar structures for the ^{99}Tc complexes **9a-d** can also be suggested. But this will have to be confirmed eventually using X-ray crystallography methods.

3.6. ***Labelling with technetium-99m***

The chemistry at the microscopic level differs from the chemistry at the macroscopic level. Even when a ^{99m}Tc complex is identified using spectroscopic and chromatographic methods, the synthetic route and the mechanism of reaction for ^{99m}Tc complexes giving high yield, high radiochemical and chemical purity at the trace level, may be different from those for corresponding "cold" ^{99}Tc complexes.

All ligands **2,3** were successfully labelled with ^{99m}Tc-pertechnetate (***Scheme 8***). Stannous tartrate $Sn(C_4H_4O_6)$ was selected as a reducing agent. Direct labelling was carried out in aqueous ethanol or water solution for lipophilic and hydrophilic compounds, respectively. Around 1 mCi of TcO_4^- was used for each synthesis, which means that TcO_4^- was present in solution in nanomolar concentrations. Since the ligand to metal ion ratio is significantly higher than in the synthesis of ^{99}Tc complexes, the reactions were complete in a few seconds. Crude complexes were

purified using normal phase silica gel Seppak cartridges.

The chemical identities of products were confirmed by comparing chromatographic mobilities to those of analogous ^{99}Tc compounds. The labelling efficiency varied from 78 to 96% (based on chromatographically separated ^{99m}Tc complexes).

Resulting water-soluble final products contained free ligand as an impurity. Since the latter does not produce any pharmacological effect and is not detectable during imaging, further purification is not mandatory for biological studies. Such a situation is common in the preparation of radiopharmaceuticals for nuclear medicine. However, if an higher degree of purity is needed, the complexes may be purified by reversed-phase HPLC.

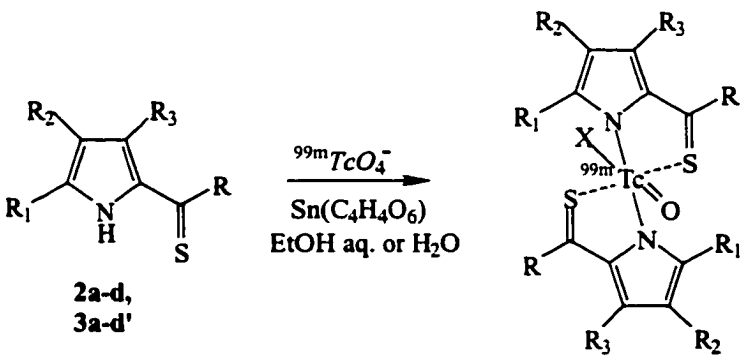

Scheme 8. Labelling with ^{99m}Tc

a: $R_1 = R_3 = H$, $R = -C_6H_5$

b: $R_1 = R_3 = H$, $R = -C_6H_4(OCH_3)$

c: $R_1 = R_3 = H$, $R = -C_6H_3(OCH_3)_2$

d: $R_1 = R_3 = H$, $R = -C_4H_2(SO_3Na)NH$

d': $R_1 = R_3 = H$, $R = -C_4H_3NH$

2,13: $R_2 = H$

3,14: $R_2 = -SO_3Na$

13: $X = -OC_2H_5$

14: $X = -OH$

The radiochemical purity of synthesised compounds was determined using thin layer chromatography (TLC) on commercially available paper strips impregnated with silica gel. In order to do this, we followed standard procedures available in nuclear medicine, which are used for quality control of technetium radiopharmaceuticals. Thereby, the absence of free pertechnetate and the reduced but uncomplexed technetium in preparation used for injection was assured. The radiochemical purity of the complexes exceeded 90% in all cases.

3.7. ***Biodistribution and pharmacokinetic studies***

Water-soluble compounds were prepared for injection in physiological saline solution, while lipophilic compounds were formulated using a water-based emulsion containing Cremophor-EL and propanol. The radioactive concentrations of these final solutions were adjusted according to specifications for biological studies and sterilised.

Biodistribution studies were performed on Balb/c mice bearing EMT6 mammary adenocarcinoma on each thigh. Complexes **13a,d** and **14** were tested for their biodistribution pattern and *in vivo* stability. (Selected results can be found in ***Supporting Data, Part 3.***)

After six hours following the injection of the radiopharmaceuticals, the blood radioactivity levels for the lipophilic complexes remain high. In contrast, their water-soluble analogues are mostly cleared from the blood.

It is worth noting that sulphonation of 2-pyrrolylthiones lowers blood and

plasma radioactivity retention, as well as radioactivity uptake by the liver, spleen, and lungs. On the other hand, kidney uptake of the complexes increases with the level of ligand sulphonation, showing the highest value for complexes with the dipyrrolylthione **3d**.

After six hours post-injection, renal uptake of the sulphonated radiopharmaceuticals **14d,d'** is still considerably high, which suggest that these compounds were trapped within the kidneys.

It should be noted that there is a major difference between the overall biodistribution of the compounds tested and that of pertechnetate, which is indicative of the strong binding of technetium to the ligands and *in vivo* stability of the synthesised complexes. However, there is still a significant accumulation of the lipophilic drugs (**13a,13d**) in thyroid, even though it is twice less than an accumulation of the free pertechnetate. It is likely that lipophilic complexes undergo partial decomposition after administration. This would release technetium species, which could be oxidised to free pertechnetate allowing for accumulation of radioactivity in the thyroid. For hydrophilic complexes thyroid accumulation is much less and comparable with that of kidney. Partial desintegration of the complexes might occur, which would explain the thyroid uptake. The results show clearly that hydrophilic complexes are much more stable than lipophilic analogues.

The biodistribution study conducted shows that 2-pyrrolylthiones are good chelating agents for ^{99m}Tc. Their biological behaviour is mostly influenced by their lipophilicity. Variations in the ligand periphery change the biological properties of the complexes. Because there was a significant kidney uptake of the sulphonated

Table 7. Percent of the injected dose per gram of tissue (average (standart error of the mean))

Compound	Brain	Tumor	Thyroid	Blood	Kidneys	Spleen	Lungs	Plasma	Skin	Muscle	Fat	Liver	Stomach
TcO4-	0.03 (0.00)	0.72 (0.08)	436.27 (37.72)	1.29 (0.12)	1.30 (0.10)	0.41 (0.03)	0.83 (0.07)	2.56 (0.37)	2.74 (0.04)	0.18 (0.02)	0.38 (0.08)	1.48 (0.08)	8.54 (1.07)
	0.30 (0.03)	2.40 (0.03)	206.05 (54.53)	11.00 (0.61)	5.38 (0.45)	3.31 (0.26)	5.21 (0.52)	17.28 (1.21)	1.03 (0.18)	0.45 (0.06)	0.93 (0.25)	16.53 (0.78)	
14a	0.03 (0.00)	1.43 (0.17)	81.94 (10.36)	1.53 (0.11)	21.80 (1.88)	0.87 (0.06)	1.69 (0.45)	2.27 (0.20)	1.19 (0.09)	0.34 (0.04)	0.94 (0.21)	4.87 (0.41)	1.93 (0.31)
14b	0.06 (0.00)	1.45 (0.37)	62.41 (7.20)	2.09 (0.11)	17.39 (1.31)	0.98 (0.04)	1.39 (0.13)	2.89 (0.25)	1.26 (0.06)	0.36 (0.03)	0.87 (0.04)	4.22 (0.19)	2.01 (0.41)
14c	0.04 (0.00)	1.91 (0.09)	61.21 (5.55)	1.94 (0.06)	18.08 (1.57)	0.95 (0.02)	2.42 (0.81)	1.94 (0.06)	1.53 (0.14)	0.44 (0.09)	0.94 (0.09)	2.93 (0.08)	1.15 (0.13)
13d	0.27 (0.01)	2.34 (0.29)	200.37 (10.79)	8.02 (0.39)	6.97 (0.42)	3.38 (0.47)	5.27 (0.82)	9.32 (0.40)	1.60 (0.24)	0.46 (0.01)	1.17 (0.16)	15.04 (0.86)	(0.00)
14d'	0.04 (0.00)	2.14 (0.20)	25.10 (2.01)	1.45 (0.09)	18.67 (0.99)	0.93 (0.05)	1.61 (0.12)	2.13 (0.12)	3.90 (0.25)	0.47 (0.03)	0.82 (0.04)	3.33 (0.10)	0.96 (0.09)
14d	0.05 (0.01)	2.21 (0.13)	53.83 (6.04)	2.02 (0.08)	24.49 (2.24)	1.93 (0.06)	2.47 (0.24)	3.42 (0.24)	1.98 (0.13)	0.52 (0.04)	1.00 (0.10)	8.29 (0.53)	1.50 (0.12)

complexes, we studied their pharmacokinetics in more detail. Rapid accumulation and slow clearance of these compounds from renal tissue prompted us to compare their properties with those of the conventional kidney imaging radiopharmaceutical ^{99m}Tc-dimercaptosuccinate (^{99m}Tc-DMSA, Succimer Injection). Although ^{99m}Tc-DMSA is the renal radiopharmaceutical currently used, it present some disadvantages in terms of clinical applications. The long time to reach optimal renal uptake results in the fact that the best contrast imaging is achived several hours postinjection. The slow excretion leads to the subsequent build-up of a considerable radiation dose. A new radiopharmaceutical that could reach peak uptake rapidly and clear quickly would represent a significant advantage for patients.

The water-soluble complexes of ^{99m}Tc **14d,d'** with mono- and disulphonated dipyrrolylthiones were administered to a group of 3 male Sprague and Dawley rats and scintigraphic images (***Figure 32***) were taken with γ-camera. The kidney images are better resolved with compound **14d** (***Figure 32***, B) than with **14d'** (***Figure 32***, C), where the liver is still apparent. The kidneys are well visualised with both, **14d** and ^{99m}Tc-DMSA (***Figure 32***, A): the outer area of the cortex appears as a dark band delineating the kidneys whereas the medulla is greyish. However, the innermost part of the kidneys (kidney pelvis, calyx area), where the urine is collected, is well defined with the ^{99m}Tc-DMSA, which is not the case for **14d**.

Analysis of the activity curves (***Figure 34***) suggests that the kidney activity reaches a plateau more rapidly with compound **14d** as compared to ^{99m}Tc-DMSA, which is an advantage of the new complex.

Comparison of the biodistribution at 1 hour post-injection (***Figure 33***) for the

tested compounds shows that ^{99m}Tc-DMSA is more rapidly cleared from the blood, followed by **14d** and **14d'** (heart area was used as a measure of blood radioactivity). As far as the overall kidney uptake is concerned, ^{99m}Tc-DMSA shows the highest activity followed by **14d** and **14d'**, which show similar values. For kidney uptake, only the left kidney was considered because the right kidney lies under the liver. The best excretion rate, as evaluated by measuring the activity found in the bladder, was obtained with **14d**.

The renal retention is greater in the cortex that in the medulla for the newly synthesised drugs, particularly for compound **14d**. This may be due to the binding of the radiopharmaceuticals to the proximal or distal convoluted tubules, which are primarily located in the renal cortex.

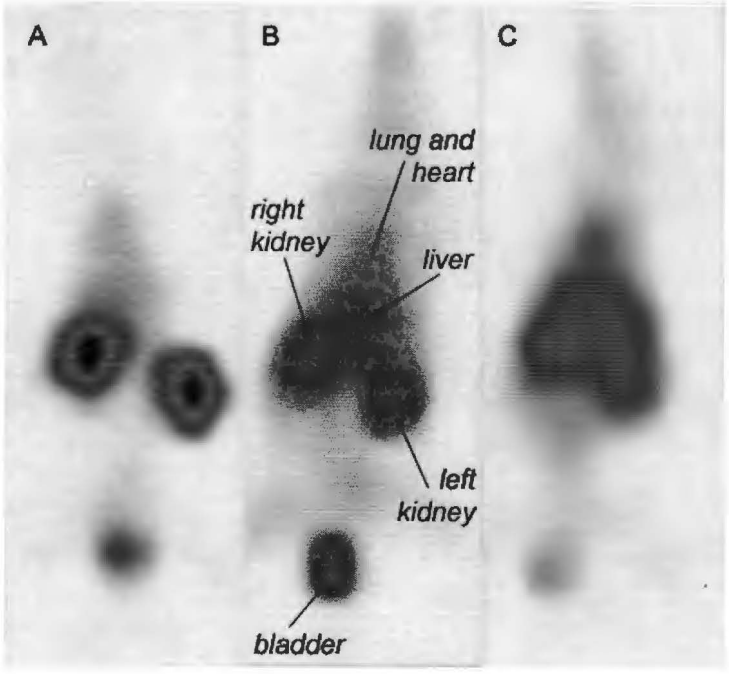

Figure 32. Scintigrafic images

A - with ^{99m}Tc-DMSA; **B** - with complex **14d**; **C**- with complex **14d'**

It is established that ^{99m}Tc-DMSA is excreted in the urine *via* glomerular filtration and tubular secretion. We suggest that compound **14d** and **14d'** are also excreted via glomerular filtration and tubular secretion. Glomerular filtration is a passive diffusion of substances through glomeruli. It is selective only with respect to the molecular size of the substances filtered. Tubular secretion is an active transport mechanism mediated by a carrier system. A saturation of the carriers might occur when concentration of the substances competing for the transport is high.

When glomerular filtrate enters the proximal tubule, the non-ionised forms of weak electrolytes may readily diffuse back into the circulation whereas the ionised or charged forms are trapped in the tubular urine and excreted. The extent to which the organic acids or bases are eliminated in the urine following secretion is dependent on their degree of ionisation within the tubular urine: the more ionised the compound is

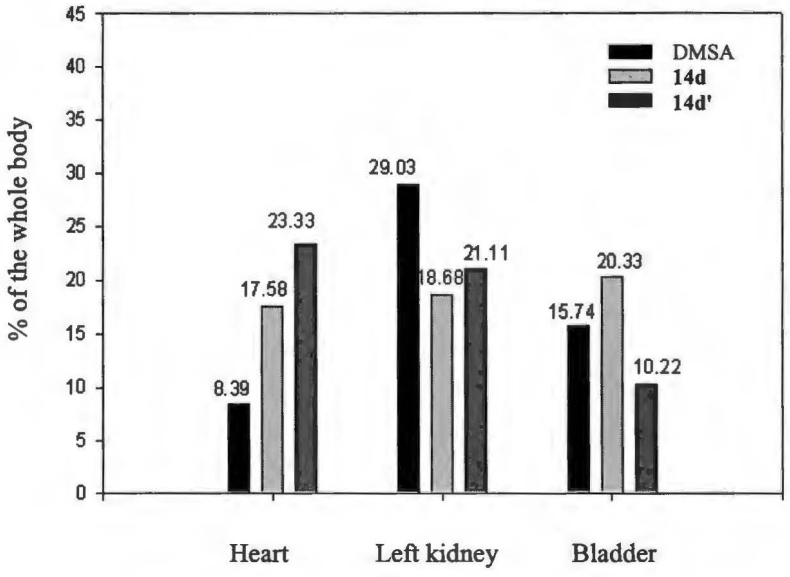

Figure 33. Biodistribution at 1 hour post-injection

– the less reabsorbtion it undergoes. We believe that little or no reabsorption occur for complexes **14d** and **14d'**, because they are salts of highly ionised acids.

It is possible that the affinity of **14d** to the carrier system is higher than affinity of ^{99m}Tc-DMSA and that protein binding of **14d** is lower comparing with ^{99m}Tc-DMSA.

The overall pharmacokinetics suggests that compound **14d** is comparable and in certain aspects superior to ^{99m}Tc-DMSA as a potential kidney scanning agent. Due to the very limited scope of animal studies that have been undertaken so far, the clinical advantages of this compound are not obvious. Our proposed next step would be to study biodistribution and pharmacokinetics of the compounds **14d** and **14d'** using other animal models. A series of specific biological test should be performed also to establish precisely protein binding rate for these novel potential radiopharmaceuticals and to determine extension to which these compounds are excreted by tubular secretion mechanism.

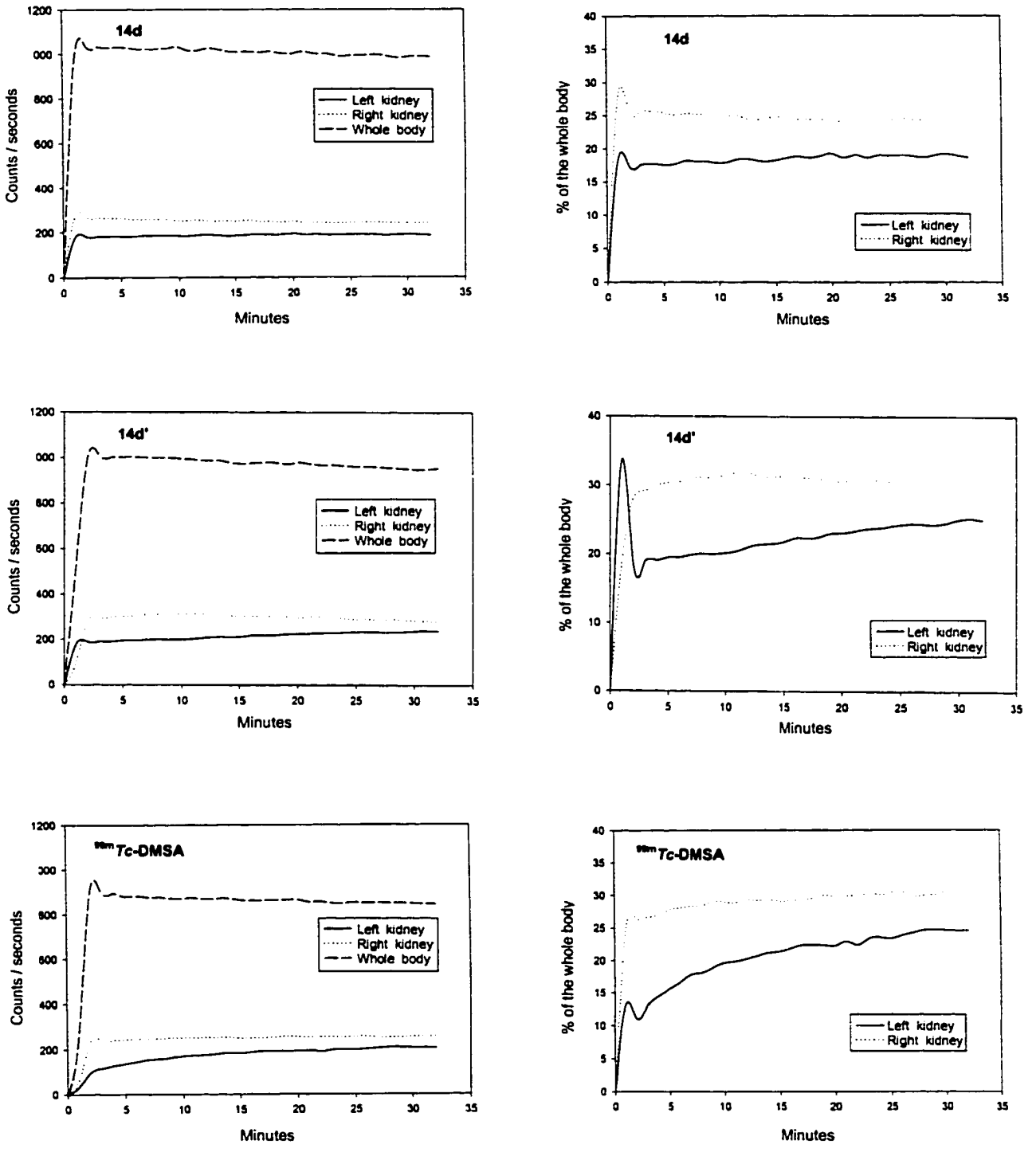

Figure 34. Activity curves for compounds **14d**, **14d'**, and ^{99m}Tc-DMSA.

Results are presented in counts per second and in percents of radioactivity of the whole body. Analysis of the activity curves suggest that the kidney activity reaches a plateau more rapidly with compounds **14d** and **14d'** as compared to ^{99m}Tc-DMSA, which is an advantage of the new complexes.

CONCLUSIONS

We have synthesised several lipophilic 2-pyrrolylthiones featuring methoxyphenyl substituents.

These compounds, along with 2,2'-dipyrrolylthione and phenyl-2-pyrrolylthione, were used as precursors for the synthesis of a series of new water-soluble analogues, i.e. sulphonated 2-pyrrolylthiones.

The chemical properties of these compounds were studied, particularly as potential chelating agents for transition metal ions, including technetium and rhenium. It was found that physical and chemical properties of the potential ligands are highly dependent on substituents in the outer periphery of the molecule. For instance, the solubility of lipophilic compounds in organic solvents and their chromatographic mobility change significantly from one ligand to another within the series. As for the synthesised sulphonated analogues, their solubility in water ranges from highly hydrophilic to amphiphilic. Thus, we have shown that the desired degree of solubility of 2-pyrrolylthiones can be achieved through the introduction of selected substituents.

A number of small-ion-radii transition metals were used in reactions with 2-pyrrolylthiones. All resulting complexes were stable and easy to synthesise using developed procedure. Despite the fact that all the sulphonated 2-pyrrolylthiones are highly soluble in water, the resulting metal complexes have different lipophilicity. Some of the nickel and copper complexes are not readily soluble in water but instead dissolve in methanol.

Technetium and rhenium complexes with 2-pyrrolylthiones were successfully prepared. ^{99}Tc and non-radioactive rhenium complexes were used to establish the chemical structures of the new compounds and to characterise them as well as to study their properties. A general complexation procedure was developed using stannous chloride as a reductant.

The resultant complexes are chemically stable compounds and can be kept for months in sealed vials. Rhenium complexes are more sensitive to air oxidation but they still can be stored for up to a few months without significant decomposition.

We found that the new 2-pyrrolylthiones, either lipophilic or water-soluble, are good ligands for a wide range of transition metals, rhenium and technetium. We have shown that the periphery of these ligands can be modified easily in order to add various specific properties to the final complexes. The suitability of these novel ligands as chelators for radiometals, such as the isotopes of technetium and rhenium, was confirmed.

In order to obtain new radioactive complexes, all synthesised 2-pyrrolylthiones were labelled directly with technetium-99m.

It was found that the biodistribution pattern of the new ^{99m}Tc-complexes greatly depends on their lipophilicity. Gradual chemical changes in the ligand periphery allow for fine-tuning of the biological properties of the corresponding technetium complexes.

Selected ^{99m}Tc-compounds were tested in rats to study their biodistribution and pharmacokinetics. One of the newly synthesised complexes (**14d**) showed promise as a radiopharmaceutical agent for kidney imaging. An overall

pharmacokinetic study showed that this novel compound is comparable to ^{99m}Tc-DMSA in terms of delineating a rat's kidney and is more favourable in terms of radiation doses absorbed: it reaches the maximum kidney uptake rapidly and clears quickly, which is a significant improvement. Due to the very limited scope of animal studies that have been undertaken so far, the clinical advantages of this compound are not obvious. Our proposed next step would be to study biodistribution and pharmacokinetics of the compound **14d** using other animal models. A series of specific biological test should be performed also to establish protein binding rate for this novel potential radiopharmaceutical and to determine extension to which this compound is excreted by tubular secretion mechanism.

Finally, we have discovered that novel 2-pyrrolylthiones could provide a new versatile class of radiopharmaceuticals for medical imaging, wherein the periphery of the molecule can be modified with various substituents, including biomolecules, while preserving the same central core.

Future research with various substituted 2-pyrrolylthiones, including testing of radioactive metal complexes in different animal models, could identify other new compounds with specific properties that might be useful in nuclear medicine.

The substituted pyrrolylthione ligands might well be used in various biological, medical, and other applications wherein chelators have an important role.

ACKNOWLEDGMENTS

I would like to thank Prof. Johannes E. van Lier for the opportunity to study at his laboratory, for his advice and encouragement, and overall for kind relationship.

I would like to thank Prof. Svetlana V. Kudrevich for her precious advice and informative discussions, for being the co-director of this project, and for her friendly encouragement and help.

I am very grateful to Dr. Jacques Rousseau for carrying out biological studies and for informative discussions on biological results.

I thank Dr. Normand Pothier, Ms. Sylvie Bilodeau, Dr. Phan Viet Minh Tan, Mr. Alain Desponts, Ms. Francine Bélanger-Gariépy, Mr. Gaston Boulay, Mr. Michael Evans for collecting NMR, IR, X-ray diffraction, mass-spectrometry data.

I would like to thank the staff of the Division of Biomedical Engineering (GBM) of the Université de Sherbrooke for the precious help with recovery of lost information from the crushed computer.

I thank the professors of the Department of Nuclear Medicine and Radiobiology for excellent courses and students of this Department for friendship.

I appreciate help of Prof. Lyudmila Alikberova in search for the older paper by Mendelejeff on the periodic law of chemical elements.

I thank Prof. Richard Wagner, Prof. André Beauchamp, and Prof. Claude Spino for the very helpful critical reviews of this manuscript.

I am grateful to my husband, Vitali Selivanov, for the review and critical comments of my thesis.

CHAPTER 3: Experimental

4.1. ***Chemistry***

4.1.1. Materials and methods

Melting points were determined on a Fisher-Johns Melting Point Apparatus and are uncorrected.

The ultraviolet - visible spectra were determined with a Hitachi U-2000 spectrophotometer.

Silica gel for preparative column chromatography was Silica gel 60 from EM Science, 0.063-0.200 nm particle size (70-230 mesh ASTM).

Reversed-phase silica gel for preparative column chromatography was C_{18} Bonda-Pac from Waters, 37-55 μm particle size, 125 Å pores.

TLC glass plates coated with C18-silica gel were TECHWARE, RPSF reversed phase hydrocarbon impregnated in silica gel W/UV254, layer thickness 250 μm, 5x20 cm, from Analthech. Silica gel coated polyester was POLYGRAM SIL G/UV_{254} for TLC, layer thickness 200 μm, particle size 5-17 μm, pore size 60 Å, 20x20 cm, from MACHEREY-NAGEL (Germany).

Infrared spectra were carried out with help of Mr. Alain Desponts of Department of Chemistry of the Université de Sherbrooke using *KBr* pellets for hydrophilic compounds and $CHCl_3$ solution for lipophilic compounds.

All the commercial reagents used were of reagent grade or higher, and were

used as received without further purification.

NMR data were recorded on a Bruker Ac-300 300 MHz nuclear magnetic resonance spectrometer by Dr. Normand Pothier from Department of Chemistry of the Université de Sherbrooke and on a 600 MHz apparatus by Ms. Sylvie Bilodeau and Dr. Phan Viet Minh Tan of the Université de Montréal. Results are given in parts per million (ppm) on the scale relative to tetramethylsilane (TMS) as internal or external standard.

Elemental analyses were performed at Guelph Chemical Laboratories (Guelph, ON, Canada) and at the Department of Chemistry, Université de Montréal (Montreal, PQ, Canada).

FAB (negative mode), SIMS, and MALDI mass spectrometry were done at the Department of Chemistry, University of British Columbia (Vancouver, BC, Canada) and by Mr. Michael Evans of the Department of Chemistry, Université de Montréal (Montreal, PQ, Canada). Either thioglycerol, 3-nitrobenzylalcohol (NBA) or glycerol-methanol mixture was used as matrices.

High performance liquid chromatography (HPLC) of products was done using a Waters Liquid Chromatograph fitted with a Waters RCM module. The chromatograph was equipped with a Nova-Pac Radial-Pac C_{18} cartridge of 8mm×100mm or 8mm×200mm size (particle size about 4 μm with pore size 60Å) to purify water-soluble compounds. They were eluted with a linear gradient running from 100 % of water or aqueous sodium phosphate buffer pH 5.0 (10mM) to 100 % of methanol (HPLC grade, Fisher Scientific) over a period of 30 minutes with a flow rate of 1 ml/minute. The chromatograph was equipped with a Nova-Pac Silica

cartridge of 8mm×100mm size (particle size about 4 μm with pore size 60Å) to purify lipophilic compounds. These were eluted with a linear gradient running from 100% chloroform to 100% methanol (both HPLC grade from Fisher Scientific) over 30 minutes with a flow rate of 1 ml/minute. Compounds were detected using an UV-Vis detector.

Radioactive doses were measured in an Accucal 2001 dose calibrator from Nuclear Pharmacy Inc. (Albuquerque, NM, U.S.A).

Scintigraphic images were recorded with a Starcam 4000i XRT Gamma camera, General Electric (Saint Albans, UK) equipped with a parallel medium energy high resolution collimator. Image analysis was performed on a Genie PNR model nuclear medicine dedicated computer General Electric (Saint Albans, UK).

The X-ray diffraction data were collected by Ms. Francine Bélanger-Gariépy of the Université de Montréal on a Bruker AXS SMART 2K/Platform diffractometer with graphite-monochromated Cu Kα radiation. Computations were carried out with SHELXS97, SHELXL96, and SHELXTL computer programs. Fractional atomic coordinates from the study have been deposited with the Cambridge Crystallographic Data Centre.

4.1.2. Safety: hazard compounds and reactions

Caution: ^{99g}Tc is a weak β-emitter ($t_{1/2}$ 2.2×10^5 yrs, β^- 0.3 MeV). ^{99m}Tc is a γ-emitter ($t_{1/2}$ 6 h, γ 140 keV). All studies using these radioisotopes were carried out

in laboratories approved for the use of radioactivity. Appropriate shielding screens used and radiation safety procedures were followed at all times.

Caution: Sulphur trioxide SO_3 is a highly hygroscopic volatile corrosive compound. Lawesson's reagent, thiophosgene, and phosphorus decasulphide P_4S_{10} are volatile and poisonous compounds. Gloves and appropriate masks should be worn for handling these chemicals in a well-ventilated fume hood.

4.1.3. Synthesis of the precursors

p-Methoxyphenyl-2-pyrrolylketone **(1b)**

This compound was prepared as described in the literature (Pesson *et al.*, 1966).

MW = 201.22

M.P. = 107-108°C (lit. 110-111°C)

3,4-Dimethoxyphenyl-2-pyrrolylketone **(1c)**

The procedure above was adapted for the synthesis of dimethoxyphenyl-2-pyrrolylketone. The Grignard derivative was prepared by slow addition of a pyrrole solution (0.7 ml, 0.01 mol) in dry ether (4 ml) to an etheral solution (5 ml) of ethylmagnesium bromide (from 0.24 g, 0.01 mol Mg; 1.50ml, 0.02 mol ethyl bromide) with stirring. The reaction mixture was heated to reflux for 30 minutes under nitrogen, then cooled. The Grignard reagent was added dropwise to a stirred solution of 3,4-dimethoxybenzoylchloride (2 g, 0.01 mol) in dry ether (5 ml) at 0°C.

The stirring was continued for 3 h at room temperature and the mixture was allowed to stand overnight. The reaction mixture was treated with saturated solution of NH_4Cl. Organic phase was separated, and the aqueous phase was extracted repeatedly with toluene. Organic extracts were combined and dried over $MgSO_4$. The solution was concentrated and chromatographed on silica gel using toluene as an eluent. The solvent was evaporated to dryness yielding 3,4-dimethoxyphenyl-2-pyrrolylketone as a pale yellow-green crystalline solid (2.13 g, 9.2 mmol, 92% yield).

MW = 231.25

M.P. = 82-83°C

LS-MS (IE), m/z = 231 (M^+)

UV-Vis ($CHCl_3$) λ_{max} (lg ε): 318 (4.20), 243 (3.88).

The single crystal X-ray diffraction data: $C_{13}H_{13}NO_3$, M_r = 231.244, orthorhombic, space group $Pca2_1$, a = 18.972(8) Å, b = 9.065(3) Å, c = 6.867(2) Å, V = 1181.0(7) Å^3, Z = 4, D_x = 1.3006 Mg/m^3. Cell parameters from 25 reflections: θ = 19.00-24.00°, μ = 0.766 mm^{-1}, T=293(2) K, block, pale grey-green, 0.76×0.36×0.21 mm.

1,4-dioxane-sulphur trioxide

1,4-Dioxane-sulphur trioxide was obtained using a method described by Bordwell and Rondestvedt. (Bordwell and Rondestvedt, 1950)

Briefly: 40g of sulphur trioxide were distilled into the cooled ethylene dichloride (1L). The resulting solution was cooled in an ice bath and the equivalent quantity of the 1,4-dioxane was added dropwise to the stirred sulphur trioxide solution. The 1,4-dioxanesulfotrioxide complex precipitated as fine granules and was

separated by filtration in a yield of 89%. This compound is unstable under atmospheric conditions and is susceptible to hydrolysis.

4.1.4. Synthesis of 2-pyrrolylthiones

***Phenyl-2-pyrrolylthione* (2a)**

The compound was obtained using a method described in the literature. (Lumbroso and Liégeois, 1984)

MW = 187.18

M.P. = 33-36°C (lit. < 40°C)

UV-Vis (*CHCl*$_3$), λ_{max} (lg ε): 527 (2.29), 392 (4.26), 316 (3.98),

(lit. (*MeOH*), λ_{max} (lg ε): 536 (2.33), 390 (4.75), 310 (4.41)).

LR-MS, m/z: 187 (M^+).

***p-Methoxyphenyl-2-pyrrolylthione* (2b)**

This compound was obtained using a method suggested in the literature. (Pesson *et al.*, 1966)

A stirred solution of *p*-methoxyphenyl-2-pyrrolylketone (4.02 g, 0.02 mol) in benzene (100 ml) was refluxed for 30 min under nitrogen. Tetraphosphorus decasulphide (4.44 g, 0.01 mol) was added in portions to the stirred solution over 30 min. The mixture was then allowed to react in an ultrasonic bath for 40 min. After removal of excess of P_4S_{10} by filtration, the solution was reduced under vacuum and the residue was chromatographed on silica gel. The column was eluted with toluene

and the first bright scarlet fraction was collected to yield p-methoxy-2-pyrrolylthione as a bright red solid (2.81 g, 0.013 mol, 65% yield).

MW = 217.29

M.P. = 97°C

^{1}H NMR ($CDCl_3$): 3.87 (s, 3H), 6.38-6.41 (m, 1H), 6.74-6.76 (m, 1H), 6.88-6.90 (m, 1H), 6.92-6.93 (m, 1H), 7.27-7.28 (m, 1H), 7.75-7.77 (m, 1H), 7.79-7.80 (m, 1H), 9.81 (s, 1H) ppm.

^{13}C NMR ($CDCl_3$): 55.38, 112.66, 113.17, 117.21, 129.57, 131.04, 139.20, 141.41, 162.37, 212.21 ppm.

IR spectra ($CHCl_3$): 3784, 3403, 2977, 2838, 2550, 1599, 1527, 1503, 1389, 1337, 1303, 1257, 1173, 1107, 1036, 961, 836 cm^{-1}.

UV-Vis ($CHCl_3$), λ_{max} (lg ε): 529 (2.69), 376 (4.38), 287 (3.57).

LR-MS, m/z: 217 (M^+).

Calculated for $C_{12}H_{11}NOS$: C, 66.34; H, 5.11; N, 6.45; S, 14.73;

found: C, 66.56; H, 5.18; N, 6.40; S, 14.42.

The single crystal X-ray diffraction data: $C_{12}H_{11}NOS$, M_r = 217.278, monoclinic, space group $P2_1/c$, a = 11.8386(1) Å, b = 11.9453(1) Å, c = 7.5061(1) Å, β = 98.676(1)°, V = 1049.33(2) Å^3, Z = 4, D_x = 1.3753 Mg/m^{-3}. Cell parameters from 11189 reflections: θ = 3.70-72.85°, μ = 2.490 mm^{-1}, T=293(2) K, block, dark red, 0.58×0.52×0.18 mm.

3,4-Dimethoxyphenyl-2-pyrrolylthione. **(2c)**

The method above gave 3,4-dimethoxyphenyl-2-pyrrolylthione with 45% yield. The compound was obtained as bright red oil, which subsequently crystallised. It is unstable at room temperature and is slowly oxidised by atmospheric oxygen.

MW = 247.31

MP = 88-90°C

^{1}H NMR ($CDCl_3$): 3.90 (s, 3H), 3.95 (s, 3H), 6.40-6.43 (m, 1H), 6.76-6.78 (m, 1H), 6.85-6.88 (m, 1H), 7.29-7.31 (m, 1H), 7.37-7.38 (m, 1H,), 7.40-7.42 (m, 1H,), 9.79 (s, 1H) ppm.

^{13}C NMR ($CDCl_3$): 56.04, 109.72, 112.77, 117.29, 122.58, 129.65, 139.28, 215.53 ppm.

IR spectra ($CHCl_3$): 3783, 3403, 2969, 2840, 2581, 1593, 1513, 1461, 1415, 1383, 1331, 1266, 1170, 1142, 1109, 1036 cm^{-1}.

UV-Vis ($CHCl_3$), λ_{max} (lg ε): 529 (2.59), 390 (4.29), 298 (3.59), 264 (3.90).

LR-MS, m/z: 247 (M^+).

Calculated for $C_{13}H_{13}NO_2S$: C, 63.14; H, 5.30; N, 5.66; S, 12.96;

found: C, 63.24; H, 5.29; N, 5.30; S, 12.85.

2,2'-Dipyrrolylthione **(2d)**

2,2'-dipyrrolylthione was obtained as suggested in the literature (Clezy *et al.*, 1970).

MW = 176.24

M.P. = 86-90°C (lit. = 96-98°C)

UV-Vis ($CHCl_3$), λ_{max} (lg ε): 404 (4.70), 302 (3.64),

(lit. ($CHCl_3$), λ_{max} (lg ε): 406 (4.56), 303 (3.47)).

4.1.5. Sulphonation of the 2-pyrrolylthiones

The general procedure. Solid 1,4-dioxane-sulphur trioxide (2 mmol) was gradually added to a stirred solution of 2-pyrrolylthione (1 mmol) in 1,4-dioxane (25 ml) under nitrogen atmosphere. The reaction mixture was allowed to stand for 10 min at room temperature. Next, the solvent was evaporated in a vacuum and the residue was redissolved in water (about 5 ml). The pH was brought to 3.6-4.6 upon addition of 1M solution of *NaOH*.

Acetone (40 ml) was added and the resulting precipitate was separated by centrifugation. The red supernatant was evaporated to dryness. The solid product was redissolved in water and chromatographed on reversed-phase silica gel with water as an eluent. Evaporation resulted in red crystalls, which were identified as sodium salt hydrate of the sulphonated 2-pyrrolylthione. Single sulphonated derivatives resulted in all cases except 2,2'-dipyrrolylthione where two products of sulphonation were found.

All synthesised sulphonated 2-pyrrolylthiones are highly soluble in water.

Phenyl-2-(4-sulpho)pyrrolylthione, sodium salt **(3a)**

Yield 50%.

MW = 307.31

^{1}H NMR (DMF-d_7): 6.75-6.76 (m, 1H), 7.45-7.48 (m, 2H), 7.50-7.60 (m, 2H), 7.66-7.69 (m, 2H), 11.81 (s, 1H) ppm.

^{13}C NMR (DMF-d_7): 116.19, 128.30, 128.81, 130.69, 130.82, 138.00, 162.60, 214.80 ppm.

IR spectra (*KBr*): 3364, 3121 (ν(*N-H*)); 1615 (δ(*C-H*)$_{ar.}$); 1591, 1531, 1458 (ν(*C-C*)); 1408, 1367 ($\nu_{as.}$(*S*(=*O*)$_2$)); 1320 (ν(*C-N*)); 1211 (ν(*C*=*S*)); 1155 ($\nu_{s.}$(*S*(=*O*)$_2$)); 1113; 1082 (ar.); 1059; 1041; 1026 (ar.), 968, 941, 852; 768, (γ(*C-H*), β-ring); 700, 667 (δ(*C-H*)); 644, 629, 617.

UV-Vis (H_2O), λ_{max} (lg ε): 513 (2.11), 382 (4.34), 320 (4.05), 215 (4.07).

LR-MS (SIMS), m/z: 266 (M^+).

Calculated for $C_{11}H_8NNaO_3S_2 \times H_2O$: C 42.99, H 3.28, N 4.56, S 20.86;

found: C 42.32, H 2.73, N 4.41, S 20.44.

p-Methoxyphenyl-2-(4-sulpho)pyrrolylthione, sodium salt **(3b)**

Yield 40%.

MW = 373.37

^{1}H NMR (DMF-d_7): 3.92 (s, 3H), 6.80-6.81 (m, 1H), 7.04-7.14 (m, 2H), 7.56-7.57 (m, 1H), 7.74-7.92 (m, 2H), 11.71 (s, 1H) ppm.

^{13}C NMR (DMF-d_7): 55.63, 113.61, 115.55, 129.72, 131.13, 131.27, 137.49, 139.94, 141.11, 213.22 ppm.

IR spectra (*KBr*): 3570 (hydrogen bonds); 3283 (ν(*N-H*)); 1597, 1531, 1504, 1460 (ν(*C-C*)); 1408, 1367 ($\nu_{as.}$(*S*(=*O*)$_2$)); 1310 (ν(*C-N*)); 1250 ($\nu_{as.}$(*C-O-C*)); 1159

($\nu_{s.}(S(=O)_2)$); 1117 (ar.); 1057; 1041; 1024 (ar., $\nu_{s.}(C\text{-}O\text{-}C)$), 950, 941, 860, 837 785 ($\gamma(C\text{-}H)$, β-ring); 671, 635 ($\gamma(C\text{-}H)$); 580.

UV-Vis (H_2O), λ_{max} (lg ε): 511 (2.35), 375 (4.40), 221 (4.03).

LR-MS (SIMS), m/z: 296 (M^+).

Calculated for $C_{12}H_{10}NNaO_4S_2 \times 3H_2O$: C 38.60, H 4.32, N 3.75, S 17.17;

found: C 38.75, H 3.63, N 3.69, S 17.38.

3,4-dimethoxyphenyl-2-(4-sulpho)pyrrolylthione, sodium salt **(3c)**

Yield 56%.

MW = 367.37

^{1}H NMR (DMF-d_7): 3.89 (s, 3H), 3.94 (s, 3H), 6.85-6.86 (m, 1H), 7.08-7.11 (m, 1H), 7.34-7.37 (m, 1H), 7.43-7.44 (m, 1H), 7.57-7.58 (m, 1H), 11.71 (s, 1H) ppm.

^{13}C NMR (DMF-d_7): 55.77, 55.89, 110.70, 113.48, 115.74, 122.60, 129.53, 129.67, 137.28, 139.94, 148.94, 152.69, 213.25 ppm.

IR spectra (*KBr*): 3443 (hydrogen bonds,$\nu(N\text{-}H)$); 3125 ($\nu(N\text{-}H)$); 1595, 1531, 1512, 1462, 1454 ($\nu(C\text{-}C)$); 1420, 1366 ($\nu_{as.}(S(=O)_2)$); 1331 ($\nu(C\text{-}N)$); 1265 ($\nu_{as.}(C\text{-}O\text{-}C)$); 1210 ($\nu(C=S)$); 1138 ($\nu_{s.}(S(=O)_2)$); 1043, 1016 ($\nu_{s.}(C\text{-}O\text{-}C)$); 941, 862, 762, 663, 635 ($\gamma(C\text{-}H)$); 478.

UV-Vis (H_2O), λ_{max} (lg ε): 508 (2.56), 382 (4.64), 264 (4.01), 221 (4.34), 197 (4.54).

LR-MS (SIMS), m/z: 326 (M^+).

Calculated for $C_{13}H_{12}NNaO_5S_2 \times H_2O$: C 42.50, H 3.84, N 3.81, S 17.45;

found: C 42.55, H 3.40, N 3.69, S 19.45.

The single crystal X-ray diffraction data: $C_{12}H_{16}NNaO_7S_2$, M_r = 373.368, orthorhombic, space group *Pnma*, a = 6.763(3) Å, b = 7.540(6) Å, c = 31.641(8) Å, V = 1613.5(15) Å^3, Z = 4, D_x = 1.5370 Mg/m^{-3}. Cell parameters from 25 reflections: θ = 20.00-25.00°, μ = 3.587 mm^{-1}, T=293(2) K, block, intense violet-pink, 0.57×0.53×0.27 mm.

2,2'-(4-Sulpho)dipyrrolylthione, sodium salt **(3d')**

This compound was obtained as a side product in sulphonation reaction of 2,2'-dipyrrolylthione **2d** with 12% yield.

MW = 314.31

^{1}H NMR (DMF-d_7): 6.37-6.39 (m, 1H), 7.00-7.07 (m, 2H), 7.37-7.43 (m, 2H), 11.47 (s, 1H), 11.63 (s, 1H), ppm.

^{13}C NMR (DMF-d_7): 111.67, 112.90, 115.62, 126.92, 128.92, 139.62, 195.26 ppm.

IR spectra (*KBr*): 3587, 3512 (hydrogen bonds); 3329, 3132 (ν(*N-H*)); 1631 (δ(*C-H*)); 1622 (δ(*N-H*)); 1529, 1462, 1404, 1350 (ν(*C-C*)); 1298, 1252 (ν(*C-N*)); 1211 (ν(*C=S*)); 1169 (ν(*S*(=*O*)$_2$)); 1121; 1099, 1059, 1028; 991, 945, 916, 879, 841, 752, 708, 677, 667, 631 (γ(*C-H*)); 586, 575, 542.

UV-Vis (H_2O), λ_{max} (lg ε): 397 (4.03), 224 (3.44).

LR-MS (SIMS), m/z: 255 (M^+).

Calculated for $C_9H_7N_2NaO_3S_2 \times 2H_2O$: C 34.39, H 3.53, N 8.91, S 20.40;

found: C 35.06, H 2.94, N 8.93, S 19.84.

2,2'-(4,4'-Disulpho)dipyrrolylthione, sodium salt **(3d)**

Yield 43%.

MW = 434.36

^{1}H NMR (DMF-d_7): 7.33-7.37 (m, 2H), 7.43-7.44 (m, 2H), 11.71 (s, 2H) ppm.

^{13}C NMR (DMF-d_7): 110.06, 112.90, 127.19, 136.38, 138.20, 195.72 ppm.

IR spectra (*KBr*): 3468, 3122 (ν(*N-H*)); 2951, 1631 (δ(*C-H*)); 1536, 1413, 1351 (ν(*C-C*)); 1218 (ν(*C=S*)); 1162 (ν(*S*(=*O*)$_2$)); 1112; 1048, 939, 916, 834, 817(γ(*C-H*)).

UV-Vis (H_2O), λ_{max} (lg ε): 389 (4.44), 222 (3.76).

LR-MS (SIMS, thioglycerol), m/z: 335 (M^+).

Calculated for $C_9H_6N_2Na_2O_6S_3\times3H_2O$: C 24.89, H 2.78, N 6.45, S 22.15;

found: C 24.62, H 2.32, N 5.76, S 20.84.

4.1.6. Synthesis of the cadmium, cobalt, copper, nickel, and zinc complexes with sulpho-2-pyrrolylthiones.

The general procedure. A solution of sulphonated 2-pyrrolylthione (3 mmol) in water (1 ml) was added to a solution of metal salt (acetate, 3.3 mmol) in water (1 ml). The colour of the reaction mixture changed rapidly.

Cd and *Co complexes*: The reaction mixture was chromatographed on reverse phase with water as an eluent. The resulting product was collected and the solvent was evaporated. The residual solid was dissolved in methanol (~ 2 ml) and then chromatographed on a normal phase column with methanol as an eluent. The single

main fraction was collected and evaporated to dryness giving the resulting complex in good yield (48-95 %). Synthesised complexes were than analysed.

Cu complexes **6a,6b** and *Ni complexes* **7a,7b,7c**: These complexes precipitate from the reaction mixture. A solvent was evaporated and the residual solid was re-dissolved in methanol and chromatographed on SiO_2. A yellow fraction was collected and dried to give a metal complex generally in good yields (45-93 %). Pure products were analysed. These compounds are poorly soluble in water and moderately soluble in methanol.

Cu complexes **6c,6d**: The colour of the reaction mixture changed from red to brown upon addition of the metal salt. Reversed-phase chromatography gave the desired products in good yields (68-82 %).

Ni complex **7d**: The colour of the reaction mixture changed from red to brown upon addition of the metal salt. Normal phase chromatography followed by reversed-phase chromatography produced the complex in moderate yield (58 %).

Zn complexes: A crude product was purified either on reverse phase with water as an eluent or on normal phase silica gel with methanol as an eluent. Single fractions of desired products were collected and evaporated to dryness. The yields were good (70-87 %).

In general, metal complexes of the **d** series are poorly soluble in methanol and other organic solvents. Water as solvent was used to dissolve these compounds for purification and analysis. Accordingly, reversed-phase chromatography was often used to purify such complexes.

1:2 Complex of cadmium with phenyl-2-(4-sulpho)pyrrolylthione (4a)

Fine orange-brown powder with a metallic shine resulted. Yield 95 %.

^{1}H NMR (DMF-d_7): 6.72-6.96 (m, 2H), 7.40-7.70 (m, 10H), 7.84-7.89 (m, 2H), 11.86 (bs, 1H), 11.99 (bs, 1H) ppm.

UV-Vis (H_2O), λ_{max} (relative intensity): 390 (1), 315 (0.61).

LR-MS (FAB, NBA), m/z: 645.5 (M^+).

Calculated for $Cd(C_{22}H_{15}N_2NaO_6S_4)\times 3H_2O$: C 36.65, H 2.94, N 3.89, S 17.79, Na 3.19;

found: C 37.81, H 2.87, N 3.94, S 16.38, Na 3.61.

1:1 Complex of cobalt with phenyl-2-(4-sulpho)pyrrolylthione (5a)

Dark red-brown powder with a metallic shine was obtained in 48 % yield.

^{1}H NMR (DMF-d_7): 6.57 (s, 1H), 6.88 (s, 1H), 7.10-7.13 (m, 2H), 7.22-7.24 (m, 2H), 7.56-7.67 (m, 4H), 7.81-7.94 (m, 4H) ppm.

UV-Vis (H_2O), λ_{max} (lg ε): 451 (4.54), 318 (4.79).

LR-MS (FAB), m/z: 322.9 (M^+)

Calculated for $Co(C_{11}H_7NO_3S_2)\times 2H_2O$: C 36.67, H 3.08, N 3.89, S 17.80;

found: C 38.00, H 3.24, N 3.91, S 17.85.

1:1 Complex of copper with phenyl-2-(4-sulpho)pyrrolylthione (6a)

Fluffy brown powder was collected in 77 % yield.

^{1}H NMR (DMF-d_7): 6.92 (s, 1H), 7.35 (s, 1H), 7.55-7.64 (m, 3H), 7.86-7.88 (m, 2H), 11.92 (m, 1H) ppm.

UV-Vis (H_2O), λ_{max} (lg ε): 450 (4.00), 347 (4.20).

LR-MS (FAB, NBA), m/z: 352.4 ($M^+ + Na$).

Calculated for $Cu(OCH_3)(C_{11}H_7NNaO_3S_2)$: C 37.65, H 2.63, N 3.66;

found: C 38.11, H 2.78, N 3.37.

1:1 Complex of nickel with phenyl-2-(4-sulpho)pyrrolylthione (7a)

A violet colloid resulted from the reaction. It dissolves well in methanol and is only moderately water-soluble. Dry complex is dark violet-bleu. Yield 47 %.

^{1}H NMR (DMF-d_7): 6.89 (s, 1H), 7.61 (m, 3H), 7.90 (s, 2H), 8.04 (s, 1H) ppm.

^{13}C NMR (DMF-d_7): 129.11, 132.38, 137.31 ppm.

UV-Vis (H_2O), λ_{max} (lg ε): 525 (3.78), 390 (4.36), 316 (4.50).

LR-MS (FAB), m/z: 325.1 (M^+)

Calculated for $Ni(OH)(C_{11}H_7NNaO_3S_2)$: C 36.30, H 2.22, N 3.85, S 17.62, Ni 16.12;

found: C 36.27, H 3.13, N 3.54, S 17.37, Ni 16.35

1:1 Complex of zinc with phenyl-2-(4-sulpho)pyrrolylthione (8a)

A compound of red-wine colour resulted. Yield 68 %.

^{1}H NMR (D_2O): 7.26-7.54 (m, 5H), 7.65-7.68 (m, 2H) ppm.

UV-Vis (H_2O), λ_{max} (relative intensity): 501 (0.009), 382 (1), 312 (0.63).

LR-MS (FAB, NBA), m/z: 329.4 (M^+).

Calculated for $Zn(OCH_3)(C_{11}H_7NNaO_3S_2)$: C 37.47, H 2.62, N 3.64;

found: C 40.23, H 3.02, N 3.41.

1:1 Complex of cadmium with p-methoxyphenyl-2-(4-sulpho)pyrrolylthione (4b)

Light-brown compound was collected in 77 % yield.

^{1}H NMR (DMF-d_7): 3.57-3.59 (m, 3H), 6.81-7.16 (m, 3H), 7.38-7.92 (m, 3H) ppm.

UV-Vis (H_2O), λ_{max} (lg ε): 390 (3.70).

Calculated for: $Cd(C_{12}H_9NNaO_4S_2)$: C 33.46, H 2.11, N 3.25, Na 5.34, S 14.89, Cd 26.10;

found: C 30.00, H 2.07, N 2.63, Na 5.20, S 15.30, Cd 26.01.

1:1 Complex of cobalt with p-methoxyphenyl-2-(4-sulpho)pyrrolylthione (5b)

Dark red-brown compound with a metallic shine was obtained. Yield 78 %.

^{1}H NMR (D_2O): 3.08-3.65 (m, 3H), 7.33-6.68 (m, 6H) ppm.

UV-Vis (H_2O), λ_{max} (lg ε): 384 (3.64).

LR-MS (FAB), m/z: 353.8 (M^+(1:1)), 671.8 (M^+(1:2)+*Na*).

Calculated for: $Co(OH)(C_{12}H_9NNaO_4S_2)$: C 36.56, H 2.56, N 3.55, Na 5.83, S 16.26, Co 14.95;

found: C 39.35, H 3.42, N 2.72, Na 6.44, S 16.81, Co 14.90

1:1 Complex of copper with p-methoxyphenyl-2-(4-sulpho)pyrrolylthione (6b)

Very fine brown powder was collected. Yield 45 %.

^{1}H NMR (D_2O): 3.57 (s, 3H), 7.39-6.91 (m, 6H) ppm.

UV-Vis (*MeOH*), λ_{max} (relative intensity): 458 (0.49), 381 (1).

LR-MS (FAB), m/z: 358.1 (M^+(1:1)), 675.7 (M^+(1:2)+*Na*).

Calculated for: $Cu(OH)(C_{12}H_9NNaO_4S_2)$: C 36.14, H 2.53, N 3.51, Na 5.76, S 16.08, Cu 15.93;

found: C 40.18, H 3.23, N 3.24, Na 5.96, S 17.09, Cu 16.08.

1:1 Complex of nickel with p-methoxyphenyl-2-(4-sulpho)pyrrolylthione (7b)

Dark brown solid was obtained in 49 % yield.

^{1}H NMR (DMF-d_7): 3.46 (br.s, 3H), 6.93 (br.s, 1H), 7.19-7.21 (m, 2H), 7.71 (br.s, 1H), 7.97-8.00 (m, 2H) ppm.

UV-Vis (*MeOH*), λ_{max} (lg ε): 607 (3.37), 531 (3.69), 406 (4.20), 357 (4.09).

LR-MS (SIMS, thioglycerol+methanol), m/z: 377 (M^+ + *Na*).

Calculated for: $Ni(OH)(C_{12}H_9NNaO_4S_2)\times 3H_2O$: C 32.17, H 3.60, N 3.13, Na 5.13, S 14.31, Ni 13.10;

found: C 33.14, H 4.07, N 3.13, Na 5.12, S 14.25, Ni 12.89.

1:1 Complex of zinc with p-methoxyphenyl-2-(4-sulpho)pyrrolylthione (8b)

Solid compound of the red-wine colour with a metallic shine resulted. Yield 87 %.

^{1}H NMR (D_2O): 3.58-3.64 (m, 3H), 6.66-6.88 (m, 3H), 7.41-7.59 (m, 3H) ppm.

UV-Vis (H_2O), λ_{max} (lg ε): 374 (3.87).

LR-MS (FAB, NBA), m/z: 365 (M^+(1:1)), 652.8 (M^+(1:2)).

Calculated for: $Zn(C_{12}H_9NNaO_4S_2)$: C 37.56, H 2.36, N 3.65, Na 5.99, S 16.71, Zn 17.04;

found: C 40.98, H 3.29, N 3.11, Na 6.12, S 16.51, Zn 17.23

1:1 Complex of cadmium with 3,4-dimethoxyphenyl-2-(4-sulpho)pyrrolylthione (4c)

A light-brown powder with a metallic shine was produced with 56 % yield.

^{1}H NMR (D_2O): 3.70-3.72 (m, 3H), 3.74-3.75 (m, 3H), 6.94-7.43 (m, 5H) ppm.

UV-Vis (H_2O), λ_{max} (relative intensity): 421 (1), 321 (0.90), 268 (0.51), 230 (0.97).

LR-MS (FAB, NBA matrix), m/z: 438.8 (M^+).

Calculated for $Cd(OH)(C_{13}H_{12}NO_5S_2)\times 3H_2O$: C 30.63, H 3.76, N 2.75, S 12.58, Na 0.00;

found: C 30.79, H 3.33, N 2.75, S 11.36, Na 0.03.

1:2 Complex of cobalt with 3,4-dimethoxyphenyl-2-(4-sulpho)pyrrolylthione (5c)

Dark brown powder with a metallic shine resulted. Yield 87 %.

UV-Vis (H_2O), λ_{max} (relative intensity): 383 (0.78), 322 (1), 268 (0.56), 231 (0.97).

LR-MS (FAB, NBA), m/z: 384.9 (M^+).

Calculated for $Co(C_{13}H_{12}NO_5S_2)_2\times 4H_2O$: C 39.85, H 4.12, N 3.57, Na 0.00, Co 7.52;

found: C 30.72, H 4.17, N 2.68, Na 0.10, Co 7.50.

1:1 Complex of copper with 3,4-dimethoxyphenyl-2-(4-sulpho)pyrrolylthione (6c)

Compound **6c** was dried using an oil pump evaporator. A fine almost black powder with a metallic shine resulted. Yield 82 %.

^{1}H NMR (DMF-d_7): 3.52 (m, 6H), 7.16-7.59 (m, 5H) ppm.

UV-Vis (H_2O), λ_{max} (relative intensity): 450 (shoulder), 323 (1), 235 (0.8).

LR-MS (FAB, NBA matrix), m/z: 389.9 (M^+).

Calculated for $Cu(OH)(C_{13}H_{12}NO_5S_2)\times 2H_2O$: C 35.25, H 3.87, N 3.16, Na 0.00;

found: C 35.45, H 4.10, N 3.12, Na 0.10.

1:1 Complex of nickel with 3,4-dimethoxyphenyl-2-(4-sulpho)pyrrolylthione (7c)

Very fine black powder was obtained. Yield 93 %.

MW = 407.03

^{1}H NMR (DMF-d_7): 3.98-4.00 (m, 6H), 7.01-7.59 (m, 5H), ppm.

UV-Vis (*MeOH*), λ_{max} (lg ε): 609 (4.25), 535 (4.55), 502 (4.53), 422 (4.94), 322 (4.67), 281 (4.78).

LR-MS (SIMS, glycerol+methanol), m/z: 407 ($M^+ + Na$).

Calculated for $Ni(C_{13}H_{11}NNaO_5S_2)$: C 38.36, H 2.72, N 3.44, S 15.75, Ni 14.42;

found: C 38.44, H 2.98, N 3.20, S 17.20, Ni 14.87.

1:1 Complex of zinc with 3,4-dimethoxyphenyl-2-(4-sulpho)pyrrolylthione (8c)

Thin dark-cherry layers of the compound **8c** resulted. Yield 72 %.

^{1}H NMR (D_2O): 3.71-3.75 (m, 6H), 6.93-6.96 (m, 2H), 7.27-7.43 (m, 3H) ppm.

UV-Vis (H_2O), λ_{max} (relative intensity): 393 (0.72), 322 (0.98), 268 (0.57), 232 (1).

LR-MS (FAB, thioglycerol matrix), m/z: 389.8 (M^+).

Calculated for $Zn(OH)(C_{13}H_{12}NO_5S_2)\times 4H_2O$: C 32.47, H 4.40, N 2.91, S 13.34, Na 0.00;

found: C 32.39, H 3.86, N 2.80, S 12.56, Na 0.13.

1:2 Complex of cadmium with 2,2'-(4,4'-disulpho)dipyrrolylthione (4d)

Thin dark red plates were collected. Yield 49 %

^{1}H NMR (D_2O): 7.03 (s, 4H), 7.19 (d, 1H), 7.33-7.38 (m, 1H), 7.43 (s, 4H), 11.51 (s, 1H) ppm.

UV-Vis (H_2O), λ_{max} (relative intensity): 389 (1).

LR-MS (FAB), m/z: 784.5(M^+)

Calculated for $Cd(C_9H_5N_2Na_2O_6S_3)_2\times 6H_2O$: C 22.08, H 2.26, N 5.72, Na 9.39;

found: C 23.25, H 2.42, N 5.88, Na 9.02.

1:2 Complex of cobalt with 2,2'-(4,4'-disulpho)dipyrrolylthione (5d)

Black solid compound was produced in 57 % yield

^{1}H NMR (DMF-d_7): 6.22-6.46 (m, 1H), 7.18-7.52 (m, 3H), 11.52 (s, 1H) ppm.

UV-Vis (H_2O), λ_{max} (relative intensity): 422 (1).

Calculated for $Co(C_9H_5N_2Na_2O_6S_3)_2\times 6H_2O$: C 23.36, H 2.40, N 6.05, Na 9.93;

found: C 23.36, H 2.50, N 3.87, Na 9.16.

1:1 Complex of copper with 2,2'-(4,4'-disulpho)dipyrrolylthione (6d)

Shiny black solid was obtained. Yield 68 %.

^{1}H NMR (D_2O): 7.03 (s, 4H), 7.19 (d, 1H), 7.33-7.38 (m, 1H), 7.43 (s, 4H), 11.52 (s, 1H) ppm.

UV-Vis (H_2O), λ_{max} (relative intensity): 469 (0.75), 419 (1).

Calculated for $Cu(OH)(C_9H_5N_2Na_2O_6S_3)\times H_2O$: C 22.62, H 1.69, N 5.86, Cu 13.30;

found: C 23.18, H 1.79, N 5.41, Cu 11.94.

1:1 Complex of nickel with 2,2'-(4,4'-disulpho)dipyrrolylthione (7d)

Black compound resulted. Yield 58 %.

^{1}H NMR (D_2O): 7.18 (m, 1H), 7.39 (s, 2H), 7.45 (m, 2H), 7.57 (s, 3H), 7.67 (m, 1H), 7.88 (s, 1H), ppm.

UV-Vis (H_2O), λ_{max} (relative intensity): 432 (1), 399 (0.92).

LR-MS (SIMS, glycerol+methanol), m/z: 437 ($M^+ + 2Na^+$)

Calculated for $Ni(OCH_3)(C_9H_5N_2Na_2O_6S_3)\times H_2O$: C 24.66, H 2.07, N 5.75, S 19.75.

found: C 24.40, H 2.44, N 5.76, S 20.35.

1:2 Complex of zinc with 2,2'-(4,4'-disulpho)dipyrrolylthione (8d)

Thin plates of light-brown colour were collected. Yield 70 %.

^{1}H NMR (DMF-d_7): 7.04 (s, 2H), 7.20-7.35 (m, 1H), 7.44 (s, 1H), 11.52 (s, 1H), ppm.

UV-Vis (H_2O), λ_{max} (relative intensity): 389 (1).

LR-MS (FAB), m/z: 458.1 ($M^+ - 4SO_3^- + 2Na^+$)

Calculated for $Zn(C_9H_5N_2Na_2O_6S_3)_2\times 4H_2O$: C 24.13, H 2.02, N 6.25, S 21.47, Zn 7.30;

found: C 24.46, H 2.01, N 5.74, S 18.50, Zn 7.26.

4.1.7. Synthesis of lipophilic technetium and rhenium complexes

General procedure. A solution of $SnCl_2$ (0.5 mmol) in 0.6 N *HCl* (5ml) purged with nitrogen was added to a solution of a 2-pyrrolylthione (0.5 mmol) in *EtOH* (100 ml) in a nitrogen atmosphere. Next, a solution of $KReO_4$ or $K^{99g}TcO_4$ (0.25 mmol) in water (10 ml) was added to the initial reactants. The reaction mixture was heated at 60°C for 15-30 minutes. The solvent was then evaporated and the residue was treated with a saturated aqueous solution of $KHCO_3$. The solid was separated by centrifugation and dissolved in an appropriate solvent for further purification by column chromatography.

Bis-(phenyl-2-pyrrolylthionato)rhenium (10a)

Repeated chromatography ($CHCl_3$) on silica-gel gave bis-(phenyl-2-pyrrolylthionato)rhenium in 40% yield.

M.W. = 619.77

^{1}H NMR (DMF-d_7): 6.38-6.78 (m, 1H), 7.06-7.30 (m, 1H), 7.53-7.97 (m, 6H) ppm.

^{13}C NMR (DMF-d_7): 121.73, 122.26, 127.91, 129.07, 130.35, 131.96, 132.25, 160.55 ppm.

IR spectra (*KBr*): 3422, 3058, 2927, 1723, 1533, 1480, 1441, 1381, 1359, 1295, 1240, 1197, 1183, 1159, 1135 1122, 1081, 1067, 1030, 999, 949, 896, 849, 817, 767, 699, 671, 645, 620, 601, 577, 483 cm^{-1}.

UV-Vis ($CHCl_3$), λ_{max} (lg ε): 454.5 (4.32), 333.5 (4.75).

LR-MS (SIMS, thioglycerol), m/z: 575 (M^+ - OC_2H_5).

R_f (SiO_2, *MeOH:CHCl₃=1:49*) = 1; (SiO_2, *MeOH:CHCl₃=0.5:99.5*) = 0.1.

Calculated for $ReO(OC_2H_5)(C_{11}H_8NS)_2$: C, 46.51; H, 3.42; N, 4.52; S, 10.35;

found: C, 46.63; H, 3.28; N, 4.31; S, 10.35.

Bis-(p-methoxyphenyl-2-pyrrolylthionato)rhenium (10b)

Normal phase column chromatography (0-2% *EtOH* in $CHCl_3$) followed by re-precipitation from hexane gave bis-(*p*-methoxyphenyl-2-pyrrolylthionato)rhenium in 69% yield.

M.W. = 679.82

^1H NMR ($CDCl_3$): 3.71-3.98 (m, 3H), 6.55-7.11 (m, 4H), 7.51-8.03 (m, 3H) ppm.

^{13}C NMR ($CDCl_3$): 55.68, 68.18, 114.43, 122.51, 128.83, 130.61, 130.89, 132.46, 162.44, 163.67 ppm.

UV-Vis ($CHCl_3$), λ_{max} (lg ε): 382 (4.53).

LR-MS (SIMS, thioglycerol), m/z: 635 (M^+ - OC_2H_5)

R_f (SiO_2, *MeOH:CHCl₃=1:49*) = 0.95; (SiO_2, *MeOH:CHCl₃=0.5:99.5*) = 0.1.

Calculated for $ReO(OC_2H_5)(C_{12}H_{10}NOS)_2$: C, 45.94; H, 3.71; N, 4.12; S, 9.43.

found: C, 47.09; H, 3.63; N, 3.82; S, 9.32.

The single crystal X-ray diffraction data:

$[Re_3O_4(C_{12}H_{10}NOS)_6]^{+1}[ReO_4]^{-1}\cdot 2CH_3CH_2OH$, M_r = 2262.556, monoclinic, space group C2/*c*, a = 34.6651(2) Å, b = 11.5694(1) Å, c = 24.6839(2) Å, β = 128.0350(4)°, V = 7797.3(1) Å^3, Z = 4, D_x = 1.9274 Mg/m^{-3}. Cell parameters from 29416 reflections: θ = 2.28-72.86°, μ = 13.923 mm^{-1}, T=293(2) K, plate, red, 0.27×0.12×0.04 mm.

Bis-(3,4-dimethoxyphenyl-2-pyrrolylthionato)rhenium (10c)

Normal phase chromatography (2-20% *EtOH* in $CHCl_3$) and reprecipitation from hexane afforded compound **10c** in 75% yield.

M.W. = 785.94

^{1}H NMR ($CDCl_3$): 3.92-3.99 (m, 3H), 4.01-4.05 (m, 3H), 6.61-6.63 (m, 1H), 6.70-6.73 (m, 1H), 7.10-7.13 (m, 1H), 7.24-7.28 (m, 1H), 7.40-7.42 (m, 1H), 7.74 (s, 1H) ppm.

^{13}C NMR ($CDCl_3$): 55.86, 56.13, 109.87, 110.23, 112.89, 113.39, 120.03, 123.47, 124.04, 126.94, 151.63, 158.76 ppm.

IR spectra (*KBr*): 3409, 3000, 2931, 2839, 2595, 2028, 1728, 1594, 1530, 1510, 1462, 1378, 1329, 1268, 1250, 1216, 1169, 1144, 1087, 1062, 1022, 990, 951, 923, 908, 871, 858, 808, 797, 765, 703, 664, 642, 613, 588, 544, 466 cm^{-1}.

UV-Vis ($CHCl_3$), λ_{max} (lg ε): 432 (4.28), 352 (4.13), 268 (4.20), 243 (4.24).

LR-MS (SIMS, thioglycerol), m/z: 695 (M^+ - OC_2H_5).

R_f (SiO_2, *MeOH:*$CHCl_3$*=1:49*) = 0.9; (SiO_2, *MeOH:*$CHCl_3$*=0.5:99.5*) = 0.3.

Calculated for

$ReO(OC_2H_5)(C_{13}H_{12}NO_2S)_2 \times C_2H_5OH$: C, 45.85; H, 4.49; N, 3.56; S, 8.16;

found: C, 46.73; H, 4.37; N, 3.56; S, 8.09.

Bis-(2,2'-dipyrrolylthionato)rhenium (10d)

A crude compound was dissolved in acetone and approximately 3 cm^3 of silica gel was added to the solution. The solvent was evaporated. A pure complex was obtained in 83% yield after column chromatography on SiO_2 using a mixture of chloroform:ethanol (95:5) as an eluent.

M.W. = 597.72

^{1}H NMR (DMF-d_7): 6.23-6.25 (m, 1H), 6.46-6.49 (m, 1H), 6.55-6.59 (m, 2H), 7.18-7.22 (m, 2H), 7.28-7.29 (m, 1H), 7.38-7.39 (m, 1H), 7.53-7.54 (m, 2H), 7.58 (s, 1H), 7.76 (s, 1H), 11.73 (s, 1H), 11.83 (s, 1H) ppm.

^{13}C NMR (DMF-d_7): 112.59, 118.62, 118.80, 119.12, 123.21, 123.57, 128.62, 155.11, 155.59, 180.33 ppm.

IR spectra (*KBr*): 3582, 3396, 3124, 3087, 2528, 1981, 1617, 1545, 1517, 1472, 1420, 1393, 1340, 1303, 1275, 1257, 1201, 1132, 1104, 1072, 1043, 1005, 992, 928, 911, 880, 816, 746, 702, 653, 597, 546, 467 cm^{-1}.

UV-Vis (*EtOH:DMF=50:1*), λ_{max} (lg ε): 628 (2.11), 425 (4.0), 301 (3.34).

LR-MS (SIMS, thioglycerol), m/z: 553 (M^+ - OC_2H_5).

R_f (SiO_2, *MeOH*) = 0.5-0.9.

Calculated for $ReO(OC_2H_5)(C_9H_7N_2S)_2$: C, 40.19; H, 3.20; N, 9.37; S, 10.73;

found: C, 40.72; H, 3.29; N, 9.10; S, 10.62.

Bis-(phenyl-2-pyrrolylthionato)technetium (9a)

Compound **9a** was obtained in 69% yield after purification on a normal phase silica gel column eluted with methanol.

M.W. = 486.50

^{1}H NMR ($CDCl_3$): 6.31-6.86 (m, 3H), 7.32-7.89 (m, 5H) ppm.

^{13}C NMR ($CDCl_3$): 92.92, 95.99, 99.05, 107.41, 111.51, 119.79, 125.52, 128.75, 129.36, 132.29 ppm.

UV-Vis ($CHCl_3$), λ_{max} (lg ε): 307 (4.35).

LR-MS (SIMS), m/z: 487 (M^+).

Bis-(p-methoxyphenyl-2-pyrrolylthionato)technetium (9b)

Compound **9b** was purified by column chromatography (2-30% *EtOH* in $CHCl_3$) followed by re-precipitation from hexane. Yield 41%.

M.W. = 546.55

^{1}H NMR ($CDCl_3$): 3.81-3.94 (m, 3H), 6.23-8.04 (m, 7H) ppm.

^{13}C NMR ($CDCl_3$): 55.40, 113.57, 130.01, 131.17, 132.21 ppm.

UV-Vis ($CHCl_3$), λ_{max} (lg ε): 696 (3.01), 368 (4.27).

LR-MS (SIMS), m/z: 547 (M^+).

Bis-(3,4-dimethoxyphenyl-2-pyrrolylthionato)technetium (9c)

Repeated purification by normal phase chromatography (eluent $CHCl_3$:*EtOH = 4:1*) and re-precipitation from hexane gave a fine black precipitate of compound **9c**. It was isolated in 43% yield.

M.W. = 606.61

^{1}H NMR (*$CDCl_3$*): 3.78-4.23 (m, 6H), 6.34-7.70 (m, 6H) ppm.

^{13}C NMR (*$CDCl_3$*): 56.05, 56.32, 110.09, 110.99, 111.57, 112.94, 121.63, 123.31, 123.75, 124.50, 126.04, 128.84, 130.89, 131.48 ppm.

UV-Vis (*$CHCl_3$*), λ_{max} (lg ε): 328 (4.23).

LR-MS (SIMS, thioglycerol), m/z: 607 (M^+), 1213 (M^+_2)

Bis-(2,2'-dipyrrolylthionato)technetium (9d)

Normal phase chromatography (0-30% *MeOH* in *$CHCl_3$*) gave pure **9d** complex in 89% yield.

M.W. = 464.46

^{1}H NMR (*DMF*): 6.28-6.53 (m, 2H), 7.17 (s, 1H), 7.25-7.31 (m, 1H), 7.51 (s, 1H), 8.35 (s, 1H), 11.74 (s, 1H) ppm.

^{13}C NMR (*DMF*): 109.97, 115.40, 120.48, 124.37, 127.45 ppm.

UV-Vis (*EtOH*), λ_{max} (lg ε): 429 (4.03).

LR-MS (SIMS), m/z: 465 (M^+).

4.1.8. Synthesis of water-soluble technetium complexes

General procedure. The *$SnCl_2$* (0.2 mmol) solution in 0.12N *HCl* (1 ml) was added to a solution of sulphonated 2-pyrrolylthione (0.2 mmol) in water (2 ml), which has been purged previously with nitrogen. After 5 minutes the solution of *$KTcO_4$* (0.1 mmol) in water (2 ml) was added to a reaction mixture, which soon became dark brown. It was further heated for 15-30 minutes at 60°C. According to the

chromatographical data, no free ligand was detected in a solution at that time. Next, the solvent was evaporated and each complex **11a-d** was purified as described below.

Bis(phenyl-2-(4-sulpho)pyrrolylthionato)technetium, sodium salt (11a)

Normal phase chromatography (eluent *MeOH*) gave the compound **11a** as dark brown solid in 75% yield.

M.W. = 690.58

^{1}H NMR (D_2O): 6.95-6.96 (m, 1H), 7.37-7.41 (m, 3H), 7.47-7.52 (m, 1H), 7.64-7.68 (m, 2H) ppm.

^{13}C NMR (D_2O): 112.64, 115.55, 120.47, 125.97, 128.68, 130.69, 193.13 ppm.

UV-Vis (H_2O), λ_{max} (relative intensity): 421 (0.44), 337 (1).

LR-MS (SIMS, thioglycerol): 649 (M^+)

Bis(p-methoxyphenyl-2-(4-sulpho)pyrrolylthionato)technetium, sodium salt (11b)

This compound was purified on a silica gel column, using methanol as an eluent. Yield 95%.

M.W. = 750.63

^{1}H NMR (D_2O): 3.64-3.69 (m, 3H), 6.87-6.94 (m, 3H), 7.38-7.39 (m, 1H), 7.66-7.69 (m, 2H) ppm.

^{13}C NMR (D_2O): 57.25, 115.61, 118.72, 127.00, 131.08, 133.21, 164.59, 187.95 ppm.

UV-Vis (H_2O), λ_{max} (relative intensity): 380 (shoulder), 311 (1).

LS-MS (SIMS, thioglycerol): 728 (M^++Na^+)

Bis(3,4-dimethoxyphenyl-2-(4-sulpho)pyrrolylthionato)technetium, sodium salt (11c)

Normal phase chromatography (eluent: methanol) gave complex **11c** in 86% yield.

M.W. = 810.69

^{1}H NMR (*D_2O*): 3.64-3.66 (m, 6H), 6.75-6.79 (m, 1H), 6.88 (s, 1H), 7.19 (s, 1H), 7.22-7.26 (m, 1H), 7.36-7.37 (m, 1H) ppm.

^{13}C NMR (*D_2O*): 57.24, 57.51, 112.38, 113.09, 118.42, 126.09, 126.88, 129.46, 130.95, 131.85, 149.39, 153.92, 177.47, 187.08, 196.87 ppm.

UV-Vis (*H_2O*), λ_{max} (relative intensity): 321 (1), 390 (shoulder).

LS-MS (SIMS, thioglycerol): 790 (M^++*Na^+*)

Bis(2,2'-(4,4'-disulpho)dipyrrolylthionato)technetium, sodium salt (11d)

This compound was dissolved in water and purified on a reversed-phase (C_{18}) preparative column using water as an eluent. The main dark brown fraction was collected and dried. Yield 95%.

M.W. = 872.62

^{1}H NMR (*D_2O*): 7.20 (d, 2H), 7.35 (d, 2H)

^{13}C NMR (*D_2O*): 115.34, 125.67, 128.55, 130.36, 175.27 ppm.

UV-Vis (*H_2O*), λ_{max} (relative intensity): 400 (0.55), 330 (1).

Bis(2,2'-(4-sulpho)dipyrrolylthionato)technetium, sodium salt. (11d')

The crude compound was dissolved in methanol and purified on silica gel column (eluent *EtOH*). A brown fraction was collected and stripped of the solvent.

Compound **11d'** was obtained in 82% yield.

M.W. = 668.54

^{1}H NMR (D_2O): 6.96-6.97 (m, 1H), 7.35-7.53 (m, 3H), 7.66-7.69 (m, 2H) ppm.

^{13}C NMR (D_2O): 97.51, 126.53, 129.16, 129.54, 131.06, 133.47 ppm.

UV-Vis (H_2O), λ_{max} (relative intensity): 421 (0.59), 337 (1).

4.1.9. Synthesis of water-soluble rhenium complexes

General procedure. The $SnCl_2$ (0.2 mmol) solution in 0.12N *HCl* (1 ml) was added to a solution of a sulphonated 2-pyrrolylthione (0.2 mmol) in water (2 ml), which had been purged previously with nitrogen. After 5 minutes the solution of $KReO_4$ (0.1 mmol) in water (2 ml) was added to a reaction mixture, which was further heated for 15 minutes at 60°C. A fine brown precipitate resulted. The end of the reaction was monitored using TLC. A precipitate was collected by prolonged centrifugation (2 hours). It was washed with water and dried.

Bis(phenyl-2-(4-sulpho)pyrrolylthionato)rhenium (12a)

Yield 12%.

M.W. = 751.83

IR spectra (*KBr*): 3405, 2923, 1703, 1630, 1593, 1535, 1474, 1443, 1354, 1298, 1227, 1176, 1155, 1046, 1025, 1006, 1000, 949, 892, 876, 818, 809, 796, 765, 717, 664, 645, 627, 593, 506 cm^{-1}.

UV-Vis (H_2O), λ_{max} (lg ε): 509 (0.82), 458 (0.89), 393 (0.91), 380 (0.91), 362 (1).

LR-MS (MALDI), m/z: 736 (M^+- *OH*), 759 (M^+ - *OH* + *Na*).

Bis(p-methoxyphenyl-2-(4-sulpho)pyrrolylthionato)rhenium (12b)

Yield 25%.

M.W. = 811.89

IR spectra (*KBr*): 3582, 2931, 1597, 1526, 1506, 1461, 1427, 1401, 1354, 1312, 1293, 1272, 1165, 1150, 1046, 1026, 941, 917, 883, 839, 810, 789, 776, 706, 683, 659, 635, 589, 503 cm^{-1}.

LR-MS (MALDI), m/z: 796 (M^+- *OH*), 818 (M^+ - *OH* + *Na*), 840 (M^+ - *OH* + 2*Na*).

Bis(3,4-dimethoxyphenyl-2-(4-sulpho)pyrrolylthionato)rhenium (12c)

Yield 21%

M.W. = 871.94

IR spectra (*KBr*): 3409, 2443, 1638, 1550, 1522, 1424, 1388, 1342, 1273, 1255, 1144, 1045, 942, 911, 875, 856, 825, 708, 659, 571, 559 cm^{-1}.

UV-Vis (H_2O), λ_{max} (relative intensity): 696 (0.13), 509 (0.72), 435 (1), 378 (0.90), 362 (0.98).

LR-MS (MALDI), m/z: 855 (M^+ - *OH*). 878 (M^+ - *OH* + *Na*), 900 (M^+ - *OH* + 2*Na*).

Calculated for $ReO(OH)(C_{13}H_{12}NO_5S_2)_2$: C 35.82, H 2.89, N 3.21;

found: C 36.82, H 3.00, N 3.17.

Bis(2,2'-(4-sulpho)dipyrrolylthionato)rhenium, sodium salt. (12d')

Yield 18%.

M.W. = 729.79

UV-Vis (H_2O), λ_{max} (relative intensity): 425 (1)

LR-MS (MALDI), m/z: 736 (M^+ - *OH* + *Na*), 758 (M^+ - *OH* + 2*Na*), 779 (M^+ - *OH* + 3*Na*).

Calculated for $ReO(OH)(C_9H_6N_2NaO_3S_2)_2 \times 6H_2O$: C 24.52, H 2.86, N 6.35, S 14.54;

found: C 25.17, H 3.09, N 5.14, S 13.86.

4.1.10. Labelling of the 2-pyrrolylthiones with ^{99m}Tc-isotope

General procedure. Direct labelling was carried out at near physiological pH. Stannous tartrate $Sn(C_4H_4O_6)$ was selected as a reducing agent. A lipophilic ligand (1 mg) was dissolved in 10 ml of methanol. A water-soluble ligand (1 mg) was dissolved in 1 ml of distilled water. Next, 20 μg of saturated solution of stannous tartrate was added, followed by a solution of sodium pertechnetate $Na^{99m}TcO_4$ in saline, as obtained from the generator (100-500 μL, according to measured radioactivity, usually approximately 3 mCi). Labelling was accomplished by incubation of a solution at 60°C for 15 minutes in a nitrogen atmosphere.

The solvent was evaporated in a vacuum. A residual solid was re-dissolved either in ethanol or water (for lipophilic and hydrophilic compounds respectively). A labelled product was purified using normal phase (SiO_2) Seppak cartridges. For the lipophilic compounds, the cartridges were pre-conditioned with chloroform. Chloroform, ethanol and acetone were used as eluents. For water-soluble

compounds, the cartridges were conditioned with water and methanol. Methanol was used as an eluent. A radioactive fraction corresponding to a ^{99m}Tc-pyrrolylthione complex was collected.

Radiochemical purity. At this point, the radiochemical purity of the product was determined using thin layer chromatography (TLC) on commercially available paper strips impregnated with silica gel. In order to do this, we followed standard procedures used for quality control of radiopharmaceuticals in nuclear medicine.

Specifically, a sample of a product was loaded on a paper strip and thoroughly dried. A strip was then immersed in a solvent in order to detect the main radioactive components that could be present in such a mixture (e.g. complex, free pertechnetate, and reduced technetium). Afterwards, the strip was dried and cut into three equal pieces. These pieces were placed in a γ-counter and the radiochemical purity of a product was calculated using the data obtained.

For lipophilic compounds, the strip was first run in chloroform to detect a radioactive complex (R_f 0.5-1.0, usually >90% of total activity). Next, the strip was immersed in acetone to detect free pertechnetate. Reduced technetium has R_f 0.0 in these solvents.

For water-soluble compounds, the strip was first chromatographed in acetone to detect free pertechnetate (R_f 1.0), then in methanol and water (a Tc-complex, R_f 1.0, usually >90% of total activity). Reduced technetium, again, remains at the origin of the chromatogram.

Labelling efficiency. The labelling efficiency was calculated based on the chromatographically purified complex. Briefly, a synthesised product was loaded on

an activated Seppak cartridge and eluted with an appropriate solvent (chloroform followed by methanol for lipophilic complexes and water followed by methanol for water-soluble compounds). Collected fractions and the cartridge itself were placed in a γ-counter and the labelling efficiency of a product was calculated using the data obtained. The values were corrected for decay of the radioisotope.

Formulation of the radiopharmaceuticals. In order to formulate solutions for injection to perform biodistribution tests, water-soluble compounds were redissolved in saline and their radioactive concentrations were adjusted according to specifications for biological studies.

The lipophilic compounds were formulated for injection using an emulsion with either Cremophor-EL or Travamulsion (Sigma-Aldrich). Emulsions were prepared as follows. For Cremophor containing emulsion 10% of Cremophor-EL, 3% of propanol and the balance of water (87%) were used. A complex was dissolved in propanol followed by the addition of Cremophor-EL. The mixture was vigorously shaken on a Vortex while water was added. For the Travamulsion mixture, the complex was dissolved in 0.5 ml of ethanol, followed by the addition of Travamulsion (4.5 ml). The mixture was shaken on a Vortex at the time of addition and for 5 more minutes after the addition. The volume of the ethanol in the final emulsion must not exceed 10%.

Finally, the solutions for injection were sterilised.

4.2. ***Biological tests***

Dr. Jacques Rousseau from our Department carried out the biodistribution and pharmacokinetics experiments.

4.2.1. Biodistribution

For biodistribution studies Balb/c mice bearing an EMT6 mammary adenocarcinoma on each thigh were injected *in vivo* with 100-200 µl (0.5 to 1 mCi) of carrier free ^{99m}Tc labelled 2-pyrrolylthones. Animals were sacrificed at 6 hours post-injection.

4.2.2. Pharmacokinetics

A group of 3 male Sprague and Dawley rats were anaesthetised by intra-muscular administration of a mixture of Ketamine Xylazine (1ml/kg). A 26 gage Butterfly was introduced into the lateral tail vein and filled with heparinised physiological saline. The animals were injected with the proper radiopharmaceutical. Acquisition started in few minutes after injection.

The camera was set to record a series of 32 images with an interval of 1 min. Animals were injected successively after the camera was started. All injections were finished within the first minute and a half. Following each injection the catheter was

flushed with 0.5 ml of physiological saline. Second dynamic acquisition was performed at a rate of one image every 10 minutes. The animals woke up 90 min after injection, when the study was terminated.

For analysis, areas were traced around the organs of interest (right and left kidneys for the dynamic study, and heart, left kidney and bladder at 60 min post-injection). The results were expressed as counts per seconds or as percent of the whole body activity at a given time.

REFERENCES

Andros G., Harper P.V., Lathrop K.A., McCardle R.J. "Pertechnetate-99m localization in man with applications to thyroid scanning and the study of thyroid physiology", *Journal of Clinical Endocrinology*, vol.25, pp.1067-1076, 1965

Arano Y. "Delivery of diagnostic agents for gamma-imaging", *Advanced Drug Delivery Reviews*, vol.37, no.1-3, pp.103-120, 1999

Ballantine J.A., Jackson A.H., Kenner G.W., McGillivray G. "Pyrroles and related compounds - IX. Syntheses and properties of certain pyrroketones", *Tetrahedron*, Supplement no.7, pp.241-259, 1966

Banbery H.J., McQuillan F.S., Hamor T.A., Jones C.J., McCleverty J.A. "The synthesis and X-ray crystal structure of the trinuclear complex $[\{ORe(OC_6H_4\text{-}2\text{-}CMe{=}NCH_2\text{-})_2(\mu\text{-}O)\}_2Re(OC_6H_4\text{-}2\text{-}CMe{=}NCH_2\text{-})_2]Cl{\times}H_2O{\times}0.5CH_2Cl_2$", *Inorganica Chimica Acta*, vol.170, pp.23-26, 1990

Baumann E.J., Searle N., Yalow A.A., Siegel E., Seidlin S.M. "Filtration of seventh group elements by thyroid, studied with radioactive isotopes" (abstract), *International Physiological Congress*, vol.19, p.194-195, 1953

Bélanger S., Beauchamp A.L. "Preparation and protonation studies of *trans*-dioxorhenium(V) complexes with imidazoles", *Inorganic Chemistry*, vol.35, no.26, pp.7836-7844, 1996

Bélanger S., Beauchamp A.L. "Oxo ligand reactivity in the $[ReO_2L_4]^+$ complex of 1-methylimidazole - preparation and crystal structures of salts containing the $ReOL_4^{3+}$ core and apical CH_3O^-, $BF_3O_2^-$, and $(CH_3O)_2PO_2^-$ groups", *Inorganic Chemistry*, vol.36, no.17, pp.3640-3647, 1997

Bélanger S., Beauchamp A.L. "μ-Oxo-bis{bis[2,2'-bi(1*H*-imidazole-N^3)]oxorhenium(V)} tetrachloride hexahydrate", *Acta Crystallographica - Section C - Crystal Structure Communications*, vol.C55 (Part 4), pp.517-521, 1999

Bordwell F.G., Rondestvedt C.S. Jr. "Mechanism for the reaction of dioxane sulfotrioxide with olefins. II. Sulfonation of styrene", *Journal of the American Chemical Society*, vol.70, no.7, p.2429-2433, 1948

Brückner C., *Ph.D. Thesis*, University of British Columbia, 1993

Brückner C., Posakony J.J., Johnson C.K., Boyle R.W., James B.R., Dolphin D. "Novel and improved syntheses of 5,15-diphenylporphyrin and its dipyrrolic precursors", *Journal of Porphyrins & Phthalocyanines*, vol.2, no.6, pp.455-465, 1998

Brückner C., Rettig S.J., Dolphin D. "2-Pyrrolylthiones as monoanionic bidentate N,S,-chelators: synthesis and molecular structure of 2-pyrrolylthionato

complexes of nickel(II), cobalt(III) and mercury(II)", *Inorganic Chemistry*, vol.39, no.26, pp.6100-6106, 2000

Bubeck B., Brandau W., Weber E., Kalble T., Parekh N., Georgi P. "Pharmacokinetics of technetium-99m-MAG_3 in humans", *Journal of Nuclear Medicine*, vol.31, no.8, pp.1285-1293, 1990

Cagnolini A., Whitener D., Jurisson S. "Comparison of the kit performance of three ^{99m}Tc myocardial perfusion agents", *Nuclear Medicine and Biology*, vol.25, no.4, pp.435-439, 1998

Carrondo M.A.A.F.deC.T., Middleton A.R., Scapski A.C., West A.P., Wilkinson G. "A novel linear *O-Re-O-Re-O-Re-O* system: the synthesis and X-ray structure of di-μ-oxo-bis{[*NN'*-ethylenebis(acetylacetiminato)]oxorhenium(V)}[*NN'*-ethylenebis(acetylacetiminato)]rhenium(V) perrhenate", *Inorganica Chimica Acta Letters*, vol.44, no.1, pp.L7-L8, 1980

Chervu L.R., Sundoro B.M., Blaufox M.D., "Technetium-99m labeled *p*-aminohippuric acid analog: a new renal agent: concise communication", *Journal of Nuclear Medicine*, vol.25, no.10, pp.1111-1115, 1984

Chi D.Y., Oneil J.P., Anderson C.J., Welch M.J., Katzenellenbogen J.A. "Homodimeric and heterodimeric bis(amino thiol) oxometal complexes with rhenium(V) and technetium(V) - control of heterodimaric complex formation and an approach to metal complexes that mimic steroid hormones", *Journal of Medicinal Chemistry*, vol.37, no.7, pp.928-937, 1994

Choi S.R., Kung M.P., Plössl K., Meegalla S., Kung H.F. "An improved kit formulation of a dopamine transporter imaging agent: [*Tc*-99m]TRODAT-1", *Nuclear Medicine & Biology*, vol.26, no.4, pp.461-466, 1999

Clezy P.S., Nichol A.W. "Chemistry of pyrrolic compounds. II. Some aspects of the chemistry of dipyrryl ketones", *Australian Journal of Chemistry*, vol.18, pp.1977-1987, 1965

Clezy P.S., Smythe G.A. "The chemistry of pyrrolic compounds. VIII. Dipyrrylthiones", *Australian Journal of Chemistry*, vol.22, pp.239-249, 1969

Clezy P.S., Liepa A.J., Nichol A.W., Smythe G.A. "The chemistry of pyrrolic compounds. IX. The synthesis of 5,5'-diformyldipyrrylketones and their derivatives", *Australian Journal of Chemistry*, vol.23, pp.589-602, 1970

Cotton F.A., Lu J., Huang Y. "A novel tetranuclear compound: crystal structure and mass-spectra of $[Re_4(C_6H_5NCOCH_3)_6(Cl)(\mu\text{-}OH)(MeOH)_3][ReO_4]_2$", *Inorganic Chemistry*, vol.35, no.7, pp.1839-1841, 1996

De Kieviet W. "Technetium radiopharmaceuticals: chemical characterization and tissue distribution of *Tc*-glucoheptonate using *Tc*-99m and carrier *Tc*-99", *Journal of Nuclear Medicine*, vol.22, no.8, pp.703-709, 1981

De Murphy C.A., Melendez-Alafort L., Montoya-Molina C., Sepulveda-Mendez J. "Technetium-99m-alendronate: a new radiopharmeceutical for bone scanning", *Archives of Medicinal Research*, vol.27, no.4, pp.481-483, 1996

Dilworth J.R., Parrotte S.J. "The biomedical chemistry of technetium and rhenium", *Chemical Society Reviews*, vol.27, no.1, pp.43-55, 1998

DiZio J.P., Fiaschi R., Davison A., Jones A.G., Katzenellenbogen J.A. "Progestin-Rhenium complexes: metal-labeled steroids with high receptor binding affinity, potential receptor-directed agents for diagnostic imaging or therapy", *Bioconjugate Chemistry*, vol.2, no.5, pp.353-366, 1991

Dyer J.R. "Spectroscopie d'absorption appliquée aux composés organiques", Prentice-Hall, Inc., Paris, 1970.

Eckelman W.C. "Radiolabeling with technetium-99m to study high-capacity and low-capacity biochemical systems", *European Journal of Nuclear Medicine*, vol.22, no.3, pp.249-263, 1995

Eckelman W.C., Richards P. "Instant ^{99m}Tc-DTPA", *Journal of Nuclear Medicine*, vol.11, no.12, p.761, 1970

Fieser L.F., Fieser M. "Reagents for organic synthesis", John Wiley & Sons, Inc., New York-Toronto, vol.1, pp.1126-1127, 1967

Fortin S., Beauchamp A.L. "Synthesis and crystal structure of a new isomer of the μ-oxo-bis[dichlorooxobis(pyridine)rhenium(v)] complex $\{ORe\mathit{Cl}_2py_2\}_2O$", *Inorganica Chimica Acta*, vol.279, no.2, pp.159-164, 1998

Fritzberg A.R., Lyster D.M., Dolphin D.H. "Evaluation of formamidine sulfinic acid and other reducing agents for use in the preparation of *Tc*-99m labeled

radiopharmaceuticals", *Journal of Nuclear Medicine*, vol.18, no.6, pp.553-557, 1977

Fritzberg A.R., Kuni C.C., Klingensmith III W.C., Stevens J., Whitney W.P. "Synthesis and biological evaluation of Tc-99m-*N,N'*-bis(mercaptoacetyl)-2,3-diaminopropanoate: a potential replacement for [^{131}I]*o*-iodohippurate", *Journal of Nuclear Medicine*, vol.23, no.7, pp.592-598, 1982

Fritzberg A.R., Kasina S., Eshima D., Johnson D.L. "Synthesis and biological evaluation of Tc-99m-MAG_3 as a hippuran replacement", *Journal of Nuclear Medicine*, vol.27, pp.111-116, 1986

Gianolli L., Dosio F., Matarrese M., Colombo F., Cutler C., Stepniakbiniakiewicz D., Deutsch E., Savi A., Lucignani G., Fazio F. "^{99m}Tc-2GAM: a tracer for renal imaging", *Nuclear Medicine and Biology*, vol.23, no.8, pp.927-933, 1996

Gilchrist T.L. "Synthesis of aromatic heterocycles", *Journal of the Chemical Society, Perkin Transactions 1*, vol.615, no.20, pp.2849-2866, 1999

Grummon G., Rajagopalan R., Palenik G.J., Koziol A.E., Nosco D.L "Synthesis, characterization and crystal structure of technetium(V)-oxo complexes useful in nuclear medicine. 1. Complexes of mercaptoacetylglycylglycylglycine (MAG_3) and its methyl ester derivative (MAG_3OMe)", *Inorganic Chemistry*, vol.34, pp.1764-1772, 1995

Gupta N.K., Bomanji J.B., Waddington W., Lui D., Costa D.C., Verbruggen A.M., Ell P.J. "Technetium-99m-*L,L*-ethylenedicysteine scintigraphy in patients with

renal disorders", *European Journal of Nuclear Medicine*, vol.22, no.7, pp.617-624, 1995

Hansen L., Lampeka Y.D., Gavrish S.P., Xu X.L., taylor A.T., Marzilli L.G. "*Re*(V) complexes with an open-chain quadridentate ligand containing two amine and two amido donors. Synthesis, characterization, and solution equilibria of Re_2O_3(dioxo-tetH_4)$_2$ and [$ReO(H_2O)$(dioxo-tetH_4)$_2$]Cl (dioxo-tetH_6 = 1,4,8,11-tetraazaundecane-5,7-dione)", *Inorganic Chemistry*, vol.39, no.25, pp.5859-5866, 2000

Harper P.V., Beck R., Charleston D., Lathrop K.A. "Optimization of a scanning", *Nucleonics*, vol.22, no.1, pp.50-54, 1964

Herzog K.M., Deutsch E., Deutsch K., Silberstein E.B., Sarangarajan R., Cacini W. "Synthesis and renal excretion of technetium-99m-labeled organic cations", *Jornal of Nuclear Medicine*, vol.33, no.12, pp.2190-2195, 1992

Holm S., Andersen A.R., Vorstrup S., Lassen N.A., Paulson O.B., Holmes R.A. "Dynamic SPECT of the brain using a lipophilic technetium-99m complex, PnAO", *Journal of Nuclear Medicine*, vol.26, no.10, pp.1129-1134, 1985

Holmes RA. Chaplin SB. Royston KG. Hoffman TJ. Volkert WA. Nowotnik DP. Canning LR. Cumming SA. Harrison RC. Higley B. Nechvatai G., Pickett R.D., Piper I.M., Neirinckx R.D. "Cerebral uptake and retention of $^{99}Tc^{m}$-hexamethylpropyleneamine oxime ($^{99}Tc^{m}$-HM-PAO)", *Nuclear Medicine Communications*, vol.6, no.8, pp.443-447, 1985

Hom R.K., Chi D.Y., Katzenellenbogen J.A. "Heterodimeric bis(amino thiol) complexes of oxorhenium(V) that mimic the structure of steroid hormones - synthesis and stereochemical issues", *Journal of Organic Chemistry*, vol.61, no.8, pp.2624-2631, 1996

Hom R.K., Katzenellenbogen J.A. "Tehcntium-99m-labeled receptor-specific small-molecule radiopharmaceuticals - recent developments and encouraging results" (review), *Nuclear Medicine & Biology*, vol.24, no.6, pp.485-498, 1997

Hom R.K., Katzenellenbogen J.A. "Synthesis of a tetradentate oxorhenium(V) complex mimic of a steroidal estrogen", *Journal of Organic Chemistry*, vol.62, no.18, pp.6290-6297, 1997

Hom R.K., Skaddan M.B., Katzenellenbogen J.A. "New structural motifs for oxorhenium (V) complexes whose structures mimic those of estrogen receptor ligands", *Journal of Labelled compounds and radiopharmaceuticals, Twelfth International Symposium on Radiopharmaceuticals Chemistry abstracts*, vol.XL, pp.510-511, 1997

Jurisson S., Schlemper E.O., Troutner D.E., Canning L.R., Nowotnik D.P., Neirinckx R.D. "Synthesis, characterization, and X-ray structural determination of technetium(V)-oxo-tetradentate amine oxime complexes", *Inorganic chemistry*, vol.25, no.4, pp.543-549, 1986

Jurisson S., Berning D., Jia W., Ma D. "Coordination compounds in nuclear medicine", *Chemical Reviews*, vol.93, no.3, pp.1137-1156, 1993

Jurisson S.S., Lydon J.D. "Potential technetium small molecule radiopharmaceuticals", *Chemical Reviews*, vol.99, no.9, pp.2205-2218, 1999

Kabasakal L., Turoglu H.T., Onsel C., Ozker K., Uslu I., Atay S., Cansiz T., Sonmezoglu K., Altiok E., Isitman A.T., Kapicioglu T., Urgancioglu I. "Clinical comparison of technetium-99m-EC, technetium-99m-MAG_3 and iodine-131-OIH in renal disorders", *Journal of Nuclear Medicine*, vol.36, no.2, pp.224-228, 1995

Karube Y., Iwamoto K., Takata J. "Cationic technetium-99m complexes of *N*-substituted pyridoxal derivatives as renal function agents", *Journal of Nuclear Medicine*, vol.35, no.10, pp.1691-1697, 1994.

Katzenellenbogen J.A. "Designing steroid receptor-based radiotracers to image breast and prostate tumors", *Journal of Nuclear Medicine*, vol.36, no.6 (Supplement), pp.S8-S13, 1995

Kenna B.T., Kuroda P.K. "Isolation of naturally occurring technetium", *Journal of Inorganic and Nuclear Chemistry*, vol.23, p.142-144, 1962

Kibar M., Noyan A., Anarat A. "$^{99}Tc^{m}$-*N*,*N*-ethylenedicysteine scintigraphy in children with various renal disorders: a comparative study with $^{99}Tc^{m}$-MAG_3", *Nuclear Medicine Communications*, vol.18, no.1, pp.44-52, 1997

Kost A.N., Gorbunova S.M., Basova L.P., Kiselev V.K., Gorbunov V.I. "2-Hydroxyacetylindoles and 2-indolylethylene glycols", Pharmaceutical Chemistry Journal, vol.8, pp.74-78, 1974. Translated from Khimiko-Farmatsevticheskii Zhurnal, vol.8, no.2, pp.8-14, 1974

Kronauge J.F., Kawamura M., Lepisto E., Holman B.L., Davison A., Jones A.G., Costello C.E., Zeng C.-H. "Metabolic studies of the myocardial perfusion agent *Tc*-MIBI", in *Technetium and Rhenium in Chemistry and Nuclear Medicine*, Nicolini M., Bandoli G., Mazzi U., eds.; Cortina international, Verona, Italy, 3th ed., pp.677-681, 1990

Kudrevich S.V., Dolphin D., Selivanova S.V., Rousseau J., van Lier J.E. "Radiometal complexes of 2-pyrrolylthiones and their use as radiopharmaceuticals for imaging and therapy" (patent pending)

Kung H.F., Kim H-J., Kung M-P., Sanath K.M., Plössl K., Lee H-K. "Imaging of dopamine transporters in humans with technetium-99m TRODAT-1", *European Journal of Nuclear Medicine*, vol.23, no.11, pp.1527-1530, 1996

Kung M.P., Stevenson D.A., Plössl K., Meegalla S.K., Beckwith A., Essman W.D., Mu M., Lucki I., Kung H.F. "[^{99m}Tc]TRODAT-1 - a novel technetium-99m complex as a dopamine transporter imaging agent", *European Journal of Nuclear Medicine*, vol.24, no.4, pp.372-380, 1997

Leonard J.P., Nowotnik D.P., Neirinckx R.D. "Technetium-99m-*D,L*-HM-PAO: a new radiopharmaceutical for imaging regional brain perfusion using SPECT -

a comparison with iodine-123 HIPDM", *Journal of Nuclear Medicine*, vol.27, no.12, pp.1819-1823, 1986

Liu S., Edwards D.S. "99mTc-Labeled small peptides as diagnostic radiopharmaceuticals", *Chemical Reviews*, vol.99, no.9, pp.2235-2268, 1999

Loberg M.D., Cooper M., Harvey E., Callery P., Faith W. "Development of new radiopharmaceuticals based on *N*-substitution of iminodiacetic acid", *Journal of Nuclear Medicine*, vol.17, no.7, pp.633-638, 1976

Loberg M.D., Fields A.T. "Chemical structure of technetium-99m-labeled *N*-(2,6-dimethylphenylcarbamoylmethyl)-iminodiacetic acid (Tc-HIDA)", *International Journal of Applied Radiation & Isotopes*, vol.29, pp.167-173, 1978

Lumbroso H., Liégeois Ch., "A dipole moment study of 2-benzoylpyrroles, di-(2-pyrryl)ketones and their sulphur analogues", *Journal of Molecular Structure*, vol.112, pp.85-99, 1984

Madras B.K., Jones A.G., Mahmood A., Zimmerman R.E., Garada B., Holman B.L., Davison A., Blundell P., Meltzer P.C. "Technepine: a high-affinity 99m-technetium probe to label the dopamine transporter in brain by SPECT imaging", *Synapse*, vol.22, no.3, pp.239-246, 1996

Mallinckrodt Medical Inc., TechneScan MAG_3^{TM} Kit for the Preparation of Technetium Tc-99m Mertiatide Diagnostic - For Intravenous Use, package insert, 1992

Mamardashvili N.Z. and Golubchikov O.A. "Synthesis of porphyrins from dipyrrolylmethanes", *Uspekhi Khimii*, vol.69, no.4, pp.337-354, 2000

McAfee J.G., Fueger C.F., Stern H.S., wagner H.N., Migita T. "Tc^{99m} Pertechnetate for brain scanning", *Journal of Nuclear Medicine*, vol.5, no.11, pp.811-827, 1964

MDS Nordion S.A., Kit for the preparation of Technetium(*Tc*-99m) Succimer Injection, package insert, 1998

Meltzer P.C., Madras B.K., Kung H.F., Kim H-J, Meegala S.K., Plossl K., Lee H.K. "Imaging of dopamine transporters in humans with technetium-99m TRODAT-1", *European Journal of Nuclear Medicine*, vol.24, no.4, pp.462-463, 1997

Mendelejeff D.I. "Die periodische gesetzmäfsigkeit der chemischen elemente" (Periodic law of the chemical elements), *Annalen der Chemie und Pharmacie*, vol.8, Suppl., no.2, pp.133-229, 1872

Mooney R.C.L. "The crystal structure of element 43", *Physical Review*, vol.72, p.1269, 1947

Motta E.E., Boyd G.E., Larson Q.V. "Production and properties of a long-lived radio-isotope of element 43", *Physical Review*, vol.72, p.1270, 1947

Murase M., Yoshida S., Hosaka T., Tobinaga S. "Synthesis of functionalized indoles by Diels-Alder reaction utilizing the diene generated by alkylation of *N*-

methyl-3-thioacetylpyrrole", *Chemical & Pharmaceutical Bulletin*, vol.39, no.2, pp.489-492, 1991

Nelson C.M., Boyd G.E., Smith W.T.Jr. "Magnetochemistry of technetium and rhenium", *Journal of the American Chemical Society*, vol.76, p.348-352, 1954

Neirinckx R.D., Canning L.R., Piper I.M., Nowotnik D.P., Pickett R.D., Holmes R.A., Volkert W.A., Forster A.M., Weisner P.S., Marriott J.A., Chaplin S.B. "Technetium-99m *D,L*-HM-PAO: a new radiopharmaceutical for SPECT imaging of regional cerebral blood perfusion", *Journal of Nuclear Medicine*, vol.28, no.2, pp.191-202, 1987

Neves M., Gano L., Ribeiro M.J., Santos A.C., Marchi A., Sawas-Dimopolou C., de Lima J.J.P. "Synthesis, characterization, and biodistribution of oxo complexes of technetium-99m with biguanide and *N*1-substituted ligands", *Nuclear Medicine and Biology*, vol.26, no.1, pp.79-83, 1999

Nikitin S.M., Kulakov V.N. "Structures of technetium(V) complexes with some tetradentate ligands", *Radiochemistry*, vol.39, no.5, pp.398-401, 1997. Translated from *Radiokhimiya*, vol.39, no.5, pp.398-400, 1997

Oya S., Plössl K., Kung M.P., Stevenson D.A., Kung H.F. "Small and neutral $Tc^{V}O$ BAT, bisaminoethanethiol (N_2S_2) complexes for developing new brain imaging agents", *Nuclear Medicine and Biology*, vol.25, no.2, pp.135-140, 1998.

Paine J.B. "Synthesis of pyrroles and of porphyrins via single-step coupling of dipyrrolic intermediates", in *The Porphyrins*, Dolphin D., ed.; Academic Press, New York, vol.1, pp.201-234, 1978

Peacock R.D. "The Chemistry of technetium and rhenium", Elsvier, Amsterdam-London-New York, 1966

Perrier C., Segré E. "Some chemical properties of element 43", *Journal of Chemical Physics*, vol.5, no.9, pp.712-716, 1937

Pesson M., Aurousseau M., Joannic M., Roquet F., "Étude chimique et pharmacologique de dérivés du pyrrole. I. Pyrryl-2-cétones", *Chimie Thérapeutique*, no.3, pp.127-136, 1966.

Pirmettis I., Mastrostamatis S., Papadopoulos M., Raptopoulou C.P., Terzis A., Chiotellis E. "Synthesis and X-ray structure determination of *N,N'*-bis-*L*-(1-carboxy-2-mercaptoethyl)ethylenediamine, oxotechnetium(V), [*TcO*(EC)]", *Journal of Labelled Compounds & Radiopharmaceuticals. 34(9):817-829, 1994*

Piwnica-Worms D., Kronauge J.F., Holman B.L., Lister-James J., Davison A., Jones A.G. "Hexakis(carbomethoxyisopropylisonitrile) technetium(I), a new myocardial perfusion imaging agent: binding characteristics in cultured chick heart cells", *Journal of Nuclear Medicine*, vol.29, no.1, pp.55-61, 1988

Rousseau J., Ali H., Lamoureux G., Lebel E., van Lier J.E. "Synthesis, tissue distribution and tumor uptake of ^{99m}*Tc*- and ^{67}*Ga*-tetrasulfophthalocyanine",

International Journal of Applied Radiation & Isotopes, vol.36, no.9, pp.709-716, 1985

Saha G.B. "Fundamentals of Nuclear Pharmacy", Fourth edition, Spring-Verlag, New-York-Berlin-Heidelberg, 1998

Sands H., Delano M.L., Camin L.L., Gallagher B.M. "Comparison of the transport of $^{42}K^{+}$, $^{22}Na^{+}$, $^{201}Tl^{+}$, and $[^{99m}Tc(dmpe)_2Cl_2]^{+}$ using human erythrocytes", *Biochimica et Biophysica Acta*, vol.812, no.3, pp.665-670, 1985

Sato Y., Sunagawa G. "Studies on seven-membered ring compounds. XXIV. Syntheses of 8-methylimino cyclohepta[*b*]pyrrole and cyclohepta[*b*]pyrrole-8(1*H*)-thione derivatives and tropone analogues of tryptamine", *Chemical & Pharmaceutical Bulletin*, vol.15, no.5, pp.634-643, 1967

Scheeren J.W., Ooms P.H.J., Nivard P.J.F. "A general procedure for the conversion of a carbonyl group into a thione group with tetraphosphorus decasulfide", *Synthesis*, no.3 (March issue), pp.149-151, 1973

Schöster F.S., Zeisler S.K. "Contribution to the coordination chemistry of technetium. II. Complexes of technetium(I) with selected ligands containing *N,O*, and *S* donor atoms", *Journal of Radioanalytical and Nuclear Chemistry*, vol.220, no.2, pp.149-154, 1997

Schwartz Z., Shani J., Soskolne W.A., Touma H., Amir D., Sela J. "Uptake and biodistribution of technetium-99m-MD^{32}P during rat tibial bone repair", *Journal of Nuclear Medicine*, vol.34, no.1, pp.104-108, 1993

Seaborg G.T., Segré E. "Nuclear isomerism in element 43", *Physical Review*, vol.55, pp.808-814, 1939

Shabana R., Rasmussen J.B., Lawesson S.-O. "Enamine chemistry, Part XXI: N- and/or C-substitution (alkylation, acylation) of ethyl 3-amino-2-butenoate. The preparation of 2-substituted 4-methyl-1,3-thiazine-6-thiones", *Bull. Soc. Chim. Belg.*, vol. 90, no.1, pp.75-82, 1981

Silversten R.M., Bassler G.C., Morrill T.C. "Spectrometric identification of organic compounds", Fifth edition, John Wiley & Sons, Inc., New York-Chichester-Brisbane-Toronto-Singapore, 1991

Sorensen L.B., Archambault M. "Visualization of the liver by scanning with Mo^{99} (molybdate) as tracer", *The Journal of Laboratory and Clinical Medicine*, vol.62, no.2, pp.330-340, 1963

Sorensen L.B., Archambault M. "Preliminary physiological studies of molybdenum (Mo^{99}) in liver scanning", *Radiology*, vol.82, no.2, pp.318-319, 1964

Sugano Y., Katzenellenbogen J.A. "Synthesis of tetradentate bisamino-bisthiol complexes of oxorhenium(V) as structural mimics of steroids", *Bioorganic & Medicinal Chemistry Letters*, vol.6, no.4, pp.361-366, 1996

Taylor A. Jr., Eshima D., Christian P.E., Milton W. "Evaluation of Tc-99m mercaptoacetyltriglycine in patients with impaired renal function", *Radiology*, vol.162, no.2, pp.365-370, 1987

Thakur M.L., Chauser B.M., Hudson R.F. "The preparation of iodine-123 labeled sodium ortho-iodo hippurate and its clearance by the rat kidneys", *International Journal of Applied Radiation and Isotopes*, vol.26, pp.319-320, 1975

Tisato F., Refosco F., Bandoli G. "Structural survey of technetium complexes", *Coordination Chemistry Reviews*, vol.135/136, pp.325-397, 1994

Troutner D.E., Volkert W.A., Hoffman T.J., Holmes R.A. "A neutral lipophilic complex of ^{99m}Tc with a multidentate amine oxime", *International Journal of Applied Radiation & Isotopes*, vol.35, no.6, pp.467-470, 1984

Tubis M., Posnik E., Nordyke R.A. "Preparation and use of I^{131} labeled sodium iodohippurate in kidney function tests", *Proceedings of the Society for Experimental Biology and Medicine*, vol.103, no.3, pp.497-498, 1960

Vanbilloen H.P., Dezutter N.A., Cleynhens B.J., Verbruggen A.M. "Characteristics and biological behaviour of ^{99m}Tc-labelled hydroxyacetyltriglycine, a potential alternative to ^{99m}Tc-MAG_3", *European Journal of Nuclear Medicine*, vol. 24, no.11, pp.1374-1379, 1997.

Van Lier J.E., Ali H., Rousseau J. "Phatlocyanines labeled ith gamma-emitting radionuclides as possible tumor scanning agents", in Porphyrin Localization and Treatment of Tumors, pp.315-319, Alan R. Liss, Inc., 1984.

Verbruggen A., Bormans G., Van Nerom C., Cleynhens B., Crombez D., de Roo M. "Isolation of the mono-ester mono-acid derivatives of ^{99m}Tc-ECD and their

biodistribution in mice", in *Technetium and rhenium in chemistry and nuclear medicine*, Nicolini M., Bandoli G., Mazzi U., eds.; Cortina International, Verona, Italy, 3th ed., pp.445-452, 1990

Volkert W.A., Hoffman T.J., Seger R.M., Troutner D.E., Holmes R.A. "^{99m}Tc-propylene amine oxime (^{99m}Tc-PnAO); a potential brain radiopharmaceutical", *European Journal of Nuclear Medicine*, vol.9, no.11, pp.511-516, 1984

Volkert W.A., Jurisson S. "Technetium-99m chelates as radiopharmaceuticals", in *Topics in Current Chemistry*, Springer-Verlag, Berlin-Heidelberg, vol.176, pp.123-148, 1996

SUPPORTING DATA

PART 1.

SPECTROSCOPIC ANALYSES OF THE SYNTHESISED COMPOUNDS (SELECTED RESULTS)

List of spectra

Compound **2b**

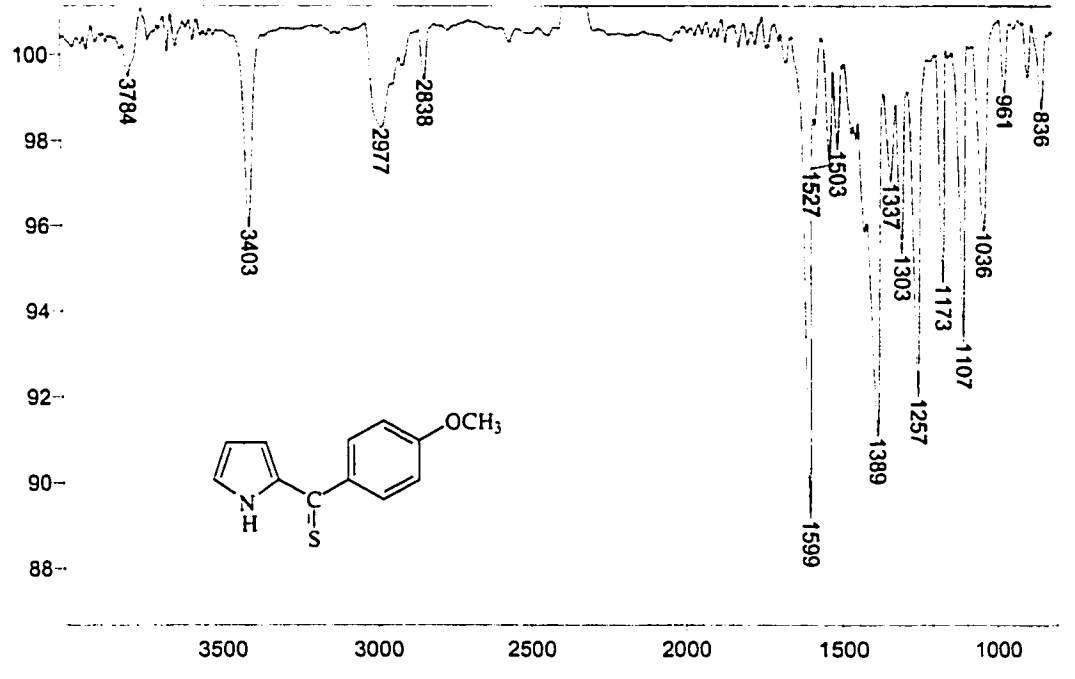

Transmittance / Wavenumber (cm-1)

Res=4cm-1

L6

Compound **2c**

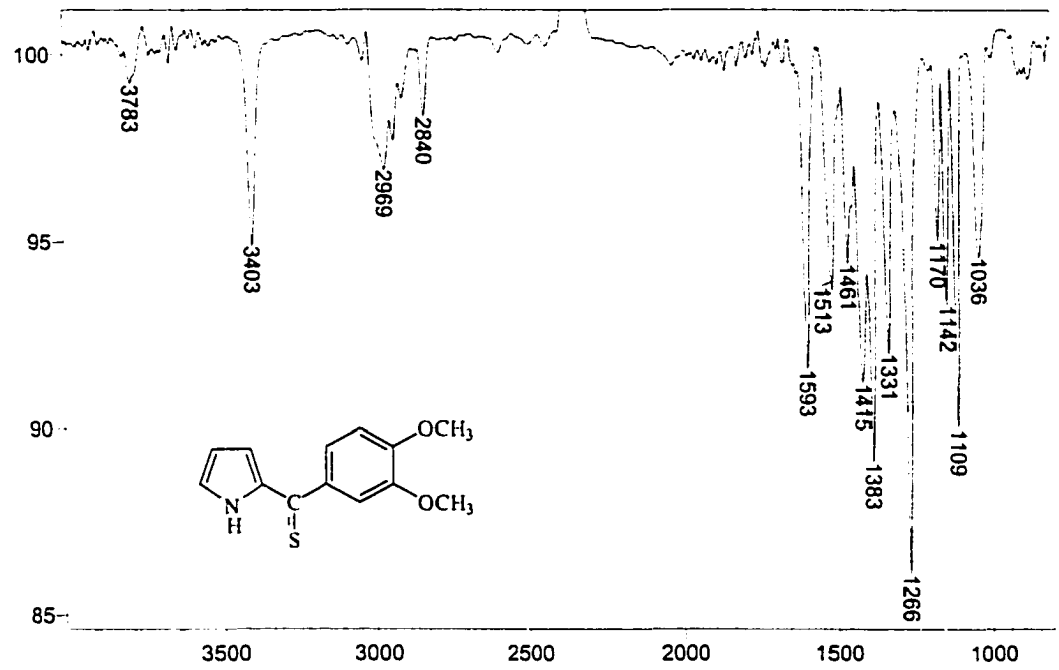

L7

Compound **3a**

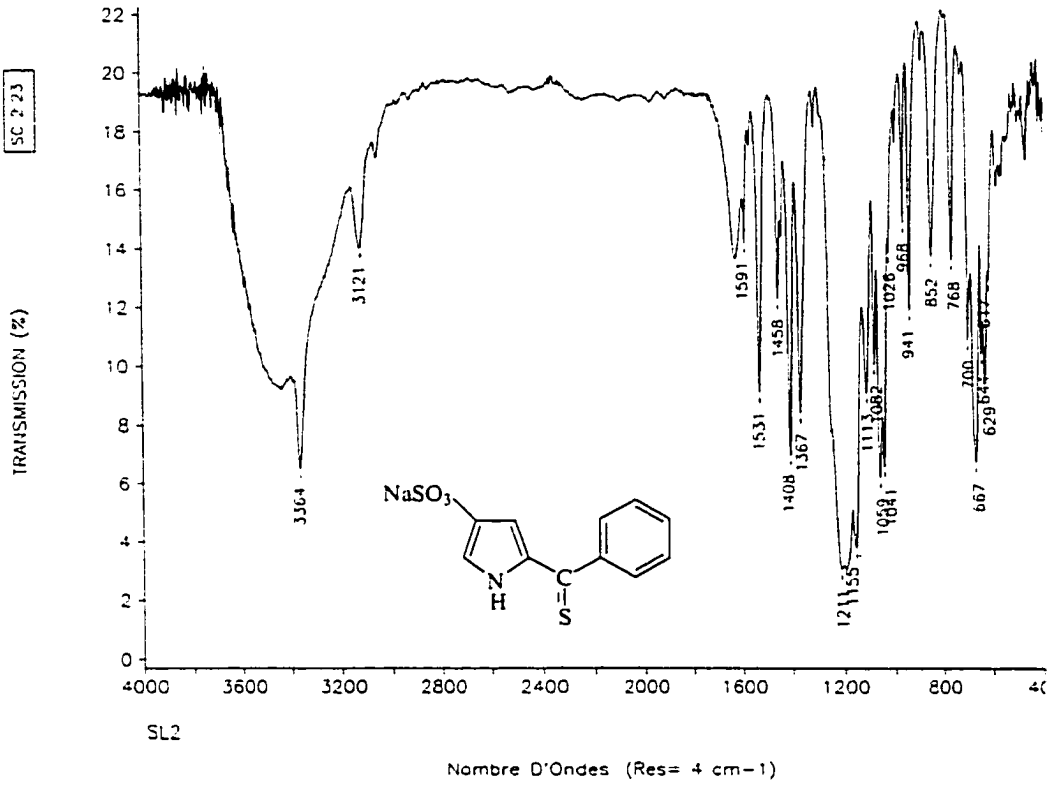
SC 223
TRANSMISSION (%)
22
20
18
16
14
12
10
8
6
4
2
0
4000
3600
3200
2800
2400
2000
1600
1200
800
3364
3121
1591
1531
1458
1408
1367
1211
1155
1113
1082
1059
1041
1026
968
941
852
768
700
667
644
629
NaSO3
N
H
C
S
SL2
Nombre D'Ondes (Res= 4 cm-1)

Compound **3a**

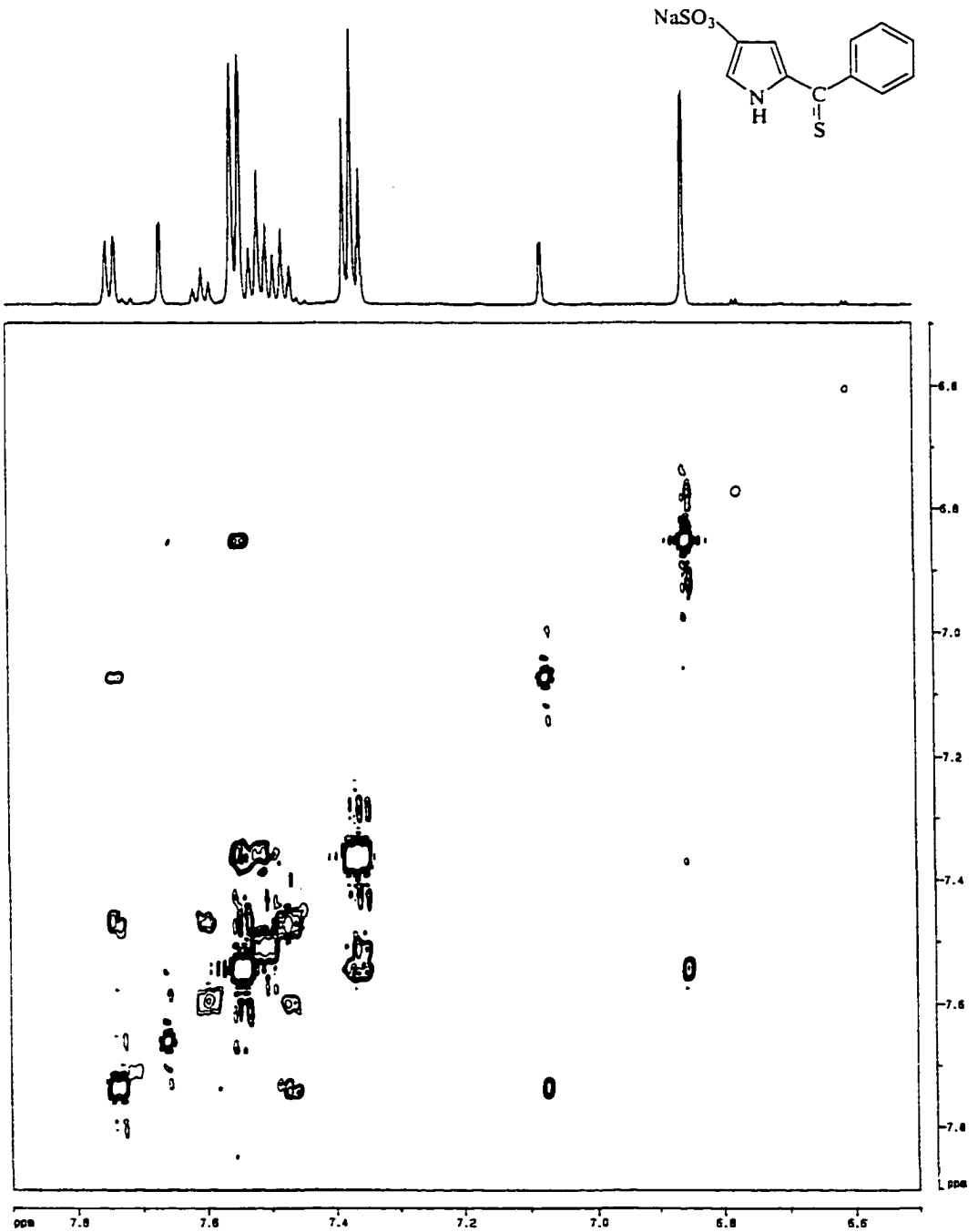

Compound **3b**

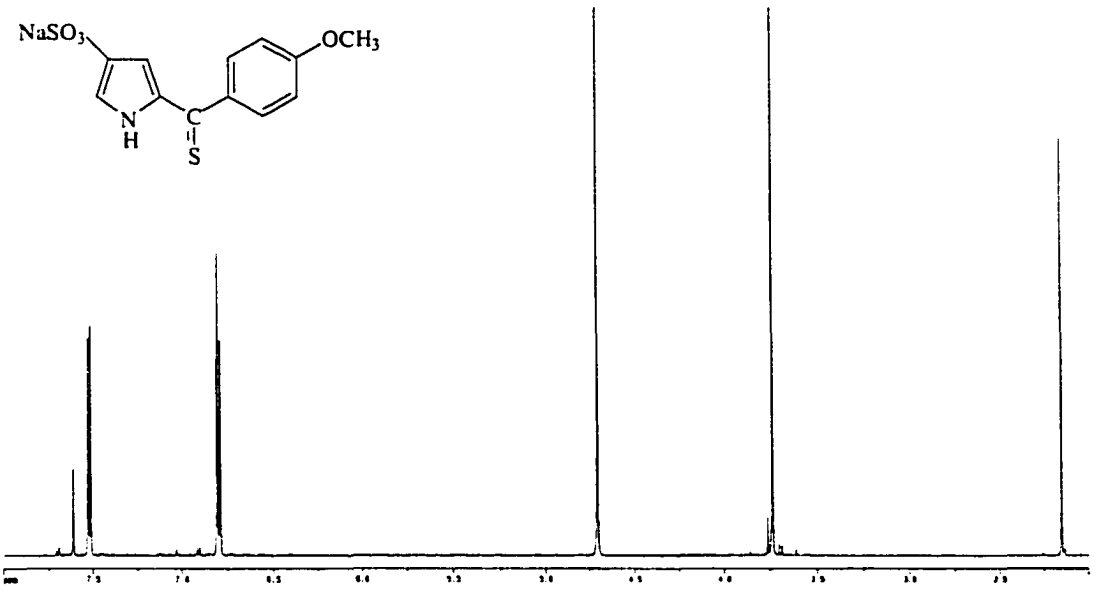
NaSO3
OCH3
N
H
C
S

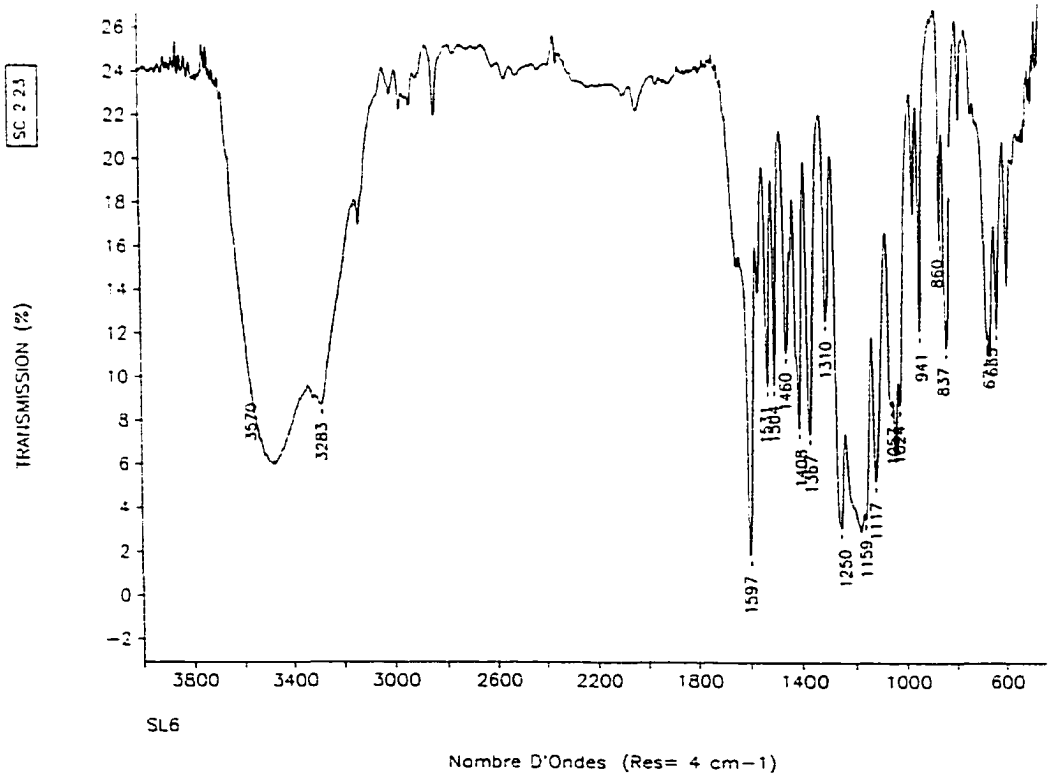
SC 2 23
TRANSMISSION (%)
26
24
22
20
18
16
14
12
10
8
6
4
2
0
-2
3570
3283
1597
1504
1460
1409
1367
1310
1250
1159
1117
941
860
837
3800
3400
3000
2600
2200
1800
1400
1000
600
SL6
Nombre D'Ondes (Res= 4 cm-1)

Compound **3c**

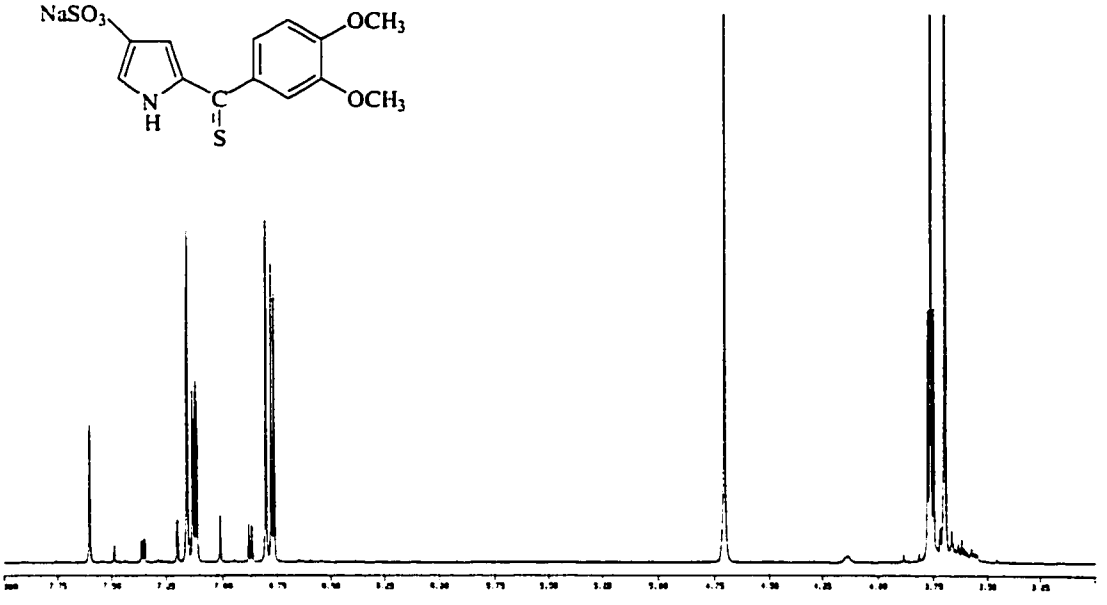
NaSO3
OCH3
OCH3
N
H
C
S

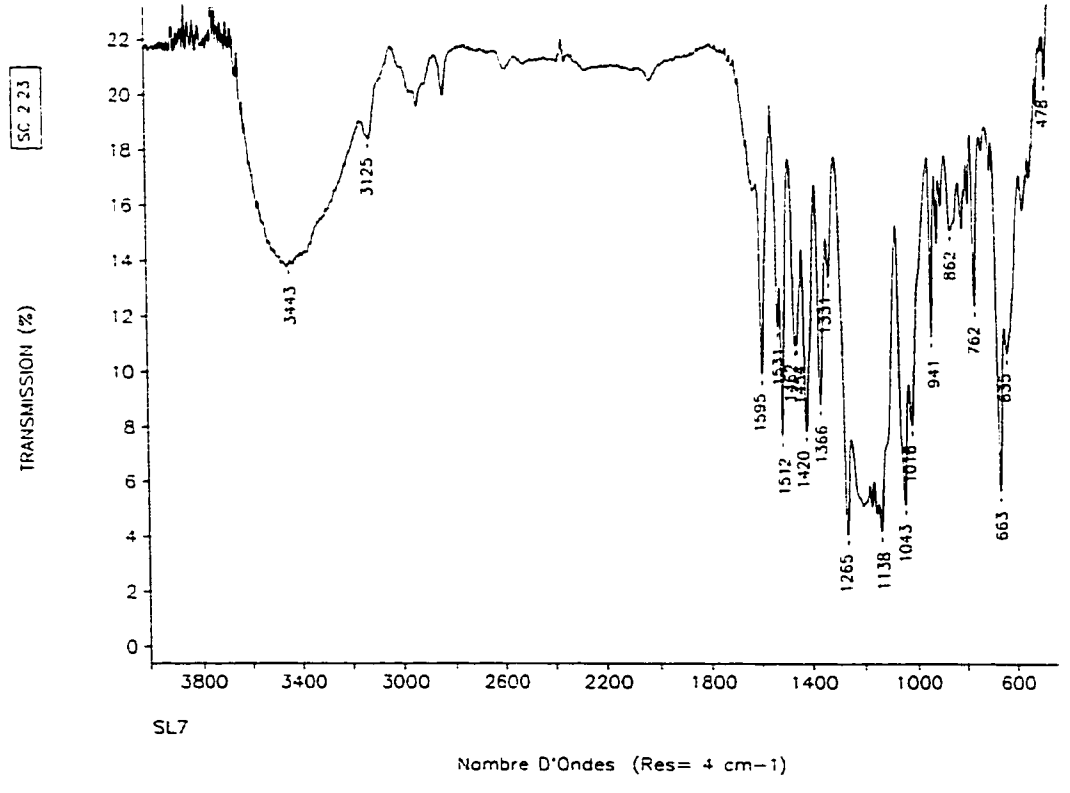
SC 223
TRANSMISSION (%)
3443
3125
1595
1512
1420
1366
1331
1265
1138
1043
941
862
762
663
478
3800
3400
3000
2600
2200
1800
1400
1000
600
SL7
Nombre D'Ondes (Res= 4 cm-1)

Compound **3d'**

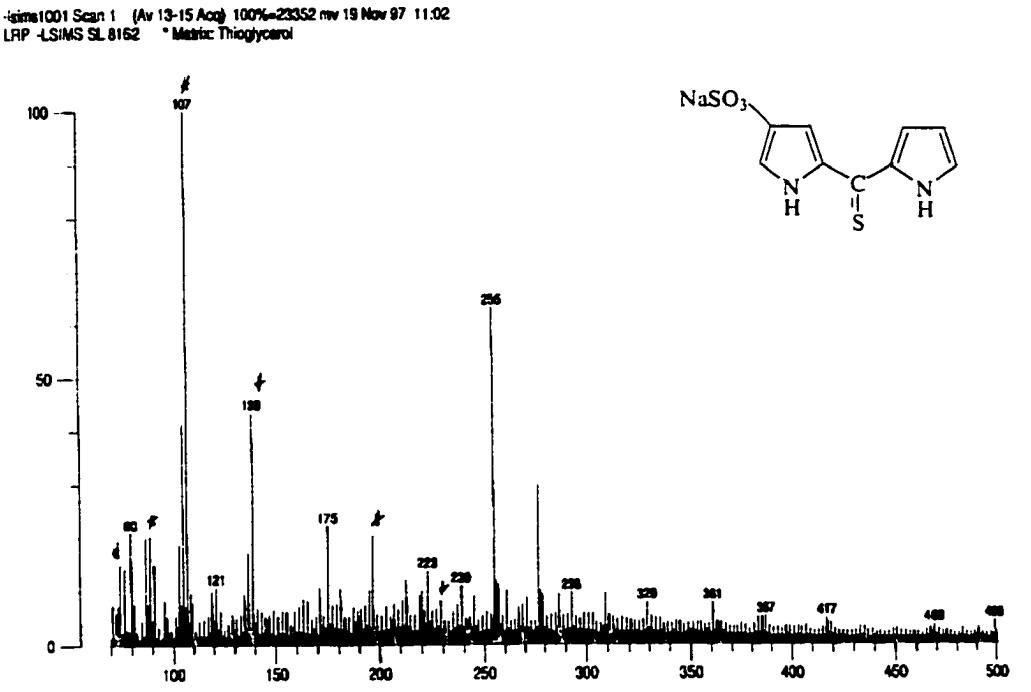
+sims1001 Scan 1 (Av 13-15 Acq) 100%=23352 mv 19 Nov 97 11:02
LRP -LSIMS SL 8162 * Matrix: Thioglycerol
NaSO3
N
H
C
S
N
H
100
50
0
107
138
175
121
223
256
100
150
200
250
300
350
400
450
500

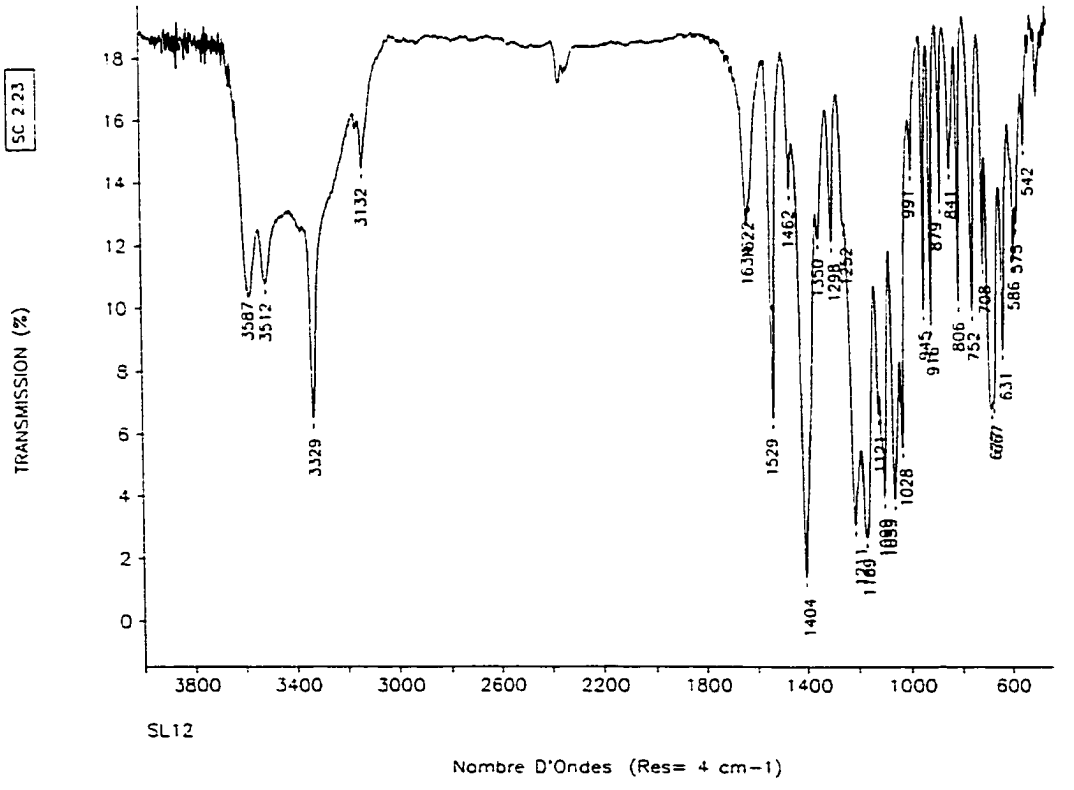
SC 223
TRANSMISSION (%)
18
16
14
12
10
8
6
4
2
0
3587
3512
3329
3132
1529
1462
1404
1350
1298
1252
1028
991
879
841
806
752
708
631
586
575
542
3800
3400
3000
2600
2200
1800
1400
1000
600
SL12
Nombre D'Ondes (Res= 4 cm-1)

Compound **3d'**

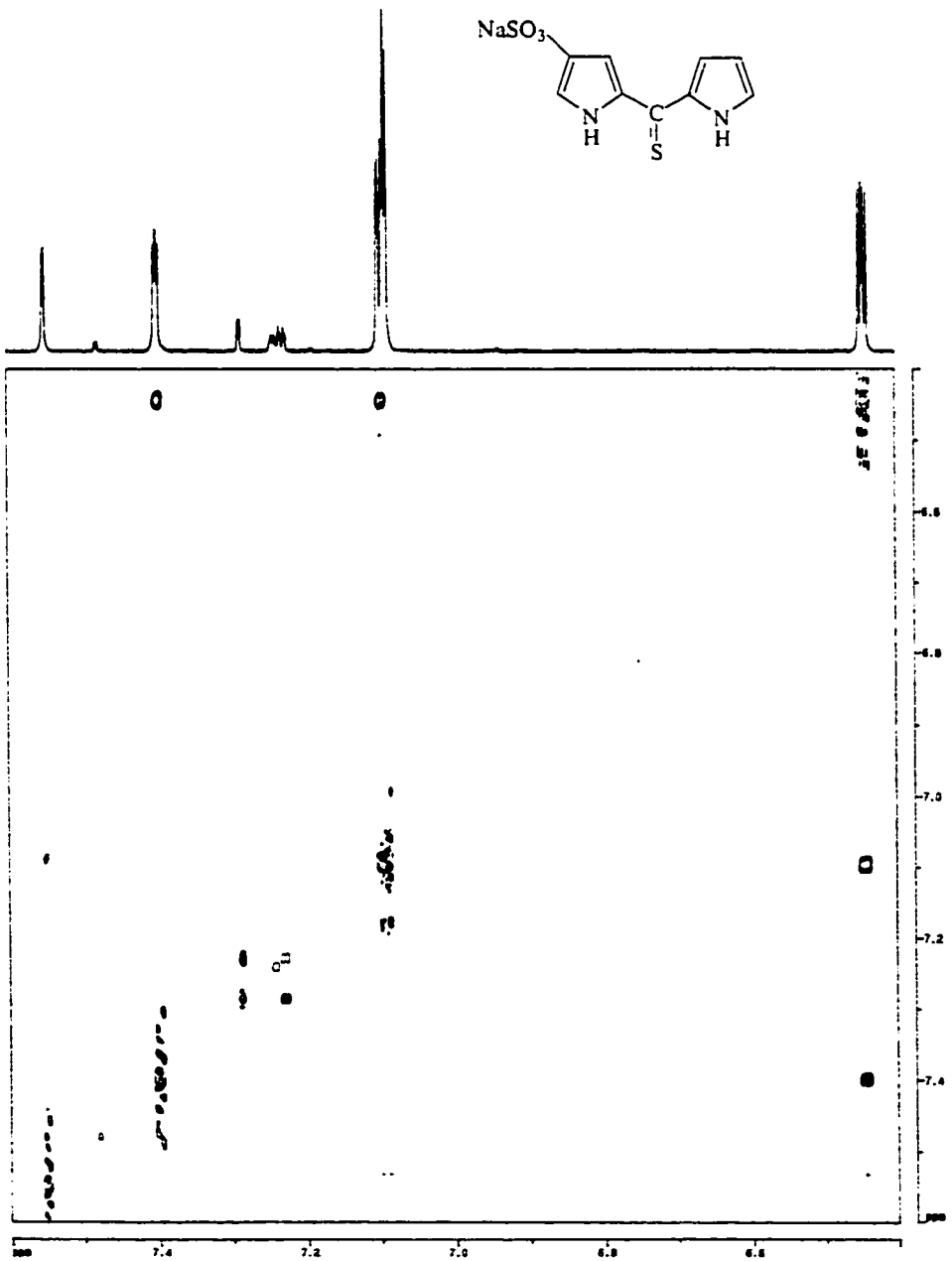

Compound **3d**

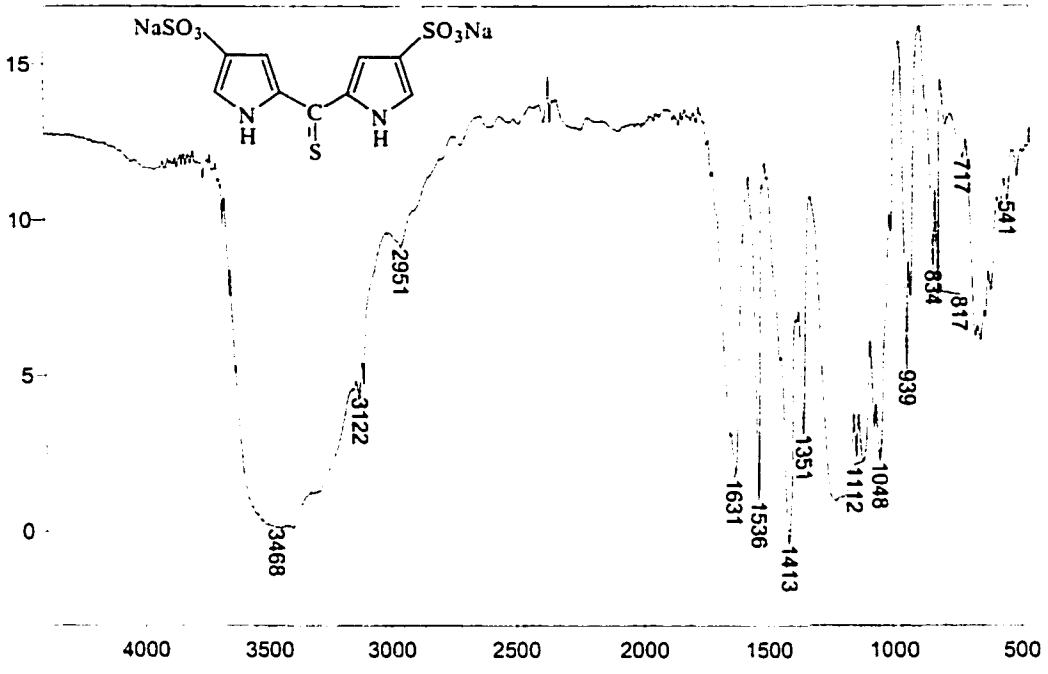

Transmittance / Wavenumber (cm-1)

Res=4cm-1

SL11

Compound **3d**

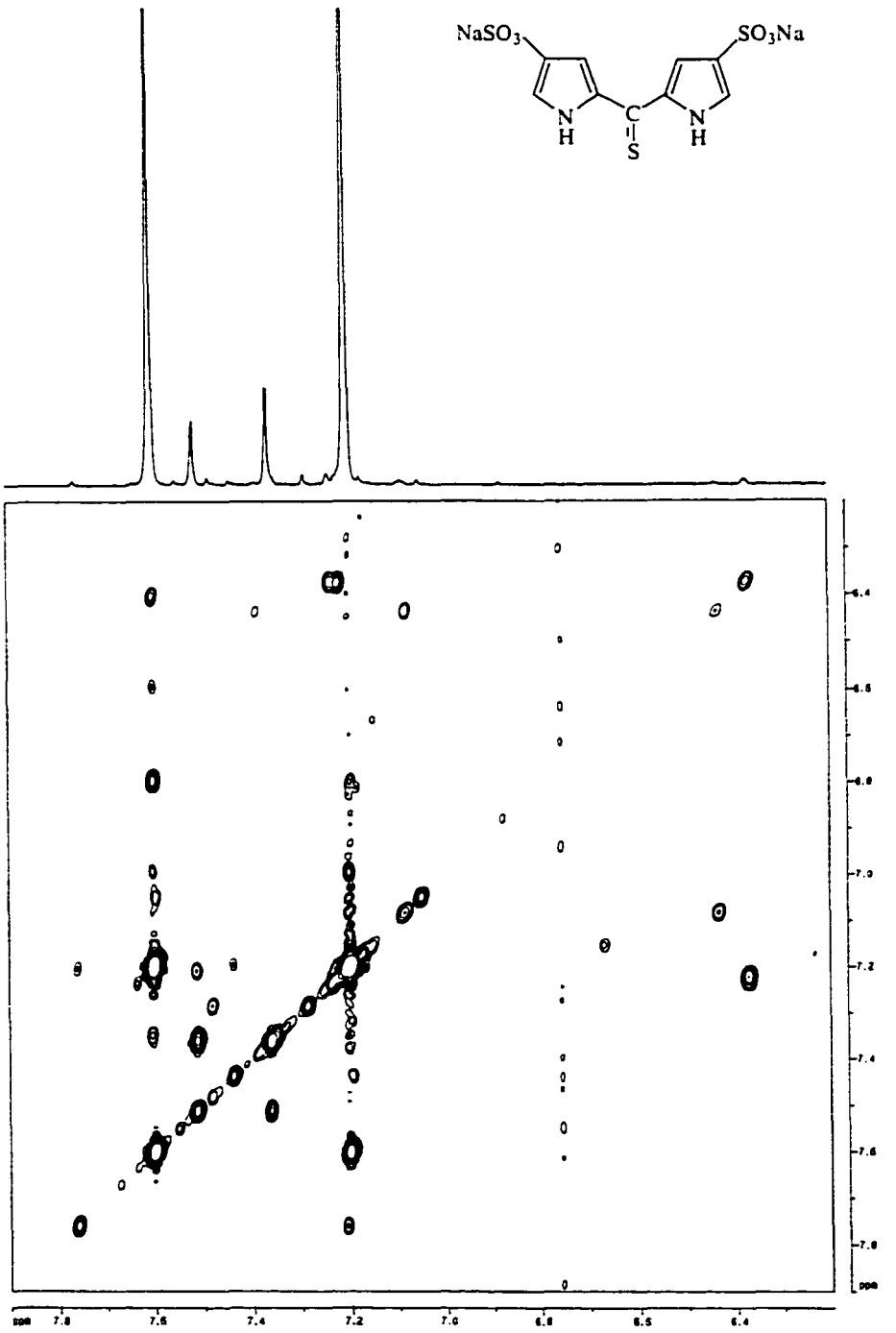

Compound **10a**

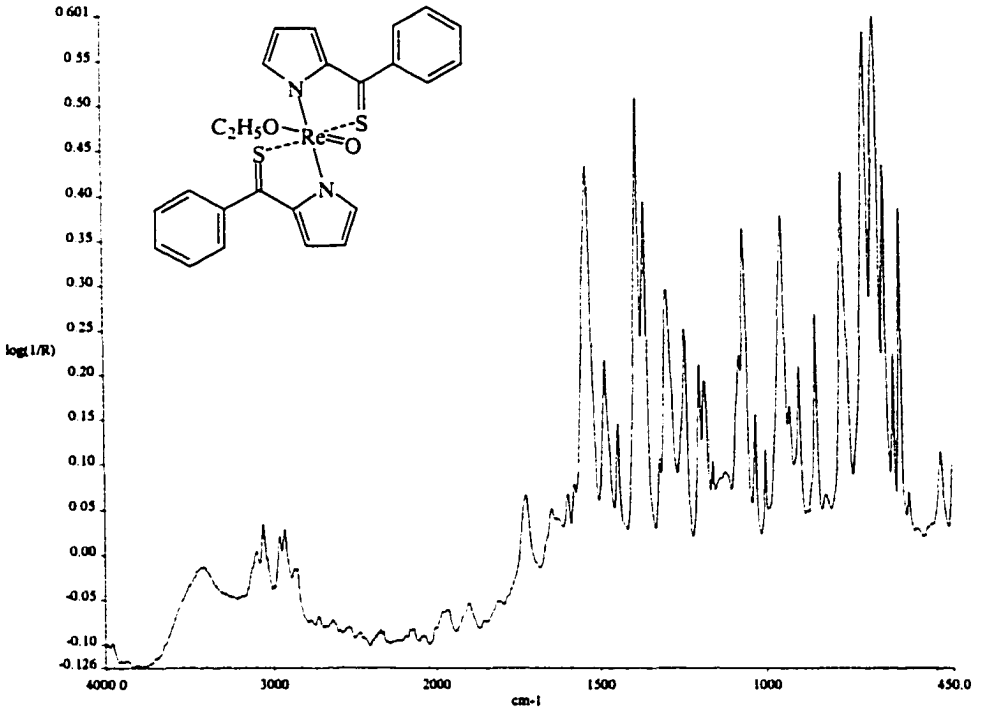

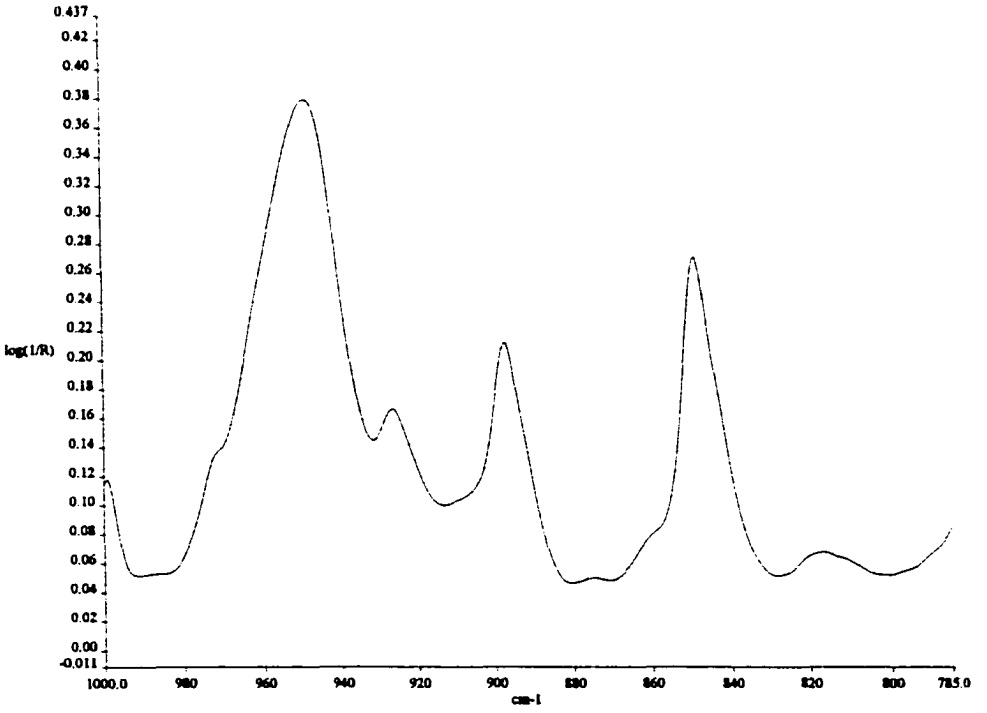

Compound **10c**

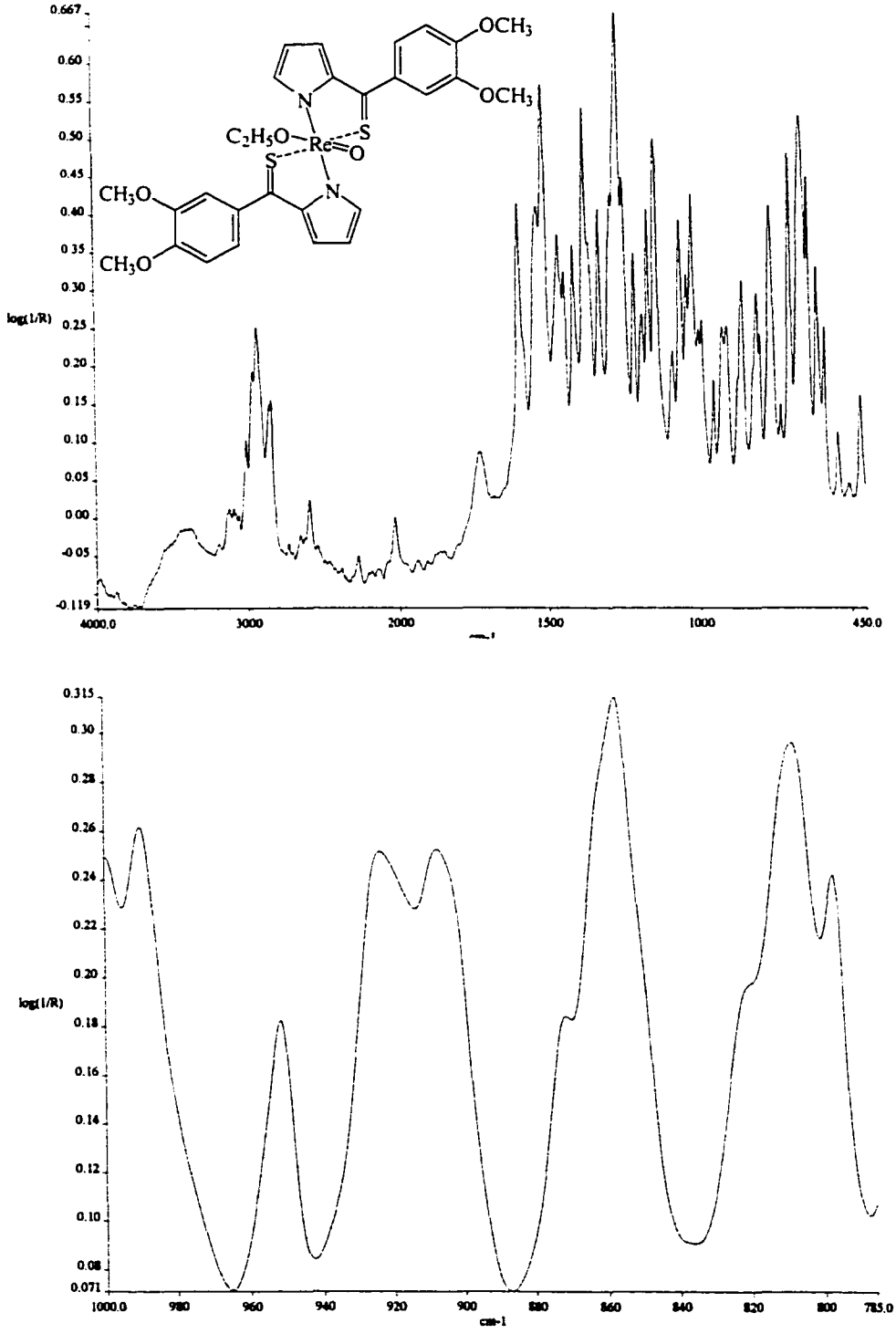

Compound **10d**

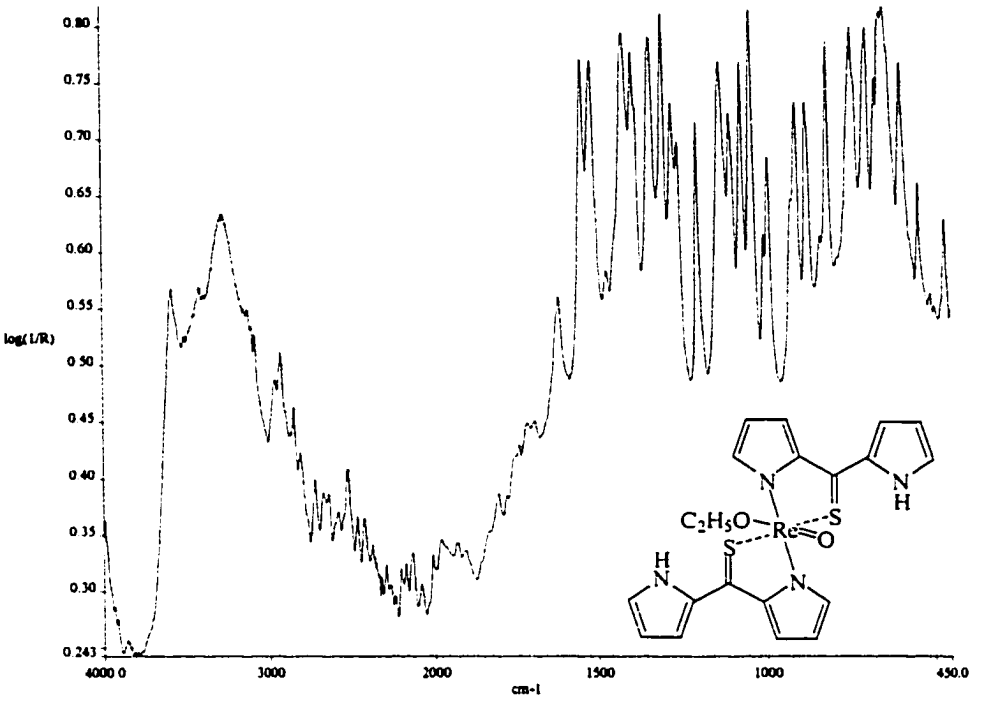

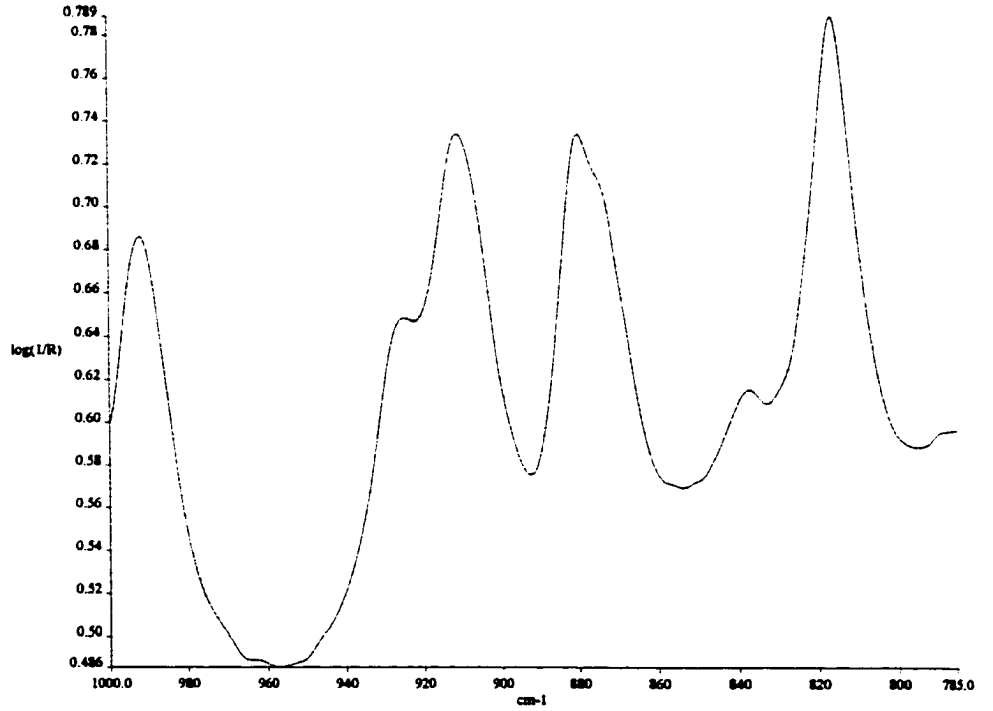

Compound **12a**

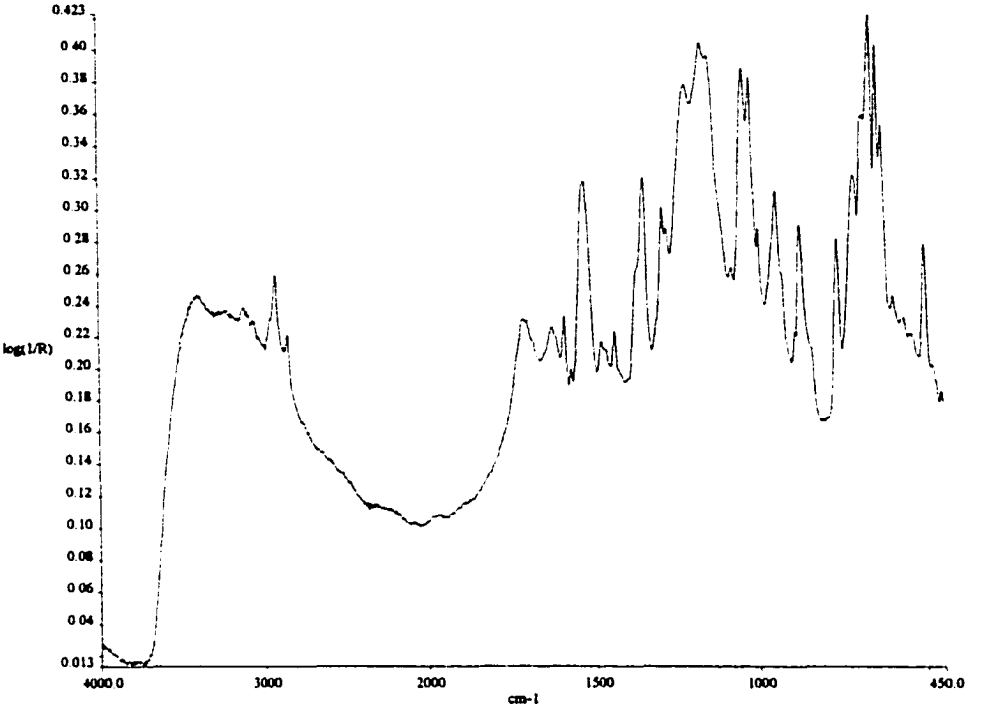

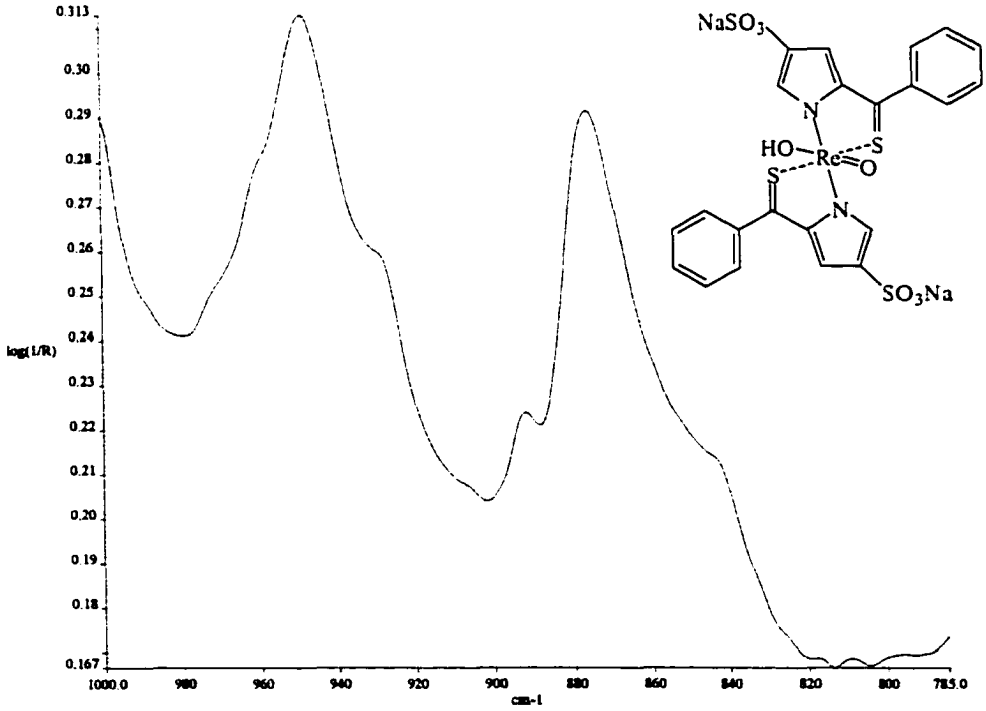

Compound **12b**

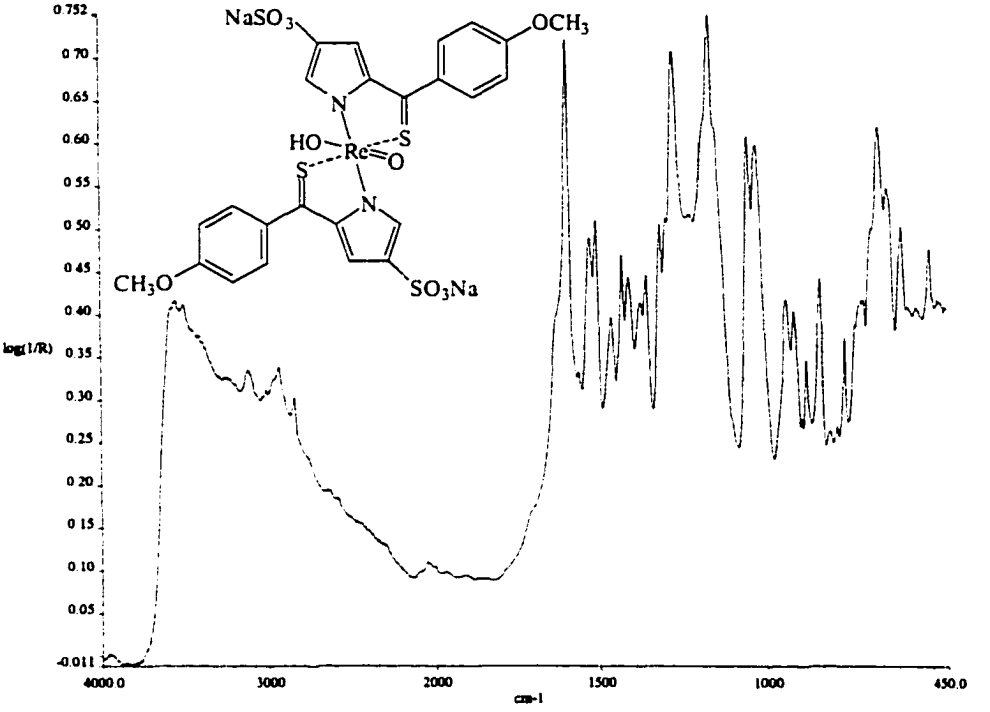

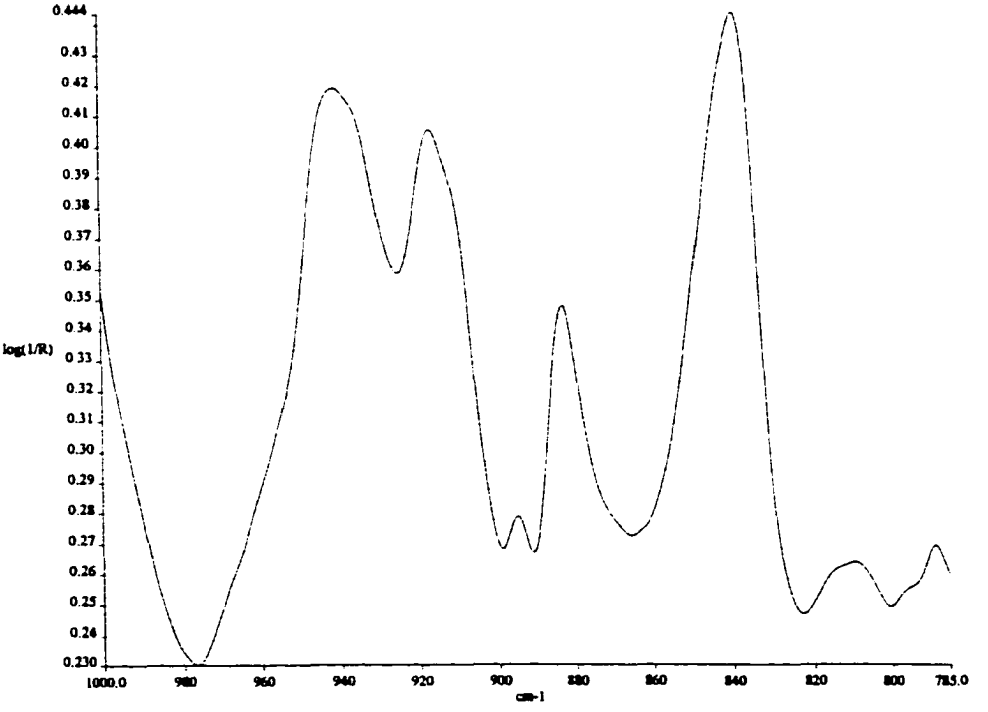

Compound **12c**

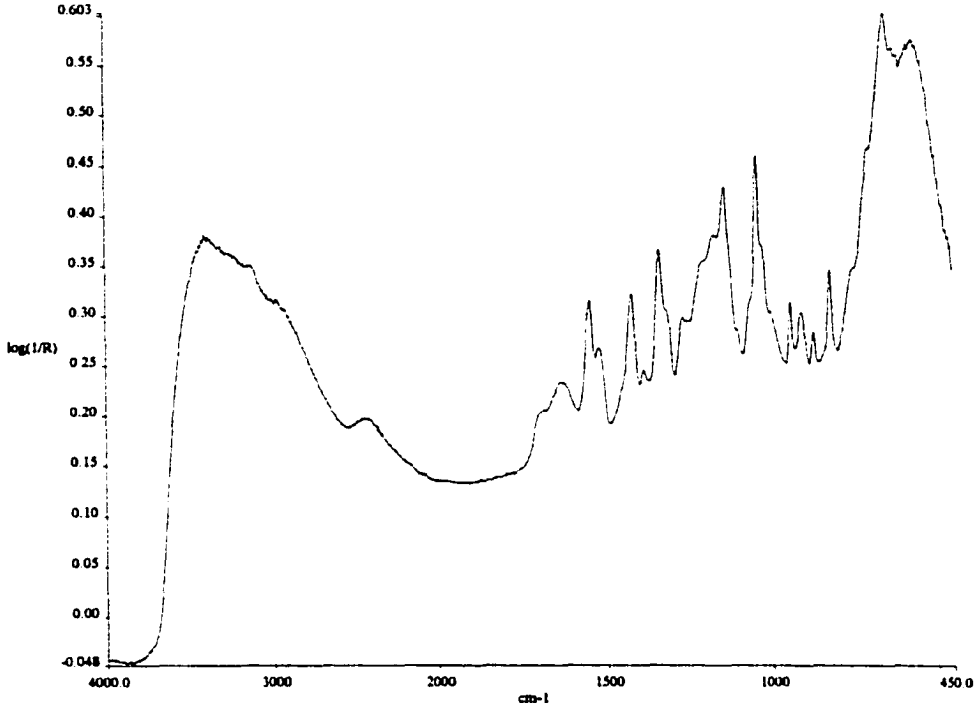

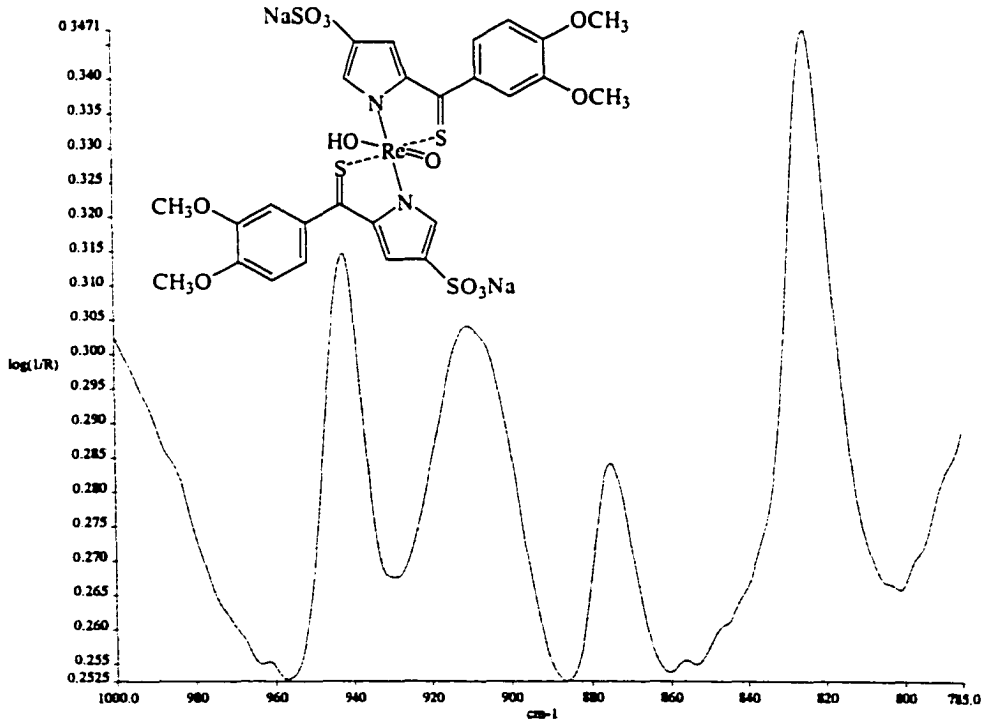

PART 2

CRYSTALLOGRAPHIC DATA

Note: Ellipsoids correspond to 30% probability in ORTEP drawings of the molecules.

Compound 1c

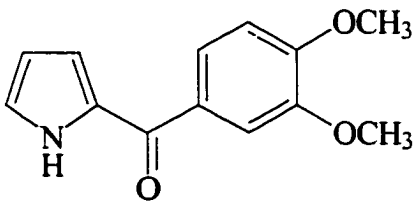

Crystal data

$C_{13}H_{13}NO_3$

$M_r = 231.244$

Orthorhombic

$Pca2_1$

$a = 18.972(8)$ Å

$b = 9.065(3)$ Å

$c = 6.867(2)$ Å

$V = 1181.0(7)$ Å^3

$Z = 4$

$D_x = 1.3006$ Mg m^{-3}

D_m not measured

Cu $K\alpha$ radiation

$\lambda = 1.54056$ Å

Cell parameters from 25 reflections

$\theta = 19.00-24.00°$

$\mu = 0.766$ mm^{-1}

$T = 293(2)$ K

Block

Pale grey-green

0.76 × 0.36 × 0.21 mm

Data collection

Nonius CAD-4 diffractometer

ω scan

Absorption correction:

by integration ABSORP in *NRCVAX*

(Gabe *et al.* 1989)

T_{min} = 0.6686, T_{max} = 0.8714

23801 measured reflections

2228 independent reflections

1743 reflections with

$>2\sigma(I)$

R_{int} = 0.045

θ_{max} = 69.82°

$h = -23 \rightarrow 23$

$k = -11 \rightarrow 11$

$l = -8 \rightarrow 8$

5 standard reflections

frequency: 60 min

intensity decay: no decay, variation 1.7%

Refinement

Refinement on F^2

$R[F^2 > 2\sigma(F^2)]$ = 0.0616

$wR(F^2)$ = 0.1485

S = 1.071

2228 reflections

157 parameters

H-atom parameters constrained

$w=1/[\sigma^2(F_o^2) + (0.1015P)^2]$

where $P = (F_o^2 + 2F_c^2)/3$

$(\Delta/\sigma)_{max}$ = 0.000

$\Delta\rho_{max}$ = 0.155 e Å^{-3}

$\Delta\rho_{min}$ = −0.160 e Å^{-3}

Extinction correction: *SHELXL*96 (Sheldrick, 1996)

Extinction coefficient: 0.0205 (19)

Scattering factors from *International Tables for Crystallography* (Vol. C)

Absolute structure: Flack (1983)

Flack parameter = 0.1 (4)

Table 1. *Selected geometric parameters (Å, °)*

O1—C1	1.231 (3)	C7—C12	1.410 (3)
C1—C2	1.453 (4)	C8—C9	1.383 (5)
C1—C7	1.479 (4)	C9—C10	1.384 (4)
C2—N3	1.371 (4)	C10—O10	1.360 (3)
C2—C6	1.385 (4)	C10—C11	1.396 (4)
N3—C4	1.354 (4)	C11—O11	1.373 (3)
C4—C5	1.348 (5)	C11—C12	1.376 (4)
C5—C6	1.396 (4)	C13—O10	1.420 (4)
C7—C8	1.375 (4)	C14—O11	1.424 (4)

O1—C1—C2	120.4 (3)	C12—C7—C1	117.0 (3)
O1—C1—C7	120.0 (3)	C7—C8—C9	120.8 (2)
C2—C1—C7	119.6 (2)	C8—C9—C10	120.0 (3)
N3—C2—C6	106.2 (2)	O10—C10—C9	124.9 (3)
N3—C2—C1	119.9 (3)	O10—C10—C11	115.2 (2)
C6—C2—C1	133.8 (3)	C9—C10—C11	119.9 (3)
C4—N3—C2	110.0 (3)	O11—C11—C12	124.5 (3)
C5—C4—N3	108.2 (3)	O11—C11—C10	115.6 (2)
C4—C5—C6	108.1 (3)	C12—C11—C10	119.8 (2)
C2—C6—C5	107.6 (3)	C11—C12—C7	120.2 (3)
C8—C7—C12	119.2 (3)	C10—O10—C13	117.2 (2)
C8—C7—C1	123.7 (2)	C11—O11—C14	117.5 (2)
O1—C1—C2—N3	5.1 (4)	C1—C7—C8—C9	177.8 (3)
C7—C1—C2—N3	−176.3 (3)	C7—C8—C9—C10	1.2 (4)
O1—C1—C2—C6	−171.6 (3)	C8—C9—C10—O10	177.6 (3)
C7—C1—C2—C6	7.0 (5)	C8—C9—C10—C11	−2.2 (4)
C6—C2—N3—C4	−1.2 (3)	O10—C10—C11—O11	0.3 (4)
C1—C2—N3—C4	−178.7 (3)	C9—C10—C11—O11	−179.8 (3)
C2—N3—C4—C5	1.1 (4)	O10—C10—C11—C12	−178.7 (2)
N3—C4—C5—C6	−0.5 (4)	C9—C10—C11—C12	1.1 (4)
N3—C2—C6—C5	0.9 (3)	O11—C11—C12—C7	−178.0 (3)
C1—C2—C6—C5	177.9 (3)	C10—C11—C12—C7	1.0 (4)
C4—C5—C6—C2	−0.2 (4)	C8—C7—C12—C11	−2.0 (4)
O1—C1—C7—C8	−142.5 (3)	C1—C7—C12—C11	−179.1 (3)
C2—C1—C7—C8	38.9 (4)	C9—C10—O10—C13	−9.9 (4)
O1—C1—C7—C12	34.6 (4)	C11—C10—O10—C13	169.9 (3)
C2—C1—C7—C12	−144.1 (3)	C12—C11—O11—C14	1.4 (4)
C12—C7—C8—C9	0.9 (4)	C10—C11—O11—C14	−177.6 (3)

Table 2. *Hydrogen-bonding geometry (Å, °)*

D—H···*A*	*D*—H	H···*A*	*D*···*A*	*D*—H···*A*
N3—H3···O1^{i}	0.86	2.37	3.127 (4)	146.5

Symmetry codes: (i) $1-x, -y, z-\frac{1}{2}$.

Data collection: CAD-4 software (Enraf–Nonius, 1989). Cell refinement: CAD-4 software (Enraf–Nonius, 1989). Data reduction: NRC-2, NRC-2A (Ahmed *et al.* 1973). Program(s) used to solve structure: *SHELXS*97 (Sheldrick, 1997). Program(s) used to refine structure: *SHELXL*96 (Sheldrick, 1996). Molecular graphics: *SHELXTL* (Bruker, 1997). Software used to prepare material for publication: *SHELXL*96 (Sheldrick, 1996).

References

Ahmed, F. R., Hall, S. R., Pippy, M. E. & Huber, C. P. (1973). NRC Crystallographic Computer Programs for the IBM/360. Accession Nos. 133–147 in *J. Appl. Cryst.* **6**, 309–346.

Enraf–Nonius (1989). CAD-4 Software. Version 5.0. Enraf–Nonius, Delft, The Netherlands.

Flack, H. D. (1983). *Acta Cryst.* **A39**, 876–881.

Flack, H. D. & Schwarzenbach, D. (1988). *Acta Cryst.* **A44**, 499–506.

Gabe, E. J., Le Page, Y., Charland, J.-P., Lee, F. L. & White, P. S. (1989). *J. Appl. Cryst.* **22**, 384–387.

International Tables for Crystallography (1992). Vol. C. Tables 4.2.6.8 and 6.1.1. **4**, Dordrecht: Kluwer Academic Publishers.

Sheldrick, G. M. (1997). *SHELXS*97. Program for the Solution of Crystal Structures. University of Gottingen, Germany.

Sheldrick, G. M. (1996). *SHELXL*96. Program for the Refinement *of Crystal Structures*. University of Göttingen, Germany.

SHELXTL (1997) Release 5.10; The Complete Software Package for Single Crystal Structure Determination. Bruker AXS Inc., Madison, WI 53719–1173.

Spek, A. L. (1995). *PLATON*, Molecular Geometry Program, July 1995 version, University of Utrecht, Utrecht, Holland.

Space group confirmed by *PLATON* program (Spek, 1995). Data reduction performed using a locally modified version of the NRC-2 program (Ahmed *et al.* 1973). The structure was solved by direct method using *SHELXS*97 (Sheldrick, 1997) and difmap synthesis using *SHELXTL* (Sheldrick, 1997) and *SHELXL*96 (Sheldrick, 1996). All non-H atoms anisotropic, H atoms isotropic. H atoms constrained to the parent site using a riding model; *SHELXL*96 defaults, C—H 0.93 to 0.96 and N—H 0.86 Å. The isotropic factors, U_{iso} , were adjusted to 50% higher value of the parent site (methyl, NH) and 20% higher (others). A final verification of possible voids was performed using the VOID routine of the *PLATON* program (Spek, 1995).

Data collection: CAD-4 software (Enraf–Nonius, 1989). Cell refinement: CAD-4 software (Enraf–Nonius, 1989). Data reduction: NRC-2, NRC-2A (Ahmed *et al.* 1973). Program(s) used to solve structure: *SHELXS*97 (Sheldrick, 1997). Program(s) used to refine structure: *SHELXL*96 (Sheldrick, 1996). Molecular graphics: *SHELXTL* (Bruker, 1997). Software used to prepare material for publication: *SHELXL*96 (Sheldrick, 1996).

Table *S*1. *Fractional atomic coordinates and equivalent isotropic displacement parameters (Å²)*

$$U_{eq} = (1/3)\Sigma_i\Sigma_j U^{ij} a^i a^j \mathbf{a}_i.\mathbf{a}_j.$$

	x	y	z	U_{eq}
O1	0.48586 (11)	0.0941 (2)	−0.2345 (4)	0.0908 (8)
C1	0.42879 (15)	0.0648 (3)	−0.1586 (5)	0.0679 (8)
C2	0.38455 (15)	−0.0513 (3)	−0.2381 (5)	0.0633 (7)
N3	0.40872 (14)	−0.1365 (3)	−0.3890 (4)	0.0770 (7)
H3	0.4496	−0.1285	−0.4419	0.116
C4	0.35869 (18)	−0.2351 (3)	−0.4424 (6)	0.0820 (9)
H4	0.3631	−0.3056	−0.5400	0.098
C5	0.30144 (17)	−0.2131 (3)	−0.3297 (6)	0.0809 (9)
H5	0.2593	−0.2654	−0.3366	0.097
C6	0.31641 (15)	−0.0983 (3)	−0.2009 (5)	0.0698 (8)
H6	0.2861	−0.0601	−0.1071	0.084
C7	0.40420 (13)	0.1502 (3)	0.0119 (4)	0.0623 (7)
C8	0.36831 (15)	0.0892 (3)	0.1660 (5)	0.0667 (7)
H8	0.3570	−0.0106	0.1640	0.080
C9	0.34886 (15)	0.1745 (3)	0.3241 (5)	0.0672 (7)
H9	0.3254	0.1316	0.4286	0.081
C10	0.36430 (14)	0.3237 (3)	0.3268 (5)	0.0626 (7)
C11	0.40169 (13)	0.3869 (3)	0.1728 (5)	0.0623 (7)
C12	0.42200 (13)	0.3011 (3)	0.0174 (5)	0.0636 (7)
H12	0.4475	0.3428	−0.0843	0.076
C13	0.2978 (2)	0.3653 (4)	0.6144 (5)	0.0875 (10)
H13A	0.2556	0.3311	0.5522	0.131
H13B	0.2864	0.4434	0.7034	0.131
H13C	0.3192	0.2854	0.6845	0.131
O10	0.34549 (11)	0.4185 (2)	0.4713 (3)	0.0800 (7)
C14	0.4502 (2)	0.6055 (3)	0.0316 (6)	0.0888 (10)
H14A	0.4949	0.5585	0.0108	0.133
H14B	0.4575	0.7077	0.0622	0.133
H14C	0.4222	0.5976	−0.0843	0.133
O11	0.41461 (11)	0.5354 (2)	0.1889 (4)	0.0764 (6)

Table *S*2. *Anisotropic displacement parameters* (Å²)

	U_{11}	U_{22}	U_{33}	U_{12}	U_{13}	U_{23}
O1	0.0756 (13)	0.0663 (11)	0.130 (2)	−0.0112 (10)	0.0339 (14)	−0.0173 (14)
C1	0.0645 (15)	0.0463 (13)	0.093 (2)	0.0012 (10)	0.0099 (15)	−0.0016 (14)
C2	0.0637 (14)	0.0449 (11)	0.0813 (18)	0.0043 (10)	0.0046 (14)	−0.0050 (12)
N3	0.0836 (16)	0.0529 (12)	0.0945 (18)	0.0004 (11)	0.0199 (14)	−0.0085 (13)
C4	0.096 (2)	0.0578 (15)	0.093 (2)	−0.0039 (15)	−0.0003 (19)	−0.0149 (16)
C5	0.0732 (17)	0.0691 (17)	0.100 (2)	−0.0064 (14)	−0.0047 (18)	−0.0112 (18)
C6	0.0618 (14)	0.0596 (14)	0.088 (2)	0.0040 (12)	0.0001 (15)	−0.0063 (15)
C7	0.0561 (13)	0.0461 (12)	0.0849 (18)	0.0007 (10)	0.0016 (13)	−0.0033 (14)
C8	0.0703 (15)	0.0465 (12)	0.0834 (19)	−0.0044 (11)	−0.0033 (15)	0.0035 (13)
C9	0.0713 (16)	0.0555 (14)	0.0749 (18)	−0.0082 (12)	−0.0024 (14)	0.0046 (14)
C10	0.0582 (13)	0.0570 (14)	0.0726 (16)	−0.0050 (10)	−0.0024 (12)	−0.0044 (13)
C11	0.0555 (12)	0.0460 (12)	0.0852 (18)	−0.0040 (10)	−0.0009 (14)	−0.0042 (12)
C12	0.0571 (13)	0.0506 (12)	0.0833 (18)	−0.0033 (11)	0.0073 (13)	−0.0007 (14)
C13	0.096 (2)	0.087 (2)	0.079 (2)	−0.0044 (18)	0.0191 (18)	−0.0021 (19)
O10	0.0880 (15)	0.0676 (12)	0.0844 (15)	−0.0135 (10)	0.0179 (11)	−0.0145 (11)
C14	0.111 (2)	0.0534 (15)	0.102 (2)	−0.0229 (16)	0.018 (2)	0.0006 (17)
O11	0.0881 (13)	0.0475 (9)	0.0937 (14)	−0.0135 (9)	0.0174 (13)	−0.0090 (10)

Table S3. *Geometric parameters (Å, °)*

O1—C1	1.231 (3)	C9—C10	1.384 (4)
C1—C2	1.453 (4)	C9—H9	0.9300
C1—C7	1.479 (4)	C10—O10	1.360 (3)
C2—N3	1.371 (4)	C10—C11	1.396 (4)
C2—C6	1.385 (4)	C11—O11	1.373 (3)
N3—C4	1.354 (4)	C11—C12	1.376 (4)
N3—H3	0.8600	C12—H12	0.9300
C4—C5	1.348 (5)	C13—O10	1.420 (4)
C4—H4	0.9300	C13—H13A	0.9600
C5—C6	1.396 (4)	C13—H13B	0.9600
C5—H5	0.9300	C13—H13C	0.9600
C6—H6	0.9300	C14—O11	1.424 (4)
C7—C8	1.375 (4)	C14—H14A	0.9600
C7—C12	1.410 (3)	C14—H14B	0.9600
C8—C9	1.383 (5)	C14—H14C	0.9600
C8—H8	0.9300		
O1—C1—C2	120.4 (3)	C8—C9—H9	119.9
O1—C1—C7	120.0 (3)	C10—C9—H9	119.9
C2—C1—C7	119.6 (2)	O10—C10—C9	124.9 (3)
N3—C2—C6	106.2 (2)	O10—C10—C11	115.2 (2)
N3—C2—C1	119.9 (3)	C9—C10—C11	119.9 (3)
C6—C2—C1	133.8 (3)	O11—C11—C12	124.5 (3)
C4—N3—C2	110.0 (3)	O11—C11—C10	115.6 (2)
C4—N3—H3	125.0	C12—C11—C10	119.8 (2)
C2—N3—H3	125.0	C11—C12—C7	120.2 (3)
C5—C4—N3	108.2 (3)	C11—C12—H12	119.9
C5—C4—H4	125.9	C7—C12—H12	119.9
N3—C4—H4	125.9	O10—C13—H13A	109.5
C4—C5—C6	108.1 (3)	O10—C13—H13B	109.5
C4—C5—H5	125.9	H13A—C13—H13B	109.5
C6—C5—H5	125.9	O10—C13—H13C	109.5
C2—C6—C5	107.6 (3)	H13A—C13—H13C	109.5
C2—C6—H6	126.2	H13B—C13—H13C	109.5
C5—C6—H6	126.2	C10—O10—C13	117.2 (2)
C8—C7—C12	119.2 (3)	O11—C14—H14A	109.5
C8—C7—C1	123.7 (2)	O11—C14—H14B	109.5
C12—C7—C1	117.0 (3)	H14A—C14—H14B	109.5
C7—C8—C9	120.8 (2)	O11—C14—H14C	109.5
C7—C8—H8	119.6	H14A—C14—H14C	109.5
C9—C8—H8	119.6	H14B—C14—H14C	109.5
C8—C9—C10	120.0 (3)	C11—O11—C14	117.5 (2)
O1—C1—C2—N3	5.1 (4)	C1—C7—C8—C9	177.8 (3)
C7—C1—C2—N3	−176.3 (3)	C7—C8—C9—C10	1.2 (4)
O1—C1—C2—C6	−171.6 (3)	C8—C9—C10—O10	177.6 (3)
C7—C1—C2—C6	7.0 (5)	C8—C9—C10—C11	−2.2 (4)
C6—C2—N3—C4	−1.2 (3)	O10—C10—C11—O11	0.3 (4)
C1—C2—N3—C4	−178.7 (3)	C9—C10—C11—O11	−179.8 (3)
C2—N3—C4—C5	1.1 (4)	O10—C10—C11—C12	−178.7 (2)
N3—C4—C5—C6	−0.5 (4)	C9—C10—C11—C12	1.1 (4)
N3—C2—C6—C5	0.9 (3)	O11—C11—C12—C7	−178.0 (3)
C1—C2—C6—C5	177.9 (3)	C10—C11—C12—C7	1.0 (4)
C4—C5—C6—C2	−0.2 (4)	C8—C7—C12—C11	−2.0 (4)
O1—C1—C7—C8	−142.5 (3)	C1—C7—C12—C11	−179.1 (3)
C2—C1—C7—C8	38.9 (4)	C9—C10—O10—C13	−9.9 (4)
O1—C1—C7—C12	34.6 (4)	C11—C10—O10—C13	169.9 (3)
C2—C1—C7—C12	−144.1 (3)	C12—C11—O11—C14	1.4 (4)
C12—C7—C8—C9	0.9 (4)	C10—C11—O11—C14	−177.6 (3)

O1
C14
C1
N3
C12
C7
C2
C4
O11
C11
C10
C8
C6
C5
O10
C9
C13

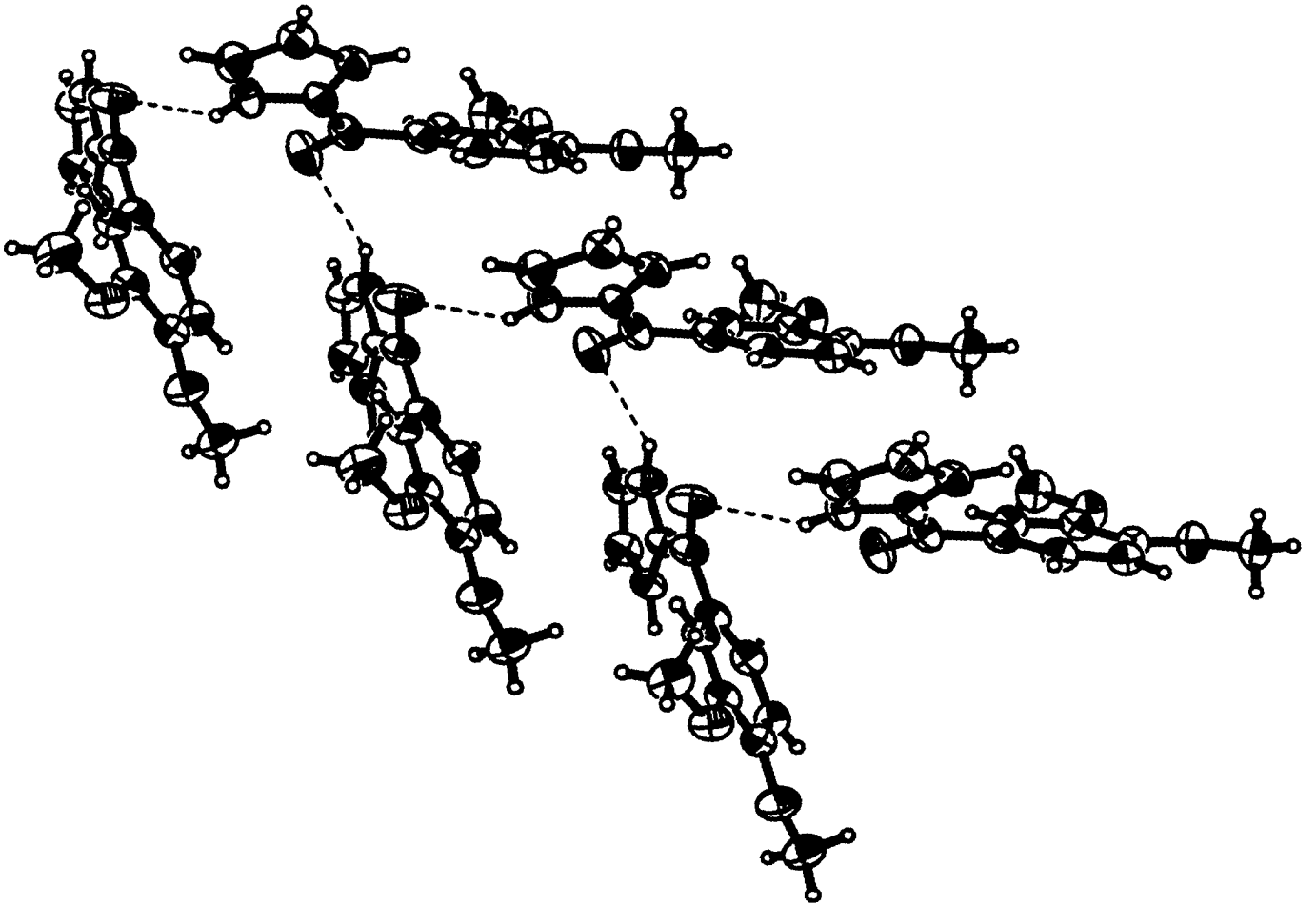

Compound **2b**

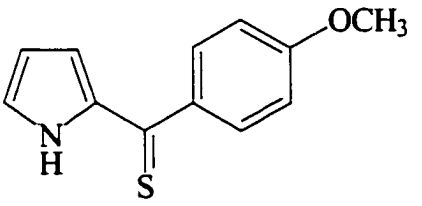

Crystal data

$C_{12}H_{11}NOS$

$M_r = 217.278$

Monoclinic

$P2_1/c$

$a = 11.8386(1)$ Å

$b = 11.9453(1)$ Å

$c = 7.5061(1)$ Å

$\beta = 98.676(1)°$

$V = 1049.33(2)$ Å^3

$Z = 4$

$D_x = 1.3753$ Mg m^{-3}

D_m not measured

Cu $K\alpha$ radiation

$\lambda = 1.54178$ Å

Cell parameters from 11189 reflections

$\theta = 3.70–72.85°$

$\mu = 2.490$ mm^{-1}

$T = 293(2)$ K

Block

Dark red

0.58 × 0.52 × 0.18 mm

Data collection

Bruker AXS SMART 2K/Platform diffractometer

ω scan

Absorption correction:

multi-scan SADABS (Sheldrick, 1996)

$T_{min} = 0.3850$, $T_{max} = 0.7390$

12236 measured reflections

2054 independent reflections

1985 reflections with $>2\sigma(I)$

$R_{int} = 0.0402$

$\theta_{max} = 72.84°$

$h = -14 \rightarrow 14$

$k = -14 \rightarrow 14$

$l = -8 \rightarrow 7$

108 standard reflections

intensity decay: none

Refinement

Refinement on F^2

$R[F^2 > 2\sigma(F^2)] = 0.0402$

$wR(F^2) = 0.1118$

$S = 1.079$

2054 reflections

138 parameters

H-atom parameters constrained

$w=1/[\sigma^2(F_o^2) + (0.0678P)^2 + 0.3079P]$

where $P = (F_o^2 + 2F_c^2)/3$

$(\Delta/\sigma)_{max} = 0.000$

$\Delta\rho_{max} = 0.294$ e Å^{-3}

$\Delta\rho_{min} = -0.330$ e Å^{-3}

Extinction correction: *SHELXL*96 (Sheldrick, 1996)

Extinction coefficient: 0.0275(19)

Scattering factors from *International Tables for Crystallography* (Vol. C)

Table 1. *Selected geometric parameters (Å, °)*

S1—C1	1.6686 (15)	C7—C8	1.396 (2)
C1—C2	1.426 (2)	C7—C12	1.403 (2)
C1—C7	1.4782 (19)	C8—C9	1.386 (2)
C2—N3	1.3779 (18)	C9—C10	1.391 (2)
C2—C6	1.399 (2)	C10—O10	1.3605 (17)
N3—C4	1.338 (2)	C10—C11	1.393 (2)
C4—C5	1.381 (3)	C11—C12	1.377 (2)
C5—C6	1.390 (2)	O10—C13	1.424 (2)
C2—C1—C7	118.60 (13)	C8—C7—C1	122.48 (13)
C2—C1—S1	121.35 (11)	C12—C7—C1	119.82 (13)
C7—C1—S1	120.04 (11)	C9—C8—C7	121.40 (13)
N3—C2—C6	105.82 (13)	C8—C9—C10	119.66 (14)
N3—C2—C1	121.46 (13)	O10—C10—C9	124.57 (14)
C6—C2—C1	132.70 (14)	O10—C10—C11	115.64 (13)
C4—N3—C2	110.46 (14)	C9—C10—C11	119.78 (13)
N3—C4—C5	108.48 (14)	C12—C11—C10	119.97 (13)
C4—C5—C6	107.12 (15)	C11—C12—C7	121.31 (14)
C5—C6—C2	108.11 (14)	C10—O10—C13	117.67 (12)
C8—C7—C12	117.70 (13)		

C7—C1—C2—N3	−174.12 (13)	S1—C1—C7—C12	35.67 (19)
S1—C1—C2—N3	6.7 (2)	C12—C7—C8—C9	3.8 (2)
C7—C1—C2—C6	8.1 (3)	C1—C7—C8—C9	−176.60 (14)
S1—C1—C2—C6	−171.08 (14)	C7—C8—C9—C10	−0.3 (2)
C6—C2—N3—C4	−0.28 (17)	C8—C9—C10—O10	178.09 (14)
C1—C2—N3—C4	−178.60 (14)	C8—C9—C10—C11	−3.1 (2)
C2—N3—C4—C5	−0.30 (19)	O10—C10—C11—C12	−178.16 (14)
N3—C4—C5—C6	0.8 (2)	C9—C10—C11—C12	2.9 (2)
C4—C5—C6—C2	−0.92 (19)	C10—C11—C12—C7	0.7 (2)
N3—C2—C6—C5	0.74 (17)	C8—C7—C12—C11	−4.0 (2)
C1—C2—C6—C5	178.79 (16)	C1—C7—C12—C11	176.40 (14)
C2—C1—C7—C8	36.9 (2)	C9—C10—O10—C13	−13.1 (2)
S1—C1—C7—C8	−143.89 (13)	C11—C10—O10—C13	168.10 (15)
C2—C1—C7—C12	−143.50 (15)		

Table 2. *Hydrogen-bonding geometry (Å, °)*

D—H···*A*	*D*—H	H···*A*	*D*···*A*	*D*—H···*A*
N3—H3···S1^{i}	0.86	2.78	3.419 (1)	132.9

Symmetry codes: (i) $1-x, 2-y, -z$.

Data collection: SMART (Bruker, 1999). Cell refinement: SAINT (Bruker, 1999). Data reduction: SAINT (Bruker, 1999). Program(s) used to solve structure: *SHELXS*97 (Sheldrick, 1997). Program(s) used to refine structure: *SHELXL*96 (Sheldrick, 1996). Molecular graphics: *SHELXTL* (Bruker, 1997). Software used to prepare material for publication: *SHELXL*96 (Sheldrick, 1996).

References

International Tables for Crystallography (1992). Vol. C. Tables 4.2.6.8 and 6.1.1. **4**. Dordrecht: Kluwer Academic Publishers.

SAINT (1999) Release 6.06; Integration Software for Single Crystal Data, Bruker AXS Inc., Madison, WI 53719-1173.

Sheldrick, G. M. (1996). SADABS, Bruker Area Detector Absorption Corrections, Bruker AXS Inc., Madison, WI 53719-1173.

Sheldrick, G. M. (1997). *SHELXS*97. Program for the Solution of Crystal Structures. University of Gottingen, Germany.

Sheldrick, G. M. (1996). *SHELXL*96. Program for the Refinement of Crystal Structures. University of Gottingen, Germany.

SHELXTL (1997) Release 5.10; The Complete Software Package for Single Crystal Structure Determination, Bruker AXS Inc., Madison, WI 53719-1173.

SMART (1999) Release 5.059; Bruker Molecular Analysis Research Tool, Bruker AXS Inc., Madison, WI 53719-1173.

Spek, A. L. (1995). July 1995 version; *PLATON*, Molecular Geometry Program, University of Utrecht, Utrecht, Holland.

XPREP (1997) Release 5.10: X-ray data Preparation and Reciprocal space Exploration Program, Bruker AXS Inc., Madison, WI 53719-1173.

Data reduction processing was carried out by the use of the program SAINT (Bruker, 1999), which applied Lorentz and polarization corrections to three-dimensionally integrated diffraction spots. The program SADABS (Sheldrick, 1996) was utilized for the scaling of diffraction data, the application of a decay correction, and an empirical absorption correction based on redundant reflections. The space group was confirmed by XPREP routine in *SHELXTL* program (Sheldrick, 1997). The structure was solved by direct method using *SHELXS*97 (Sheldrick, 1997) and difmap synthesis using *SHELXL*96 (Sheldrick, 1996). All non-H atoms anisotropic, hydrogen atoms isotropic. H atoms constrained to the parent site using a riding model; *SHELXL*96 defaults, C—H 0.93 to 0.96, N—H 0.86 Å. The isotropic factors, U_{iso} , were adjusted to 50% higher value of the parent site (methyl and NH) and 20% higher (others). A final verification of possible voids was performed using the VOID routine of the *PLATON* program (Spek, 1995).

Data collection: SMART (Bruker, 1999). Cell refinement: SAINT (Bruker, 1999). Data reduction: SAINT (Bruker, 1999). Program(s) used to solve structure: *SHELXS*97 (Sheldrick, 1997). Program(s) used to refine structure: *SHELXL*96 (Sheldrick, 1996). Molecular graphics: *SHELXTL* (Bruker, 1997). Software used to prepare material for publication: *SHELXL*96 (Sheldrick, 1996).

Table *S1*. *Fractional atomic coordinates and equivalent isotropic displacement parameters (Å²)*

$$U_{eq} = (1/3)\Sigma_i\Sigma_j U^{ij} a^i a^j \mathbf{a}_i.\mathbf{a}_j.$$

	x	*y*	*z*	U_{eq}
S1	0.69294 (3)	0.96827 (4)	−0.00753 (6)	0.0522 (2)
C1	0.73243 (12)	0.91650 (12)	0.1989 (2)	0.0349 (3)
C2	0.65056 (12)	0.89250 (12)	0.3149 (2)	0.0341 (3)
N3	0.53491 (10)	0.90014 (11)	0.25519 (19)	0.0395 (3)
H3	0.5050	0.9178	0.1473	0.059
C4	0.47567 (14)	0.87621 (14)	0.3888 (2)	0.0444 (4)
H4	0.3965	0.8763	0.3802	0.053
C5	0.55197 (14)	0.85136 (15)	0.5415 (2)	0.0452 (4)
H5	0.5338	0.8310	0.6533	0.054
C6	0.66114 (13)	0.86246 (13)	0.4967 (2)	0.0400 (4)
H6	0.7294	0.8518	0.5742	0.048
C7	0.85458 (12)	0.89605 (12)	0.26610 (19)	0.0332 (3)
C8	0.89195 (12)	0.80525 (12)	0.3765 (2)	0.0354 (3)
H8	0.8389	0.7532	0.4045	0.042
C9	1.00643 (12)	0.79106 (12)	0.4454 (2)	0.0364 (3)
H9	1.0297	0.7302	0.5193	0.044
C10	1.08636 (12)	0.86825 (13)	0.4036 (2)	0.0353 (3)
C11	1.05160 (13)	0.95607 (13)	0.2858 (2)	0.0376 (4)
H11	1.1053	1.0059	0.2532	0.045
C12	0.93771 (13)	0.96911 (12)	0.2178 (2)	0.0366 (4)
H12	0.9154	1.0275	0.1383	0.044
O10	1.20008 (9)	0.86421 (11)	0.46760 (16)	0.0457 (3)
C13	1.23672 (15)	0.79024 (17)	0.6136 (3)	0.0536 (5)
H13A	1.1902	0.8012	0.7065	0.080
H13B	1.3151	0.8054	0.6610	0.080
H13C	1.2295	0.7143	0.5718	0.080

Table *S2*. *Anisotropic displacement parameters* (Å²)

	U_{11}	U_{22}	U_{33}	U_{12}	U_{13}	U_{23}
S1	0.0393 (3)	0.0775 (4)	0.0385 (3)	0.00640 (18)	0.00165 (18)	0.01798 (19)
C1	0.0328 (7)	0.0363 (7)	0.0347 (8)	0.0010 (6)	0.0021 (6)	0.0008 (5)
C2	0.0286 (7)	0.0358 (7)	0.0370 (8)	0.0006 (5)	0.0018 (5)	0.0003 (5)
N3	0.0301 (6)	0.0467 (7)	0.0404 (7)	0.0016 (5)	0.0009 (5)	0.0013 (5)
C4	0.0336 (8)	0.0458 (9)	0.0551 (10)	−0.0014 (6)	0.0110 (7)	0.0003 (7)
C5	0.0442 (9)	0.0476 (9)	0.0459 (9)	0.0013 (7)	0.0137 (7)	0.0058 (7)
C6	0.0354 (8)	0.0458 (8)	0.0382 (8)	0.0020 (6)	0.0037 (6)	0.0036 (6)
C7	0.0303 (7)	0.0381 (7)	0.0310 (7)	0.0012 (5)	0.0041 (5)	0.0003 (5)
C8	0.0321 (7)	0.0375 (7)	0.0368 (8)	−0.0022 (5)	0.0060 (6)	0.0033 (6)
C9	0.0347 (7)	0.0386 (7)	0.0356 (8)	0.0037 (6)	0.0048 (6)	0.0052 (6)
C10	0.0289 (7)	0.0450 (8)	0.0321 (7)	0.0011 (6)	0.0051 (5)	−0.0037 (6)
C11	0.0335 (8)	0.0431 (8)	0.0374 (8)	−0.0050 (6)	0.0090 (6)	0.0018 (6)
C12	0.0376 (8)	0.0389 (8)	0.0338 (8)	0.0003 (6)	0.0067 (6)	0.0059 (5)
O10	0.0281 (5)	0.0636 (8)	0.0446 (7)	−0.0004 (4)	0.0027 (4)	0.0075 (5)
C13	0.0356 (8)	0.0750 (12)	0.0476 (10)	0.0057 (8)	−0.0022 (7)	0.0096 (8)

Table *S3. Geometric parameters (Å, °)*

S1—C1	1.6686 (15)	C8—C9	1.386 (2)
C1—C2	1.426 (2)	C8—H8	0.9300
C1—C7	1.4782 (19)	C9—C10	1.391 (2)
C2—N3	1.3779 (18)	C9—H9	0.9300
C2—C6	1.399 (2)	C10—O10	1.3605 (17)
N3—C4	1.338 (2)	C10—C11	1.393 (2)
N3—H3	0.8600	C11—C12	1.377 (2)
C4—C5	1.381 (3)	C11—H11	0.9300
C4—H4	0.9300	C12—H12	0.9300
C5—C6	1.390 (2)	O10—C13	1.424 (2)
C5—H5	0.9300	C13—H13A	0.9600
C6—H6	0.9300	C13—H13B	0.9600
C7—C8	1.396 (2)	C13—H13C	0.9600
C7—C12	1.403 (2)		
C2—C1—C7	118.60 (13)	C9—C8—H8	119.3
C2—C1—S1	121.35 (11)	C7—C8—H8	119.3
C7—C1—S1	120.04 (11)	C8—C9—C10	119.66 (14)
N3—C2—C6	105.82 (13)	C8—C9—H9	120.2
N3—C2—C1	121.46 (13)	C10—C9—H9	120.2
C6—C2—C1	132.70 (14)	O10—C10—C9	124.57 (14)
C4—N3—C2	110.46 (14)	O10—C10—C11	115.64 (13)
C4—N3—H3	124.8	C9—C10—C11	119.78 (13)
C2—N3—H3	124.8	C12—C11—C10	119.97 (13)
N3—C4—C5	108.48 (14)	C12—C11—H11	120.0
N3—C4—H4	125.8	C10—C11—H11	120.0
C5—C4—H4	125.8	C11—C12—C7	121.31 (14)
C4—C5—C6	107.12 (15)	C11—C12—H12	119.4
C4—C5—H5	126.4	C7—C12—H12	119.4
C6—C5—H5	126.4	C10—O10—C13	117.67 (12)
C5—C6—C2	108.11 (14)	O10—C13—H13A	109.5
C5—C6—H6	125.9	O10—C13—H13B	109.5
C2—C6—H6	125.9	H13A—C13—H13B	109.5
C8—C7—C12	117.70 (13)	O10—C13—H13C	109.5
C8—C7—C1	122.48 (13)	H13A—C13—H13C	109.5
C12—C7—C1	119.82 (13)	H13B—C13—H13C	109.5
C9—C8—C7	121.40 (13)		
C7—C1—C2—N3	−174.12 (13)	S1—C1—C7—C12	35.67 (19)
S1—C1—C2—N3	6.7 (2)	C12—C7—C8—C9	3.8 (2)
C7—C1—C2—C6	8.1 (3)	C1—C7—C8—C9	−176.60 (14)
S1—C1—C2—C6	−171.08 (14)	C7—C8—C9—C10	−0.3 (2)
C6—C2—N3—C4	−0.28 (17)	C8—C9—C10—O10	178.09 (14)
C1—C2—N3—C4	−178.60 (14)	C8—C9—C10—C11	−3.1 (2)
C2—N3—C4—C5	−0.30 (19)	O10—C10—C11—C12	−178.16 (14)
N3—C4—C5—C6	0.8 (2)	C9—C10—C11—C12	2.9 (2)
C4—C5—C6—C2	−0.92 (19)	C10—C11—C12—C7	0.7 (2)
N3—C2—C6—C5	0.74 (17)	C8—C7—C12—C11	−4.0 (2)
C1—C2—C6—C5	178.79 (16)	C1—C7—C12—C11	176.40 (14)
C2—C1—C7—C8	36.9 (2)	C9—C10—O10—C13	−13.1 (2)
S1—C1—C7—C8	−143.89 (13)	C11—C10—O10—C13	168.10 (15)
C2—C1—C7—C12	−143.50 (15)		

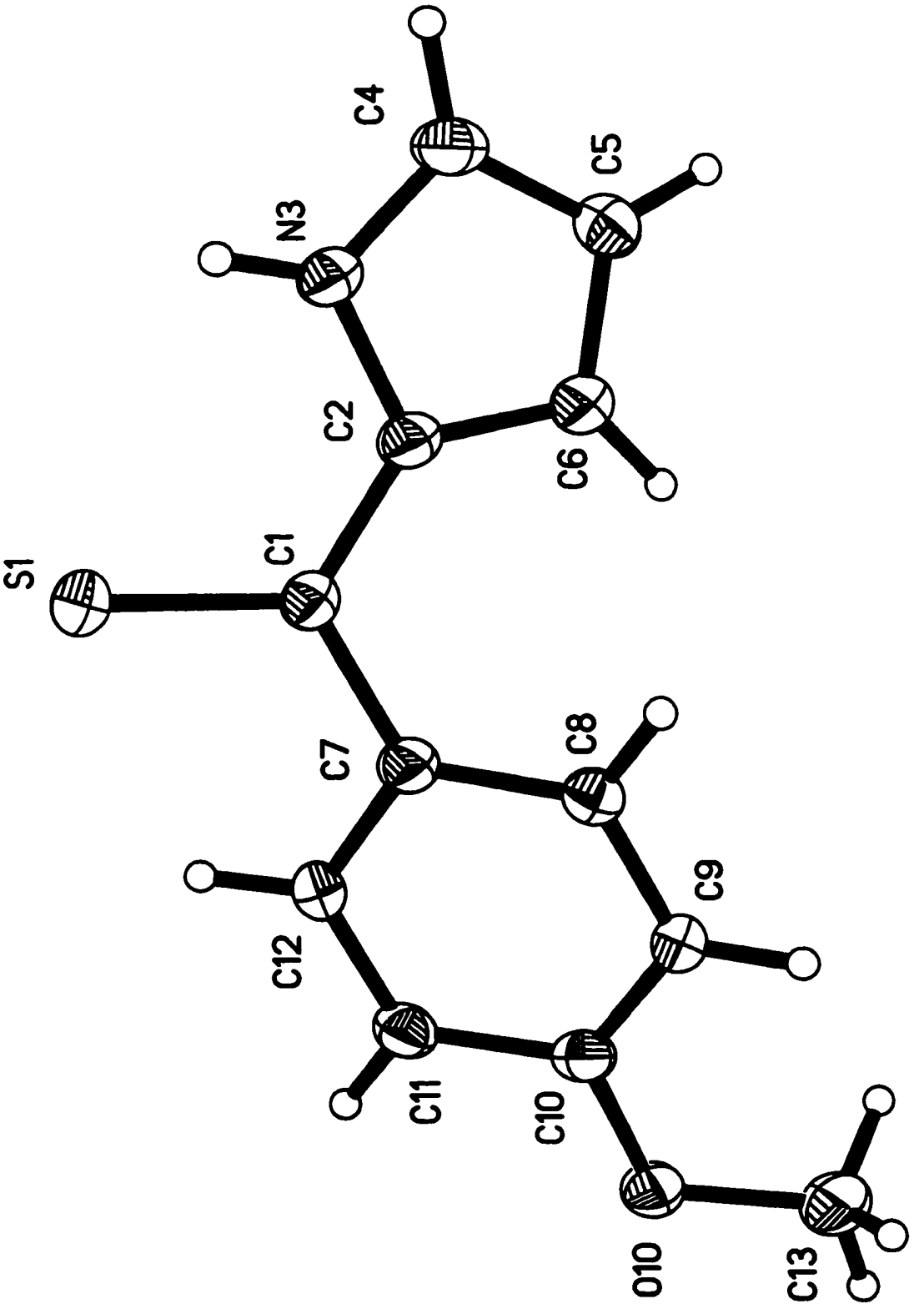
C4
C5
N3
C2
C6
S1
C1
C7
C8
C9
C12
C11
C10
O10
C13

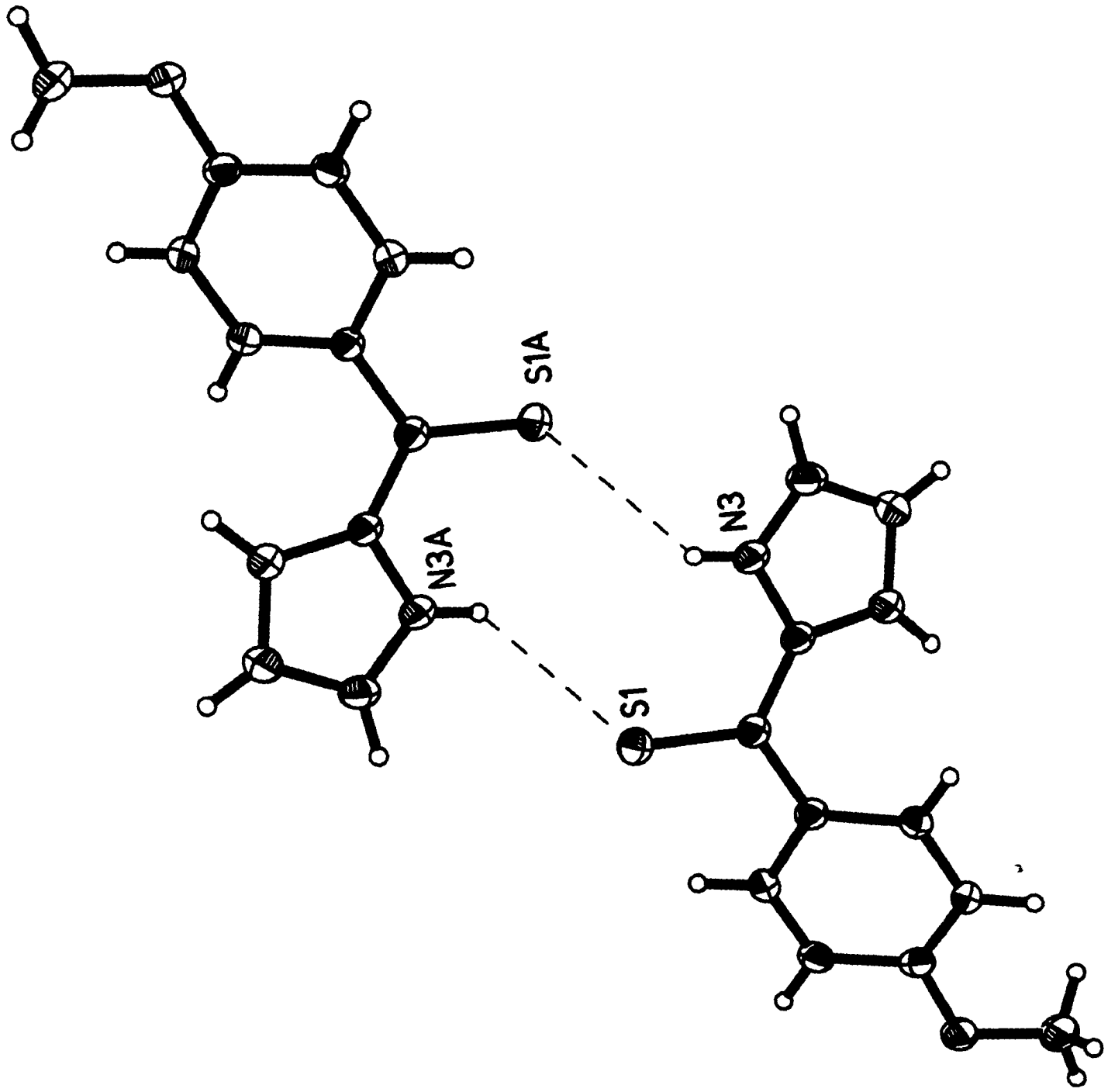
S1A
N3
N3A
S1

Compound 3b

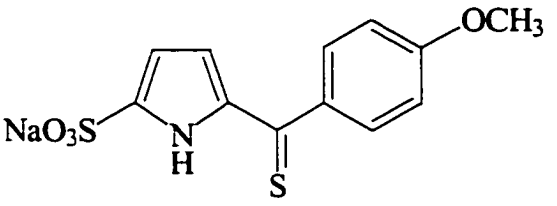

Crystal data

$C_{12}H_{16}NNaO_7S_2$
$M_r = 373.368$
Orthorhombic
Pnma
$a = 6.763(3)$ Å
$b = 7.540(6)$ Å
$c = 31.641(8)$ Å
$V = 1613.5(15)$ Å^3
$Z = 4$
$D_x = 1.5370$ Mg m^{-3}
D_m not measured
Cu $K\alpha$ radiation
$\lambda = 1.54178$ Å

Cell parameters from 25 reflections
$\theta = 20.00-25.00°$
$\mu = 3.587$ mm^{-1}
$T = 293(2)$ K
Block
Intense violet-pink
0.57 × 0.53 × 0.27 mm

Data collection

Nonius CAD-4 diffractometer

$\omega/2\theta$ scan

Absorption correction:
by integration ABSORP in *NRCVAX* (Gabe *et al.* 1989)

$T_{min} = 0.1775$, $T_{max} = 0.4530$

16409 measured reflections

1655 independent reflections

1507 reflections with $>2\sigma(I)$

$R_{int} = 0.031$

$\theta_{max} = 69.92°$

$h = -8 \rightarrow 8$

$k = -9 \rightarrow 9$

$l = -38 \rightarrow 38$

5 standard reflections
frequency: 60 min
intensity decay: no decay, variation 0.8%

Refinement

Refinement on F^2

$R[F^2 > 2\sigma(F^2)] = 0.0286$

$wR(F^2) = 0.0817$

$S = 1.107$

1655 reflections

177 parameters

H-atom parameters constrained

$w=1/[\sigma^2(F_o^2) + (0.0536P)^2 + 0.2229P]$
where $P = (F_o^2 + 2F_c^2)/3$

$(\Delta/\sigma)_{max} = 0.010$

$\Delta\rho_{max} = 0.359$ e Å^{-3}

$\Delta\rho_{min} = -0.266$ e Å^{-3}

Extinction correction: *SHELXL*96 (Sheldrick, 1996)

Extinction coefficient: 0.0146 (6)

Scattering factors from *International Tables for Crystallography* (Vol. C)

Table 1. *Selected geometric parameters (Å, °)*

Na—O2^{i}	2.4455 (12)	C1—C2	1.450 (3)
Na—O2	2.4455 (12)	C1—C7	1.492 (2)
Na—O2^{ii}	2.4538 (12)	C2—C3	1.383 (5)
Na—O2^{iii}	2.4538 (12)	C2—N6	1.382 (3)
Na—O1^{iv}	2.4572 (12)	C3—C4	1.411 (3)
Na—O1	2.5129 (13)	C4—C5	1.361 (3)
Na—Na^{iv}	3.4331 (15)	C5—N6	1.335 (3)
Na—Na^{iii}	3.4331 (15)	C7—C8	1.3900
O1—Na^{iii}	2.4571 (12)	C7—C12	1.3900
O2—Na^{iv}	2.4538 (12)	C8—C9	1.3900
S1—C1	1.646 (2)	C9—C10	1.3900
S4—O42	1.4534 (12)	C10—O10	1.373 (2)
S4—O42^{v}	1.4534 (13)	C10—C11	1.3900
S4—O41	1.4578 (13)	C11—C12	1.3900
S4—C4^{v}	1.743 (2)	O10—C13	1.358 (3)
S4—C4	1.743 (2)		

$O2^{i}$—Na—O2	81.90 (6)	$O42^{v}$—S4—O41	112.17 (5)
$O2^{i}$—Na—$O2^{ii}$	165.09 (4)	O42—S4—$C4^{v}$	112.38 (12)
O2—Na—$O2^{ii}$	96.32 (5)	$O42^{v}$—S4—$C4^{v}$	102.43 (12)
$O2^{i}$—Na—$O2^{iii}$	96.32 (5)	O41—S4—$C4^{v}$	105.72 (9)
O2—Na—$O2^{iii}$	165.09 (4)	O42—S4—C4	102.43 (12)
$O2^{ii}$—Na—$O2^{iii}$	81.57 (6)	$O42^{v}$—S4—C4	112.38 (11)
$O2^{i}$—Na—$O1^{iv}$	74.40 (3)	O41—S4—C4	105.72 (9)
O2—Na—$O1^{iv}$	74.40 (3)	$C4^{v}$—S4—C4	11.5 (2)
$O2^{ii}$—Na—$O1^{iv}$	90.83 (3)	C2—C1—C7	119.79 (17)
$O2^{iii}$—Na—$O1^{iv}$	90.83 (3)	C2—C1—S1	120.42 (17)
$O2^{i}$—Na—O1	120.42 (3)	C7—C1—S1	119.78 (15)
O2—Na—O1	120.42 (3)	C3—C2—N6	106.4 (2)
$O2^{ii}$—Na—O1	73.27 (3)	C3—C2—C1	133.2 (2)
$O2^{iii}$—Na—O1	73.27 (3)	N6—C2—C1	120.34 (19)
$O1^{iv}$—Na—O1	158.76 (4)	C2—C3—C4	106.8 (4)
$O2^{i}$—Na—Na^{iv}	45.61 (3)	C5—C4—C3	107.9 (2)
O2—Na—Na^{iv}	45.61 (3)	C5—C4—S4	124.63 (16)
$O2^{ii}$—Na—Na^{iv}	124.29 (3)	C3—C4—S4	127.4 (3)
$O2^{iii}$—Na—Na^{iv}	124.29 (3)	N6—C5—C4	108.16 (19)
$O1^{iv}$—Na—Na^{iv}	46.99 (3)	C5—N6—C2	110.45 (19)
O1—Na—Na^{iv}	154.26 (4)	C8—C7—C12	120.0
$O2^{i}$—Na—Na^{iii}	139.00 (3)	C8—C7—C1	119.06 (12)
O2—Na—Na^{iii}	139.00 (3)	C12—C7—C1	120.92 (12)
$O2^{ii}$—Na—Na^{iii}	45.42 (3)	C9—C8—C7	120.0
$O2^{iii}$—Na—Na^{iii}	45.42 (3)	C8—C9—C10	120.0
$O1^{iv}$—Na—Na^{iii}	113.12 (4)	O10—C10—C9	124.54 (13)
O1—Na—Na^{iii}	45.64 (3)	O10—C10—C11	113.69 (16)
Na^{iv}—Na—Na^{iii}	160.10 (5)	C9—C10—C11	120.0
Na^{iii}—O1—Na	87.37 (4)	C12—C11—C10	120.0
Na—O2—Na^{iv}	88.97 (5)	C11—C12—C7	120.0
O42—S4—$O42^{v}$	111.46 (10)	C13—O10—C10	122.08 (19)
O42—S4—O41	112.16 (5)		

$O2^{i}$—Na—O1—Na^{iii}	−130.53 (3)	$O42^{v}$—S4—C4—C3	−47.1 (12)
O2—Na—O1—Na^{iii}	130.53 (3)	O41—S4—C4—C3	−169.8 (11)
$O2^{ii}$—Na—O1—Na^{iii}	43.00 (3)	$C4^{v}$—S4—C4—C3	−78.2 (12)
$O2^{iii}$—Na—O1—Na^{iii}	−43.00 (3)	C3—C4—C5—N6	−5.3 (10)
$O1^{iv}$—Na—O1—Na^{iii}	0.0	S4—C4—C5—N6	178.6 (2)
Na^{iv}—Na—O1—Na^{iii}	180.0	C4—C5—N6—C2	3.2 (3)
$O2^{i}$—Na—O2—Na^{iv}	31.85 (2)	C3—C2—N6—C5	0.2 (10)
$O2^{ii}$—Na—O2—Na^{iv}	−133.22 (4)	C1—C2—N6—C5	177.5 (2)
$O2^{iii}$—Na—O2—Na^{iv}	−52.28 (10)	C2—C1—C7—C8	144.06 (17)
$O1^{iv}$—Na—O2—Na^{iv}	−44.13 (2)	S1—C1—C7—C8	−36.5 (2)
O1—Na—O2—Na^{iv}	152.49 (4)	C2—C1—C7—C12	−37.7 (3)
Na^{iii}—Na—O2—Na^{iv}	−151.59 (7)	S1—C1—C7—C12	141.75 (14)
C7—C1—C2—C3	−8.5 (13)	C12—C7—C8—C9	0.0
S1—C1—C2—C3	172.1 (12)	C1—C7—C8—C9	178.28 (17)
C7—C1—C2—N6	175.1 (2)	C7—C8—C9—C10	0.0
S1—C1—C2—N6	−4.3 (3)	C8—C9—C10—O10	−163.9 (3)
N6—C2—C3—C4	−3.3 (15)	C8—C9—C10—C11	0.0
C1—C2—C3—C4	179.9 (4)	O10—C10—C11—C12	165.5 (2)
C2—C3—C4—C5	5.4 (15)	C9—C10—C11—C12	0.0
C2—C3—C4—S4	−178.7 (6)	C10—C11—C12—C7	0.0
O42—S4—C4—C5	−112.0 (3)	C8—C7—C12—C11	0.0
$O42^{v}$—S4—C4—C5	128.2 (3)	C1—C7—C12—C11	−178.24 (17)
O41—S4—C4—C5	5.6 (3)	C9—C10—O10—C13	−149.4 (4)
$C4^{v}$—S4—C4—C5	97.2 (3)	C11—C10—O10—C13	45.8 (5)
O42—S4—C4—C3	72.6 (12)		

Symmetry codes: (i) $x, \frac{1}{2}-y, z$; (ii) $x-\frac{1}{2}, y, \frac{3}{2}-z$; (iii) $x-\frac{1}{2}, \frac{1}{2}-y, \frac{3}{2}-z$; (iv) $\frac{1}{2}+x, \frac{1}{2}-y, \frac{3}{2}-z$; (v) $x, \frac{3}{2}-y, z$.

Table 2. *Hydrogen-bonding geometry (Å, °)*

D—H···*A*	*D*—H	H···*A*	*D*···*A*	*D*—H···*A*
O1—H1···$O42^{i}$	0.82	2.24	2.999 (2)	154.1
O2—H2A···$O42^{ii}$	0.82	2.04	2.845 (1)	165.7
O2—H2B···$O41^{iii}$	0.82	2.01	2.833 (2)	176.8
N6—H6···$O42^{iv}$	0.86	2.29	3.022 (2)	142.8

Symmetry codes: (i) $\frac{1}{2}+x, y-1, \frac{3}{2}-z$; (ii) $\frac{3}{2}+x, y-1, \frac{3}{2}-z$; (iii) $1+x, y-1, z$; (iv) $1+x, y, z$.

Data collection: CAD-4 software (Enraf–Nonius, 1989). Cell refinement: CAD-4 software (Enraf–Nonius, 1989). Data reduction: NRC-2, NRC-2A (Ahmed *et al.* 1973). Program(s) used to solve structure: *SHELXS*97 (Sheldrick, 1997). Program(s) used to refine structure: *SHELXL*96 (Sheldrick, 1996). Molecular graphics: *SHELXTL* (Bruker, 1997). Software used to prepare material for publication: *SHELXL*96 (Sheldrick, 1996).

References

Ahmed, F. R., Hall, S. R., Pippy, M. E. & Huber, C. P. (1973). NRC Crystallographic Computer Programs for the IBM/360. Accession Nos. 133–147 in *J. Appl. Cryst.* **6**, 309–346.

Enraf–Nonius (1989). CAD-4 Software. Version 5.0. Enraf–Nonius, Delft, The Netherlands.

Gabe, E. J., Le Page, Y., Charland, J.-P., Lee, F. L. & White, P. S. (1989). *J. Appl. Cryst.* **22**, 384–387.

International Tables for Crystallography (1992). Vol. C. Tables 4.2.6.8 and 6.1.1. **4**, Dordrecht: Kluwer Academic Publishers.

Sheldrick, G. M. (1997). *SHELXS*97. Program for the Solution of Crystal Structures. University of Gottingen, Germany.

Sheldrick, G. M. (1996). *SHELXL*96. Program for the Refinement *of Crystal Structures*. University of Göttingen, Germany.

SHELXTL (1997) Release 5.10; The Complete Software Package for Single Crystal Structure Determination, Bruker AXS Inc., Madison, WI 53719–1173.

Spek, A. L. (1995). *PLATON*, Molecular Geometry Program, July 1995 version, University of Utrecht, Utrecht, Holland.

Space group confirmed by *PLATON* program (Spek, 1995). Data reduction performed using a locally modified version of the NRC-2 program (Ahmed *et al.* 1973). The structure was solved by direct method using *SHELXS*97 (Sheldrick, 1997) and difmap synthesis using *SHELXTL* (Sheldrick, 1997) and *SHELXL*96 (Sheldrick, 1996). Most atoms were displaced from the mirror and two models were observed for this complexe/The constraint AFIX 66 applied to phenuyl ring was used to help congergence. All non-H atoms anisotropic, H atoms isotropic. H atoms constrained to the parent site using a riding model; *SHELXL*96 defaults, C—H 0.93 to 0.96, N—H 0.86 and O—H 0.82 Å. The isotropic factors, U_{iso} , were adjusted to 50% higher value of the parent site (CH3, NH,OH) and 20% higher (others). A final verification of possible voids was performed using the VOID routine of the *PLATON* program (Spek, 1995).

Table *S1*. *Fractional atomic coordinates and equivalent isotropic displacement parameters (Å²)*

$$U_{eq} = (1/3)\Sigma_i\Sigma_j U^{ij} a^i a^j \mathbf{a}_i.\mathbf{a}_j.$$

	Occupancy	*x*	*y*	*z*	U_{eq}
Na	1	0.72210 (11)	1/4	0.74063 (2)	0.04139 (19)
O1	1	0.42033 (12)	1/4	0.69429 (2)	0.0506 (4)
H1	1	0.3904 (6)	0.1674 (4)	0.67869 (13)	0.076
O2	1	0.98904 (7)	0.03743 (4)	**0.728284** (13)	0.0453 (2)
H2A	1	1.0440 (3)	−0.0015 (6)	0.70713 (7)	0.068
H2B	1	0.9786 (12)	−0.0464 (3)	0.74464 (9)	0.068
S1	0.50	0.59191 (9)	0.81257 (11)	0.96292 (2)	0.0517 (2)
S4	1	−0.14359 (6)	3/4	**0.827640** (12)	0.02936 (11)
O41	1	−0.0635 (2)	3/4	0.78487 (4)	0.0437 (3)
O42	1	−0.25712 (14)	0.90929 (13)	0.83659 (3)	0.0429 (2)
C1	0.50	0.3504 (3)	0.7905 (3)	0.95933 (7)	0.0327 (8)
C2	0.50	0.2546 (3)	0.7884 (3)	0.91834 (7)	0.0310 (8)
C3	1	0.0630 (3)	0.754 (3)	0.90545 (6)	0.0300 (6)
H3	0.50	−0.0433	0.7242	0.9227	0.036
C4	0.50	0.0596 (3)	0.7732 (5)	0.86111 (6)	0.0212 (7)
C5	0.50	0.2483 (4)	0.8019 (3)	0.84788 (7)	0.0398 (7)
H5	0.50	0.2899	0.8099	0.8199	0.048
N6	0.50	0.3634 (3)	0.8167 (3)	0.88198 (6)	0.0394 (5)
H6	0.50	0.4878	0.8406	0.8814	0.059
C7	0.50	0.22905 (17)	0.7743 (3)	0.99851 (3)	0.0309 (6)
C8	0.50	0.30484 (18)	0.6807 (3)	1.03270 (4)	0.0389 (6)
H8	0.50	0.4280	0.6265	1.0307	0.047
C9	0.50	0.1965 (2)	0.6680 (3)	1.06992 (4)	0.0415 (6)
H9	0.50	0.2472	0.6053	1.0928	0.050
C10	1	0.01242 (19)	0.7489 (3)	1.07294 (3)	0.0375 (4)
C11	0.50	−0.06337 (18)	0.8426 (3)	1.03874 (4)	0.0362 (6)
H11	0.50	−0.1866	0.8968	1.0408	0.043
C12	0.50	0.04493 (19)	0.8553 (2)	1.00153 (4)	0.0335 (5)
H12	0.50	−0.0058	0.9180	0.9787	0.040
O10	0.50	−0.0852 (2)	0.7811 (5)	1.11022 (5)	0.0455 (10)
C13	0.50	−0.2856 (4)	0.7825 (8)	1.11272 (9)	0.0576 (16)
H13A	0.50	−0.3325	0.9024	1.1105	0.086
H13B	0.50	−0.3262	0.7332	1.1393	0.086
H13C	0.50	−0.3398	0.7131	1.0901	0.086

Table *S2*. *Anisotropic displacement parameters* (Å²)

	U_{11}	U_{22}	U_{33}	U_{12}	U_{13}	U_{23}
Na	0.0302 (4)	0.0505 (4)	0.0435 (4)	0.000	0.0017 (3)	0.000
O1	0.0638 (9)	0.0551 (9)	0.0328 (6)	0.000	−0.0011 (6)	0.000
O2	0.0511 (5)	0.0414 (5)	0.0435 (5)	0.0033 (5)	0.0129 (4)	−0.0035 (4)
S1	0.0220 (3)	0.0839 (6)	0.0491 (3)	−0.0008 (3)	−0.0041 (2)	0.0000 (3)
S4	0.0289 (2)	0.0349 (2)	0.02428 (19)	0.000	−0.00192 (15)	0.000
O41	0.0510 (8)	0.0553 (8)	0.0249 (6)	0.000	0.0036 (5)	0.000
O42	0.0408 (5)	0.0454 (5)	0.0424 (5)	0.0139 (4)	−0.0043 (4)	−0.0017 (4)
C1	0.0255 (9)	0.037 (2)	0.0358 (10)	0.0009 (8)	−0.0034 (8)	−0.0005 (9)
C2	0.0255 (9)	0.038 (2)	0.0300 (9)	−0.0007 (9)	0.0026 (8)	0.0015 (9)
C3	0.0241 (8)	0.0385 (16)	0.0274 (7)	0.001 (6)	0.0025 (6)	−0.001 (6)
C4	0.0255 (8)	0.008 (2)	0.0297 (8)	−0.0001 (8)	0.0000 (7)	−0.0002 (9)
C5	0.0317 (11)	0.058 (2)	0.0300 (10)	−0.0035 (10)	0.0066 (8)	0.0034 (10)
N6	0.0219 (8)	0.0609 (14)	0.0355 (10)	−0.0044 (9)	0.0036 (7)	0.0024 (9)

C7	0.0252 (9)	0.0363 (17)	0.0311 (9)	−0.0023 (10)	−0.0041 (7)	0.0039 (11)
C8	0.0278 (11)	0.0492 (13)	0.0397 (12)	0.0028 (10)	−0.0085 (10)	0.0012 (10)
C9	0.0390 (12)	0.0543 (15)	0.0312 (11)	−0.0001 (13)	−0.0127 (10)	0.0054 (11)
C10	0.0384 (10)	0.0480 (10)	0.0261 (7)	−0.002 (9)	−0.0040 (7)	0.001 (9)
C11	0.0319 (11)	0.0464 (15)	0.0302 (11)	0.0040 (11)	−0.0034 (9)	−0.0025 (11)
C12	0.0294 (12)	0.0415 (14)	0.0298 (10)	0.0024 (10)	−0.0049 (9)	0.0023 (10)
O10	0.0463 (9)	0.063 (3)	0.0275 (6)	−0.0014 (11)	0.0000 (6)	−0.0023 (9)
C13	0.0537 (14)	0.074 (5)	0.0456 (12)	0.0062 (18)	0.0137 (11)	0.0064 (17)

Table *S*3. *Geometric parameters (Å, °)*

Na—O2^{i}	2.4455 (12)	C2—N6	1.382 (3)
Na—O2	2.4455 (12)	C3—C4	1.411 (3)
Na—O2^{ii}	2.4538 (12)	C3—H3	0.9300
Na—O2^{iii}	2.4538 (12)	C4—C5	1.361 (3)
Na—O1^{iv}	2.4572 (12)	C5—N6	1.335 (3)
Na—O1	2.5129 (13)	C5—H5	0.9300
Na—Na^{iv}	3.4331 (15)	N6—H6	0.8600
Na—Na^{iii}	3.4331 (15)	C7—C8	1.3900
O1—Na^{iii}	2.4571 (12)	C7—C12	1.3900
O1—H1	0.8200	C8—C9	1.3900
O2—Na^{iv}	2.4538 (12)	C8—H8	0.9300
O2—H2A	0.8200	C9—C10	1.3900
O2—H2B	0.8200	C9—H9	0.9300
S1—C1	1.646 (2)	C10—O10	1.373 (2)
S4—O42	1.4534 (12)	C10—C11	1.3900
S4—O42^{v}	1.4534 (13)	C11—C12	1.3900
S4—O41	1.4578 (13)	C11—H11	0.9300
S4—C4^{v}	1.743 (2)	C12—H12	0.9300
S4—C4	1.743 (2)	O10—C13	1.358 (3)
C1—C2	1.450 (3)	C13—H13A	0.9600
C1—C7	1.492 (2)	C13—H13B	0.9600
C2—C3	1.383 (5)	C13—H13C	0.9600

$O2^{i}$—Na—O2	81.90 (6)	O41—S4—C4	105.72 (9)
$O2^{i}$—Na—$O2^{ii}$	165.09 (4)	$C4^{v}$—S4—C4	11.5 (2)
O2—Na—$O2^{ii}$	96.32 (5)	C2—C1—C7	119.79 (17)
$O2^{i}$—Na—$O2^{iii}$	96.32 (5)	C2—C1—S1	120.42 (17)
O2—Na—$O2^{iii}$	165.09 (4)	C7—C1—S1	119.78 (15)
$O2^{ii}$—Na—$O2^{iii}$	81.57 (6)	C3—C2—N6	106.4 (2)
$O2^{i}$—Na—$O1^{iv}$	74.40 (3)	C3—C2—C1	133.2 (2)
O2—Na—$O1^{iv}$	74.40 (3)	N6—C2—C1	120.34 (19)
$O2^{ii}$—Na—$O1^{iv}$	90.83 (3)	C2—C3—C4	106.8 (4)
$O2^{iii}$—Na—$O1^{iv}$	90.83 (3)	C2—C3—H3	126.6
$O2^{i}$—Na—O1	120.42 (3)	C4—C3—H3	126.6
O2—Na—O1	120.42 (3)	C5—C4—C3	107.9 (2)
$O2^{ii}$—Na—O1	73.27 (3)	C5—C4—S4	124.63 (16)
$O2^{iii}$—Na—O1	73.27 (3)	C3—C4—S4	127.4 (3)
$O1^{iv}$—Na—O1	158.76 (4)	N6—C5—C4	108.16 (19)
$O2^{i}$—Na—Na^{iv}	45.61 (3)	N6—C5—H5	125.9
O2—Na—Na^{iv}	45.61 (3)	C4—C5—H5	125.9
$O2^{ii}$—Na—Na^{iv}	124.29 (3)	C5—N6—C2	110.45 (19)
$O2^{iii}$—Na—Na^{iv}	124.29 (3)	C5—N6—H6	124.8
$O1^{iv}$—Na—Na^{iv}	46.99 (3)	C2—N6—H6	124.8
O1—Na—Na^{iv}	154.26 (4)	C8—C7—C12	120.0
$O2^{i}$—Na—Na^{iii}	139.00 (3)	C8—C7—C1	119.06 (12)
O2—Na—Na^{iii}	139.00 (3)	C12—C7—C1	120.92 (12)
$O2^{ii}$—Na—Na^{iii}	45.42 (3)	C9—C8—C7	120.0
$O2^{iii}$—Na—Na^{iii}	45.42 (3)	C9—C8—H8	120.0
$O1^{iv}$—Na—Na^{iii}	113.12 (4)	C7—C8—H8	120.0
O1—Na—Na^{iii}	45.64 (3)	C8—C9—C10	120.0
Na^{iv}—Na—Na^{iii}	160.10 (5)	C8—C9—H9	120.0
Na^{iii}—O1—Na	87.37 (4)	C10—C9—H9	120.0
Na^{iii}—O1—H1	111.7	O10—C10—C9	124.54 (13)
Na—O1—H1	123.5	O10—C10—C11	113.69 (16)
Na—O2—Na^{iv}	88.97 (5)	C9—C10—C11	120.0
Na—O2—H2A	134.4	C12—C11—C10	120.0
Na^{iv}—O2—H2A	105.6 (2)	C12—C11—H11	120.0
Na—O2—H2B	109.9	C10—C11—H11	120.0
Na^{iv}—O2—H2B	107.8 (5)	C11—C12—C7	120.0
H2A—O2—H2B	106.2	C11—C12—H12	120.0
$O42$—S4—$O42^{v}$	111.46 (10)	C7—C12—H12	120.0
O42—S4—O41	112.16 (5)	C13—O10—C10	122.08 (19)
$O42^{v}$—S4—O41	112.17 (5)	O10—C13—H13A	109.5
O42—S4—$C4^{v}$	112.38 (12)	O10—C13—H13B	109.5
$O42^{v}$—S4—$C4^{v}$	102.43 (12)	H13A—C13—H13B	109.5
O41—S4—$C4^{v}$	105.72 (9)	O10—C13—H13C	109.5
O42—S4—C4	102.43 (12)	H13A—C13—H13C	109.5
$O42^{v}$—S4—C4	112.38 (11)	H13B—C13—H13C	109.5

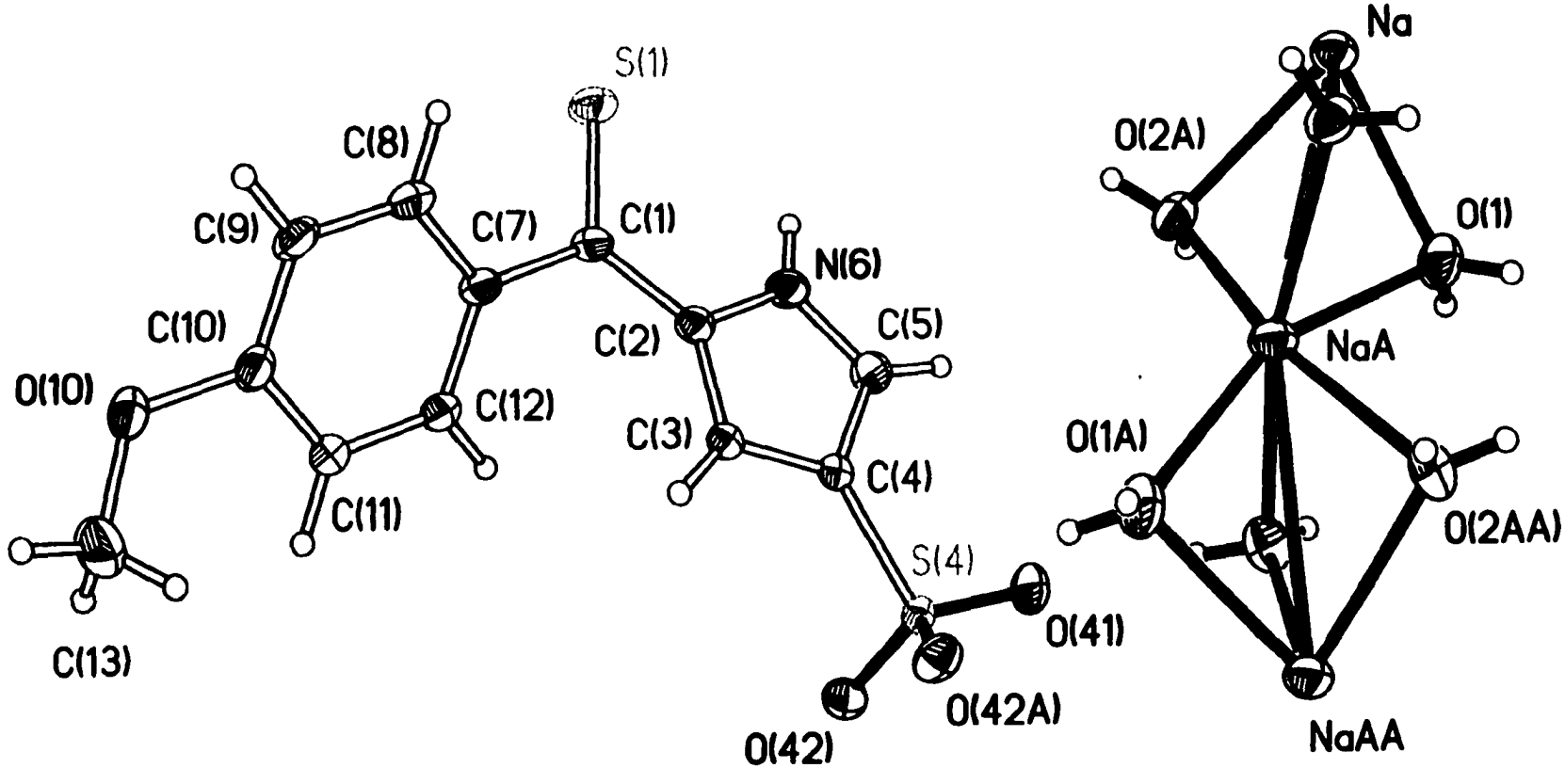
S(1)
C(8)
C(9)
C(7)
C(1)
N(6)
C(10)
C(2)
C(5)
O(10)
C(12)
C(3)
C(4)
C(11)
S(4)
O(41)
C(13)
O(42A)
O(42)
Na
O(2A)
O(1)
NaA
O(1A)
O(2AA)
NaAA

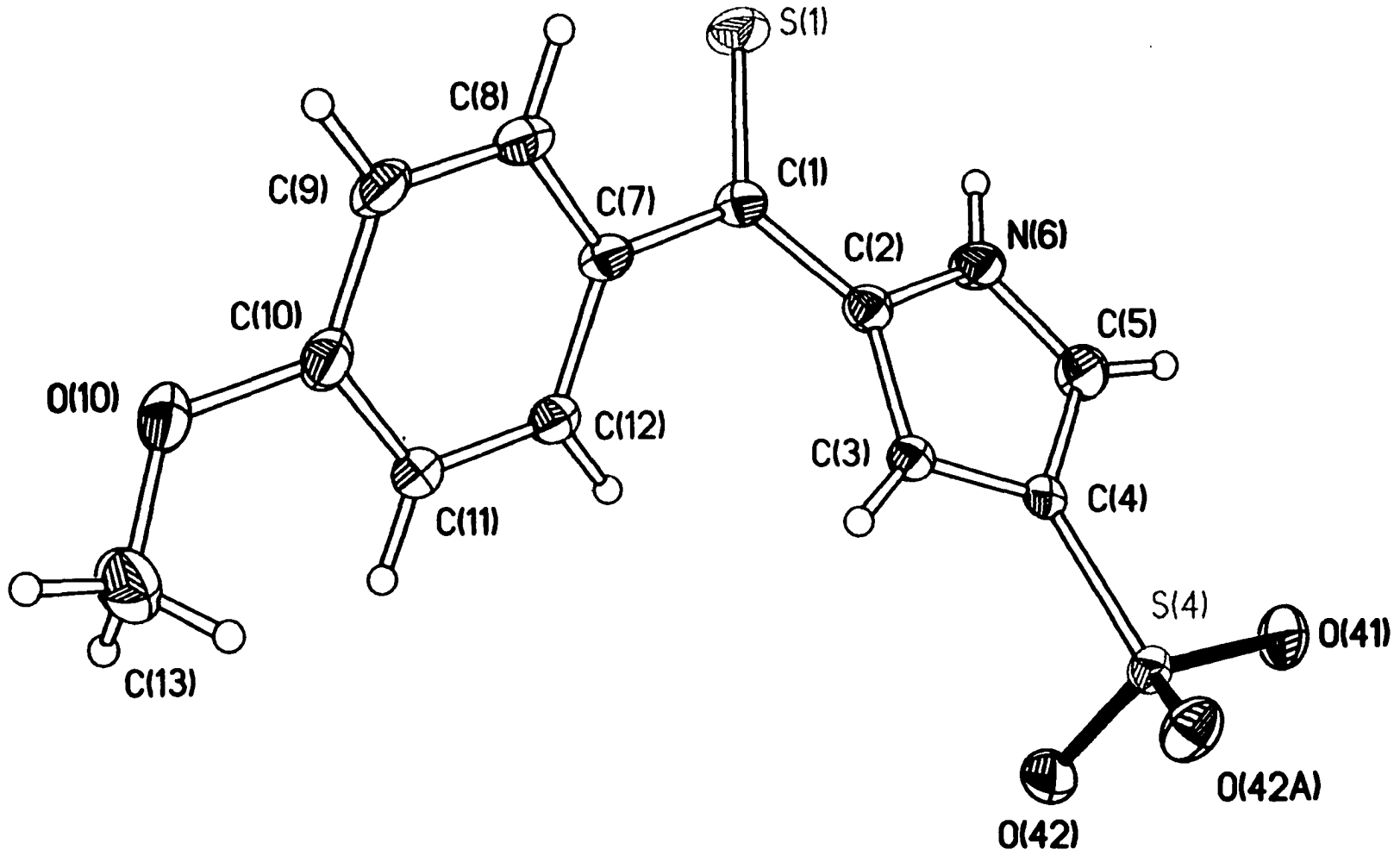
S(1)
C(8)
C(9)
C(7)
C(1)
C(2)
N(6)
C(10)
C(5)
O(10)
C(12)
C(3)
C(4)
C(11)
S(4)
O(41)
C(13)
O(42A)
O(42)

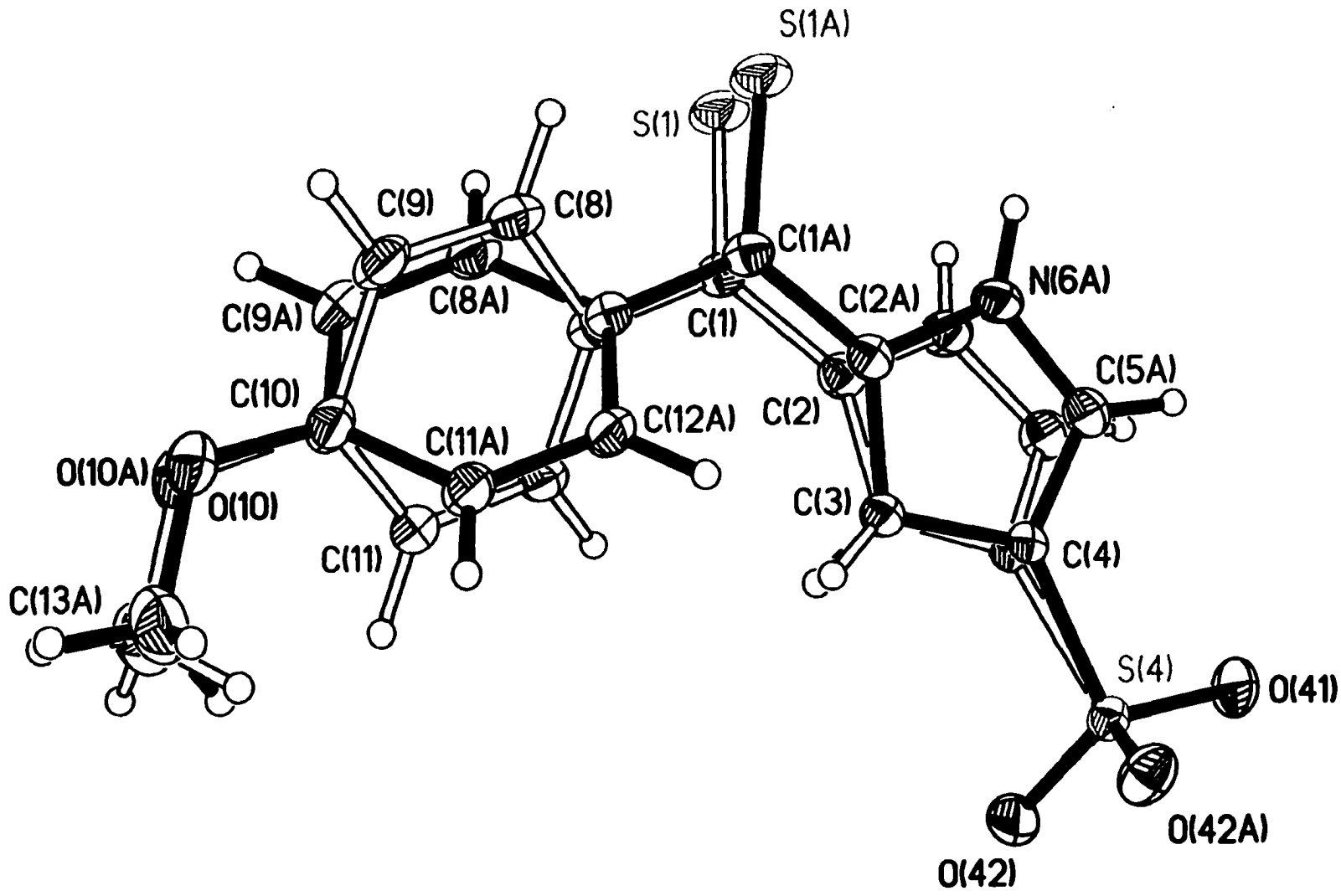
S(1A)
S(1)
C(9)
C(8)
C(1A)
C(9A)
C(8A)
C(1)
C(2A)
N(6A)
C(10)
C(5A)
C(12A)
C(2)
C(11A)
O(10A)
O(10)
C(3)
C(11)
C(4)
C(13A)
S(4)
O(41)
O(42A)
O(42)

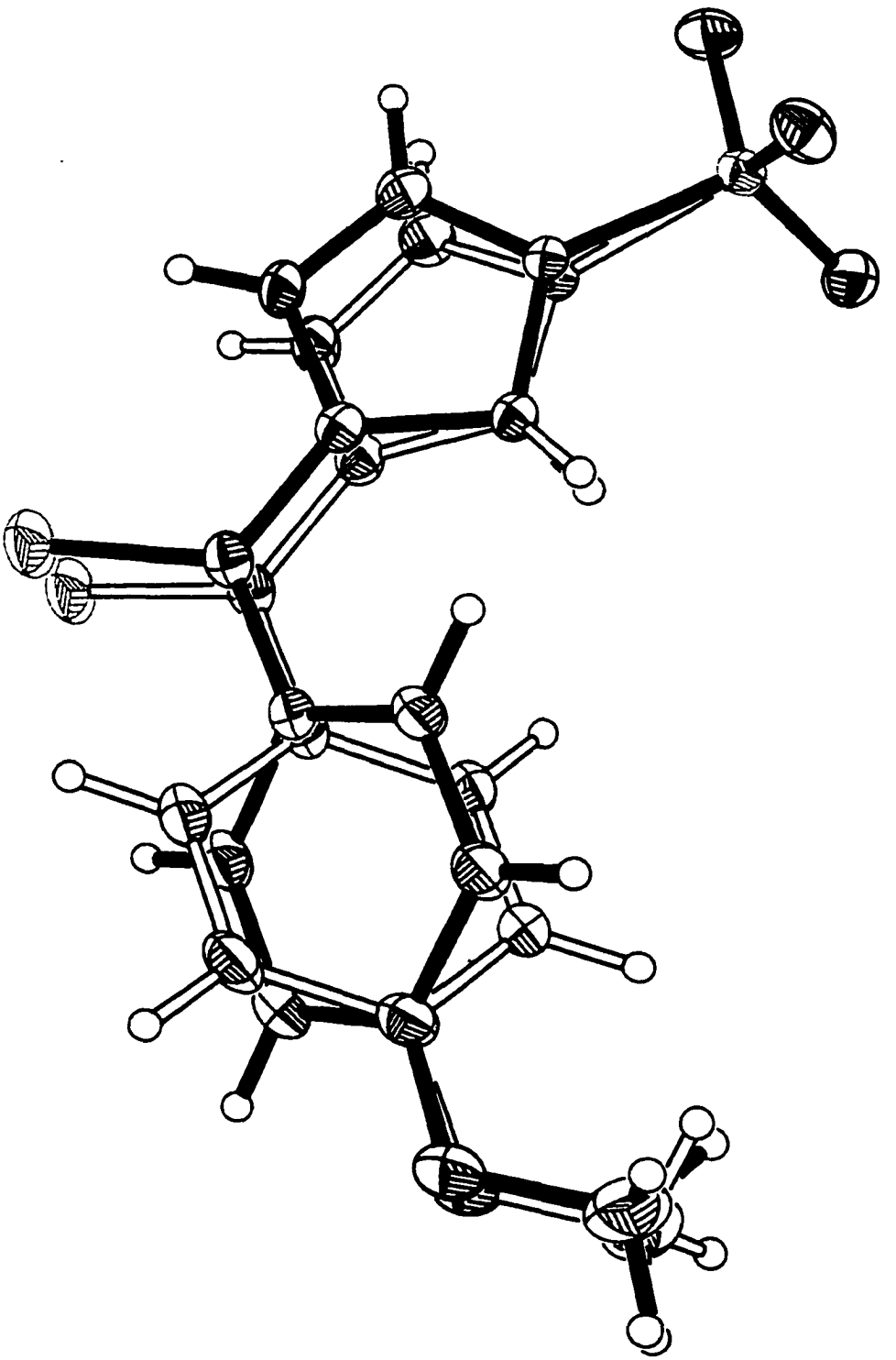

Compound 10b

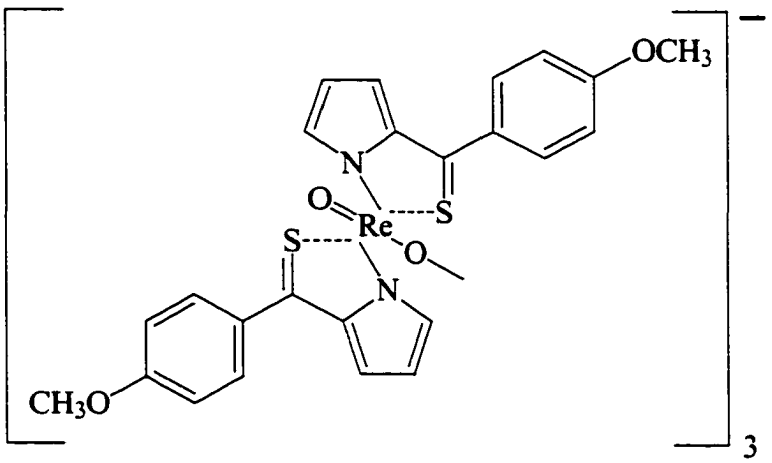

Crystal data

$C_{76}H_{72}N_6O_{16}Re_4S_6$

M_r = 2262.556

Monoclinic

$C2/c$

a = 34.6651 (2) Å

b = 11.5694 (1) Å

c = 24.6839 (2) Å

β = 128.0350 (4)°

V = 7797.3 (1) Å^3

Z = 4

D_x = 1.9274 Mg m^{-3}

D_m not measured

Cu $K\alpha$ radiation

λ = 1.54178 Å

Cell parameters from 29416 reflections

θ = 2.28–72.86°

μ = 13.923 mm^{-1}

T = 293 (2) K

Plate

Red

0.27 × 0.12 × 0.04 mm

Data collection

Bruker AXS SMART 2K/Platform diffractometer

ω scan

Absorption correction:

multi-scan SADABS (Sheldrick, 1996)

$T_{min} = 0.3700, T_{max} = 0.6900$

45747 measured reflections

7583 independent reflections

6201 reflections with $>2\sigma(I)$

$R_{int} = 0.0627$

$\theta_{max} = 72.91°$

$h = -42 \rightarrow 42$

$k = -14 \rightarrow 14$

$l = -24 \rightarrow 29$

318 standard reflections

intensity decay: none

Refinement

Refinement on F^2

$R[F^2 > 2\sigma(F^2)] = 0.0619$

$wR(F^2) = 0.1710$

$S = 1.156$

7583 reflections

486 parameters

H-atom parameters constrained

$w=1/[\sigma^2(F_o^2) + (0.1012P)^2 + 59.7091P]$

where $P = (F_o^2 + 2F_c^2)/3$

$(\Delta/\sigma)_{max} = 0.003$

$\Delta\rho_{max} = 2.248$ e Å^{-3}

$\Delta\rho_{min} = -1.598$ e Å^{-3}

Extinction correction: none

Scattering factors from *International Tables for Crystallography* (Vol. C)

Table 1. *Selected geometric parameters (Å, °)*

Re1—O1	1.667 (8)	C141—C142	1.3900
Re1—N113	2.064 (8)	O143—C143	1.417 (16)
Re1—N133	2.066 (3)	C147—C148	1.3900
Re1—O2	2.082 (6)	C147—C152	1.3900
Re1—S111	2.384 (3)	C148—C149	1.3900
Re1—S131	2.406 (2)	C149—C150	1.3900
O2—Re2	1.779 (6)	C150—O153	1.365 (14)
S111—C111	1.704 (10)	C150—C151	1.3900
C111—C112	1.371 (11)	C151—C152	1.3900
C111—C117	1.481 (9)	O153—C153	1.415 (18)
C112—N113	1.404 (11)	Re2—O2^{i}	1.779 (6)
C112—C116	1.431 (12)	Re2—N213^{i}	2.088 (7)
N113—C114	1.327 (11)	Re2—N213	2.088 (7)
C114—C115	1.412 (13)	Re2—S211^{i}	2.418 (2)
C115—C116	1.339 (12)	Re2—S211	2.418 (2)
C117—C118	1.3900	S211—C211^{i}	1.711 (9)
C117—C122	1.3900	C211—C212	1.386 (9)
C118—C119	1.3900	C211—C217	1.486 (8)
C119—C120	1.3900	C211—S211^{i}	1.710 (8)
C120—O123	1.3581	C212—N213	1.420 (9)
C120—C121	1.3900	C212—C216	1.421 (10)
C121—C122	1.3900	N213—C214	1.329 (10)
O123—C123	1.4273	C214—C215	1.418 (12)
S131—C131	1.7145	C215—C216	1.348 (11)
C131—C132	1.3889	C217—C218	1.3900
C131—C137	1.473 (8)	C217—C222	1.3900
C131—C147	1.544 (12)	C218—C219	1.3900
C132—N133	1.4073	C219—C220	1.3900
C132—C136	1.4396	C220—O223	1.366 (7)
N133—C134	1.3392	C220—C221	1.3900
C134—C135	1.4341	C221—C222	1.3900
C135—C136	1.3705	O223—C223	1.435 (11)
C137—C138	1.3900	Re11—O11	1.664 (10)
C137—C142	1.3900	Re11—O11^{ii}	1.664 (10)
C138—C139	1.3900	Re11—O12^{ii}	1.712 (11)
C139—C140	1.3900	Re11—O12	1.712 (11)
C140—O143	1.352 (12)	O21—C22	1.466 (19)
C140—C141	1.3900	C22—C23	1.46 (2)

O1—Re1—N113	97.9 (4)	O1—Re1—N133	99.5 (3)
N113—Re1—N133	162.6 (2)	C132—C131—C137	120.9 (6)
O1—Re1—O2	178.2 (4)	C132—C131—C147	123.9 (8)
N113—Re1—O2	80.7 (3)	C132—C131—S131	118.7
N133—Re1—O2	81.96 (19)	C137—C131—S131	117.5 (6)
O1—Re1—S111	98.3 (4)	C147—C131—S131	114.5 (7)
N113—Re1—S111	81.6 (2)	C131—C132—N133	120.8
N133—Re1—S111	95.79 (10)	C131—C132—C136	131.6
O2—Re1—S111	82.66 (17)	N133—C132—C136	107.6
O1—Re1—S131	96.4 (4)	C134—N133—C132	109.2
N113—Re1—S131	96.0 (2)	C134—N133—Re1	131.81 (7)
N133—Re1—S131	82.12 (8)	C132—N133—Re1	118.86 (7)
O2—Re1—S131	82.56 (17)	N133—C134—C135	107.9
S111—Re1—S131	165.22 (9)	C136—C135—C134	109.2
Re2—O2—Re1	177.6 (3)	C135—C136—C132	106.0
C111—S111—Re1	99.5 (3)	C138—C137—C142	120.0
C112—C111—C117	124.0 (8)	C138—C137—C131	123.7 (8)
C112—C111—S111	119.9 (7)	C142—C137—C131	116.2 (8)
C117—C111—S111	116.1 (6)	C137—C138—C139	120.0
C111—C112—N113	119.2 (9)	C140—C139—C138	120.0
C111—C112—C116	133.8 (9)	O143—C140—C141	115.5 (11)
N113—C112—C116	106.9 (8)	O143—C140—C139	124.5 (11)
C114—N113—C112	108.0 (8)	C141—C140—C139	120.0
C114—N113—Re1	132.4 (7)	C140—C141—C142	120.0
C112—N113—Re1	119.6 (6)	C141—C142—C137	120.0
N113—C114—C115	109.3 (9)	C140—O143—C143	119.3 (17)
C116—C115—C114	108.6 (9)	C148—C147—C152	120.0
C115—C116—C112	107.1 (9)	C148—C147—C131	124.6 (13)
C118—C117—C122	120.0	C152—C147—C131	115.2 (13)
C118—C117—C111	120.8 (4)	C149—C148—C147	120.0
C122—C117—C111	119.1 (4)	C148—C149—C150	120.0
C117—C118—C119	120.0	O153—C150—C151	121.2 (15)
C120—C119—C118	120.0	O153—C150—C149	118.8 (15)
O123—C120—C119	122.2	C151—C150—C149	120.0
O123—C120—C121	117.8	C150—C151—C152	120.0
C119—C120—C121	120.0	C151—C152—C147	120.0
C122—C121—C120	120.0	C150—O153—C153	123 (3)
C121—C122—C117	120.0	O2—Re2—O2^{i}	179.996 (2)
C120—O123—C123	117.9	O2—Re2—N213^{i}	90.8 (3)
C131—S131—Re1	99.47 (6)	O2^{i}—Re2—N213^{i}	89.2 (3)

O2—Re2—N213	89.2 (3)	N213—C214—C215	110.6 (8)
O2^{i}—Re2—N213	90.8 (3)	C216—C215—C214	107.3 (8)
N213^{i}—Re2—N213	180.0	C215—C216—C212	107.9 (8)
O2—Re2—S211^{i}	89.34 (19)	C218—C217—*C*222	120.0
O2^{i}—Re2—S211^{i}	90.7 (2)	C218—C217—C211	119.9 (4)
N213^{i}—Re2—S211^{i}	98.37 (18)	*C*222—C217—C211	120.0 (4)
N213—Re2—S211^{i}	81.63 (18)	C219—C218—C217	120.0
O2—Re2—S211	90.66 (19)	C218—C219—C220	120.0
O2^{i}—Re2—S211	89.3 (2)	O223—C220—C221	115.3 (5)
N213^{i}—Re2—S211	81.63 (18)	O223—C220—C219	124.7 (5)
N213—Re2—S211	98.37 (18)	C221—C220—C219	120.0
S211^{i}—Re2—S211	180.0	*C*222—C221—C220	120.0
C211^{i}—S211—Re2	99.0 (3)	C221—*C*222—C217	120.0
C212—C211—C217	121.9 (7)	C220—O223—C223	118.5 (8)
C212—C211—S211^{i}	120.9 (6)	O11—Re11—O11^{ii}	117.6 (13)
C217—C211—S211^{i}	117.2 (5)	O11—Re11—O12^{ii}	108.8 (11)
C211—C212—N213	118.8 (7)	O11^{ii}—Re11—O12^{ii}	108.7 (11)
C211—C212—C216	133.5 (8)	O11—Re11—O12	108.7 (11)
N213—C212—C216	107.3 (7)	O11^{ii}—Re11—O12	108.8 (10)
C214—N213—C212	106.9 (7)	O12^{ii}—Re11—O12	103.3 (18)
C214—N213—Re2	133.6 (6)	C23—C22—O21	108 (2)
C212—N213—Re2	119.4 (5)		
O1—Re1—O2—Re2	28 (16)	C116—C112—N113—C114	1.4 (12)
N113—Re1—O2—Re2	−12 (8)	C111—C112—N113—Re1	3.4 (12)
N133—Re1—O2—Re2	168 (8)	C116—C112—N113—Re1	−177.4 (7)
S111—Re1—O2—Re2	−95 (8)	O1—Re1—N113—C114	−83.5 (10)
S131—Re1—O2—Re2	85 (8)	N133—Re1—N113—C114	96.5 (12)
O1—Re1—S111—C111	−95.9 (5)	O2—Re1—N113—C114	95.3 (10)
N113—Re1—S111—C111	1.0 (4)	S111—Re1—N113—C114	179.2 (10)
N133—Re1—S111—C111	163.7 (4)	S131—Re1—N113—C114	13.9 (10)
O2—Re1—S111—C111	82.6 (4)	O1—Re1—N113—C112	94.9 (8)
S131—Re1—S111—C111	82.6 (5)	N133—Re1—N113—C112	−85.1 (10)
Re1—S111—C111—C112	0.4 (9)	O2—Re1—N113—C112	−86.3 (7)
Re1—S111—C111—C117	−178.9 (6)	S111—Re1—N113—C112	−2.4 (7)
C117—C111—C112—N113	176.8 (8)	S131—Re1—N113—C112	−167.7 (7)
S111—C111—C112—N113	−2.4 (13)	C112—N113—C114—C115	−2.1 (13)
C117—C111—C112—C116	−2.1 (18)	Re1—N113—C114—C115	176.4 (8)
S111—C111—C112—C116	178.7 (11)	N113—C114—C115—C116	2.2 (16)
C111—C112—N113—C114	−177.8 (10)	C114—C115—C116—C112	−1.2 (15)

C111—C112—C116—C115	178.9 (12)	S111—Re1—N133—C134	9.87 (10)
N113—C112—C116—C115	0.0 (14)	S131—Re1—N133—C134	175.1
C112—C111—C117—C118	−37.9 (11)	O1—Re1—N133—C132	95.3 (4)
S111—C111—C117—C118	141.3 (4)	N113—Re1—N133—C132	−84.7 (8)
C112—C111—C117—C122	144.6 (8)	O2—Re1—N133—C132	−83.51 (18)
S111—C111—C117—C122	−36.2 (7)	S111—Re1—N133—C132	−165.22 (10)
C122—C117—C118—C119	0.0	S131—Re1—N133—C132	0.04 (9)
C111—C117—C118—C119	−177.5 (4)	C132—N133—C134—C135	−3.6
C117—C118—C119—C120	0.0	Re1—N133—C134—C135	−179.03 (10)
C118—C119—C120—O123	−179.0	N133—C134—C135—C136	2.2
C118—C119—C120—C121	0.0	C134—C135—C136—C132	0.0
O123—C120—C121—C122	179.0	C131—C132—C136—C135	179.1
C119—C120—C121—C122	0.0	N133—C132—C136—C135	−2.1
C120—C121—C122—C117	0.0	C132—C131—C137—C138	34.1 (14)
C118—C117—C122—C121	0.0	C147—C131—C137—C138	140 (2)
C111—C117—C122—C121	177.6 (4)	S131—C131—C137—C138	−126.4 (10)
C119—C120—O123—C123	165.3	C132—C131—C137—C142	−142.0 (8)
C121—C120—O123—C123	−13.7	C147—C131—C137—C142	−36.1 (18)
O1—Re1—S131—C131	−97.8 (3)	S131—C131—C137—C142	57.4 (10)
N113—Re1—S131—C131	163.5 (2)	C142—C137—C138—C139	0.0
N133—Re1—S131—C131	0.88 (7)	C131—C137—C138—C139	−176.0 (14)
O2—Re1—S131—C131	83.74 (18)	C137—C138—C139—C140	0.0
S111—Re1—S131—C131	83.7 (4)	C138—C139—C140—O143	178 (2)
Re1—S131—C131—C132	−1.87 (6)	C138—C139—C140—C141	0.0
Re1—S131—C131—C137	159.1 (7)	O143—C140—C141—C142	−177.9 (19)
Re1—S131—C131—C147	−163.6 (8)	C139—C140—C141—C142	0.0
C137—C131—C132—N133	−158.1 (7)	C140—C141—C142—C137	0.0
C147—C131—C132—N133	162.2 (8)	C138—C137—C142—C141	0.0
S131—C131—C132—N133	2.3	C131—C137—C142—C141	176.3 (13)
C137—C131—C132—C136	20.6 (7)	C141—C140—O143—C143	−175 (2)
C147—C131—C132—C136	−19.1 (8)	C139—C140—O143—C143	7 (4)
S131—C131—C132—C136	−179.1	C132—C131—C147—C148	−19.5 (15)
C131—C132—N133—C134	−177.5	C137—C131—C147—C148	−116 (2)
C136—C132—N133—C134	3.6	S131—C131—C147—C148	141.2 (10)
C131—C132—N133—Re1	−1.32 (8)	C132—C131—C147—C152	155.4 (9)
C136—C132—N133—Re1	179.73 (8)	C137—C131—C147—C152	59.4 (18)
O1—Re1—N133—C134	−89.6 (4)	S131—C131—C147—C152	−43.9 (12)
N113—Re1—N133—C134	90.4 (8)	C152—C147—C148—C149	0.0
O2—Re1—N133—C134	91.59 (18)	C131—C147—C148—C149	174.7 (15)

C147—C148—C149—C150	0.0	$N213^{i}$—Re2—N213—C214	129 (8)
C148—C149—C150—O153	179 (2)	$S211^{i}$—Re2—N213—C214	−171.3 (9)
C148—C149—C150—C151	0.0	S211—Re2—N213—C214	8.7 (9)
O153—C150—C151—C152	−179 (2)	O2—Re2—N213—C212	−84.6 (6)
C149—C150—C151—C152	0.0	$O2^{i}$—Re2—N213—C212	95.4 (6)
C150—C151—C152—C147	0.0	$N213^{i}$—Re2—N213—C212	−55 (9)
C148—C147—C152—C151	0.0	$S211^{i}$—Re2—N213—C212	4.8 (6)
C131—C147—C152—C151	−175.2 (13)	S211—Re2—N213—C212	−175.2 (6)
C151—C150—O153—C153	6 (4)	C212—N213—C214—C215	0.5 (11)
C149—C150—O153—C153	−173 (3)	Re2—N213—C214—C215	177.0 (7)
Re1—O2—Re2—$O2^{i}$	−55 (10)	N213—C214—C215—C216	−1.4 (13)
Re1—O2—Re2—$N213^{i}$	162 (8)	C214—C215—C216—C212	1.8 (13)
Re1—O2—Re2—N213	−18 (8)	C211—C212—C216—C215	−173.4 (11)
Re1—O2—Re2—$S211^{i}$	−100 (8)	N213—C212—C216—C215	−1.5 (12)
Re1—O2—Re2—S211	80 (8)	C212—C211—C217—C218	−43.1 (10)
O2—Re2—S211—$C211^{i}$	95.4 (4)	$S211^{i}$—C211—C217—C218	133.5 (5)
$O2^{i}$—Re2—S211—$C211^{i}$	−84.6 (4)	C212—C211—C217—*C*222	139.8 (7)
$N213^{i}$—Re2—S211—$C211^{i}$	4.6 (4)	$S211^{i}$—C211—C217—*C*222	−43.6 (8)
N213—Re2—S211—$C211^{i}$	−175.4 (4)	*C*222—C217—C218—C219	0.0
$S211^{i}$—Re2—S211—$C211^{i}$	−173 (14)	C211—C217—C218—C219	−177.1 (6)
C217—C211—C212—N213	174.4 (7)	C217—C218—C219—C220	0.0
$S211^{i}$—C211—C212—N213	−2.1 (12)	C218—C219—C220—O223	178.0 (7)
C217—C211—C212—C216	−14.4 (16)	C218—C219—C220—C221	0.0
$S211^{i}$—C211—C212—C216	169.1 (9)	O223—C220—C221—*C*222	−178.2 (7)
C211—C212—N213—C214	173.9 (9)	C219—C220—C221—*C*222	0.0
C216—C212—N213—C214	0.6 (10)	C220—C221—*C*222—C217	0.0
C211—C212—N213—Re2	−3.2 (11)	C218—C217—*C*222—C221	0.0
C216—C212—N213—Re2	−176.5 (6)	C211—C217—*C*222—C221	177.1 (6)
O2—Re2—N213—C214	99.2 (9)	C221—C220—O223—C223	−176.2 (9)
$O2^{i}$—Re2—N213—C214	−80.8 (9)	C219—C220—O223—C223	5.7 (12)

Symmetry codes: (i) $\frac{1}{2}-x, \frac{3}{2}-y, 1-z$; (ii) $1-x, y, \frac{3}{2}-z$.

Data collection: SMART (Bruker, 1999). Cell refinement: SAINT (Bruker, 1999). Data reduction: SAINT (Bruker, 1999). Program(s) used to solve structure: *SHELXS*97 (Sheldrick, 1997). Program(s) used to refine structure: *SHELXL*96 (Sheldrick, 1996). Molecular graphics: *SHELXTL* (Bruker, 1997). Software used to prepare material for publication: *SHELXL*96 (Sheldrick, 1996).

References

International Tables for Crystallography (1992). Vol. C. Tables 4.2.6.8 and 6.1.1. **4**, Dordrecht: Kluwer Academic Publishers.

SAINT (1999) Release 6.06; Integration Software for Single Crystal Data, Bruker AXS Inc., Madison, WI 53719–1173.

Sheldrick, G. M. (1996). SADABS, Bruker Area Detector Absorption Corrections. Bruker AXS Inc., Madison, WI 53719–1173.

Sheldrick, G. M. (1997). *SHELXS*97. Program for the Solution of Crystal Structures. University of Gottingen, Germany.

Sheldrick, G. M. (1996). *SHELXL*96. Program for the Refinement of Crystal Structures. University of Gottingen, Germany.

SHELXTL (1997) Release 5.10; The Complete Software Package for Single Crystal Structure Determination. Bruker AXS Inc., Madison, WI 53719–1173.

SMART (1999) Release 5.059; Bruker Molecular Analysis Research Tool, Bruker AXS Inc., Madison, WI 53719–1173.

Spek, A. L. (1995). July 1995 version; *PLATON*, Molecular Geometry Program, University of Utrecht, Utrecht, Holland.

XPREP (1997) Release 5.10; X-ray data Preparation and Reciprocal space Exploration Program. Bruker AXS Inc., Madison, WI 53719–1173.

Data reduction processing was carried out by the use of the program SAINT (Bruker, 1999), which applied Lorentz and polarization corrections to three-dimensionally integrated diffraction spots. The program SADABS (Sheldrick, 1996) was utilized for the scaling of diffraction data, the application of a decay correction, and an empirical absorption correction based on redundant reflections. The space group was confirmed by XPREP routine in *SHELXTL* program (Sheldrick, 1997). The structure was solved by direct method using *SHELXS*97 (Sheldrick, 1997) and difmap synthesis using *SHELXL*96 (Sheldrick, 1996). All non-H atoms anisotropic, hydrogen atoms isotropic. H atoms constrained to the parent site using a riding model; *SHELXL*96 defaults, C—H 0.93 to 0.97 and O—H 0.82 Å. The isotropic factors, U_{iso} , were adjusted to 50% higher value of the parent site (methyl and hydroxyl) and 20% higher (others). A final verification of possible voids was performed using the VOID routine of the *PLATON* program (Spek, 1995).

Data collection: SMART (Bruker, 1999). Cell refinement: SAINT (Bruker, 1999). Data reduction: SAINT (Bruker, 1999). Program(s) used to solve structure: *SHELXS*97 (Sheldrick, 1997). Program(s) used to refine structure: *SHELXL*96 (Sheldrick, 1996). Molecular graphics: *SHELXTL* (Bruker, 1997). Software used to prepare material for publication: *SHELXL*96 (Sheldrick, 1996).

Table S1. *Fractional atomic coordinates and equivalent isotropic displacement parameters (Å²)*

$$U_{eq} = (1/3)\Sigma_i\Sigma_j U^{ij} a^i a^j \mathbf{a}_i.\mathbf{a}_j.$$

	Occupancy	x	y	z	U_{eq}
Re1	1	**0.215259** (17)	1.01072 (4)	0.55963 (2)	0.05695 (17)
O1	1	0.2024 (3)	1.1271 (8)	0.5857 (5)	0.087 (3)
O2	1	0.2327 (2)	0.8687 (5)	0.5267 (3)	0.0466 (13)
S111	1	0.24794 (11)	0.8918 (3)	0.65804 (14)	0.0653 (7)
C111	1	0.3087 (4)	0.9193 (8)	0.7020 (5)	0.067 (3)
C112	1	0.3237 (4)	0.9942 (8)	0.6752 (5)	0.062 (3)
N113	1	0.2886 (3)	1.0440 (7)	0.6104 (4)	0.0559 (19)
C114	1	0.3120 (5)	1.1091 (10)	0.5947 (6)	0.077 (3)
H114	1	0.2973	1.1498	0.5539	0.093
C115	1	0.3627 (5)	1.1071 (11)	0.6498 (6)	0.086 (4)
H115	1	0.3867	1.1479	0.6518	0.104
C116	1	0.3705 (4)	1.0365 (11)	0.6987 (6)	0.076 (3)
H116	1	0.4007	1.0184	0.7401	0.092
C117	1	0.34252 (14)	0.8572 (4)	0.76798 (14)	0.075 (3)
C118	1	0.38702 (13)	0.8146 (4)	0.78778 (19)	0.098 (5)
H118	1	0.3965	0.8276	0.7603	0.117
C119	1	0.41740 (16)	0.7526 (5)	0.8487 (2)	0.132 (7)
H119	1	0.4472	0.7242	0.8619	0.158
C120	1	0.40327 (19)	0.7332 (5)	0.88979 (18)	0.138 (8)
C121	1	0.3588 (2)	0.7758 (5)	0.86999 (15)	0.115 (6)
H121	1	0.3493	0.7628	0.8975	0.137
C122	1	0.32839 (18)	0.8377 (4)	0.80909 (13)	0.084 (4)
H122	1	0.2986	0.8662	0.7958	0.101
O123	1	0.4320 (2)	0.6748 (6)	0.9502 (2)	0.202 (8)
C123	1	0.4203 (3)	0.6828 (6)	0.99636 (18)	0.41 (3)
H12A	1	0.4464	0.7212	1.0378	0.622
H12B	1	0.4161	0.6065	1.0073	0.622
H12C	1	0.3905	0.7260	0.9750	0.622
S131	1	0.18747 (9)	1.0884 (2)	0.45056 (13)	0.0651 (7)
C131	1	0.13008 (9)	1.0284 (2)	0.39871 (13)	0.079 (4)
C132	1	0.11573 (8)	0.9554 (3)	0.42803 (15)	0.071 (3)
N133	1	0.14692 (9)	0.9341 (3)	0.49930 (15)	0.062 (2)
C134	1	0.12562 (11)	0.8577 (4)	0.51412 (18)	0.077 (3)
H134	1	0.1394	0.8264	0.5572	0.092
C135	1	0.07777 (11)	0.8329 (5)	0.4518 (2)	0.084 (4)
H135	1	0.0549	0.7842	0.4481	0.101
C136	1	0.07110 (10)	0.8920 (4)	0.39848 (19)	0.075 (3)
H136	1	0.0434	0.8914	0.3526	0.090
C137	0.50	0.0935 (4)	1.0839 (13)	0.3317 (5)	0.054 (5)
C138	0.50	0.0476 (4)	1.1195 (14)	0.3096 (6)	0.065 (5)
H138	0.50	0.0393	1.1132	0.3388	0.078
C139	0.50	0.0141 (4)	1.1646 (15)	0.2438 (7)	0.080 (7)
H139	0.50	−0.0166	1.1885	0.2291	0.096
C140	0.50	0.0266 (5)	1.1740 (17)	0.2002 (5)	0.077 (7)
C141	0.50	0.0725 (6)	1.138 (2)	0.2223 (7)	0.107 (14)

H141	0.50	0.0808	1.1447	0.1930	0.129
C142	0.50	0.1060 (4)	1.0933 (18)	0.2880 (7)	0.068 (7)
H142	0.50	0.1367	1.0694	0.3028	0.082
O143	0.50	−0.0039 (6)	1.2129 (19)	0.1347 (7)	0.100 (6)
C143	0.50	−0.0499 (9)	1.260 (3)	0.1097 (16)	0.129 (14)
H14A	0.50	−0.0727	1.1984	0.0966	0.193
H14B	0.50	−0.0619	1.3079	0.0705	0.193
H14C	0.50	−0.0463	1.3056	0.1451	0.193
C147	0.50	0.1057 (6)	1.0307 (18)	0.3212 (6)	0.064 (6)
C148	0.50	0.0775 (7)	0.9417 (15)	0.2755 (9)	0.103 (9)
H148	0.50	0.0744	0.8724	0.2916	0.124
C149	0.50	0.0539 (7)	0.9561 (18)	0.2056 (8)	0.113 (10)
H149	0.50	0.0350	0.8965	0.1750	0.136
C150	0.50	0.0585 (7)	1.060 (2)	0.1815 (6)	0.107 (9)
C151	0.50	0.0867 (9)	1.1486 (18)	0.2272 (11)	0.110 (14)
H151	0.50	0.0898	1.2179	0.2110	0.132
C152	0.50	0.1104 (8)	1.1342 (16)	0.2971 (9)	0.102 (14)
H152	0.50	0.1293	1.1938	0.3276	0.122
O153	0.50	0.0355 (10)	1.071 (3)	0.1127 (9)	0.175 (12)
C153	0.50	0.0422 (17)	1.168 (4)	0.085 (2)	0.23 (3)
H15A	0.50	0.0659	1.2189	0.1210	0.351
H15B	0.50	0.0117	1.2079	0.0539	0.351
H15C	0.50	0.0537	1.1427	0.0596	0.351
Re2	1	1/4	3/4	0.5000	0.03744 (16)
S211	1	0.29990 (8)	0.67193 (19)	0.61536 (10)	0.0467 (5)
C211	1	0.2414 (3)	0.9230 (7)	0.3933 (4)	0.0468 (19)
C212	1	0.2891 (3)	0.9276 (8)	0.4536 (4)	0.047 (2)
N213	1	0.3028 (2)	0.8546 (6)	0.5092 (3)	0.0461 (16)
C214	1	0.3508 (3)	0.8670 (9)	0.5574 (5)	0.058 (2)
H214	1	0.3693	0.8283	0.5994	0.069
C215	1	0.3700 (3)	0.9474 (11)	0.5361 (5)	0.069 (3)
H215	1	0.4024	0.9713	0.5615	0.083
C216	1	0.3324 (3)	0.9826 (9)	0.4722 (5)	0.061 (3)
H216	1	0.3345	1.0339	0.4451	0.073
C217	1	0.2232 (2)	1.0038 (4)	0.3354 (2)	0.0416 (18)
C218	1	0.2351 (2)	1.1205 (5)	0.3484 (2)	0.055 (2)
H218	1	0.2557	1.1472	0.3935	0.066
C219	1	0.2163 (3)	1.1972 (4)	0.2941 (3)	0.060 (2)
H219	1	0.2242	1.2752	0.3029	0.073
C220	1	0.1855 (2)	1.1572 (5)	0.2267 (3)	0.054 (2)
C221	1	0.1736 (2)	1.0406 (5)	0.2137 (2)	0.061 (2)
H221	1	0.1530	1.0139	0.1686	0.073
C222	1	0.1924 (2)	0.9639 (4)	0.2680 (3)	0.060 (2)
H222	1	0.1845	0.8858	0.2592	0.072
O223	1	0.1639 (3)	1.2255 (6)	0.1698 (4)	0.071 (2)
C223	1	0.1768 (6)	1.3457 (9)	0.1790 (7)	0.098 (5)
H22A	1	0.1654	1.3833	0.2015	0.147
H22B	1	0.1618	1.3810	0.1350	0.147
H22C	1	0.2117	1.3533	0.2068	0.147
Re11	1	1/2	0.89117 (12)	0.7500	0.1346 (5)
O11	1	0.4486 (5)	0.8167 (15)	0.7149 (8)	0.200 (7)
O12	1	0.4919 (11)	0.983 (2)	0.6893 (10)	0.45 (3)
O21	1	0.4537 (8)	0.967 (2)	0.4866 (15)	0.226 (10)
H21	1	0.4626	0.9308	0.4676	0.340
C22	1	0.4963 (12)	0.997 (3)	0.5568 (15)	0.218 (15)
H22D	1	0.4861	1.0409	0.5794	0.261
H22E	1	0.5124	0.9269	0.5832	0.261
C23	1	0.5299 (17)	1.065 (5)	0.553 (3)	0.41 (4)
H23A	1	0.5294	1.1441	0.5642	0.610
H23B	1	0.5199	1.0614	0.5068	0.610
H23C	1	0.5625	1.0349	0.5844	0.610

Table S2. *Anisotropic displacement parameters* ($Å^2$)

	U_{11}	U_{22}	U_{33}	U_{12}	U_{13}	U_{23}
Re1	0.0683 (3)	0.0472 (3)	0.0678 (3)	−0.00266 (19)	0.0482 (3)	−0.01265 (19)
O1	0.083 (6)	0.081 (6)	0.103 (7)	0.006 (4)	0.060 (5)	−0.021 (5)
O2	0.052 (3)	0.044 (3)	0.046 (3)	−0.003 (3)	0.031 (3)	−0.005 (2)
S111	0.0753 (16)	0.0754 (18)	0.0632 (15)	−0.0149 (13)	0.0518 (14)	−0.0139 (12)
C111	0.097 (8)	0.054 (6)	0.065 (6)	−0.007 (6)	0.057 (6)	−0.018 (5)
C112	0.079 (7)	0.048 (6)	0.065 (6)	−0.011 (5)	0.047 (6)	−0.007 (4)
N113	0.064 (5)	0.052 (5)	0.058 (5)	−0.008 (4)	0.041 (4)	−0.014 (4)
C114	0.107 (10)	0.056 (7)	0.089 (8)	−0.010 (6)	0.071 (8)	0.004 (6)
C115	0.097 (10)	0.077 (9)	0.099 (10)	−0.030 (7)	0.068 (9)	−0.001 (7)
C116	0.074 (7)	0.078 (8)	0.074 (7)	−0.015 (6)	0.044 (6)	−0.006 (6)
C117	0.090 (8)	0.070 (7)	0.061 (6)	−0.038 (6)	0.045 (6)	−0.018 (5)
C118	0.075 (8)	0.107 (11)	0.079 (8)	−0.017 (8)	0.031 (7)	0.021 (7)
C119	0.091 (10)	0.144 (15)	0.118 (13)	−0.021 (10)	0.043 (9)	0.041 (11)
C120	0.120 (13)	0.153 (15)	0.082 (10)	−0.040 (11)	0.032 (9)	0.044 (10)
C121	0.142 (13)	0.116 (12)	0.077 (9)	−0.063 (11)	0.063 (9)	−0.005 (8)
C122	0.112 (10)	0.073 (8)	0.068 (7)	−0.030 (7)	0.057 (7)	−0.017 (6)
O123	0.144 (11)	0.266 (17)	0.128 (10)	−0.042 (12)	0.049 (9)	0.087 (11)
C123	0.41 (5)	0.47 (5)	0.29 (4)	−0.12 (4)	0.18 (4)	0.17 (4)
S131	0.0662 (15)	0.0458 (13)	0.0792 (17)	0.0048 (11)	0.0426 (14)	0.0103 (11)
C131	0.072 (7)	0.056 (7)	0.098 (9)	0.012 (5)	0.047 (7)	0.033 (6)
C132	0.061 (6)	0.075 (7)	0.082 (8)	0.020 (6)	0.047 (6)	0.019 (6)
N133	0.069 (5)	0.053 (5)	0.071 (5)	0.008 (4)	0.046 (5)	−0.003 (4)
C134	0.079 (8)	0.085 (9)	0.084 (8)	−0.011 (7)	0.059 (7)	−0.003 (6)
C135	0.086 (8)	0.090 (9)	0.098 (9)	−0.012 (7)	0.067 (8)	0.000 (7)
C136	0.065 (7)	0.077 (8)	0.082 (8)	−0.004 (6)	0.045 (6)	0.005 (6)
C137	0.046 (10)	0.042 (11)	0.066 (12)	0.012 (8)	0.031 (9)	0.004 (9)
C138	0.061 (12)	0.067 (14)	0.062 (12)	0.001 (10)	0.035 (10)	0.007 (10)
C139	0.043 (12)	0.092 (17)	0.073 (14)	0.010 (11)	0.019 (11)	0.008 (13)
C140	0.057 (12)	0.099 (19)	0.066 (14)	0.018 (12)	0.033 (11)	0.031 (13)
C141	0.13 (3)	0.12 (3)	0.09 (3)	0.01 (3)	0.08 (2)	0.02 (2)
C142	0.045 (12)	0.085 (19)	0.066 (15)	0.025 (11)	0.029 (11)	0.002 (14)
O143	0.079 (12)	0.137 (17)	0.065 (10)	0.007 (12)	0.036 (9)	0.025 (11)
C143	0.09 (2)	0.17 (4)	0.09 (2)	0.06 (2)	0.039 (18)	0.04 (2)
C147	0.048 (11)	0.051 (12)	0.081 (14)	0.011 (9)	0.034 (10)	0.013 (11)
C148	0.097 (17)	0.12 (2)	0.107 (19)	0.026 (16)	0.071 (15)	0.021 (16)
C149	0.078 (16)	0.14 (2)	0.12 (2)	0.007 (16)	0.062 (16)	−0.002 (18)
C150	0.063 (14)	0.16 (2)	0.081 (17)	0.015 (16)	0.036 (12)	0.029 (17)
C151	0.084 (17)	0.11 (3)	0.13 (3)	0.019 (16)	0.064 (17)	0.03 (2)
C152	0.11 (2)	0.10 (2)	0.10 (2)	0.013 (16)	0.072 (18)	0.015 (16)
O153	0.122 (18)	0.22 (2)	0.16 (2)	0.027 (18)	0.077 (16)	0.053 (19)
C153	0.14 (3)	0.35 (6)	0.25 (5)	0.00 (4)	0.14 (4)	0.09 (4)
Re2	0.0449 (3)	0.0339 (3)	0.0352 (3)	0.0000 (2)	0.0255 (2)	−0.00139 (18)
S211	0.0485 (11)	0.0471 (12)	0.0387 (10)	−0.0033 (9)	0.0239 (9)	0.0028 (8)
C211	0.052 (5)	0.041 (5)	0.043 (4)	−0.006 (4)	0.027 (4)	−0.006 (3)
C212	0.050 (5)	0.061 (6)	0.041 (4)	−0.009 (4)	0.033 (4)	−0.010 (4)
N213	0.047 (4)	0.045 (4)	0.042 (4)	−0.007 (3)	0.025 (3)	−0.003 (3)
C214	0.053 (5)	0.068 (6)	0.051 (5)	0.004 (5)	0.032 (4)	0.005 (4)
C215	0.051 (6)	0.089 (8)	0.058 (6)	−0.014 (5)	0.029 (5)	−0.005 (6)
C216	0.064 (6)	0.066 (7)	0.054 (6)	−0.012 (5)	0.037 (5)	0.001 (5)
C217	0.055 (5)	0.038 (4)	0.035 (4)	0.002 (3)	0.029 (4)	0.000 (3)
C218	0.059 (5)	0.053 (6)	0.049 (5)	−0.008 (4)	0.032 (4)	−0.005 (4)
C219	0.088 (7)	0.040 (5)	0.068 (6)	−0.003 (5)	0.056 (6)	0.002 (4)
C220	0.069 (6)	0.050 (5)	0.058 (5)	0.001 (4)	0.047 (5)	0.005 (4)
C221	0.071 (6)	0.066 (6)	0.044 (5)	−0.004 (5)	0.035 (5)	−0.003 (4)
C222	0.088 (7)	0.052 (6)	0.054 (6)	0.002 (5)	0.051 (5)	0.006 (4)
O223	0.108 (6)	0.060 (4)	0.059 (4)	0.013 (4)	0.059 (4)	0.015 (3)
C223	0.156 (14)	0.057 (7)	0.082 (9)	−0.001 (8)	0.073 (10)	0.018 (6)
Re11	0.0569 (5)	0.1163 (9)	0.1588 (11)	0.000	0.0304 (6)	0.000
O11	0.177 (15)	0.217 (17)	0.173 (15)	−0.067 (14)	0.092 (13)	−0.040 (14)
O12	0.32 (3)	0.45 (4)	0.50 (4)	−0.01 (3)	0.21 (3)	0.28 (3)
O21	0.135 (13)	0.31 (3)	0.26 (2)	0.014 (15)	0.137 (16)	0.05 (2)
C22	0.15 (2)	0.21 (2)	0.29 (3)	0.037 (17)	0.13 (2)	0.06 (2)
C23	0.40 (6)	0.44 (6)	0.46 (6)	0.02 (5)	0.31 (5)	0.04 (5)

Table S3. *Geometric parameters (Å, °)*

Re1—O1	1.667 (8)	C147—C148	1.3900
Re1—N113	2.064 (8)	C147—C152	1.3900
Re1—N133	2.066 (3)	C148—C149	1.3900
Re1—O2	2.082 (6)	C148—H148	0.9300
Re1—S111	2.384 (3)	C149—C150	1.3900
Re1—S131	2.406 (2)	C149—H149	0.9300
O2—Re2	1.779 (6)	C150—O153	1.365 (14)
S111—C111	1.704 (10)	C150—C151	1.3900
C111—C112	1.371 (11)	C151—C152	1.3900
C111—C117	1.481 (9)	C151—H151	0.9300
C112—N113	1.404 (11)	C152—H152	0.9300
C112—C116	1.431 (12)	O153—C153	1.415 (18)
N113—C114	1.327 (11)	C153—H15A	0.9600
C114—C115	1.412 (13)	C153—H15B	0.9600
C114—H114	0.9300	C153—H15C	0.9600
C115—C116	1.339 (12)	Re2—O2^{i}	1.779 (6)
C115—H115	0.9300	Re2—N213^{i}	2.088 (7)
C116—H116	0.9300	Re2—N213	2.088 (7)
C117—C118	1.3900	Re2—S211^{i}	2.418 (2)
C117—C122	1.3900	Re2—S211	2.418 (2)
C118—C119	1.3900	S211—C211^{i}	1.711 (9)
C118—H118	0.9300	C211—C212	1.386 (9)
C119—C120	1.3900	C211—C217	1.486 (8)
C119—H119	0.9300	C211—S211^{i}	1.710 (8)
C120—O123	1.3581	C212—N213	1.420 (9)
C120—C121	1.3900	C212—C216	1.421 (10)
C121—C122	1.3900	N213—C214	1.329 (10)
C121—H121	0.9300	C214—C215	1.418 (12)
C122—H122	0.9300	C214—H214	0.9300
O123—C123	1.4273	C215—C216	1.348 (11)
C123—H12A	0.9600	C215—H215	0.9300
C123—H12B	0.9600	C216—H216	0.9300
C123—H12C	0.9600	C217—C218	1.3900
S131—C131	1.7145	C217—C222	1.3900
C131—C132	1.3889	C218—C219	1.3900
C131—C137	1.473 (8)	C218—H218	0.9300
C131—C147	1.544 (12)	C219—C220	1.3900
C132—N133	1.4073	C219—H219	0.9300
C132—C136	1.4396	C220—O223	1.366 (7)
N133—C134	1.3392	C220—C221	1.3900
C134—C135	1.4341	C221—C222	1.3900
C134—H134	0.9300	C221—H221	0.9300
C135—C136	1.3705	C222—H222	0.9300
C135—H135	0.9300	O223—C223	1.435 (11)
C136—H136	0.9300	C223—H22A	0.9600
C137—C138	1.3900	C223—H22B	0.9600
C137—C142	1.3900	C223—H22C	0.9600
C138—C139	1.3900	Re11—O11	1.664 (10)
C138—H138	0.9300	Re11—O11^{ii}	1.664 (10)
C139—C140	1.3900	Re11—O12^{ii}	1.712 (11)
C139—H139	0.9300	Re11—O12	1.712 (11)
C140—O143	1.352 (12)	O21—C22	1.466 (19)
C140—C141	1.3900	O21—H21	0.8200
C141—C142	1.3900	C22—C23	1.46 (2)
C141—H141	0.9300	C22—H22D	0.9700
C142—H142	0.9300	C22—H22E	0.9700
O143—C143	1.417 (16)	C23—H23A	0.9600
C143—H14A	0.9600	C23—H23B	0.9600
C143—H14B	0.9600	C23—H23C	0.9600
C143—H14C	0.9600		

O1—Re1—N113	97.9 (4)	O1—Re1—N133	99.5 (3)
N113—Re1—N133	162.6 (2)	C137—C131—S131	117.5 (6)
O1—Re1—O2	178.2 (4)	C147—C131—S131	114.5 (7)
N113—Re1—O2	80.7 (3)	C131—C132—N133	120.8
N133—Re1—O2	81.96 (19)	C131—C132—C136	131.6
O1—Re1—S111	98.3 (4)	N133—C132—C136	107.6
N113—Re1—S111	81.6 (2)	C134—N133—C132	109.2
N133—Re1—S111	95.79 (10)	C134—N133—Re1	131.81 (7)
O2—Re1—S111	82.66 (17)	C132—N133—Re1	118.86 (7)
O1—Re1—S131	96.4 (4)	N133—C134—C135	107.9
N113—Re1—S131	96.0 (2)	N133—C134—H134	126.1
N133—Re1—S131	82.12 (8)	C135—C134—H134	126.1
O2—Re1—S131	82.56 (17)	C136—C135—C134	109.2
S111—Re1—S131	165.22 (9)	C136—C135—H135	125.4
Re2—O2—Re1	177.6 (3)	C134—C135—H135	125.4
C111—S111—Re1	99.5 (3)	C135—C136—C132	106.0
C112—C111—C117	124.0 (8)	C135—C136—H136	127.0
C112—C111—S111	119.9 (7)	C132—C136—H136	127.0
C117—C111—S111	116.1 (6)	C138—C137—C142	120.0
C111—C112—N113	119.2 (9)	C138—C137—C131	123.7 (8)
C111—C112—C116	133.8 (9)	C142—C137—C131	116.2 (8)
N113—C112—C116	106.9 (8)	C137—C138—C139	120.0
C114—N113—C112	108.0 (8)	C137—C138—H138	120.0
C114—N113—Re1	132.4 (7)	C139—C138—H138	120.0
C112—N113—Re1	119.6 (6)	C140—C139—C138	120.0
N113—C114—C115	109.3 (9)	C140—C139—H139	120.0
N113—C114—H114	125.3	C138—C139—H139	120.0
C115—C114—H114	125.3	O143—C140—C141	115.5 (11)
C116—C115—C114	108.6 (9)	O143—C140—C139	124.5 (11)
C116—C115—H115	125.7	C141—C140—C139	120.0
C114—C115—H115	125.7	C140—C141—C142	120.0
C115—C116—C112	107.1 (9)	C140—C141—H141	120.0
C115—C116—H116	126.4	C142—C141—H141	120.0
C112—C116—H116	126.4	C141—C142—C137	120.0
C118—C117—C122	120.0	C141—C142—H142	120.0
C118—C117—C111	120.8 (4)	C137—C142—H142	120.0
C122—C117—C111	119.1 (4)	C140—O143—C143	119.3 (17)
C117—C118—C119	120.0	O143—C143—H14A	109 (2)
C117—C118—H118	120.0	O143—C143—H14B	109.5 (15)
C119—C118—H118	120.0	H14A—C143—H14B	109.5
C120—C119—C118	120.0	O143—C143—H14C	109.5 (16)
C120—C119—H119	120.0	H14A—C143—H14C	109.5
C118—C119—H119	120.0	H14B—C143—H14C	109.5
O123—C120—C119	122.2	C148—C147—C152	120.0
O123—C120—C121	117.8	C148—C147—C131	124.6 (13)
C119—C120—C121	120.0	C152—C147—C131	115.2 (13)
C122—C121—C120	120.0	C149—C148—C147	120.0
C122—C121—H121	120.0	C149—C148—H148	120.0
C120—C121—H121	120.0	C147—C148—H148	120.0
C121—C122—C117	120.0	C148—C149—C150	120.0
C121—C122—H122	120.0	C148—C149—H149	120.0
C117—C122—H122	120.0	C150—C149—H149	120.0
C120—O123—C123	117.9	O153—C150—C151	121.2 (15)
O123—C123—H12A	109.5	O153—C150—C149	118.8 (15)
O123—C123—H12B	109.5	C151—C150—C149	120.0
H12A—C123—H12B	109.5	C150—C151—C152	120.0
O123—C123—H12C	109.5	C150—C151—H151	120.0
H12A—C123—H12C	109.5	C152—C151—H151	120.0
H12B—C123—H12C	109.5	C151—C152—C147	120.0
C131—S131—Re1	99.47 (6)	C151—C152—H152	120.0
C132—C131—C137	120.9 (6)	C147—C152—H152	120.0
C132—C131—C147	123.9 (8)	C150—O153—C153	123 (3)
C132—C131—S131	118.7	O153—C153—H15A	109

O153—C153—H15B	109	C219—C218—C217	120.0
H15A—C153—H15B	109.5	C219—C218—H218	120.0
O153—C153—H15C	109	C217—C218—H218	120.0
H15A—C153—H15C	109.5	C218—C219—C220	120.0
H15B—C153—H15C	109.5	C218—C219—H219	120.0
O2—Re2—O2^{i}	179.996 (2)	C220—C219—H219	120.0
O2—Re2—N213^{i}	90.8 (3)	O223—C220—C221	115.3 (5)
O2^{i}—Re2—N213^{i}	89.2 (3)	O223—C220—C219	124.7 (5)
O2—Re2—N213	89.2 (3)	C221—C220—C219	120.0
O2^{i}—Re2—N213	90.8 (3)	*C*222—C221—C220	120.0
N213^{i}—Re2—N213	180.0	*C*222—C221—H221	120.0
O2—Re2—S211^{i}	89.34 (19)	C220—C221—H221	120.0
O2^{i}—Re2—S211^{i}	90.7 (2)	C221—*C*222—C217	120.0
N213^{i}—Re2—S211^{i}	98.37 (18)	C221—*C*222—H222	120.0
N213—Re2—S211^{i}	81.63 (18)	C217—*C*222—H222	120.0
O2—Re2—S211	90.66 (19)	C220—O223—C223	118.5 (8)
O2^{i}—Re2—S211	89.3 (2)	O223—C223—H22A	109.5
N213^{i}—Re2—S211	81.63 (18)	O223—C223—H22B	109.5
N213—Re2—S211	98.37 (18)	H22A—C223—H22B	109.5
S211^{i}—Re2—S211	180.0	O223—C223—H22C	109.5
C211^{i}—S211—Re2	99.0 (3)	H22A—C223—H22C	109.5
C212—C211—C217	121.9 (7)	H22B—C223—H22C	109.5
C212—C211—S211^{i}	120.9 (6)	O11—Re11—O11^{ii}	117.6 (13)
C217—C211—S211^{i}	117.2 (5)	O11—Re11—O12^{ii}	108.8 (11)
C211—C212—N213	118.8 (7)	O11^{ii}—Re11—O12^{ii}	108.7 (11)
C211—C212—C216	133.5 (8)	O11—Re11—O12	108.7 (11)
N213—C212—C216	107.3 (7)	O11^{ii}—Re11—O12	108.8 (10)
C214—N213—C212	106.9 (7)	O12^{ii}—Re11—O12	103.3 (18)
C214—N213—Re2	133.6 (6)	C22—O21—H21	109.5
C212—N213—Re2	119.4 (5)	C23—C22—O21	108 (2)
N213—C214—C215	110.6 (8)	C23—C22—H22D	110
N213—C214—H214	124.7	O21—C22—H22D	110.1
C215—C214—H214	124.7	C23—C22—H22E	110
C216—C215—C214	107.3 (8)	O21—C22—H22E	110.1
C216—C215—H215	126.3	H22D—C22—H22E	108.4
C214—C215—H215	126.3	C22—C23—H23A	109
C215—C216—C212	107.9 (8)	C22—C23—H23B	109
C215—C216—H216	126.0	H23A—C23—H23B	109.5
C212—C216—H216	126.0	C22—C23—H23C	109
C218—C217—*C*222	120.0	H23A—C23—H23C	109.5
C218—C217—C211	119.9 (4)	H23B—C23—H23C	109.5
*C*222—C217—C211	120.0 (4)		
O1—Re1—O2—Re2	28 (16)	O1—Re1—N113—C114	−83.5 (10)
N113—Re1—O2—Re2	−12 (8)	N133—Re1—N113—C114	96.5 (12)
N133—Re1—O2—Re2	168 (8)	O2—Re1—N113—C114	95.3 (10)
S111—Re1—O2—Re2	−95 (8)	S111—Re1—N113—C114	179.2 (10)
S131—Re1—O2—Re2	85 (8)	S131—Re1—N113—C114	13.9 (10)
O1—Re1—S111—C111	−95.9 (5)	O1—Re1—N113—C112	94.9 (8)
N113—Re1—S111—C111	1.0 (4)	N133—Re1—N113—C112	−85.1 (10)
N133—Re1—S111—C111	163.7 (4)	O2—Re1—N113—C112	−86.3 (7)
O2—Re1—S111—C111	82.6 (4)	S111—Re1—N113—C112	−2.4 (7)
S131—Re1—S111—C111	82.6 (5)	S131—Re1—N113—C112	−167.7 (7)
Re1—S111—C111—C112	0.4 (9)	C112—N113—C114—C115	−2.1 (13)
Re1—S111—C111—C117	−178.9 (6)	Re1—N113—C114—C115	176.4 (8)
C117—C111—C112—N113	176.8 (8)	N113—C114—C115—C116	2.2 (16)
S111—C111—C112—N113	−2.4 (13)	C114—C115—C116—C112	−1.2 (15)
C117—C111—C112—C116	−2.1 (18)	C111—C112—C116—C115	178.9 (12)
S111—C111—C112—C116	178.7 (11)	N113—C112—C116—C115	0.0 (14)
C111—C112—N113—C114	−177.8 (10)	C112—C111—C117—C118	−37.9 (11)
C116—C112—N113—C114	1.4 (12)	S111—C111—C117—C118	141.3 (4)
C111—C112—N113—Re1	3.4 (12)	C112—C111—C117—C122	144.6 (8)
C116—C112—N113—Re1	−177.4 (7)	S111—C111—C117—C122	−36.2 (7)

C122—C117—C118—C119	0.0	C141—C140—O143—C143	−175 (2)
C111—C117—C118—C119	−177.5 (4)	C139—C140—O143—C143	7 (4)
C117—C118—C119—C120	0.0	C132—C131—C147—C148	−19.5 (15)
C118—C119—C120—O123	−179.0	C137—C131—C147—C148	−116 (2)
C118—C119—C120—C121	0.0	S131—C131—C147—C148	141.2 (10)
O123—C120—C121—C122	179.0	C132—C131—C147—C152	155.4 (9)
C119—C120—C121—C122	0.0	C137—C131—C147—C152	59.4 (18)
C120—C121—C122—C117	0.0	S131—C131—C147—C152	−43.9 (12)
C118—C117—C122—C121	0.0	C152—C147—C148—C149	0.0
C111—C117—C122—C121	177.6 (4)	C131—C147—C148—C149	174.7 (15)
C119—C120—O123—C123	165.3	C147—C148—C149—C150	0.0
C121—C120—O123—C123	−13.7	C148—C149—C150—O153	179 (2)
O1—Re1—S131—C131	−97.8 (3)	C148—C149—C150—C151	0.0
N113—Re1—S131—C131	163.5 (2)	O153—C150—C151—C152	−179 (2)
N133—Re1—S131—C131	0.88 (7)	C149—C150—C151—C152	0.0
O2—Re1—S131—C131	83.74 (18)	C150—C151—C152—C147	0.0
S111—Re1—S131—C131	83.7 (4)	C148—C147—C152—C151	0.0
Re1—S131—C131—C132	−1.87 (6)	C131—C147—C152—C151	−175.2 (13)
Re1—S131—C131—C137	159.1 (7)	C151—C150—O153—C153	6 (4)
Re1—S131—C131—C147	−163.6 (8)	C149—C150—O153—C153	−173 (3)
C137—C131—C132—N133	−158.1 (7)	Re1—O2—Re2—O2^{i}	−55 (10)
C147—C131—C132—N133	162.2 (8)	Re1—O2—Re2—N213^{i}	162 (8)
S131—C131—C132—N133	2.3	Re1—O2—Re2—N213	−18 (8)
C137—C131—C132—C136	20.6 (7)	Re1—O2—Re2—S211^{i}	−100 (8)
C147—C131—C132—C136	−19.1 (8)	Re1—O2—Re2—S211	80 (8)
S131—C131—C132—C136	−179.1	O2—Re2—S211—C211^{i}	95.4 (4)
C131—C132—N133—C134	−177.5	O2^{i}—Re2—S211—C211^{i}	−84.6 (4)
C136—C132—N133—C134	3.6	N213^{i}—Re2—S211—C211^{i}	4.6 (4)
C131—C132—N133—Re1	−1.32 (8)	N213—Re2—S211—C211^{i}	−175.4 (4)
C136—C132—N133—Re1	179.73 (8)	S211^{i}—Re2—S211—C211^{i}	−173 (14)
O1—Re1—N133—C134	−89.6 (4)	C217—C211—C212—N213	174.4 (7)
N113—Re1—N133—C134	90.4 (8)	S211^{i}—C211—C212—N213	−2.1 (12)
O2—Re1—N133—C134	91.59 (18)	C217—C211—C212—C216	−14.4 (16)
S111—Re1—N133—C134	9.87 (10)	S211^{i}—C211—C212—C216	169.1 (9)
S131—Re1—N133—C134	175.1	C211—C212—N213—C214	173.9 (9)
O1—Re1—N133—C132	95.3 (4)	C216—C212—N213—C214	0.6 (10)
N113—Re1—N133—C132	−84.7 (8)	C211—C212—N213—Re2	−3.2 (11)
O2—Re1—N133—C132	−83.51 (18)	C216—C212—N213—Re2	−176.5 (6)
S111—Re1—N133—C132	−165.22 (10)	O2—Re2—N213—C214	99.2 (9)
S131—Re1—N133—C132	0.04 (9)	O2^{i}—Re2—N213—C214	−80.8 (9)
C132—N133—C134—C135	−3.6	N213^{i}—Re2—N213—C214	129 (8)
Re1—N133—C134—C135	−179.03 (10)	S211^{i}—Re2—N213—C214	−171.3 (9)
N133—C134—C135—C136	2.2	S211—Re2—N213—C214	8.7 (9)
C134—C135—C136—C132	0.0	O2—Re2—N213—C212	−84.6 (6)
C131—C132—C136—C135	179.1	O2^{i}—Re2—N213—C212	95.4 (6)
N133—C132—C136—C135	−2.1	N213^{i}—Re2—N213—C212	−55 (9)
C132—C131—C137—C138	34.1 (14)	S211^{i}—Re2—N213—C212	4.8 (6)
C147—C131—C137—C138	140 (2)	S211—Re2—N213—C212	−175.2 (6)
S131—C131—C137—C138	−126.4 (10)	C212—N213—C214—C215	0.5 (11)
C132—C131—C137—C142	−142.0 (8)	Re2—N213—C214—C215	177.0 (7)
C147—C131—C137—C142	−36.1 (18)	N213—C214—C215—C216	−1.4 (13)
S131—C131—C137—C142	57.4 (10)	C214—C215—C216—C212	1.8 (13)
C142—C137—C138—C139	0.0	C211—C212—C216—C215	−173.4 (11)
C131—C137—C138—C139	−176.0 (14)	N213—C212—C216—C215	−1.5 (12)
C137—C138—C139—C140	0.0	C212—C211—C217—C218	−43.1 (10)
C138—C139—C140—O143	178 (2)	S211^{i}—C211—C217—C218	133.5 (5)
C138—C139—C140—C141	0.0	C212—C211—C217—*C*222	139.8 (7)
O143—C140—C141—C142	−177.9 (19)	S211^{i}—C211—C217—*C*222	−43.6 (8)
C139—C140—C141—C142	0.0	*C*222—C217—C218—C219	0.0
C140—C141—C142—C137	0.0	C211—C217—C218—C219	−177.1 (6)
C138—C137—C142—C141	0.0	C217—C218—C219—C220	0.0
C131—C137—C142—C141	176.3 (13)	C218—C219—C220—O223	178.0 (7)
C218—C219—C220—C221	0.0	C218—C217—*C*222—C221	0.0
O223—C220—C221—*C*222	−178.2 (7)	C211—C217—*C*222—C221	177.1 (6)
C219—C220—C221—*C*222	0.0	C221—C220—O223—C223	−176.2 (9)
C220—C221—*C*222—C217	0.0	C219—C220—O223—C223	5.7 (12)

Symmetry codes: (i) $\frac{1}{2}-x,\frac{3}{2}-y,1-z$; (ii) $1-x,y,\frac{3}{2}-z$.

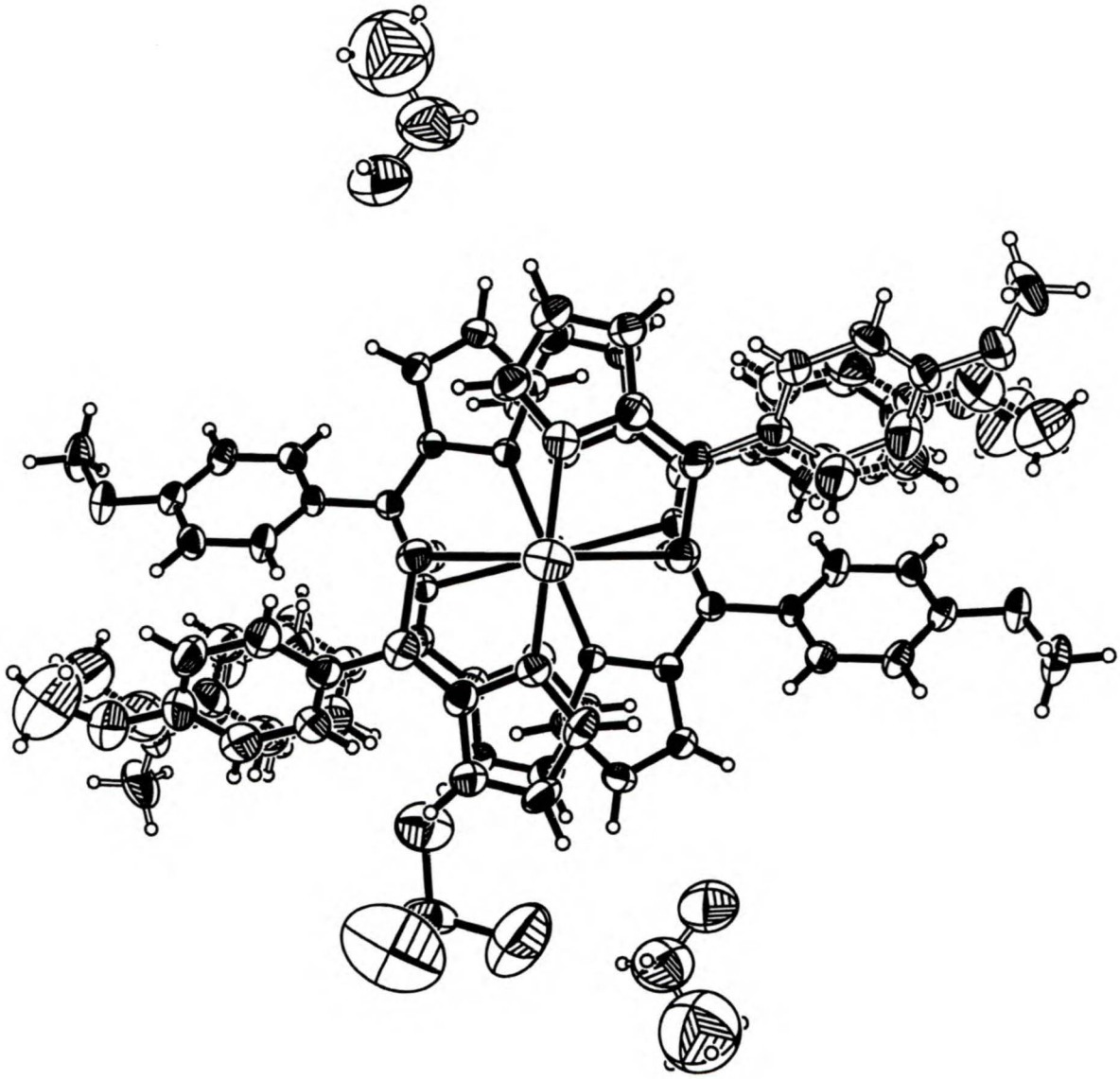

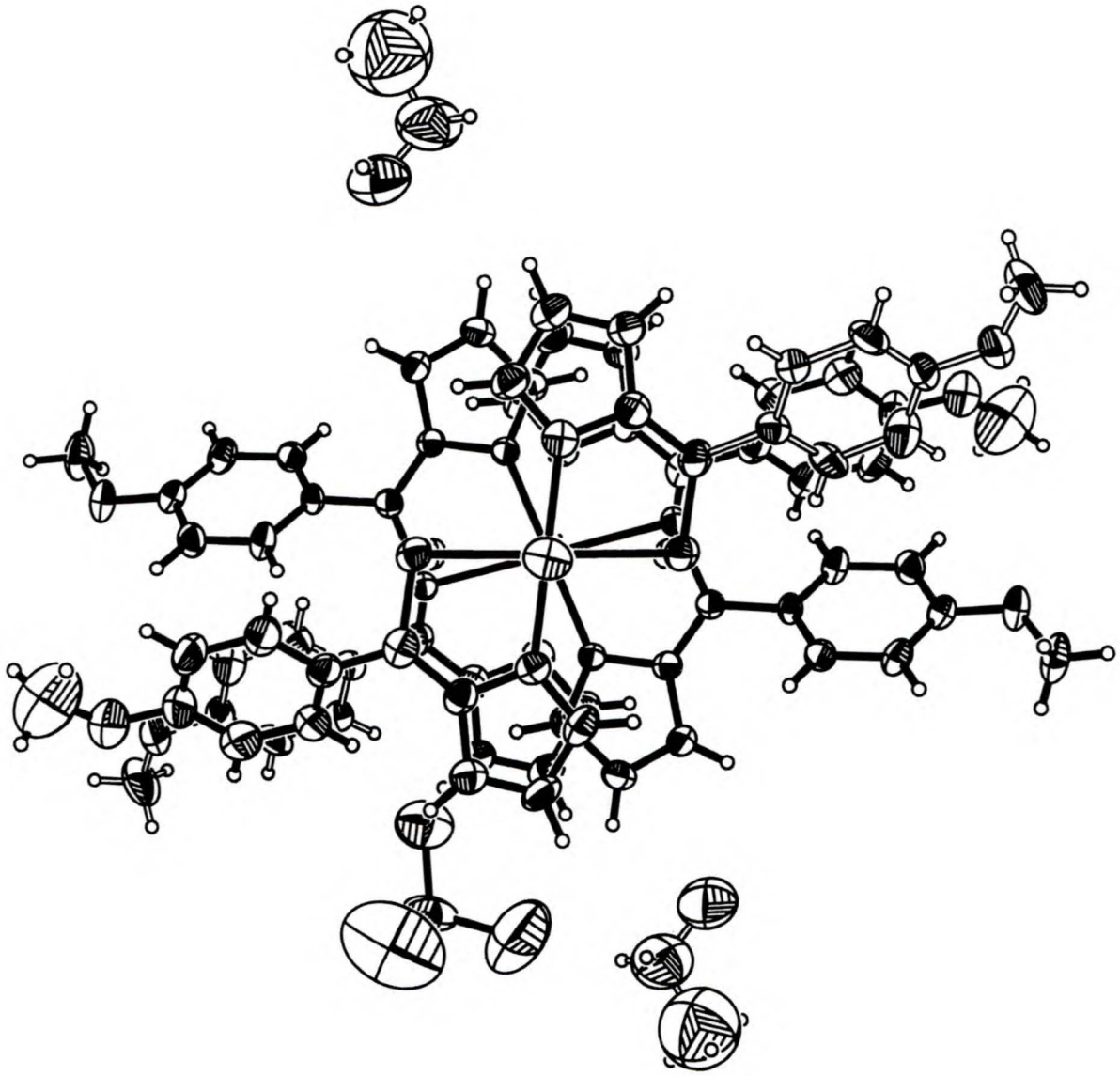

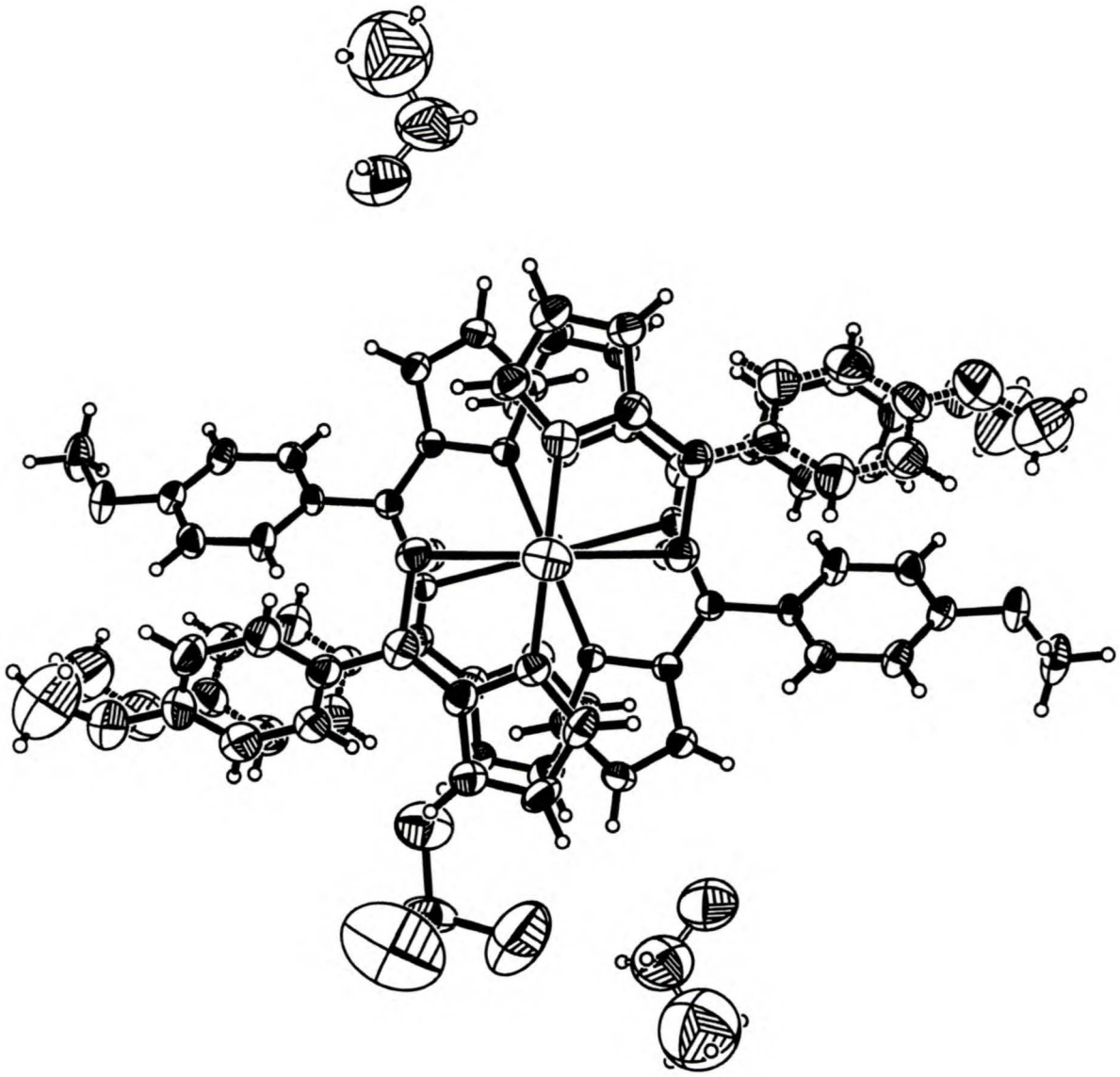

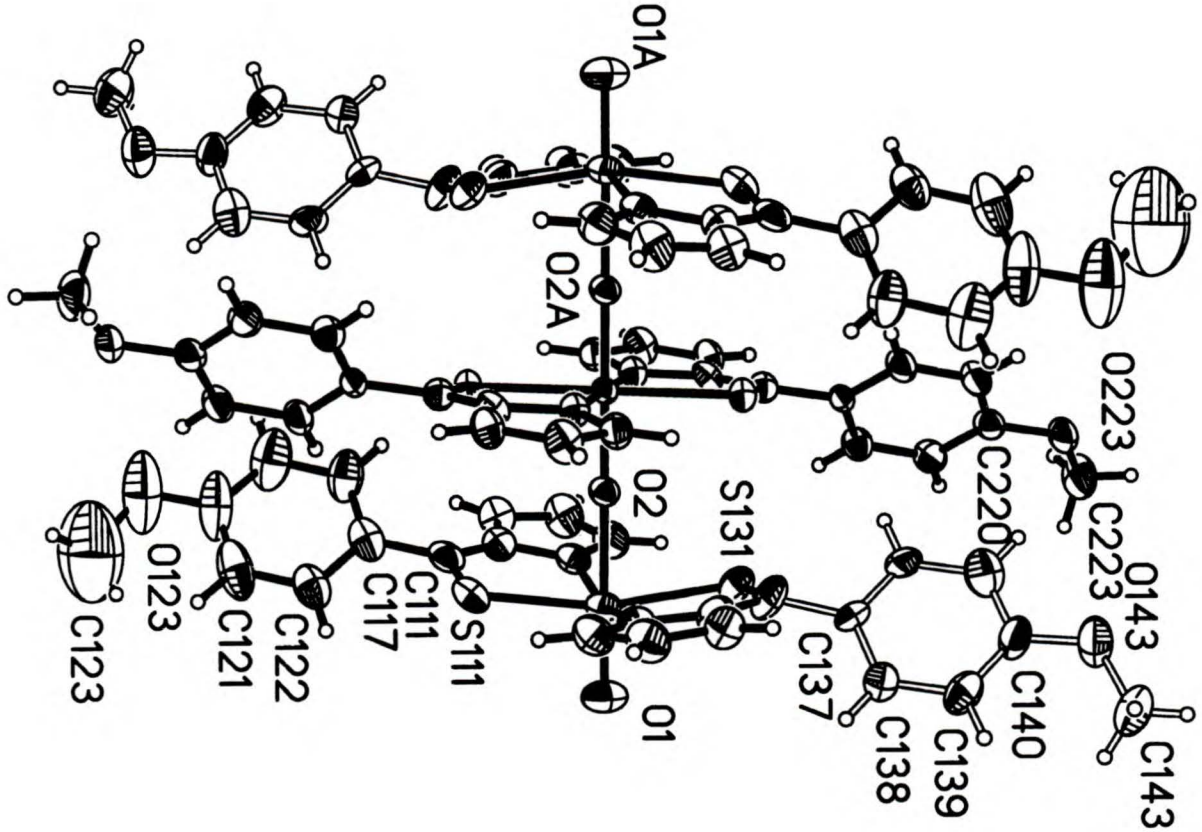
O1A
O2A
O223
C223
O143
C143
C220
C140
C139
C138
C137
S131
O2
O1
S111
C111
C117
C121
C122
O123
C123

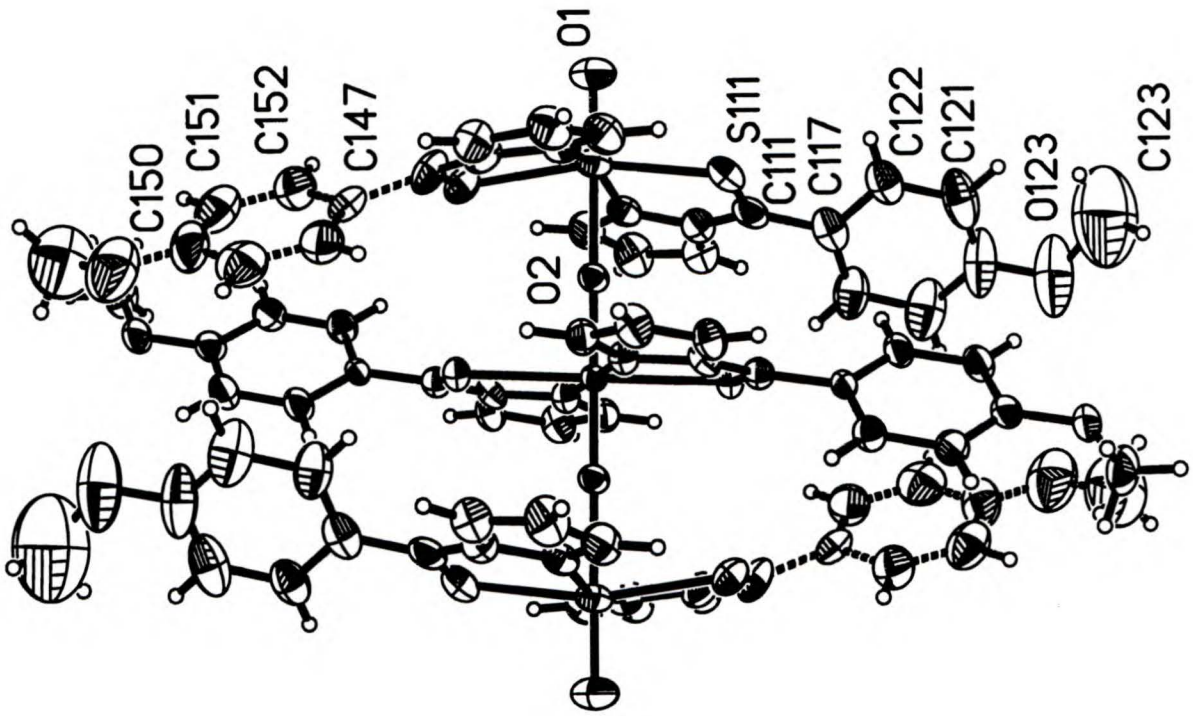
O1
S111
C111
C117
C122
C121
O123
C123
C147
C152
C151
C150
O2

PART 3

BIOLOGICAL STUDIES (SELECTED RESULTS)

In vitro data

Biodistribution chart 1.

Comparison of the biodistribution of the free pertechnetate, lipophilic compound **13a**, and water-soluble **14a**

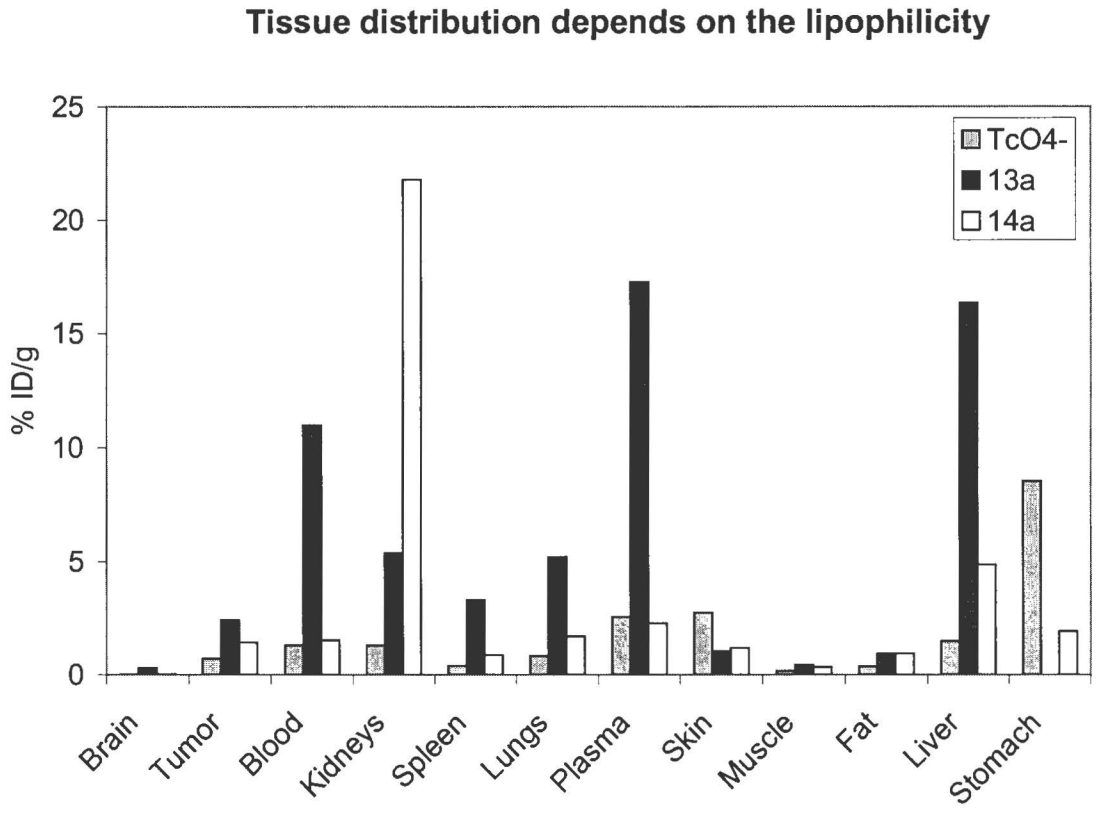

Biodistribution chart 2

Comparison of the biodistribution of the compounds with different level of the sulphonation, increasing in the row **13d**, **14d'**, **14d**.

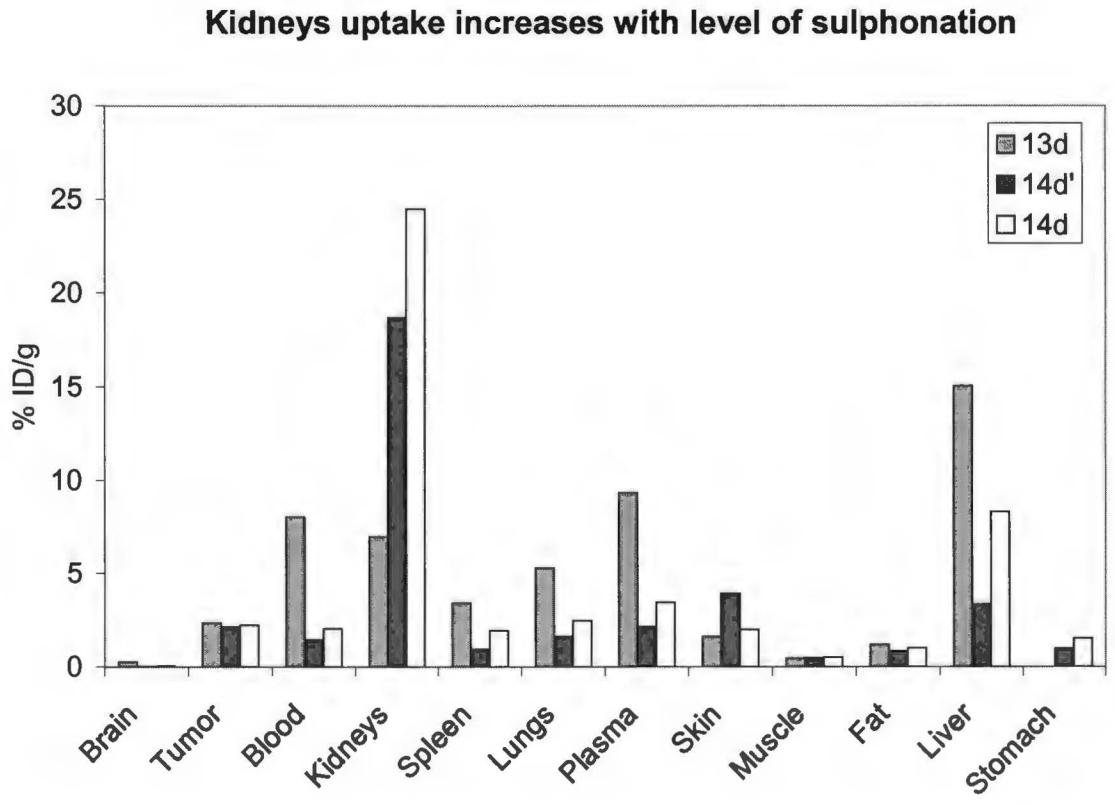

Biodistribution chart 3

Comparison of the biodistribution of the compounds with various substituents in the phenolic ring of the ligand molecule, where **12a** is the unsubstituted compound, **12b** has a methoxy-group, and **12c** has two methoxy-groups in the phenolic ring.